PHYSICAL REVIEW

A JOURNAL OF EXPERIMENTAL AND THEORETICAL PHYSICS

PUBLISHED BY THE

AMERICAN PHYSICAL SOCIETY

AMERICAN PHYSICAL SOCIETY

OFFICERS OF THE SOCIETY

	HENRY G. GALE	University of Chicago, Chicago, Ill.
	W. F. G. SWANN	Bartol Research Foundation, Philadelphia, Pa.
	W. L. SEVERINGHAUS	Columbia University, New York City
	G. B. PEGRAM	Columbia University, New York City
	JOHN T. TATE	University of Minnesota, Minneapolis, Minn.
for		
Coast:	L. R. LOSH	University of California, Berkeley, Calif.

THE PHYSICAL REVIEW

ished by the American Physical Society at 450 Ahnaip St., Menasha, Wis. office: University of Minnesota, Minneapolis, Minn. Two volumes annually, issues per volume.

series. From July 1, 1893, to January 1, 1913, the REVIEW was conducted by Ed- Nichols, Ernest Merritt and Frederick Bedell, with the financial support of Cor- versity. The first four volumes were issued annually; subsequent volumes, semi- thirty-five volumes in all.

series. On January 1, 1913, the REVIEW was transferred to the American Society as announced on the first page of the new series which was then begun. it has been conducted by a Board of Editors elected by the Society. Semi- olumes begin in January and July. Beginning July 1, 1919, the REVIEW will semi-monthly instead of monthly as heretofore.

are referred to page 2 of the advertisements for further information.

Subscription, throughout the Postal Union, $10.00 in advance.

ingles of current volume, $.60.

Index, 1893-1920, $4.00, in advance.

Volumes, $6.00 per volume; Back Numbers, $1.00 per copy for issues prior to (Vols. 1-33), $.60 per copy for issues subsequent thereto. Postage is free accompanies order; otherwise postage is extra. No bound volumes can be The REVIEW offers to purchase a limited number of First Series, Vol. 1, No. 1 each); Second Series, Vol. 7, No. 1, January 1916; Vol. 7, No. 2, February No. 4, April 1916; and Vol. 7, No. 5, May 1916 (at $1.00 each).

Rates will be supplied by the Editor on request. Copy for each num- received at Minneapolis two weeks prior to the date of issue; old copy is new copy is received. Send electrotypes direct to the printers, George Banta Co., Menasha, Wis.

of ten percent is allowed subscription agencies and members of the American ciety.

of address and Complaints of failure to receive the REVIEW, in the case of of the Physical Society, should be addressed to the Treasurer; in the case of bers to 450 Ahnaip St., Menasha, Wis.; or to the Editor. New copies can in response to complaint of non-delivery only if notice of non-delivery is within three months of date of issue.

Correspondence should be addressed to the PHYSICAL REVIEW, University of Minneapolis, Minn.

Entered at the postoffice at Menasha, Wis., as second class matter.
Acceptance for mailing at special rate of postage provided for in section 1103, Act of October 3, 1917, authorized September 6, 1918.

Second Series *July 15, 1929* *Vol. 34, No. 2*

THE

PHYSICAL REVIEW

THE CONTINUOUS X-RAY SPECTRUM

By Carl Eckart
Ryerson Physical Laboratory, University of Chicago

(Received May 13, 1929)

Abstract

Under the assumption that the target of an x-ray tube is a plane mirror which completely reflects the electron waves, the characteristics of the continuous x-ray spectrum are deduced from the principles of wave-mechanics. It is also assumed that the velocity of the electrons is so small that its square may be neglected in comparison to c^2. The conclusions are: (1) The component of momentum parallel to the plane of the target is conserved, the momentum of the emitted radiation being taken to be $h\kappa$, (κ = wave-number). The radiation due to a single transition is practically unidirectional, the direction of the beam (Nadelstrahl) being determined by the conservation laws of energy and momentum. The angular opening of the beam agrees with the uncertainty principle, using the linear dimensions of the target as Δx in the formula $\Delta x \Delta p_x = h/2\pi$. (2) No light of $\kappa > \kappa_m$ is emitted (short wave-length limit). κ_m is determined primarily by the energy of motion normal to the target, and not by the total energy. This result is due to the simplified model, and not to general principles. (3) The total intensity is proportional to κ_m^2 (empirically verified). The intensity in the wave-number interval $d\kappa$ is proportional to $[\kappa_m(\kappa_m - \kappa)]^{1/2} d\kappa$. (4) The intensity has a maximum in the azimuth of the velocity of the incident electron, the normal to the target being the polar axis. The plane of the target is one of mirror symmetry for the intensity distribution—a result which is again inseparable from the model. (5) For very small velocities, the radiation is linearly polarized parallel to the normal of the target (spectroscopic sense of the phrase). For higher velocities, the polarizaton cannot be so simply described, but in any direction whose azimuth is that of the incident velocity, the light should be plane polarized, the electric vector lying in the plane determined by the direction of observation and the normal to the target. These results also have no very general validity. The conclusions seem in satisfactory agreement with experiment, the schematic character of the model being taken into account.

THE continuous x-ray spectrum has never been satisfactorily treated by any theory, though its outstanding characteristic, the "short wave limit" has served for a direct determination for the value of h/e. The object of this paper is to indicate the ability of the present quantum theory to account for various features of the spectrum. As the calculations involved in the discussion are not the simplest it has seemed advisable to apply the theory to a very schematic model, which, though leading to incorrect quantitative results, yet brings out the theoretical principles involved. The ap-

plication to a less idealized model will doubtless improve the quantitative results.

The fundamental principles are those of wave-mechanics, with the interpretation of $-e\psi\psi'^*$ as the density of virtual charges associated to the transition from the state ψ to the state ψ'. The consequences of this interpretation have usually been investigated only in the case where $\psi\psi'^*$ is practically zero except in a region whose dimensions are small compared to the wave-length of the light emitted. As is well known, this case leads to the interpretation of

$$\int \cdots \int \Sigma e_i x_i \psi\psi'^* d\tau_1 \cdots d\tau_N$$

as the amplitude of the virtual oscillator producing the radiation. The conquences of the general case, in which $\psi\psi'^*$ may have a finite value in a larger region, have not yet been fully investigated, though G. Breit[1] has shown that the unidirectional character of the radiation from an atom of finite mass can be deduced in this way. The virtual charges concerned in the production of the continuous x-ray spectrum are of course spread over the macroscopic region between cathode and anticathode, so that the ordinary approximation of a dipole radiator is certainly not justifiable. In a conversation with Professor A. Sommerfeld it became clear that the more general view was not only logically necessary, but would account for some of the characteristics of this radiation which seemed inexplicable on any virtual dipole theory.

The model to which the general theory will be applied is that of an infinite plane (coinciding with $x_3=0$) which specularly and completely reflects the incident electron waves. The energy of the electron (measured in frequency units) will be designated by ω, and its momentum, in wave-numbers, by the vector $\boldsymbol{k}$, where

$$\frac{1}{2m}h^2\boldsymbol{k}^2 = h\omega \tag{1}$$

Relativistic complications are useless, since there is at present no theory which can be considered as satisfactory. The physically inadmissable transition from an energy $h\omega = +mc^2/(1-\beta^2)^{1/2}$ to $h\omega' = -mc^2/(1-\beta^2)^{1/2}$ could not be excluded by any consistent application of quantum mechanics, and it seems useless to multiply the examples illustrating this difficulty. The wave function representing this state of motion of the electron, in the absence of the reflecting plane, would be $u(\boldsymbol{k}) = e^{2\pi i\,(\boldsymbol{k}\cdot\boldsymbol{x}-\omega t)}$ where $\boldsymbol{x} = (x_1, x_2, x_3)$ is the vector to a point in space. To take account of the reflection at the target, the function

$$\psi = \frac{1}{i(2)^{1/2}}\{u(\boldsymbol{k}) - u(\boldsymbol{k}_r)\}, \quad x_3 > 0\,; \quad \psi = 0, \quad x_3 < 0 \tag{2}$$

[1] G. Breit, J.O.S.A. **14**, 374 (1927).

must be used, where $\boldsymbol{k}_r=(k_1, k_2,-k_3)$ is the momentum of the reflected electron. This represents an average density of one electron per cm³, and the average number of electrons reflected from one cm² of the target per second is accordingly $hk_3/2m$. The intensity of emission to be calculated will thus refer to unit charge density and not, as is customary, to unit current density. The virtual charges associated with a transition are then given by[2]

$$\begin{aligned}\rho&=-e\psi\psi'^*\\&=-\frac{e}{2}\{u(k)u(-k')-u(k)u(-k_r')+u(k_r)u(-k_r')-u(k_r)u(-k')\}\\&=-e\Sigma a e^{2\pi i[(k-k')\cdot x-\nu t]},\end{aligned}\tag{3}$$

where

$$\nu=\omega-\omega'.\tag{4}$$

The virtual currents are

$$\begin{aligned}J&=\frac{h}{4\pi im}\{\psi'^*\nabla\psi-\psi\nabla\psi'^*\}\\&=-\frac{eh}{2m}\Sigma a(k+k')e^{2\pi i[(k-k')\cdot x-\nu t]}.\end{aligned}\tag{5}$$

If these charges were viewed from a system moving with the velocity

$$v_1=\frac{h}{2m}(k_1+k_1'),\qquad v_2=\frac{h}{2m}(k_2+k_2'),\qquad v_3=0,$$

which is the component parallel to the target of the average of the velocity of the electron before and after the transition, the components J_1 and J_2 would vanish. This follows since the vectors $\boldsymbol{k}+\boldsymbol{k}'$, $\boldsymbol{k}_r+\boldsymbol{k}_r'$ have the same components in the 1 and 2 directions. In this moving system there would then be complete symmetry of distribution about the normal to the target. Hence all azimuthal asymmetry of the intensity distribution must be introduced by the transformation from this system to that of the observer; this is the result of Sommerfeld's classical considerations[3] modified to apply to this model. The asymmetry in polar distribution cannot be treated in this way.

These virtual charges may also be represented by a continuous distribution of dipoles, whose density is

$$L=-\frac{eh}{2m}\ \Sigma\ a\ \frac{k+k'}{2\pi i\nu}\ e^{2\pi i[(k-k')\cdot x-\nu t]}.\tag{6}$$

[2] It is understood that only the real parts of these and similar expressions have any significance.

[3] A. Sommerfeld, Atombau, 3rd Ed. Append. 1. p. 649 (1922).

The charge and current densities are then, as is well known, derivable from the equations

$$\rho = \nabla \cdot \boldsymbol{L}, \quad \boldsymbol{J} = -\partial \boldsymbol{L}/\partial t$$

Whenever this is possible, it is known that the electro-magnetic field is derivable from the single Hertzian vector $\boldsymbol{Q}$:

$$\boldsymbol{E}\boldsymbol{Q} = -\nabla \times (\nabla \times \boldsymbol{Q}), \quad \boldsymbol{H} = -\frac{1}{c}\frac{\partial}{\partial t}(\nabla \times \boldsymbol{Q}),$$
$$\boldsymbol{Q} = \int\int\int ([\boldsymbol{L}]/R)\, d\tau. \tag{7}$$

The term $4\pi \boldsymbol{L}$ is omitted from the expression for $\boldsymbol{E}$ since the observer is certainly not in the stream of cathode rays. In the equation defining $\boldsymbol{Q}$, R denotes the distance from the point of integration, $\boldsymbol{x}$, to the point of observation, $\boldsymbol{r}$, and the symbol [ ] denotes retardation of the enclosed function. The integral is to be extended over all space above the plane $x_3 = 0$.

It is apparent from the nature of the problem that the radiation can come only from the surface of the target, for the electron is not accelerated except when it is actually in contact with the target. Alternatively, it may also be seen by remarking that the radiation from successive crests of the electron wave will destructively interfere, except at the boundary of the distribution, where the succession of waves ceases. This finds its mathematical expression in the transformation of the volume integral into a surface integral. To do this, it is necessary to treat each term of the sum, Eq. (6), separately. Letting V denote the variable part of a typical term

$$[V]/R = V(e^{+2\pi i \nu R/c})/R = VG$$

where obviously

$$\nabla^2 V + 4\pi^2 (\boldsymbol{k} - \boldsymbol{k}')^2 V = 0$$
$$\nabla^2 G + 4\pi^2 \kappa^2 G = 0, \quad \kappa = \nu/c.$$

An application of Green's theorem immediately yields[4]

$$\int\int\int [V]/R\, d\tau = \frac{1}{4\pi^2 [(\boldsymbol{k} - \boldsymbol{k}')^2 - \kappa^2]} \int\int \boldsymbol{n} \cdot \{G\nabla V - V\nabla G\}\, dS, \tag{8}$$

in which the surface integral is to be extended over the whole of the plane $x_3 = 0$, and over the infinite hemisphere above it. For obvious physical reasons, it will suffice to calculate the contribution from a finite region of the plane. This area may be taken to be rectangular, with two sides extending along the coordinate axes, and of lengths l_1, l_2. The point of observation $\boldsymbol{r}$ will be assumed so far distant from the origin that the approximation

[4] It might appear that this expression could become infinite, but, from $(\boldsymbol{k} - \boldsymbol{k}')^2 = \kappa^2$ and $\nu = \omega - \omega'$ it may be deduced that $h|\boldsymbol{k} + \boldsymbol{k}'| \geqq 2mc$, which contradicts the necessary assumption that the velocity of the electron be less than that of light.

$$R=r-\boldsymbol{\alpha}\cdot\mathbf{x}, \quad \boldsymbol{\alpha}=\mathbf{r}/r,$$

suffices at every point within the rectangle.

Since $\boldsymbol{n}$ is now a constant unit vector along the x_3-axis Eq.(8) reduces to

$$\iiint \frac{[V]}{R}d\tau=\frac{k_3-k_3'+\kappa\alpha_3}{2\pi[(k-k')^2-\kappa^2]}\,\frac{1}{r}e^{-2\pi i\nu(t-r/c)}\iint e^{2\pi i\,[\mathbf{k}-\mathbf{k}'-\kappa\boldsymbol{\alpha}]\,\cdot\,\mathbf{x}}dS$$

The surface integral is to be extended over the rectangle, and is readily seen to be equal to

$$\frac{e^{4\pi i\delta_1 l_1}-1}{4\pi i\delta_1}\cdot\frac{e^{4\pi i\delta_2 l_2}-1}{4\pi i\delta_2}$$

where

$$2\delta_1=k_1-k_1'-\kappa\alpha_1$$
$$2\delta_2=k_2-k_2'-\kappa\alpha_2.$$

This is a function typical of the theory of diffraction, and has a very sharp maximum when $\delta_1=0, \delta_2=0$. Since δ_1 and δ_2 have the same value for every term of the summation, it follows that the radiation will be negligible except in one direction α which satisfies these equations. The radiation due to a single transition will thus consist of a single sharply defined beam (Nadelstrahlung) which may be taken as the path of the photon. The equations determining its direction are precisely those expressing the conservation of momentum in the x_1 and x_2 directions, the momentum of the photon being taken as $h\nu/c$ gm cm sec^{-1}. The action of the forces causing the reflection makes it impossible to demand conservation in the third direction.[5] The sharpness of the maximum allows $(\boldsymbol{k}-\boldsymbol{k}')^2-\kappa^2$ to be replaced by $(k_3-k_3')^2-\kappa\alpha_3^2$ without serious error, although the two expressions are in general not even approximately equal. Thus the Hertzian vector may be written

$$\boldsymbol{Q}=-\frac{eh}{4\pi m}\boldsymbol{B}Q_0 \tag{9}$$

where

$$\boldsymbol{B}=\Sigma a\frac{\boldsymbol{k}+\boldsymbol{k}'}{k_3-k_3'-\kappa\alpha_3}$$

and

$$Q_0=\frac{1}{2\pi\nu r}e^{-2\pi i[\nu(t-r/c)-\delta_1 l_1-\delta_2 l_2]}\frac{\sin 2\pi\delta_1 l_1\sin 2\pi\delta_2 l_2}{(2\pi)^2\delta_1\delta_2} \tag{10}$$

is independent of k_3 and k_3'. An algebraic reduction yields the components of $\boldsymbol{B}$:

[5] The width of the beam is readily seen to be that required by the uncertainty principle because of the restriction that the electron impinge on the finite area of the rectangle.

$$B_1 = A\kappa\alpha_3(k_1 + k_1')$$
$$B_2 = A\kappa\alpha_3(k_2 + k_2') \tag{11}$$
$$B_3 = A(k_3^2 - k_3'^2)$$

where

$$A = \frac{4k_3k_3'}{[k_3^2 - k_3'^2 + \kappa^2\alpha_3^2]^2 - 4k_3^2\kappa^2\alpha_3^2}. \tag{12}$$

The expression for the electromagnetic field follows from Eq. (7):

$$\boldsymbol{E} = \frac{eh\nu}{2mc^2}\boldsymbol{\alpha}\times(\boldsymbol{\alpha}\times\boldsymbol{B})\,Q_0$$
$$\boldsymbol{H} = -\frac{eh\nu}{2mc^2}\boldsymbol{\alpha}\times\boldsymbol{B}\,Q_0 \tag{13}$$

(terms of order $1/r^2$ are of no significance and have been neglected). The average energy flux due to the virtual charges is

$$\overline{\boldsymbol{E}\times\boldsymbol{H}} = \frac{1}{2}\left(\frac{eh\nu}{2mc^2}\right)^2(\boldsymbol{\alpha}\times\boldsymbol{B})^2\frac{1}{r^2}\,\frac{\sin^2 2\pi\delta_1 l_1 \sin^2 2\pi\delta_2 l_2}{(2\pi)^4\delta_1^2\delta_2^2}. \tag{14}$$

This expression, multiplied by $dk_1'\,dk_2'\,dk_3'$ and integrated over all $k_1'k_2'k_3'$ for which $\omega \geqq \omega'$ gives the probable energy radiated per cm^2 per sec in the direction α. The integrations with respect to k_1' and k_2' are readily carried out for, approximately

$$\int_0^{k_m'} F(k')\frac{\sin^2 2\pi\delta l}{(2\pi)^2\delta^2}dk'$$
$$= F(k'_{\delta=0})\int_{-\infty}^{\infty}\frac{\sin^2 2\pi\delta l}{(2\pi)^2\delta^2}dk'$$
$$= lF(k'_{\delta=0})$$

if $\delta = 0$ can be satisfied for a value $k' < k_m'$; otherwise the integral is negligibly small. Hence the probable energy flux may be written

$$\frac{l_1 l_2}{2r^2}\int\left(\frac{eh\kappa}{2mc}\right)^2(\boldsymbol{\alpha}\times\boldsymbol{B})^2 dk_3' \tag{15}$$

in which the integrand is a function of k_3' only, k_1', k_2', κ being eliminated by means of the equations $\delta_1 = 0$ $\delta_2 = 0$ and $\nu = \omega - \omega'$ which may be written

$$k_1 = k_1' + \kappa\alpha_1$$
$$k_2 = k_2' + \kappa\alpha_2$$
$$\frac{h}{2mc}\boldsymbol{k}^2 = \kappa + \frac{h}{2mc}\boldsymbol{k}'^2 \tag{16}$$

This elimination is simplified by the fact that terms of order β^2 ($\beta = h|\boldsymbol{k}|/mc$) are not significant, the variability of the mass of the electron giving rise to other terms of the same magnitude. The Eqs. (16) reduce to

$$\kappa = \frac{h}{2mc}\left\{ k_3^2 - k_3'^2 + 2\kappa(k_1\alpha_1 + k_2\alpha_2) - \kappa^2(\alpha_1^2 + \alpha_2^2)\right\}$$

or, approximately

$$\kappa = \frac{h\gamma}{2mc}(k_3^2 - k_3'^2) \tag{17}$$

where

$$\gamma = 1 + \frac{h}{mc}(k_1\alpha_1 + k_2\alpha_2) \tag{18}$$

From this it immediately follows that the largest value of κ for which k_3' can be real is

$$\kappa_m = \frac{h\gamma}{2mc}k_3^2 = \kappa_0\gamma. \tag{19}$$

This is the wave-number of the short wave-length limit of the spectrum. It is not determined by the total energy of the incident electron, but (to a first approximation) by that part of its energy which is due to its motion normal to the target only. This is obviously a direct result of the absence of forces parallel to the surface of the target, and in no way conflicts with experiment. Another consequence of Eq. (17), since $\kappa < \kappa_m$, is that $h\kappa/mc$, κ^2/k^2 are negligible quantities; remembering this, Eq. (12) may be reduced to

$$A = \frac{2h\gamma}{mc}\,\frac{[\kappa_m(\kappa_m - \kappa)]^{1/2}}{\kappa^2} \tag{20}$$

and Eq. (11) to

$$\begin{aligned} B_1 &= (hk_1/mc)\alpha_3 B_3 \\ B_2 &= (hk_2/mc)\alpha_3 B_3 \\ B_3 &= (4/\kappa)[\kappa_m(\kappa_m - \kappa)]^{1/2}. \end{aligned} \tag{21}$$

To this approximation, the average momentum may be replaced by the momentum of the electron before impact on the target. A simple calculation yields

$$(\boldsymbol{\alpha}\times\boldsymbol{B})^2 = 16\frac{\kappa_m(\kappa_m - \kappa)}{\kappa^2}(1 - \alpha_\beta^2\gamma^2) \tag{22}$$

so that the total energy flux is

$$\frac{l_1 l_2}{2r^2}\left(\frac{eh}{2mc}\right)^2 \cdot 16\int_0^{k_3} \kappa_m(\kappa_m - \kappa)(1 - \alpha_3^2\gamma^2)\,dk_3'.$$

To compare this expression with experiment, it is convenient to change the variable of integration from k_3' to κ and to reduce to the intensity I per one electron striking the target per sec. By Eq. (17)

$$\frac{dk_3'}{d\kappa}=\frac{-1}{2\left(\frac{h\gamma}{2mc}(\kappa_m-\kappa)\right)^{1/2}}$$

and the number of electrons striking the target in one second is (cf. p. 3)

$$l_1 l_2 \frac{hk_3}{2m}=l_1 l_2 \frac{c}{\gamma}\left(\frac{h\gamma}{2mc}\kappa_m\right)^{1/2}$$

hence the expression for I is

$$I=2\frac{e^2h}{mc^2}\frac{1}{r^2}(1-\alpha_3{}^2\gamma^2)\int_0^{\kappa_m}(\kappa_m(\kappa_m-\kappa))^{1/2}d\kappa. \tag{23}$$

The integrand of this expression obviously gives the spectral distribution of the intensity, as a function of the wave-number of the light. The distribution curve is a parabola:

$$I(\kappa)\sim(\kappa_m(\kappa_m-\kappa))^{1/2}$$

whose vertex is at the short wave-length limit of the spectrum. The most recent experimental work indicates that the empirical curve more nearly approximates a rectangle, or even has a slight maximum near κ_m.[6] The perpendicular descent to zero at κ_m is borne out, however.

The Eq. (23) also contains the empirical law, $I\sim\kappa_m{}^2$ but the constant of proportionality is here determined by absolute constants (except for the dependence on angle), whereas it is found empirically to be a linear function of the atomic number of the metal composing the target. The model could not be expected to furnish this relation.

The dependence of the intensity on the azimuth of observation, as has been pointed out, must be considered to be satisfactory and need not be explicitly considered here. The dependence on polar angle of observation must be discussed, however, and the result is not very satisfactory. The dependence on the direction is contained in the expression

$$I\sim\kappa_m{}^2(1-\alpha_3{}^2\gamma^2)=\kappa_0{}^2\gamma^2(1-\alpha_3{}^2\gamma^2)$$

whose value is unchanged when the polar angle is replaced by its supplement. The plane of the target is thus a plane of mirror-symmetry for the intensity distribution, which is at variance with experiment. Considerations which need not be reproduced here, show that this conclusion is definitely dependent on the simplifications introduced by the model, and not at all of general

[6] W. W. Nicholas, Bur. Stand. Journ. of Res. **2**, 837 (1929). The suggestion made there that the shape of this curve is due to the structure of the electron ($\psi\psi^*\sim\sin kx/x$) does not seem to be in accord with the general principles of quantum theory.

validity; presumably almost any other model would give a more satisfactory result.

According to Eq. (13) the radiation is polarized in the same manner as that from a linear oscillator whose direction of oscillation is given by the vector $\boldsymbol{B}$. In a direction α whose azimuth is that of the incident electron, the light will thus always be plane polarized, the plane of the electric vector and α passing through the normal to the target. It is true that $\boldsymbol{B}$ is not independent of the direction α, so that a different oscillator must be considered for each direction; if the velocity of the electron is very small compared to that of light, however, this dependence disappears, and the radiation is linearly polarized parallel to the x_3-axis (the phrase is used in the sense current in spectroscopy). This result is also inseparably related to the absence of forces in the x_3 direction.

In summary, it may be said that the theory accounts for many of the characteristics of the continuous x-ray spectrum, and that discrepancies between theory and experiment seem rather to be due to the schematic model on which the calculations are based than to the fundamental principles of the quantum theory.

RESOLUTION OF THE LINE $L\beta_2$ INTO ITS DIAGRAM COMPONENTS AND THE RELATIVE WIDTHS OF SOME X-RAY SPECTRUM LINES

By Samuel K. Allison
University of California, Berkeley

(Received May 25, 1929)

Abstract

According to the energy-level diagram applicable to atoms which have lost one electron from an inner level the line $L\beta_2$ should be double, since it consists of electron transitions from the levels $N_{IV}N_V \rightarrow L_{III}$. The weaker component is designated as $L\beta_{15}$ following Crofutt. The present paper describes the results of an investigation of the line in 77 Ir, 81 Tl, and 92 U, using the double spectrometer. In 77 Ir the line $L\beta_2$ has such a great intrinsic width that β_{15} could not be separated from it although the dispersion and resolving power of the instrument were ample. In Tl 81 a better but not complete resolution was obtained. In 92 U a practically complete separation was found. The average of the wave-length separations observed in two experiments on uranium is 1.86 X.U. Using the combination principle and Lindberg's M-series measurements the separation should be 1.94 X.U. The Burger-Dorgelo rules predict a relative intensity of 9:1 and this was found to represent the facts within the rather large experimental error. Experiments are reported on the intrinsic widths of certain lines in the L-series of thallium and lead, taken at 34 kilovolts. The data reveal the following facts (1) Although the wave-length breadth ($\Delta\lambda$) of $L\alpha_1$ is greater than any of the other lines measured except $L\beta_4$, the energy breadth (ΔV) is less than that of the other lines. (2) $\Delta\lambda$ for $L\beta_4$ is 2–3 times as great as that of any other line measured. These results are compared with certain remarks by Coster on the width of x-ray spectrum lines.

THIS paper concerns investigations in the L-series carried out with the double x-ray spectrometer as previously used by Ehrenberg and Mark,[1] Ehrenberg and von Susich,[2] and Bergen Davis[3] and his associates. A description of the double spectrometer used in this work will appear soon in another journal.[4] The x-ray tube was of the usual water cooled type described in previous papers by the author.[5] All the investigations reported were carried out at 34 kilovolts and 8 milliamperes. It is well known that one of the advantages of the double spectrometer is the possibility of using wide slits. This meant the use of a wide window on the x-ray tube to pass the rather soft rays under consideration. Mica windows proved unsatisfactory due to electrostatic puncturing, so an aluminum foil window 0.0035 cm thick was used. The original intention in undertaking the work reported here was

[1] Ehrenberg and Mark, Zeits. f. Physik **42**, 807 (1927).

[2] Ehrenberg and v. Susich, Zeits. f. Physik **42**, 823 (1927).

[3] Bergen Davis and Harris Purks, Proc. Nat. Acad. Sci. USA **13**, 419 (1927) and succeeding papers.

[4] J. W. Williams and S. K. Allison, J.O.S.A. and R.S.I. in print.

[5] S. K. Allison, Phys. Rev. **30**, 245 (1927).

to supplement some relative intensity measurements made by the author with a single spectrometer in thallium, lead, and bismuth where the lines $L\beta_1$ and $L\beta_2$ were not resolved. Although complete resolution of these lines was obtained in thallium it became apparent that there are complicating factors which make it essential that great care be used in making intensity measurements with the double spectrometer and that several subsidiary researches would have to be carried out before the meaning of the measurements would become clear. Accordingly the original project was temporarily abandoned and other somewhat less exacting investigations carried out.

The intensity-wave-length curves for Tl $L\beta_2$ showed unmistakable evidence of a weak component on the long wave-length side. This is due to the double character of this line, representing the transitions $N_{IV}N_V \rightarrow L_{III}$. The transition $N_V L_{III}$ is the main line $L\beta_2$, $N_{IV}L_{III}$ the weaker component of

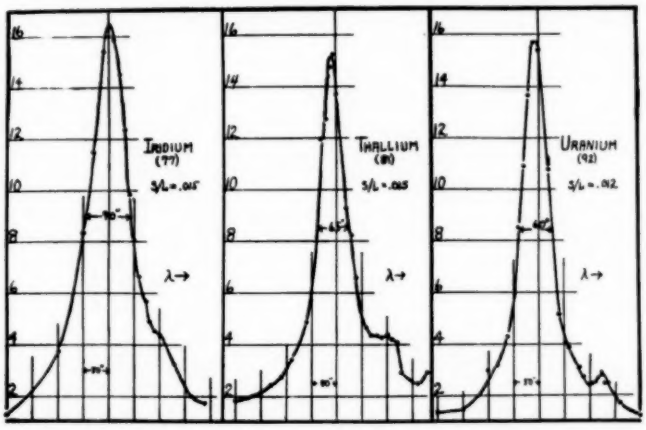

Fig. 1. The $L\beta_2$ and its weaker component in iridium, thallium, and uranium. Ordinates are proportional to electrometer deflections in millimeters per second.

longer wave-length. The situation is exactly analogous to that of $L\alpha_1\alpha_2$ and the extension of the sum rules of Burger and Dorgelo to x-ray spectra by Sommerfeld[6] and Coster and Goudsmit[7] predict the intensity ratio 9:1 in both cases. Fig. 1 shows the $L\beta_2$ line as it appeared in these experiments in iridium, thallium, and uranium. These curves were taken with both crystals at first order so the dispersion is twice that of a single crystal spectrometer at first order. In an analysis of the double spectrometer Schwarzschild[8] has shown that the condition that the width of the lines observed should not be due to geometrical factors in the instrument is

$$s/L << \{(\text{angular width measured})/\tfrac{1}{2}(\tan\theta_1 \pm \tan\theta_2)\}^{1/2}$$

providing the faces of both crystals are vertical. s is the effective height of the slits, L the distance between the stops controlling the vertical height

[6] A. Sommerfeld, Ann. d. Physik **76,** 284 (1925).
[7] Coster and Goudsmit, Naturwissenschaften **1,** 11 (1925).
[8] Schwarzschild, Phys. Rev. **32,** 162 (1928).

and θ_1 and θ_2 the glancing angles on crystals A and B respectively. The + sign is to be taken in the anti-parallel position, and the − sign in the parallel position. In the experiments on $L\beta_2$ s/L was 0.015 for iridium and thallium, and 0.012 for uranium. The factor on the right hand side of Schwarzschild's criterion was 0.048 for Ir, 0.044 for Tl, and 0.048 for U. An appreciable fraction of the width observed may therefore be due to geometric causes. Nevertheless it is clear that the wave-length width of Ir $L\beta_2$ is considerably greater than Tl $L\beta_2$ or U $L\beta_2$.

It has been previously claimed by Crofutt[9] that the components of $L\beta_2$ in tungsten had been resolved using a single spectrometer with a rock-salt crystal. The failure of the double spectrometer with calcite crystals to resolve these lines in iridium indicates that the separation observed by Crofutt was spurious. Crofutt denotes the weaker component by β_{15} and that symbol will be used in this discussion. As is seen in Fig. 1 the separation in uranium is almost complete. Results of the measurements on thallium and uranium are shown in Table I.

TABLE I. *Separation and relative intensity of L* β_2, β_{15}.

	$\Delta\theta$	$\Delta\lambda$	$\Delta\lambda$ (calc)	Intensity ratio
Thallium	110 sec.	1.60 XU.	1.74 XU.	9:1
Uranium	123	1.80		13:1
Uranium	132	1.93		10:1
Uranium ave.	128	1.86	1.94 Av	11:1

The values of $\Delta\lambda$(calc.) were obtained by the combination principle from the data of Lindberg[10] on the M-series wave-lengths since the same frequency difference should exist between the lines $M_{III}N_{IV}$ and $M_{III}N_V$. The relative intensities are the maximum ordinates of the curves representing the two components, with base lines computed on the same assumptions as used by Allison and Armstrong[11] in their work on the separation and relative intensities of the components of Mo$K\beta_1$. The assumption is made that $L\beta_2$ and $L\beta_{15}$ have the same width which means that the intensity estimates are rather crude. These two lines are part of the compound doublet $\gamma_1\beta_2\beta_{15}$, analogous to $\beta_1\alpha_1\alpha_2$ and the present measurements, together with previous work shows that these two compound doublets obey the Burger-Dorgelo rules as extended to x-ray spectra.

Figure 2 shows curves obtained for the widths of certain lines in the L-series of lead and thallium. These were obtained at 34 kilovolts and 8 milliamperes. For all these experiments the ratio s/L was 0.012. The results on these wave-length breadths are not considered final, in the sense that all contribution to the breadths in Fig. 2 are due to the intrinsic widths of the lines themselves compounded with the width of reflection of a single wave-

[9] Crofutt, Phys. Rev. **24**, 9 (1924).
[10] Lindberg, Zeits. f. Physik **50**, 82 (1928).
[11] Allison and Armstrong, Phys. Rev. **26**, 701 (1925).

length from a highly perfect calcite crystal. The width of the rocking curves at the parallel position as shown in Fig. 2 was 24 seconds at half maximum. All widths of curves given in this paper refer to the total width at half maximum. The widths referred to in the papers of Ehrenberg and Mark, and Ehrenberg and v. Susich are the half-breadths at half maximum. The width

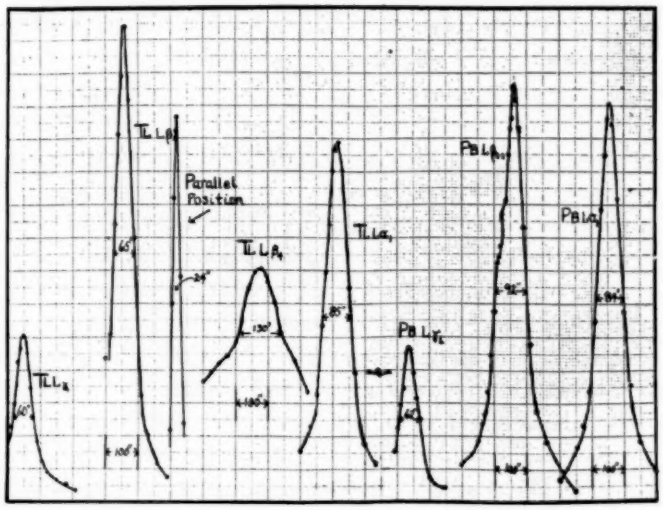

Fig. 2. Curves showing relative widths of certain x-ray lines. Ordinates are proportional to rates of deflection of the electrometer.

of 24 seconds was taken at a glancing angle of 9°19′. This indicates that the crystals used were not as perfect as have been obtained by other investigators. Work is now going on in an attempt to make the results more precise and trustworthy. Due to the relation

$$H_\lambda = (H_2^2 + H_1^2)^{1/2}$$

where $H\lambda$ is the intrinsic width at half maximum, H_2 and H_1 are the observed widths in the anti-parallel and parallel positions respectively; for the large H_2's measured here the H_1 of 24 seconds introduced no large correction. It was assumed that H_1 is constant throughout the wave-length region measured.

TABLE II.

Line	H_2	$(H_2^2 - H_1^2)^{1/2}$	$\Delta\lambda$	ΔV
Tl $L\alpha_1$	84.5 sec.	80.8	1.16 XU.	9.8 volts
Tl $L\beta_4$	130	128	1.86	21.3
Tl $L\beta_1$	65	60.4	0.87	10.4
Tl $L\gamma_1$	60	55.0	0.80	13.2
Pb $L\alpha_1$	84	80.6	1.16	10.4
Pb $L\gamma_1$	62.5	57.6	0.84	14.8

The column headed $\Delta\lambda$ was calculated from the preceding column by the formula

$$\Delta\lambda = \tfrac{1}{2}\lambda \cot \theta \Delta\theta .$$

Two important facts appear in Table II are (1) Although the wave-length breadth of $L\alpha_1$ is greater than $L\beta_1$ or $L\gamma_1$, the voltage breadth is less, (2) The line $L\beta_4$, the only line measured involving the level L_1, is very much broader than these other lines, both in wave-length and voltage.

Figure 2 also shows an attempt to separate the lines $L\beta_1$ and $L\beta_2$ of lead. The lines are not separated but it is clear that $L\beta_2$ is on the short wave-length side of $L\beta_1$.

The results on the widths of the lines may be compared with some comments of Coster[12] on the width of x-ray lines. Coster states that in general the widths of lines involving transitions between so-called "elliptic orbits" on the classical quantum theory is greater than those involving circular orbits. This is not entirely confirmed here inasmuch as it applies to $L\alpha_1$, for in these experiments this line had a greater wave-length breadth than any other line measured involving the L_{II} L_{III} orbits. It must be noted, however, that the voltage or energy width of the $L\alpha_1$ line is less than that for any of the others measured which agrees with the ideas underlying Coster's remarks. Probably the two chief causes of the widths observed here are (1) "spark" lines on the short wave-length side of the diagram lines, and (2) deviation of the energy levels from true doublet levels due to Hund coupling with incompleted outer shells in the atom. The great width of $L\beta_4$ involving the orbits $L_I M_{II}$ is perhaps the best illustration of the effect of "elliptic" orbits. It is interesting to note that this class of lines constitutes the exceptions to the Burger-Dorgelo rules.

[12] Coster, Zeits. f. Physik **45**, 797 (1927).

UNUSUAL REFLECTING POWER OF A PAIR OF CALCITE CRYSTALS

By Bergen Davis and Harris Purks
Physics Laboratories, Columbia University

(Received May 13, 1929)

Abstract

Reflection characteristics of the calcite (Iceland spar) crystal are reported. Two split calcite crystals were mounted on double x-ray spectrometer in parallel position. Coefficient of reflection, percent reflection and width of rocking curve were measured at both first and second order reflections and for three wave-lengths: λ0.209A, λ0.7077A and λ1.537A. The percent reflection was as great as 48.5 at first order for λ1.537. The corresponding coefficient of reflection was small. The rocking curves were surprisingly narrow, being as small as 1.25″ at second order for λ0.7078A. This width is less than is to be expected from the Darwin equation using previously determined values of the structure factor. Crystals of these properties are especially valuable for use on the double crystal spectrometer, when high resolving power is desired.

THE resolving power of the double x-ray spectrometer is largely dependent on the perfection of the crystals. In the search for the best crystals a pair was found whose properties were so near those of a "perfect" crystal that it seemed desirable to bring it to the attention of those who are interested in theories of crystal reflection.

The specimen of calcite (Iceland spar) was obtained from the Ward Natural Science Establishment of Rochester, New York. A portion about $2\times2\times10$ cm was split from the large crystal. This was then carefully split into two equal crystals 1 cm thick and 10 cm long. They were mounted so that the two contiguous faces of the last splitting formed the two reflecting surfaces. These crystals were mounted on the spectrometer in the parallel position in the manner previously described.[1] When the crystals are placed in this position the width of rocking curves is independent of the properties of the radiation. It depends only on the crystals.

The instrument and the technique have been improved so that it is possible to read rocking angles to a part of a second of arc. An important matter in the technique of two-crystal spectrometry is that the axis of rotation of the second crystal B should be parallel to that of the first crystal A. Lack of parallelism increases the width of the rocking curves.

Measurements were made at first and second orders on both crystals. The wave-lengths used were W $K\alpha_1$(0.209A), Mo $K\alpha_1$(0.7077A) and Cu $K\alpha_1$(1.537A). The rocking curves obtained are shown in the figures. They are plotted on the same scale with first order curves in Figure 1, and second order curves in Figure 2. The results are also given in Table I. The coefficient

[1] Bergen Davis and W. M. Stempel, Phys. Rev. **17**, 608 (1921).

of reflection is the value of $E\omega/I$. The unit of angle is one degree of arc. The intensity I of the beam coming from crystal A is obtained by throwing crystal B back out of direct path of beam and allowing it to enter the ionization

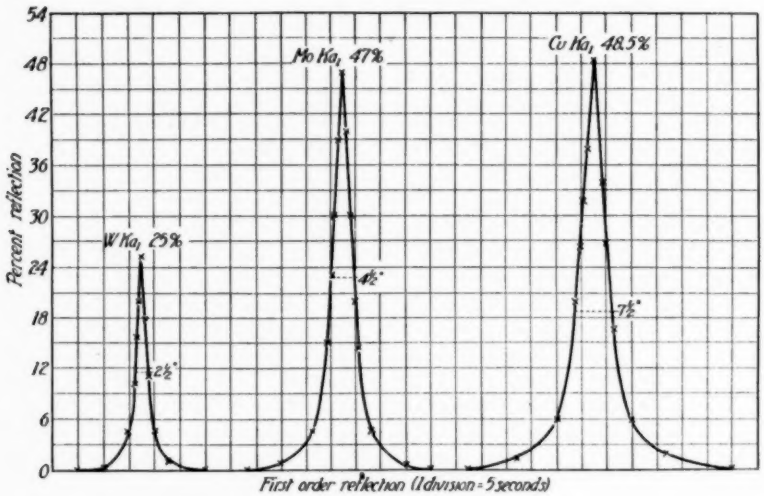

Fig. 1. Rocking curves, first order.

chamber. The term $E\omega$ which is the integrated intensity after reflection from crystal B is often obtained by the method of sweeps. In the present instance it was obtained directly from the rocking curves by a method previously

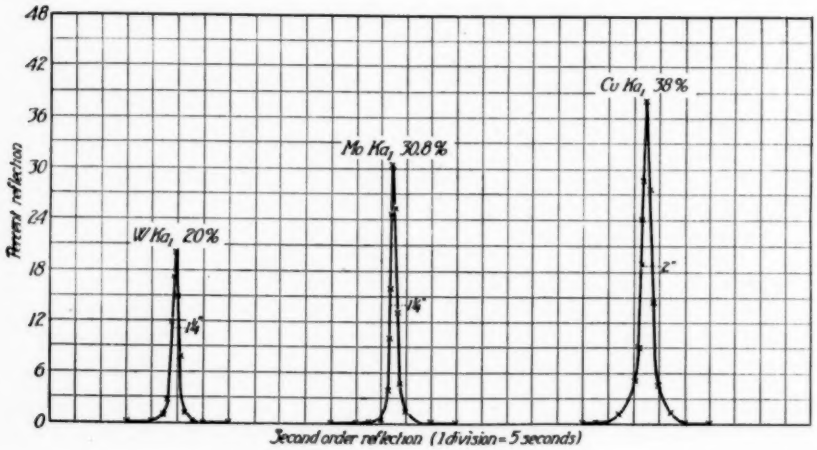

Fig. 2. Rocking curves, second order.

described.[2] The percent reflection is the ratio of the intensity from crystal A to that from crystal B, when B is in the position of maximum reflection. In the next column is given the observed width at half-maximum of the rock-

[2] Bergen Davis and H. M. Terrill, Phil. Mag., Vol. XLV, March, 1923.

ing curves in seconds of arc. If the width depends on some property of the crystals it will be present equally in both crystals. Each crystal will contribute to the width. This contribution, however, is not directly additive. A reasonable method of correction has been given by Ehrenberg and Mark[3] and by M. Schwarzschild.[4] The contribution of crystal A to the width observed from crystal B is the factor $2^{1/2}$. The corrected width given in the last column is obtained by dividing the observed width by $2^{1/2}$. This column should represent the actual width of rocking curve due to crystal B when a strictly parallel beam is reflected from it.

TABLE I.

λ	Order	Coef. R	Percent R	Width (seconds)	Corrected width
0.209A	1	0.00026	25	2.5	1.78
	2	0.0001	20	1.25	0.9
0.7077	1	0.00035	47	4.5	3.2
	2	0.0001	31	1.25	0.9
1.537	1	0.0011	48.5	7.5	5.4
	2	0.00022	38	2	1.67

The structure factor:—An expression for the width of rocking curve for reflection from a perfect crystal has been derived by C. G. Darwin.[5] It has the form (for unpolarized rays)

$$\Delta\Theta = \frac{4}{3\pi} nF \frac{e^2}{mc^2} \lambda^2 \cot\theta,$$

where n is the number of molecules per cc, θ is the angle of reflection, and F is the term known as the structure factor. It represents the effect of distribution of electrons on the reflection. If the electrons belonging to a molecular layer all lie in one plane $F=Z$, where Z is the number of electrons in a molecule. As used here $Z=50$ for a calcite crystal.

The values of the structure factors for the constituents of calcite have been experimentally determined by the powdered crystal method. We are indebted to Dr. R. W. G. Wyckoff and Miss Alice H. Armstrong, of the Rockefeller Institute for Medical Research, for advanced unpublished values of F for oxygen and carbon. The values of F for calcium are taken from Havighurst.[6] The structure factor is a constant function of $\sin\theta/\lambda$ and has the same value for all wave-lengths but depends on the order of reflection. These values of the structure factor are designated by F_1 in the third column of Table II. The next column of the table gives the widths calculated by the

[3] Ehrenberg and Mark, Zeits. f. Physik **42,** 807 (1927).
[4] M. Schwarzschild, Phys. Rev. **32,** 1928.
[5] A. H. Compton, X-rays and Electrons, p. 141.
[6] R. J. Havighurst, Phys. Rev. **28,** 869 (1926).

Darwin equation for $F=Z$. The last column gives the widths for $F=F_1$. This column ($F=F_1$) is to be compared to the last column of Table I. It will be noticed that the observed widths are less than the calculated values for a perfect crystal except in the case of W $K\alpha_1$(0.209A).

TABLE II.

λ	Order	F_1	Calculated width $F=z$	$F=F_1$
0.209A	1	25.1	2.55″	1.28″
	2	11	1.27	0.28
0.7077	1	25.1	8.6	4.3
	2	11	4.2	0.92
1.537	1	25.1	17.2	8.6
	2	11	12.3	2.7

The crystals, however, can not be regarded as perfect. The percent reflection does not rise to a greater value than 48.5 percent in any case, while theory predicts 100 percent reflection for a perfect crystal. The observed widths for W $K\alpha_1$ are greater than is to be expected from theory. The experimental difficulties were much greater at this small wave-length. The glancing angle is quite small. It was difficult to exclude the scattered radiation from the ionization chamber.

The resolution that is to be expected with the double x-ray spectrometer is about the same order of magnitude as the width of rocking curves with parallel crystals. Fine structure in spectral lines should be measureable to this degree of refinement provided the natural breadth is not greater than this. Also the natural breadth of a spectral line can be measured to this small angle provided it contains no fine structure. This may be illustrated by the case of second order reflection for wave-lengths near the Mo $K\alpha_1$, where the width is one second of arc. The resolution is given by $2\Delta\lambda = 2d\cos\theta_2\, d\theta_2$. If $d\theta_2 = 1''$ arc, the measureabie fine structure will be 0.015X-units. Also the breadth of a spectral line may be measured to 0.015 X-units, which is much less than the classical breadth of 0.12 X-units.

We wish to express our appreciation of the trouble taken by Miss Alice H. Armstrong in preparing for us the structure factor data used in this article.

THE ARC SPECTRUM OF PLATINUM

By J. J. Livingood
Palmer Physical Laboratory, Princeton University

(Received May 24, 1929)

Abstract

Eight new levels and forty-four new combinations have been found in Pt I. Fifty-six new lines have been measured in the ultra-violet. An examination of the *Zeeman effect* and the subsequent determination of the g-values for most of the terms has permitted a reasonable interpretation of many levels. Low structures are d^9s, d^8s^2 and d^{10}; middle terms arise from d^9p and d^8sp; high configurations are $d^9 \cdot s$, $d^8s \cdot s$, with an indication of $d^8s \cdot d$. Quintet terms appear in the middle and high sets. From the failure of the intensity and interval rules and the irregularity of the g-values, it is evident that the Russell-Saunders coupling has almost completely broken down, as is to be expected from the position of platinum in the periodic table. There is only an approximate similarity with the theoretically analogous spectrum of Ni I. Ionization potentials are approximately calculated as 8.9 volts for d^9s to d^9 and 9.7 volts for d^9s to d^8s.

THE platinum arc spectrum has received attention from a number of investigators. The more recent contributions are wave-length determinations in the visible by Meggers,[1] the discovery of many of the term values by McLennan and McLay,[2] the examination of the absorption spectrum in the under water spark by Meggers and Laporte,[3] and a more comprehensive analysis with the aid of the Zeeman effect by Haussmann.[4] The purpose of the present investigation was the discovery of new levels, the classification of more lines, further wave-length measurements in the ultra-violet and the determination of g-values from Zeeman effects for as many of the levels as possible in order to add to the knowledge of the types of terms involved.

The present paper lists 8 new levels, 44 newly classified lines, 41 remeasured and 56 newly measured lines. The g-values for almost all the eighty terms have been found, aiding considerably in their classification. The conclusion of the previous investigators has been confirmed that the outer electron structures are d^{10}, d^8s^2 and d^9s for the low terms, and evidence is presented that the middle terms are due to d^9p and d^8sp, while the high terms come from $d^9 \cdot s$, $d^8s \cdot s$ and probably $d^8s \cdot d$, in conformity with the predictions of Hund. As is to be expected from the position of platinum in the periodic table, the interval rule is found to be useless, the g-values depart very markedly from the Landé values (although the g-sums, where it is possible to form them, are correct within experimental error) and the intensity rules are satisfied only very approximately.

[1] W. F. Meggers, Scientific Papers, Bur. of Standards **20**, No. 499 (1925).
[2] J. C. McLennan and A. B. McLay, Trans. Royal Soc. of Canada, (3rd series) **20**, (1926).
[3] W. F. Meggers and O. Laporte, Phys. Rev. **28**, 642 (1926).
[4] A. C. Haussmann, Astrophys. J. **66**, 333 (1927).

Experimental Procedure

A Hilger E1 quartz spectrograph was employed, with Cramer Contrast and Hilger Schumann plates. Rods of extremely pure platinum were used as electrodes in photographs for wave-length determinations. Arc and spark pictures were taken, to assist in classification. It was found necessary to use a mechanical vibrator, for with a steady arc in air the cathode became red hot in several seconds and the arc flared up and out. At 250 volts and an arc current of 1½ amperes, exposures ranged from a few seconds for lines near the visible to one and a half hours for those around λ1900.

Zeeman effect photographs were taken from λ3408 to 2043 with the same instrument and an electromagnet giving a field of about 34700 gauss with pole faces 10 mm in diameter separated by a 3 mm air gap. A platinum wire fused into a bead at the end, attached to the vibrator arm, served as cathode, the anode being a copper plate clamped against one of the pole pieces. This arrangement was found to give the easiest running arc in the magnetic field, and only a few copper lines appeared on the plates. The separation of Cu λ2442 ($^2S-{}^4P_{1/2}$) was used to determine the field, all other exposures in different ranges of the spectrograph being taken under identical conditions. Measurements of Cu λ2356 and 2276, whose Zeeman patterns could be simply calculated, were consistent with the choice of the field constant. A current of 1 ampere at 115 volts was used for the Zeeman pictures, the exposures lasting from three minutes to an hour. A quartz double image prism separated the parallel and perpendicular components of the patterns.

Haussmann's wave-lengths above λ4498 were taken from Meggers's paper, and below that from Kayser's Tables, with Exner and Haschek's values where Kayser listed no lines. In continuing the search to allocate lines, the author has preferred Exner and Haschek's values rather than Kayser's. The wave-length and intensity of most of the lines below λ2200 classified by Haussmann were taken from measurements made by Meggers and Laporte, and it was seen that the listed wave-numbers were consistenly higher than the combination of terms predicted, the greatest error of over two units occurring at the short wave-length end of the list. Consequently, all the lines from λ2246 to 2039 have been remeasured by the author, with copper arc and spark lines for standards, since their wave-numbers have been fixed to within about two tenths of a unit by Shenstone's use of the combination principle.[5] From λ2039 to 1911 the silver spark was used for comparison, with wave-numbers supplied in a private communication from C. W. Gartlein of Cornell University. The new measurements are in much better agreement with the computed wave-numbers.

Zeeman Effect Analysis

Of the 225 arc lines examined for Zeeman effect, the vast majority appeared as triplets only, due to the low resolving power of the instrument. However, fairly accurate determinations of the g-values from these "blends" were

[5] A. G. Shenstone, Phys. Rev. **29**, 380 (1927).

possible by the use of formulae developed by A. G. Shenstone[6] from considerations of the intensities of the various lines in the parallel and perpendicular components. It is shown that $2\sigma = g_x(J_x+1) - g_yJ_y$, where $J_x = J_y+1$ and σ is the separation of the "center of gravity" of the blend from the normal (undeviated) position, in terms of the Lorentz separation as unity. For $J_x = J_y$ the center of gravity lies of course at $2\sigma = g_x+g_y$. For the π components, separated blends occur only when $J_x = J_y$; the ratios of the intensities follow a somewhat more complicated law and Shenstone has shown that the separation of the center of gravity from the normal (again measured on the basis of the Lorentz displacement) is given by $(g_x-g_y)\{1+C(J-1)\}$ for odd multiplicity, and by $(g_x-g_y)\{\frac{1}{2}+C'(J-\frac{1}{2})\}$ for even multiplicity. C and C' are complicated functions of J, and a table is appended giving their numerical magnitudes for various values of J. Both these expressions can be reduced to a single more convenient form by substituting in the values of C,C' and J. The result is that the separation of the center of gravity of the π components from the normal position is given by $\pi = k(g_x-g_y)$, where

Even Multiplicity				Odd Multiplicity			
for $J=\frac{1}{2}$	$k=0.50$	$J=3\frac{1}{2}$	$k=2.96$	for $J=1$	$k=1.00$	$J=4$	$k=3.34$
$1\frac{1}{2}$	1.40	$4\frac{1}{2}$	3.70	2	1.80	5	4.08
$2\frac{1}{2}$	2.18	$5\frac{1}{2}$	4.45	3	2.58	6	4.85
						7	5.56

Haussmann's Zeeman patterns were almost always somewhat greater in value than the author's determinations and in many cases were quite self-inconsistent. These may be the patterns "perturbed so that they were no longer symmetrical," mentioned by him. In as much as the author's measurements are much more self-consistent, it is probable that with the greater dispersion of Haussmann's gratings, the components were separated in some cases to such an extent (though still unresolved) that the cross hairs of the comparator would be set nearer to the strongest line than to the center of gravity, and hence the pattern would be amenable neither to a "completely resolved" or a "blended" analysis. Particularly bad disagreements in measurement were found in the lines λ2929, 2830 and 2677, for which Haussmann gave the patterns (0)1.64, (0)1.52 and (0)1.71 respectively, while the author obtained (0)1.27, (0)1.37 and (0)1.50. The use of Haussmann's values in such cases gave g-values quite at variance with other determinations, whereas the author's measurements fitted in very nicely. Among the longer wavelengths above the author's range, some of Haussmann's patterns had to be discarded as they could not be interpreted at all; for example, (0) 1.20, 1.80 for λ3638 and (.36) 1.41, .92 for λ4164. He gives (.44) $\overline{1.27}$, 1.61 for λ3699, and assuming g-values of 1.20 and 1.40 from other combinations, calculates the pattern (.20, .$\overline{40}$,) 1.00, $\overline{1.20}$, $\overline{1.40}$, 1.60, which is not at all in accord with his observation.

No attempt was made in the present paper to determine both g's involved in each of the several completely resolved patterns. Instead, g's were as-

[6] To appear in Phil. Mag.

sumed to have Landé values for those levels of which there was but one with a given J in the whole number of levels due to any particular electron structure; i.e., the g-sum rule was applied to those cases where there was but one item in the sum. This procedure gave five unambiguous g-values among the low terms. Then by applying the blend formulae to lines involving these terms, other g's could be found and averages finally taken.

Notation

The notation used in this paper is that recently adopted by an informal committee, consisting of H. N. Russell, A. G. Shenstone and L. A. Turner, appointed at a meeting of the Physical Society last spring.[6a]

The type of term is denoted by the customary $SPD\cdots$ corresponding to the quantum numbers $L=0\ 1\ 2\cdots$. The multiplicity is given by a superscript to the left and the J value by a subscript at the right. Terms for which the l-sum of the component electrons is odd (an odd number of p and f electrons) are followed by the superscript°; those for which the l-sum is even (an even number of p and f electrons) have no such index. Thus the present notation is

$$\text{Even terms } S\ P\ D\ F\cdots$$
$$\text{Odd terms } S^\circ\ P^\circ\ D^\circ\ F^\circ\cdots$$

replacing the older usage of $S\ P'\ D\ F'$ for even and $S'\ P\ D'\ F$ for odd terms.

The arbitrary numerical designation given by Haussmann to unidentified middle group terms is in conformity with the suggestions of the committee and so is retained, except that the "°" has been added. Haussmann's arbitrary capital letters to indicate unclassified high terms are not in strict accord with the committee's recommendations, but the usage is continued in this paper as a change would be unnecessarily confusing.

Among the low terms the arbitrary label "a" is prefixed to each of the different levels; "b", "c", "d", to the following higher terms of the same S, L and J. Similarly, the middle group levels are marked z, y, x in succession, and the high group levels e, f, g.

Electron structure in the outermost shells is given by, e.g., $5d^8\ 6s^2$, the letter indicating the type of electron, the prefix its total quantum number and the superscript the number of electrons of that type present. As an abbreviation, a dot before a letter indicates that the total quantum number of the electron is greater than it is when the electron is in its lowest state.

It seems unnecessary to repeat the wave-length, frequency, intensity and term combination list given by Haussmann, as the changes made by this analysis are almost all in the designation given the various levels. Table I gives the complete list of all terms known in Pt I, with Haussmann's arbitrary and suggested designations and in addition the author's identifications and the probable electron structures. To indicate the reality of the terms, the numbers of combinations they make are also included. The most probable g-values, obtained by averaging, as explained above, are given, as well as the theoretical Landé values. The number of π and σ components from which the g's were averaged and the mean deviation of the

[6a] H. N. Russell, A. G. Shenstone and L. A. Turner, Phys. Rev. **33**, 900 (1929).

TABLE I. *Terms of Pt I. New terms marked*.*

ν (Vac.)	Author's suggested Structure	Author's sugg. desig.	Arbit. designation	Hauss. designation	No. of comb.	g obs.	g Landé	No. of comp. for g	Mean dev. of g
0.0	$5d^96s$	a^3D_3		$^3D_3$	26	(1.33)			
775.9	$5d^96s$	a^3D_2		a^1D_2	29	1.01	1.17	4	0.03
823.7	$5d^86s^2$	a^3F_4		$^3F_4'$	20	1.25	1.25	5	.02
6140.0	$5d^{10}$	a^1S_0		$^1S_0$	8	(0/0)			
6567.5	$5d^86s^2$	a^3P_2		$^3D_2$	34	1.12	1.50	6	.05
10116.8	$5d^86s^2$	a^3F_3		$^3F_3'$	28	(1.08)			
10132.0	$5d^96s$	a^3D_1		$^3D_1$	25	(.50)			
13496.3	$5d^96s$	a^1D_2		$^3P_2'$	35	1.17	1.00	5	.02
15501.8	$5d^86s^2$	a^3F_2		$^3F_2'$	35	.92	.67	6	.00
18566.5	$5d^86s^2$	a^3P_1		$^3P_1'$	21	(1.50)			
21967.1	$5d^86s^2$	a^1G_4		$^1G_4$	12	1.+?	1.00	3	.13
26638.6	$5d^86s^2$	b^1D_2		b^1D_2	15	.97	1.00	7	.03
*30157.0	$5d^86s6p$	$z^5D_4^\circ$	46_4°		6	1.46	1.50	2	.01
32620.0	$5d^96p$	$z^3P_2^\circ$	1_2°	D_2	12	1.39	1.50	3	.02
33680.5	$5d^86s6p$	$z^5G_5^\circ$	2_5°	G_5	7	1.32	1.27	1	
34122.1	$5d^96p$	$z^3F_3^\circ$	3_3°	F_3	13	1.21	1.08	6	.01
35321.7	$5d^86s6p$	$z^5D_3^\circ$	4_3°	D_3 or F_3	13	1.33	1.50	4	.03
*36781.6	$5d^86s6p$	$z^5G_6^\circ$	47_6°		2	1.33	1.33	1	
36844.7	$5d^86s6p$		5_1°	D_1	10	1.09		5	.05
37342.1	$5d^86s6p$		6_2°	D_2	18	1.15		3	.01
37590.7	$5d^96p$	$z^3F_4^\circ$	7_4°	F_4	11	1.25	1.25	2	.02
37769.0	$5d^86s6p$		8_3°	D_3	16	1.17		4	.10
38536.2	$5d^86s6p$	$z^5F_5^\circ$	9_5°	G_5	8	1.30	1.40	1	
38815.9	$5d^96p$	$z^3D_2^\circ$	10_2°	F_2	13	.88	1.17	3	.03
40194.2	$5d^86s6p$	$z^5F_4^\circ$	11_4°	F_4	11	1.21	1.35	2	.00
40516.3	$5d^86s6p$	$z^5D_2^\circ$	12_2°	D_2	13	1.38	1.50	5	.02
40787.9	$5d^86s6p$		13_2°	D_2	11	1.20		5	.07
40873.5	$5d^86s6p$		14_0°	P_0	3		0/0		
40970.1	$5d^96p$	$z^3D_3^\circ$	15_3°	F_3	19	1.12	1.33	5	.02
41802.7	$5d^96p$	$z^3P_1^\circ$	16_1°	P_1	8	.92	1.50	4	.07
42660.2	$5d^86s6p$		17_3°	D_3	14	1.19		4	.01
43187.8	$5d^86s6p$		18_1°	P_1 or D_1	11	1.39		4	.11
43945.7	$5d^86s6p$		19_3°	D_3 or F_3	8	1.21		3	.03
44432.7	$5d^86s6p$		20_4°	F_4	7	1.20		2	.01
44444.4	$5d^96p$	$z^3F_2^\circ$	21_2°	D_2	9	1.21	.67	5	.02
44730.3	$5d^86s6p$		22_3°	F_3	15	1.19		5	.04
45398.4	$5d^86s6p$	$z^5D_1^\circ$	23_1°	P_1	6	1.52	1.50	1	
*46007.3	$5d^86s6p$	$z^5D_0^\circ$	48_0°		2		0/0		
46170.4	$5d^86s6p$		24_2°	D_2	11	1.01		6	.12
46419.4	$5d^86s6p$		25_2°	D_2	11	.87		4	.05
46433.9	$5d^96p$	$z^3P_0^\circ$	26_0°	P_0	3		0/0		
46622.5	$5d^86s6p$		27_3°	F_3	12	1.15		6	.01
*46793.9	$5d^86s6p$		49_2°		3				
46965.1	$5d^86s6p$		28_4°	G_4	5	1.34		1	
47740.6	$5d^86s6p$	$y^3P_1^\circ$ or $^5D_1^\circ$	29_1°	P_1 or D_1	10	1.43	1.50	2	.01
48351.9	$5d^86s6p$		30_4°	G_4	3	1.25		2	.02
48535.6	$5d^86s6p$		31_2°	P_2	8	1.02		2	.05
48779.3	$5d^86s6p$		32_3°	D_3	7	1.22		3	.01
49286.1	$5d^96p$	$z^1F_3^\circ$	33_3°		9	1.19	1.00	6	.04
49544.5	$5d^96p$	$z^1P_1^\circ$	34_1°		7	1.24	1.00	2	.01
49880.8	$5d^86s6p$		35_2°		7	1.12		5	.06
50055.3	$5d^96p$	$z^3D_1^\circ$	36_1°		8	.87	.50	3	.01
*51097.5	$5d^86s6p$		50_3°		6	1.21		3	.02
51286.9	$5d^96p$	$z^1D_2^\circ$	37_2°		8	1.13	1.00	2	.02
51545.5	$5d^86s6p$		38_2°		5	1.25		3	.17
51752.3	$5d^86s6p$		39_2°		5	1.34		4	.02
52071.6	$5d^86s6p$		40_1°		5	1.22		4	.03
52379.3	$5d^97s$	e^3D_2	A_2		9	1.32	1.33	2	.00
52667.2	$5d^97s$	e^3D_2	B_2		8	1.04	1.17	1	
52708.3	$5d^86s6p$	$y^3P_2^\circ$ or $^5D_2^\circ$	41_2°		5	1.46	1.50	3	.02

TABLE I. (continued)

ν (Vac.)	Author's suggested Structure	Author's sugg. desig.	Arbit. designation	Hauss. designation	No. of comb	g-obs.	g Landé	No. of comp. for g	Mean dev. of g
53019.2	$5d^56s6p$		42_1°		6	1.08		4	.08
53955.3	$5d^56s6p$		43_2°		5	1.32		3	.01
54839.2	$5d^56s6p$		44_2°		4	1.21		3	.01
55216.8	$5d^56s6p$		45_1° or 2		4	.96		4	.12
55640.7	$5d^56s7s$	e^5F_5	C_5		5	1.41	1.40	2	.01
56784.4	$5d^56s7s$	e^5F_4	D_4		11	1.27	1.35	4	.05
*59731.5			Q_3		10	1.3		1	
59751.2			E_3		7				
59764.3	$5d^56s7s$	e^5F_3	F_3		10	1.27	1.25	6	.12
59782.8			G_1		8	1.07		2	.01
59872.1			H_3		8	1.23		3	.04
59882.4			I_4		7	1.17		2	.01
59908.1			J_2		7	1.02		2	.03
60357.8	$5d^97s$	e^3D_1	K_1		8	.52	.50	4	.04
60640.6	$5d^97s$	e^1D_2	L_2		13	1.08	1.00	3	.03
60790.4			M_3		11	1.07		4	.02
60884.0			N_4		9	1.29		3	.01
*64129.1			$R_{4 \text{ or } 5}$		3				
*64141.3	$5d^56s6d$	e^5G_6 or $^5H_6$	T_6		3				
64505.9			O_4		7				

Terms	g-sums obs.	g-sums Landé	Terms	g-sums obs.	g-sums Landé
d^9s			d^9p		
$J=2$	2.18	2.17	$J=1$	3.03	3.00
d^8s^2			$J=2$	4.61	4.34
$J=2$	3.01	3.17	$J=3$	3.52	3.41
$J=4$	2.25?	2.25	$d^9 \cdot s$		
			$J=2$	2.12	2.17

TABLE II. *Newly classified lines*. Remeasured lines. New lines ‡.*

λ (Air)	Int.	Auth.	ν (Vac.)	Combination	ν obs. − ν calc.
*7830.45	1	M	12767.3	$28_4^\circ - Q_3$	0.9
*7626.27	1	M	13109.0	$27_3^\circ - Q_3$	.0
*7257.76	1u	E	13774.6	$48_6^\circ - G_1$	−.9
*7094.77	7	M	14091.0	$49_3^\circ - N_4$	.9
*6332.88	0	M	15786.2	$19_3^\circ - Q_3$	.4
*5328.60	2	M	18761.4	$15_3^\circ - Q_3$	.0
*5301.02	25	M	18859.1	$47_6^\circ - C_5$	.0
*5117.49	1	E	19535.4	$11_4^\circ - Q_3$	−1.9
*4551.94	3	M	21962.5	$8_3^\circ - Q_3$	.0
*4498.75	20	M	22222.2	$46_4^\circ - A_3$	−.1
*4465.13	1	E	22389.5	$6_2^\circ - Q_3$	.1
*3922.97	10	E	25483.6	$46_4^\circ - C_5$	−.1
*3906.27	1	E	25592.6	$9_5^\circ - R_{4,5}$	−.3
*3904.39	2	E	25605.0	$9_5^\circ - T_6$	−.1
*3903.70	2	E	25609.5	$3_3^\circ - Q_3$	.1
*3687.46	4	E	27111.2	$1_2^\circ - Q_3$	−.3

TABLE II. (continued)

λ (Air)	Int.	Auth.	ν (Vac.)	Combination	ν obs.−ν calc.
*3654.00	1	E	27359.5	$47_6^\circ - T_6$	−.2
*3643.17	5	E	27440.8	$a^3P_1 - 48_0^\circ$	.0
*3431.86	2	E	29130.4	$a^1G_4 - 50_3^\circ$	.0
*3408.13	15	E	29333.2	$a^3F_4 - 46_4^\circ$	−.1
*3315.03	8	E	30156.9	$a^3D_3 - 46_4^\circ$	−.1
*3283.26	4	E	30448.8	$2_5^\circ - R_{4,5}$	.2
*3281.96	5	E	30460.9	$2_5^\circ - T_6$	.1
*3002.26	10	E	33298.6	$a^1D_2 - 49_3^\circ$ $a^3F_4 - 3_3^\circ$	1.0 .2
*2942.77	4	E	33971.7	$46_4^\circ - R_{4,5}$	−.4
*2910.46	1	E	34348.8	$46_4^\circ - O_4$	−.1
*2808.49	2	E	35595.9	$a^3F_2 - 50_3^\circ$	.2
*2658.69	2	E	37601.3	$a^1D_2 - 50_3^\circ$	.1
*2614.61	1	E	38235.2	$a^3F_3 - 30_4^\circ$	.1
*2439.45	1	K	40980.4	$a^3F_3 - 50_3^\circ$	−.3
*2244.93	8	L	44531.0	$a^3P_2 - 50_3^\circ$	1.0
‡2241.20	4	L	44605.0		
†2240.31	3	L	44622.7	$a^3D_2 - 23_1^\circ$	.2
‡*2235.46	3	L	44719.6	$a^3P_2 - 37_2^\circ$	.2
2234.91	8	L	44730.6	$a^3D_3 - 22_3^\circ$	.3
‡2227.53	2	L	44892.7		
‡2224.51	4	L	44939.7		
2222.60	8	L	44978.4	$a^3P_2 - 38_2^\circ$	.4
2217.33	7	L	45085.2	$a^3D_1 - 45_{1,2}^\circ$	.4
‡2213.93	3	L	45154.5		
‡2208.77	2	L	45260.0		
2202.20	8	L	45394.9	$a^3D_2 - 24_2^\circ$	.4
2201.08	7	L	45418.1		
‡2199.68	5	L	45446.9		
2196.90	5	L	45504.5	$a^3P_2 - 40_1^\circ$	.4
‡2192.49	3	L	45595.9		
‡2190.78	5	L	45631.5		
2190.16	6	L	45644.5	$a^3D_2 - 25_2^\circ$	.5
‡2188.33	2	L	45682.7		
2182.76	6	L	45799.1	$a^3F_4 - 27_2^\circ$	.3
2180.49	8	L	45846.9	$a^3D_2 - 27_2^\circ$	.3
‡2180.31	6	L	45850.7		
‡*2176.46	3	L	45931.7	$a^1S_0 - 40_1^\circ$	.1
*2174.64	10	L	45970.2	$a^3F_4 - 49_3^\circ$	.0
‡2170.71	4	L	46053.4		
‡2169.25	5	L	46084.3		
2166.62	6	L	46140.3	$a^3P_2 - 41_2^\circ$ $a^3F_4 - 28_4^\circ$	−.5 −1.1
2165.14	9	L	46171.8	$a^3D_3 - 24_2^\circ$	1.4
‡2164.28	3	L	46190.2		
2153.54	8	L	46420.6	$a^3D_3 - 25_2^\circ$	−.7
‡2153.38	2u	L	46423.9		
2152.07	6	L	46452.3	$a^3P_2 - 42_1^\circ$	.6
2150.64	5	L	46483.1		
‡2147.38	2	L	46553.6		
‡2145.02	6	L	46604.8		
2144.22	10	L	46622.2	$a^3D_3 - 27_3^\circ$	−.3
2135.15	5	L	46820.4		
‡2134.62	3	L	46831.9		
‡*2132.46	2	L	46879.4	$a^1S_0 - 42_1^\circ$	.2
‡2131.07	2	L	46910.0		
2128.62	8	L	46963.9	$a^3D_2 - 29_1^\circ$ $a^3D_3 - 28_4^\circ$	−.8 1.2
2122.56	5	L	47097.9		
‡2119.88	4	L	47157.5		
‡2114.22	2	L	47283.8		

TABLE II. (continued)

λ (Air)	Int.	Auth.	ν (Vac.)	Combination	ν obs.−ν calc.
*2109.65	7	L	47386.2	$a^3P_2-43_2°$	−1.6
2109.49	6	L	47389.7		
‡2103.48	2u	L	47525.2		
2103.33	6	L	47528.5	$a^3F_4-30_4°$	.3
‡2101.64	5	L	47566.7		
‡2098.75	3	L	47632.3		
‡2097.30	3	L	47665.2		
‡2095.45	2	L	47707.1		
‡2094.71	1	L	47724.1		
‡2094.00	1	L	47740.4		
‡2088.97	4	L	47855.3		
‡2088.32	5	L	47870.0		
2084.62	7	L	47955.0	$a^3F_4-32_3°$	−.6
‡2084.36	3	L	47961.0		
2083.38	5	L	47983.6		
2082.55	5	L	48002.7	$a^3D_2-32_3°$	−.7
‡2076.25	2	L	48148.4		
2073.62	3	L	48209.5		
2070.96	6	L	48271.3	$a^3P_2-44_3°$	−.4
‡2070.36	1	L	48285.2		
2067.53	5	L	48351.4	$a^3D_3-30_4°$	−.5
2066.95	4	L	48364.9		
2062.81	5	L	48462.0	$a^3F_4-33_3°$	−.4
2060.78	5	L	48509.7	$a^3D_2-33_2°$	−.5
2059.70	3	L	48535.1	$a^3D_3-31_2°$	−.5
‡2058.42	1	L	48565.4		
‡*2049.84	3	L	48768.5	$a^3D_2-34_1°$	−.1
2049.38	6	L	48779.6	$a^3D_3-32_3°$	.3
‡2041.47	1	L	48968.6		
2040.33	3	L	48995.9		
2039.70	3	L	49011.1		
2036.46	8	L	49089.0		
2035.79	4	L	49105.2		
2032.42	5	L	49186.5		
2030.64	6	L	49229.5		
‡*2028.58	2	L	49279.6	$a^3D_2-36_1°$	.2
‡*2028.32	1	L	49285.9	$a^3D_3-33_3°$	−.2
‡2025.86	2	L	49345.7		
‡2024.63	1	L	49375.8		
‡2020.90	2	L	49467.1		
‡2016.72	1	L	49569.3		
‡*2004.13	3	L	49880.7	$a^3D_3-35_2°$	−.1
λ (Vac.)					
‡1995.91	3	L	50102.5		
‡1991.59	2	L	50211.2		
‡*1989.11	2	L	50273.7	$a^3F_4-50_3°$	−.1
‡1987.79	1	L	50307.4		
‡*1979.78	2u	L	50510.7	$a^3D_2-37_2°$	−.3
‡*1969.69	2	L	50769.5	$a^3D_2-38_2°$	−.1
‡1963.17	1	L	50938.3		
‡1949.92	1	L	51284.1		
‡*1949.81	1	L	51287.0	$a^3D_3-37_2°$	.1
‡1929.25	3	L	51833.5		
‡1928.85	1	L	51844.4		

E—Exner and Haschek.
K—Kayser.
L—Author.

† By some mistake Haussmann gave to $a^3D_2-23_1°$, instead of the value here shown, the wave-length 2245.51, which is a strong spark line.

various values from their average are given in the last two columns to give an estimate of the reliability. The five low term g-values that were assumed to have Landé values, as explained before, are given in parentheses. New levels found in the present investigation are marked with an asterisk. Table II gives the newly classified lines, and all the lines remeasured below λ2246, including 64 hitherto not observed. The author's intensity estimates are on the basis of 10 as maximum. Levels are referred to by their arbitrary symbols, except for the lower group, where the author's suggested names are used.

Term Designation

McLennan and McLay were of the opinion that the lowest term in the platinum arc spectrum was of the triplet F type, by analogy with the analysis by Bechert and Sommer[7] of the nickel arc, to which the spectrum of platinum should be similar. On that assumption they assigned tentative L-values and multiplicities to the twelve low terms. Shortly thereafter, Meggers and Laporte published their work on the absorption spectrum, but by considerations of the general dependence of level separations on atomic number they were led to a different assignment of L-values, so that the lowest state was named $^3D_3$. Haussmann, from a study of Zeeman patterns, reached the conclusion that the designations suggested by Meggers were preferable to those of McLennan.

The present analysis offers three changes in the names of the low terms and suggests designations for many of the middle and high terms, as well as assigning electron structures in most cases. Considerable assistance was received from a very complete analysis of Ni I recently made by H. N. Russell, confirming and amplifying the results of Bechert and Sommer.

According to Hund's theory the low group (even) structures of platinum and their resulting terms should be $5d^{10}\ ^1S_0$; $5d^9 6s\ ^3D_{321}\ ^1D_2$; $5d^8\ 6s^2\ ^3F_{432}\ ^3P_{210}\ ^1G_4\ ^1D_2\ ^1S_0$. Haussmann made an identification of all these with the exception of one $^1S_0$ and the $^3P_0$. The author has made a very thorough search and has also been unable to detect any terms to which these two designations might be applied. It seems probable that the missing $^1S_0$ is from d^8s^2, since that term from such a structure never has been definitely found in other spectra.

It was first pointed out by Grotrian[8] and later shown more extensively by Laporte[9] and by Goudsmit's[10] use of the Γ sum rule, that the total separation of the triplet arising from d^9s or p^5s is (neglecting a small correction in the screening) the same as that of the doublet of the ion d^9 or p^5 of the same atom. The separation of the doublet follows the x-ray regular doublet law of Sommerfeld:

[7] Bechert and Sommer, Bayr. Akad. **7**, 9 (1925).
[8] W. Grotrian, Zeits. f. Physik **8**, 116 (1922).
[9] O. Laporte, Phys. Rev. **29**, 650 (1927).
[10] S. Goudsmit, Phys. Rev. **31**, 496 (1928).

$$\Delta\nu = \frac{R\alpha^2(Z-\sigma)^4}{n^3 l(l+1)}$$

where $R\alpha^2$ is a universal constant, n and l are quantum numbers of the d or p electron lacking from the closed shell d^{10} or p^6, and σ is an empirical screening number depending on n and l but only slightly on the atomic number Z. Goudsmit and Back[11] showed that in the case of the configuration ps the singlet and triplet merge into two pairs of levels, as one considers successively Si $3p4s$, $Z=14$; Sn $5p6s$, $Z=50$; Pb $6p7s$, $Z=82$; i.e., that the triplet separation increases greatly with increasing atomic number and that the relative distance of the singlet from the nearest member of the triplet, compared to the separation of the triplet itself, decreases as Z increases. Recent work by J. E. Mack[12] confirms this, in a study of the d^9s configuration in the spectra of Ni I PdI Pt I, Cu II Ag II Au II, Zn III Cd III Hg III, Ga IV In IV Tl IV, and Ge V Sn V Pb V. Hence it appears that in platinum the structure $5d^96s$ should give $^3D_3$ and $^3D_2$ close together, with $^3D_1$ and $^1D_2$ considerably higher and also near each other. On the basis of the above considerations and the fact that Shenstone[5,13] had found in the $d^9 \cdot ns$ series of Ni I, Cu II, Pd I and Ag II that the $^3D_2$, rather than $^1D_2$, closes in on $^3D_3$, the term at 775.9 in Pt I was changed [14] from Haussmann's designation of $^1D_2$ to $^3D_2$. The present paper suggests the further alteration of the level at 13496.3 from $^3P_2$ to $^1D_2$ to make the assignment conform with the arguments given above. It is true that these names, $^3D_2$ and $^1D_2$, if turned about, would give g-values almost exactly in accord with Landé's predictions, but as the g's throughout the rest of the spectrum are decidedly irregular, it seems plausible that such an agreement is fortuitous. With the present arrangement, the g's for the $J=2$ levels in $5d^96s$ are irregular, but their sum of 2.18 is in good agreement with the Landé sum 2.17.

This assignment means that the term at 6567.5 must be called $5d^86s^2\ ^3P_2$. The g-sum for $J=2$ from this structure comes out as 3.01, differing from the Landé sum of 3.17 by 5 percent, which is about the limit of accuracy to be obtained from these blended patterns. The observed g-value of $5d^8 6s^2\ ^3F_4$ is 1.25, exactly the Landé value, so that $^1G_4$ should have a g equal to 1.00 if the g-sum is to be correct. There are but three patterns available for this level, giving computed g-values of 1.00, 1.22, and 1.17, with an average of 1.13, but as they are all Haussmann's determinations, which seem to be consistently too high, it is possible that the g of $^1G_4$ is close to the Landé value of 1.00. With the levels as widely separated as these are—22104 units—it is not surprising that the g's of $^3F_4$ and $^1G_4$ are so close to the theoretical values, although the departures are so great among the rest of the terms.

Among the middle group of terms (odd), the structure $5d^96p$ is to be expected, giving singlet and triplet P° D° F° terms; twelve levels in all.

[11] S. Goudsmit and E. Back, Zeits. f. Physik **40**, 530 (1926).
[12] J. E. Mack, Phys. Rev. **34**, 17 (1929).
[13] A. G. Shenstone, Phys. Rev. **31**, 317 (1928).
[14] J. E. Mack, O. Laporte and R. J. Lang, Phys. Rev. **3** , 748 (1928).

Arguing by analogy and extrapolation from the behavior of the d^9p levels in the elements mentioned above, Mack has made a tentative identification of all these, (given in this paper), with but four disagreements from Haussmann's determinations. The triplets F° and D° are partially re-inverted, while triplet P° is wholly inverted. The g-sums are correct within a few percent, although the individual values are very irregular.

Before discussing the remainder of the middle group of terms, it will be profitable to consider the high set. They are probably due to the configurations $5d^97s$, $5d^86s7s$, $5d^86s6d$, and $5d^96d$, giving a large number of singlet, triplet and quintet *SPDFGHI* terms. In Ni I the lowest level of the group is $d^9 \cdot s\ ^3D_3$ and is thus the second series member of the d^9s structure. The same might be expected in Pt I, and for this reason the term A_3 has been called $5d^97s\ ^3D_3$. Excellent confirmation of this choice is the computed g-value of 1.32, in accord with the Landé value 1.33 (there being but one $J=3$ level in the configuration.) The levels B_2 and L_2 are then certainly $5d^97s\ ^3D_2$ and $^1D_2$ respectively, their g-sums being correct to within $2\frac{1}{2}$ percent. Level K_1 has a g-value of 0.52 making it appear to be $^3D_1$ from the same structure, in which it is the only $J=1$ level. The triplet D separation in the low terms is 10132, and this assignement of A_3 and K_1 makes the separation of the second member of the triplet D series only 7978. In the analogous spectra Ni I Cu II Pd I and Ag II this triplet separation is constant to within a few units in the first and second members of the series,[13,5] so the marked diminution in the second member of platinum is another indication of the abnormality of its spectrum.

After d^97s the most important high term should be ^5F due to $d^8s \cdot s$. By analogy with Ni I this should be slightly higher than $d^9 \cdot s\ ^3D$ but lower than the terms arising from $d^9 \cdot d$ and $d^8s \cdot d$. Actually, the next lowest level of the high terms, after $d^9 \cdot s\ ^3D_3$ and $^3D_2$, has a $J=5$, and g 1.41 and hence is doubtless $5d^8\ 6s7s\ ^5F_5$ (Landé g 1.40). This assignment is corroborated by the intensities of its combinations with the middle set of terms. With somewhat less assurance the levels D_4 and F_3 may be called $^5F_4$ and $^5F_3$ from the same structure.

Nothing can be said of the remainder of the high terms, except that T_6 is probably either $^5G_6$ or $^5H_6$ from $5d^86s6d$. It may be noted that λ4465.13, from the combination $6_2^\circ - Q_3$, has a pattern given by Haussman as (.31) 1.24, indicating that it should belong to a transition where $\Delta J=0$. However, since there are several instances where he has definitely been in error, it is possible that this particular pattern is also incorrect. The wave-length is too great for the Zeeman effect to be determined with the quartz instrument. Haussman classifies λ5108.45 as $13_2^\circ - K_1$ and $11_4^\circ - F_3$, both very accurately as to wave-number, but the g-value calculated for the high terms show that the main intensity of the line is due to the latter combination. Similarly, λ3925.34, assigned by Haussman to $^3F_2 - 15_3^\circ$ and to $4_3^\circ - M_3$ without the explicit statement of the duality, gives g-values showing that the former transition is more intense.

Returning to the middle group of terms, one would expect the remainder of them to be due to $5d^8\,6s6p$, forming a great many singlets, triplets and quintets. Of these, $^5D_4°$, if it could be found, should combine strongly with the high $^5F_5$ and $^3D_3$ and the low $^3F_4$ and $^3D_3$. In Ni I the lowest level of $d^8\,s^2$ is 204 units below the lowest level of d^9s, and in Pt I the lowest level of d^8s^2 is 823 above the lowest of d^9s. Consequently the d^8s ion structure is about 1000 units higher in Pt than it is in Ni, relative to the d^9 basis. In Ni $d^8sp\ ^5D_4°$ lies about 2800 units below $d^9p\ ^3P_2°$ so that in Pt one might expect $^5D_4°$ to appear about 1800 lower than $^3P_2°$, i.e., at 30800. A level with $J=4$ was searched for in that region and $46_4°$ was found, combining strongly with the terms mentioned above and less intensely with O_4 and $R_{4,5}$ and has therefore been designated $z^5D_4°$. It is the lowest level in the middle group. Its g is close to the Landé value of 1.50; the Zeeman effect of its combination with A_3, measured by Haussmann, is, however, discordant, but there can be no doubt as to the level's reality and nature. The levels $4_3°$, $12_2°$, $23_1°$ and $48_0°$ follow with decreasing assurance as the remainder of the $d^8sp^5D°$ multiplet. The reality of the last named level is somewhat doubtful.

Among the d^8sp terms there should be but two levels with $J=6$, namely $^3H_6°$ and $^5G_6°$. The latter should be lower and might be expected to combine two or three times with the high terms, (strongly with e^5F_5.) Level $47_6°$ was found and met these requirements and has been labelled $z^5G_6°$. Its combination with e^5F_5 is the strongest line in that region of the spectrum. Level $2_5°$, designated as $G_5°$ by Haussmann, is then probably $z^5G_5°$ since it is the lowest $J=5$ level in the middle group, although this means a (partial, at least) re-inversion of the multiplet, which is not the case in nickel. From the strength of its combinations with e^5F_5 and e^5F_4, the level $9_5°$ seems to be $d^8sp\ ^5F_5°$ rather than the $G_5°$ suggested by Haussmann. Furthermore, it is the only $J=5$ level available to give an inverted partial multiplet with $11_4°$, which is doubtless $z^5F_4°$ as it combines quite strongly with the high e^5F_4.

Level $30_4°$ has been altered from 48353.8 to 48351.9. One of its combinations, with O_4, given by Haussmann, for λ6188.77, involved the large error of 1.7 wave-numbers, whereas the same line is given also by the combination $22_3°-N_4$ with an error of only 0.1 units. Consequently $30_4°-O_4$ has been abandoned and $30_4°$ readjusted to give a better fit with its other two combinations and a new one, namely with a^3F_3 to give λ2614.61.

Haussmann classified λ2659.44 as $a^3D_3-7_4°$ although the Zeeman pattern he obtained was (.40) 1.20, which would mean that $\Delta J=0$. The author's measurements gave (0) 1.15, thus confirming Haussmann's classification but showing that his Zeeman separation was in error In this connection it should be noted that a similar doubt arises for his pattern of (.33) 1.17 for λ4862.40, classified as $19_3°-O_4$. The author could not settle this point as the resolution was not great enough to be of value at that wave length.

The pattern of λ2144.22, $a^3D_3-27_3°$ is (0) 1.32, giving a g-value for $27_3°$ of 1.31, calculated from the unambiguous Landé value of 1.33 for a^3D_3. This is decidedly anomalous, as six other patterns give for g of $27_3°$ the values

1.16, 1.15, 1.15, 1.14, 1.14, 1.14. Including 1.31 the average is 1.17; excluding it, it is 1.15, which is the value given in Table I. If the assignment of this line is correct, the intensities of its Zeeman components may be irregular.

Levels 40°, 42°, and 45°, given with J either 1 or 2 by Haussmann, may now definitely be assigned the J value of 1, due to their Zeeman patterns with a^3D_1 and the combination of the first two with a^1S_0. However, λ2217.33, $a^3D_1-45_1°$, is very peculiar, since its pattern, (.54) .81, gives g of $45_1°$ to be 1.08 as the average computed from the π and σ components, whereas combinations with a^1D_2 and a^3F_2 show that g of $45_1°$ is .81 and .88 respectively. The value given in Table I is the average of the four determinations. Because of their g-values, the levels $29_1°$ and $41_2°$ have been designated $5d^86s6p\ ^3P°$ or $^5D°$.

The spectrum of an atom of so heavy an atomic weight and so complicated an electron structure can be expected to exhibit very wide deviations from the Russell-Saunders coupling. In other words, the spectrum is approaching the condition of jj-coupling wherein there are no resultant L and S vectors for the atom and hence the assignment of term names becomes meaningless. In such cases it has usually been found possible to designate some of the levels with considerable certainty, but in general there will be a large number of levels to which J-values only can be assigned. This is the case in platinum. The evidence has been given for the assignment of L and S-values to a few of the levels; the remainder do not yield to the methods ordinarily employed in multiplet analysis. This is particularly evident among the middle terms, where half of the levels are still unidentified. They are probably due to the configuration d^8sp and will include the representatives of further singlet, triplet and quintet terms. Comparison with spectra of the same structure usually assists in identification, and such a method has been used here with Ni I and Pt I, but the similarity does not lead very far.

Ionization Potentials

The application of a Rydberg formula to the two members of the series $5d^96s\ ^3D_3$ and $5d^97s\ ^3D_3$ puts the limit at 74821 wave-numbers. This corresponds to an energy of 9.2 volts for the removal of an electron from d^9s to form the ion d^9. The limits similarly calculated from the $^3D_2$, $^3D_1$ and $^1D_2$ series are 75003, 82369 and 82402 respectively, indicating that $^3D_3$ and $^3D_2$ are approaching a common limit of about 74912, while $^3D_1$ and $^1D_2$ converge to a limit of about 82385. The closeness with which the four series converge to two limits is additional evidence for the correctness of the assignment of the second series members. The difference of the two average limits, 7473, should be the approximate separation of the $5d^9\ ^2D$ ion of Pt II. A check on this prediction will be afforded when the analysis of the spark spectrum, now in progress, is completed.

The use of a Rydberg formula, however to a series due to the removal of an s electron usually gives too high a limit. H. N. Russell has given[15]

[15] H. N. Russell, Astrophys. J. **65**, 233 (1927).

an empirical equation to correct such a computation for elements in the first long period, obtained from comparison of the limits given by the Rydberg and the more accurate Ritz formulae in cases where there were three series members known:

$$\text{Percent error} = 4.5 \times 10^{-5} \times \text{length of series.}$$

Applying this to the value of the $^3D_3$ series given above, we obtain 72300 or 8.9 volts. It should be noted that the application of this formula to the platinum spectrum is without justification except in the fact that the spectra are of such similar structure. A better approximation might be expected from the readjustment of the factor 4.5 from data taken from spectra in the same row of the periodic table as platinum. For Au I the factor is 4.8 and for Hg I it is 5.5, giving an average of 5.2. The use of this number, however, introduces a change in the ionization potential only in the second decimal place, beyond the accuracy of a Rydberg formula, so that the correction is trivial.

There will also be an ionizing potential corresponding to the removal of an s electron from the configuration d^8s^2. In cases of this sort, the limit is usually calculated from the lowest term of $d^{n-2}s^2$ and the term of the same type and multiplicity in $d^{n-2}s \cdot s$. Empirically it is found, however, in cases where it can be checked, that a much better approximation to the correct ionization potential is obtained by using as the second member the term of the same type but of higher multiplicity, which is always present. For example, in Ca I $s^2\ ^1S$ and $s \cdot s\ ^3S$ put the limit only 127 units higher than the Ritz equation, and in Ni I the use of $d^8s^2\ ^3F_4$ and $d^8s \cdot s\ ^5F_5$ places it 154 too high, whereas a Rydberg formula applied in the usual way gives errors of 2133 and 2557 in the two cases. The method has been tested on other spectra of a similar nature and always gives a limit much nearer the Ritz value, although it is sometimes too high and sometimes too low. Thus in platinum, using $5d^86s^2\ ^3F_4$ and $5d^86s7s\ ^5F_5$, we obtain the limit 77730, and adding 824, by which a^3F_4 lies above the lowest term, ($5d^96s\ ^3D_3$) the energy difference between d^9s and d^8s is 78554 or 9.7 volts.

It gives the author the greatest pleasure to acknowledge the expert assistance given him by Dr. A. G. Shenstone, who has been a continual source of friendly advice and criticism throughout the work. Sincere thanks are also given to Dr. J. E. Mack for his interpretation of many of the levels.

THE MEAN LIFE FOR THE MERCURY SPARK SPECTRUM

By Louis R. Maxwell*
Bartol Research Foundation of the Franklin Institute

(Received June 5, 1929)

Abstract

By using the method previously described by the writer for measuring the average life of excited ions, a mean life of 9×10^{-7} and 8×10^{-7} seconds was found for the 3114 and 2572 lines, respectively, of Hg IV, 6×10^{-7}, 4×10^{-7} and 4×10^{-7} seconds for the 3090, 3312 and 4797 lines respectively of Hg III. The prominent lines of Hg II are estimated to have a mean life of the order of 10^{-8} seconds. These results indicate that the greater the charge of the ion producing the line the longer the mean life. The formula derived for determining the mean life is discussed and experimental results are given which agree quite satisfactorily with the theory developed for measuring the mean life. Intensity-current relations of the spark lines show that they are produced as the result of single electron collisions, which substantiates the assumptions made in the above theory. It is pointed out that lines due to electrons jumping from the same energy level should have the same mean life regardless of the level to which the electrons may jump. The above lines have not been classified so a correlation between the electron transitions and mean lives cannot at present be made.

Discussion of Formula for Determining the Mean Life

RECENTLY the writer[1] has described a new method for determining the life in the excited state which is applicable to lines of the spark spectrum. Electrons in mercury vapor were confined in a beam by a magnetic field. Perpendicular to the beam, an electric field withdrew the positive ions. The light emitted was projected on to the slit of a spectroscope in such a manner that the slit was parallel to the direction of motion of the ions. Several of the spark lines were shown to suffer a displacement along their length and the following formula was derived in order to calculate the mean life $\tau=1/\beta$ after measuring the distance the most intense portion of the line had been shifted,

$$2e^{-\beta(2mx'/Xe)^{1/2}}-e^{-\beta[2m(a+x')/Xe]^{1/2}}-1=0 \qquad (9)$$

where X is the cross field, m/e the ratio of mass to charge of the ion and a is one half the width of the beam.

Part 1. The Displacement as a Function of the Mean Life

We shall now consider how the displacement x' will vary with respect to the mean life τ as given by the above equation. Eq. (9) can be written as follows:

$$f(x'\beta)=2e^{-c\beta}-e^{-d\beta}-1=0$$

* National Research Fellow.

[1] L. R. Maxwell, Phys. Rev. **32**, 715–726 (1928).

where $e=(2mx'/Xe)^{1/2}$ and $d=[2m(a+x')/Xe]^{1/2}$. We shall now consider the field X as being constant and determine how x' varies with respect to β. Let us first consider the curve representing the function $f(x'\beta)$ plotted with respect to β holding x' constant and equal to some value greater than zero and less than infinity. For β very great $f(x'\beta)$ will approach -1 and for $\beta=0$, $f(x'\beta)$ will be zero. The slope of the curve is

$$\frac{df(x'\beta)}{d\beta}=de^{-d\beta}-2ce^{-c\beta}=e^{-d\beta}(d-2ce^{(d-c)\beta}) \tag{10}$$

and for β approaching zero we have

$$\left(\frac{df(x'\beta)}{d\beta}\right)_{\beta\to 0}=d-2c$$

if $d>2c$ then the slope near the origin will be positive and hence the curve will initially rise. Since d is always greater than c, $2ce^{d-c\beta}$ will increase as β increases, making, therefore, the slope of the curve decrease as shown by Eq. (10). As β takes on larger values the slope eventually becomes zero,

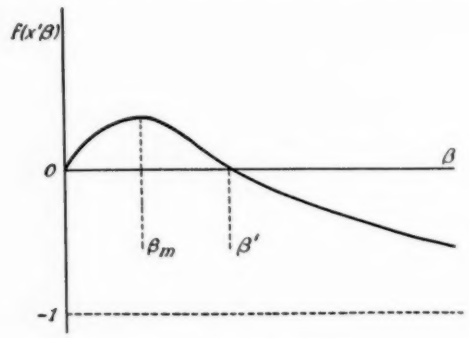

Fig. 1.

and then negative. Thus the curve will reach a maximum and then decrease to negative values for large values of β and for β infinite the curve will approach the value -1. This estimated shape of the curve is illustrated in Fig. 1. The value of β which locates the maximum we shall designate by β_m and it is evaluated by setting the slope given by Eq. (10) equal to zero which gives

$$\beta_m=[1/(d-c)]\log(d/2c). \tag{11}$$

The point where the curve crosses the axis gives β' the root of the equation, i.e., the value of β which satisfies Eq. (9). We see that β_m will always be less than β'.

If $d<2c$, then the slope will always be negative and the curve will drop from the origin and proceed to the value -1 as β approaches ∞. Similarly, for $d=2c$ the function is negative. For these two cases there exists no root of the Eq. (9) except that for $\beta=0$.

We therefore have shown that in order to obtain β' a solution of Eq. (9) different than zero d must be greater than $2c$. That is

$$\left(\frac{2m}{Xe}(a+x')\right)^{1/2} > 2\left(\frac{2mx'}{Xe}\right)^{1/2}$$

which means that x' must be always less than $a/3$.

Let us now consider how x' varies with β_m. When $x'=0$, i.e. when $c=0$, and $d=(2ma/Xe)^{1/2}$ then $\beta_m=\infty$ as given by Eq. (11). When $x'=a/3$ then $\beta_m=0$. Since it can be shown that $d\beta_m/dx$ is always negative, we then know

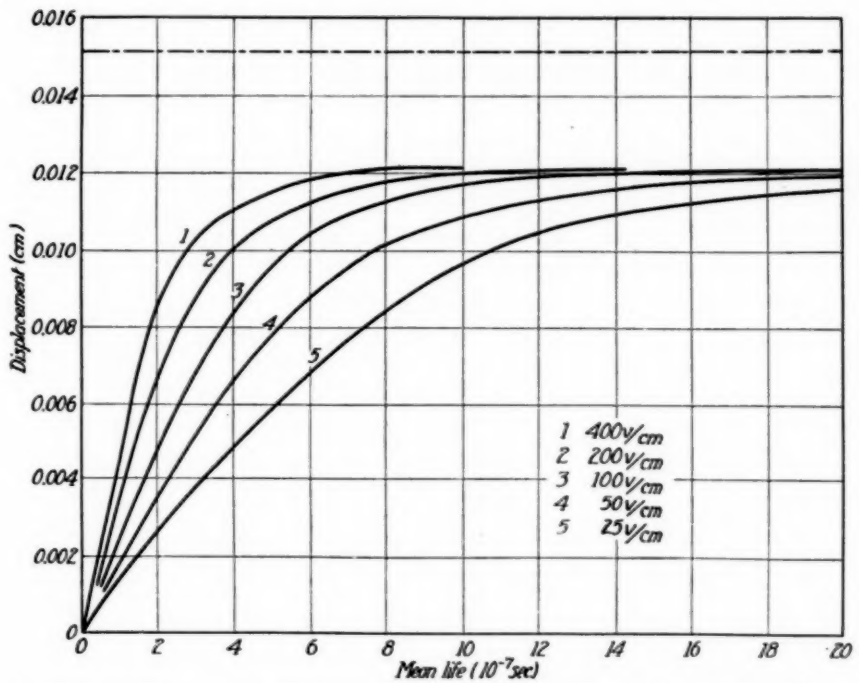

Fig. 2. Relation between the displacement and the mean life for lines of Hg III. Each curve represents results calculated for the particular cross field indicated.

that a curve representing β_m plotted with respect to x' will be a curve without maxima and minima which will extend to infinity at $x'=0$ and cut the abscissae at $x'=a/3$.

It is now easy to obtain x' as a function of β' for we have shown that for $x'=a/3$, $\beta_m=0$, therefore for this value of x', $\beta_m=\beta'$. Let us now choose a β_m very large. Then the corresponding value of x' which satisfies Eq. (11) is very small. But for this value of β_m and x', there exists a $\beta'>\beta_m$ which is a solution of Eq. (9). Therefore, we know the end points of an x', β' curve. It is now necessary to determine if there exist maxima or minima lying between these end points $x'=a/3$, $\beta'=0$ and $x=0$, $\beta'=\infty$. The number of maxima or minima which exist is equal to the number of sets of values x', β' which satisfy Eq. (9) and also the following equation

$$de^{-d\beta} - 2ce^{-c\beta} = 0 \tag{12}$$

which is obtained by differentiating (9) with respect to β and imposing the condition that $dx'/d\beta = 0$. This equation simply specifies which of all those sets of values x', β' that satisfy Eq. (9), will locate a maxima or minima on an x', β' graph. It can be shown that according to these considerations, there is only one maximum and that is at $\beta' = 0$, i.e., $x' = a/3$, $\beta' = 0$ is the only set of values which fulfill the above conditions. Therefore, we have proved that the curve between the end points has no maxima or minima, and that the largest value of the displacement $(a/3)$ is obtained for $\beta' = 0$, or $\tau = \infty$. In Fig. 2 we have x' plotted with respect to the mean life as calculated directly by numerical substitution in Eq. (9) for different cross fields as indicated by the full curves. The horizontal broken line is the limiting value of $a/3$ for the displacements. We see that the displacements approach this value as the mean life is made large.

Part II. The Displacement as a Function of the Cross Field

We shall now consider β to be kept constant and determine how the displacement x' will depend upon the cross field X. We have just shown the relationship between the displacements and the mean life $1/\beta$ for a constant X. The present case is analogous to the above, for here we shall determine how x' depends upon X holding β constant. The relation between x' and

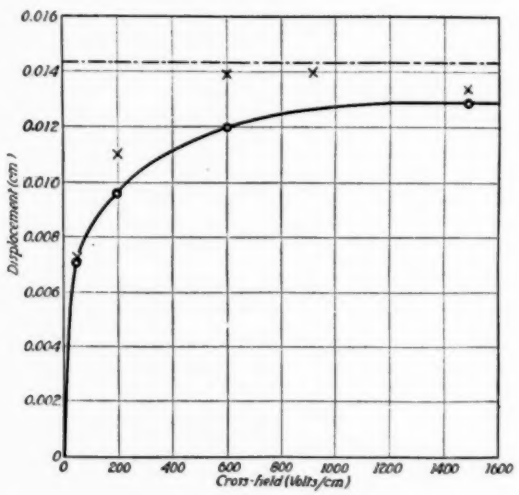

Fig. 3. Relation between the displacement and the cross field for the 4797 line of Hg III. The dots represent the theoretical values of the displacements and the crosses the experimental values.

$X^{1/2}$ will be the same as that found to exist between x' and $1/\beta$ as shown by Eq. (9). Therefore we know that the displacements will never be greater than $a/3$, i.e., $x = a/3$ for $X = \infty$. In Fig. 3 is shown a curve representing x' plotted as a function of X as given by the full line curve. These values are those which were found to satisfy Eq. (9) by direct numerical substitution and hence give the theoretical prediction of how the displacements depend

upon the field. The horizontal broken line gives the limiting value of $a/3$ for the displacements. It is noticed that the curve approaches this value asymptotically as the field becomes large.

Experimental Arrangement and Results

The apparatus used in the present work was the same as that previously described except that it was designed to accommodate greater cross fields. This was accomplished by placing the tube between the pole pieces of an electro-magnet which produced a magnetic field of 2500 gauss and hence permitted large values of the cross field to be used without disturbing the electron beam. The new apparatus was considerably smaller but the essential parts of it were the same as in the former tube. The same type of filament and similar placement of the side plates were used. The shape of the electron beam is determined by the shape of the filament. The filament was a straight wire which caused the beam to be of a ribbon-like character. The electrode S_2 was omitted and a Faraday cage of one centimeter depth was used in place of the long cage C. Inside the Faraday cylinder a non-uniform cross field was used to prevent the return of secondary electrons into the region photographed.

Fig. 4. A reproduction of a portion of two typical plates showing the displaced 4797 line of Hg III indicated by the dot and the undisplaced 4916 Hg arc line. The direction of motion of the ions is indicated by the arrow. The cross field applied for the upper photograph was 600 volts/cm while for the lower 200 volts/cm was used.

Figure 4 is a reproduction of a portion of one of the spectrum plates. The ions were moving in the direction indicated by the arrow. The slit of the spectrograph was purposely made very wide so that the lines would be of sufficient width to allow intensity measurements along their length. The line indicated by the dot is the 4797 of Hg III and the other is the 4916 line of the mercury arc spectrum. It can be easily seen that the spark line is distorted and the line actually pulled up in the direction of motion of the ions. The arc line is of course not affected by the field. In the upper set of lines the cross-field was 600 volts/cm while in the lower, the field was 200 volts/cm. Photographs were also taken with this spark line for other fields and the results are given in Fig. 3. The actual displacements were measured and are indicated by the crosses. The full line curve located by the dots gives the

theoretical values as mentioned above. The value of the mean life is taken to be 4×10^{-7} sec. We see that the agreement between the experimental results and the theory is quite satisfactory.

The accuracy with which the mean life can be measured depends greatly upon the value of the cross field. For example, suppose we were to examine a line which had a mean life of 1×10^{-6} sec and were to use a cross field of 400 volts/cm. We see from Fig. 2 that the displacement which we would measure would lie on the curve at a point where the slope was about zero. Therefore, any small error in the measurement of the displacement would produce a very great error in the determination of the mean life. We see from the figure that a choice of a field of 25 volts/cm would give a decidedly more accurate measurement of the mean life. In general the value of the field should be so adjusted that the point representing a displacement corresponding to a certain mean life lies on that part of the curve where the slope is the greatest.

The results obtained for the mean life for the lines of the mercury spark spectrum are presented in Table I. The mean life for the 3832 line of Hg IV

TABLE I. *Mean life of various spark lines of mercury.*

Wave-length (A)	Type of spectrum	Mean life (sec.)
3090	Hg III (E_2)	6×10^{-7}
3312	Hg III (E_2)	4×10^{-7}
4797	Hg III (E_2)	4×10^{-7}
3114	Hg IV (E_3)	9×10^{-7}
2572	Hg IV (E_3)	8×10^{-7}

was estimated to be of the same order of magnitude as those given in the table. The prominent lines of the first spark spectrum of mercury such as the 2848, 2947, 3208, 3708 and many others did not exhibit any appreciable displacement so that their mean life could not be measured. A mean life of 10^{-8} seconds would produce a very small displacement as illustrated in Fig. 2 for lines of the Hg III spectrum while for the Hg II spectrum the displacements would be still less. Thus we see that it is impossible (for the cross field used) to measure mean lives of 10^{-8} seconds for the Hg II spectrum. Therefore these undisplaced spark lines of Hg II probably have a mean life of that order of magnitude. The lines 2262 and 2916 of Hg II did show a noticeable displacement in the case of high cross fields, but the mean life for these lines has not been measured. However, we conclude that in general the mean life for the first spark spectrum is of the order of 10^{-8} seconds. For the second and third spark spectra, the life is considerably greater, while the lines of Hg IV show slightly higher mean lives than do the lines of Hg III. These results indicate that the greater the ionic charge the longer the life in the excited state.

It has been assumed in this method of calculating the mean life that the line is produced as a result of a single electron collision, i.e., the atom is multiply ionized and excited at the moment of collision of the atom and

electron. Since the concentration of positive ions is small, the probability of collision between electrons and unexcited ions is so small that the number of excited ions formed as a result of this double collision process would not be great enough to produce any light. The pressure of the mercury vapor in the tube was about 0.001 mm so that the total ion current was of the order of 10^{-5} amperes which necessitates that the ion concentration be small. Valasek[2] has shown that many of the spark lines of mercury formed under similar conditions were produced as the result of single collisions. This conclusion was arrived at after he found that the intensity of the spark lines was directly proportional to the exciting electron current. In fact, Valasek found no lines due to multiple collisions. In the present work similar intensity-current relations were measured for the 3208 of Hg II, 3090 and 3312 of Hg III, 3114, 2572 of Hg IV and the relationships were found to be linear. All of the measurements of this character show that the mercury spark lines are the result of single collisions which substantiates the assumptions that have been made in the above calculations.

The value of the charge of the ion responsible for the lines quoted in the above table was obtained from the results of L. and E. Bloch,[3] who, by means of an electrodeless discharge tube, have classified a large number of the spark lines of mercury into either the first, second or third spark spectrum. From Eq. (9) we see that in order to calculate the mean life, it is necessary to know e the total charge of the ion; and any error in e which might arise in the measurements of L. and E. Bloch will alter the value of the mean life given in Table I. On the other hand, if we knew the mean life for the spark line it would be possible to measure, by the present method, the charge of the ion producing the line.

Discussion of Results

Let us be concerned with determining how the mean life should depend upon the electron transitions. If N be the number of atoms which at any time t have an electron in a certain excited state designated by the quantum numbers nk; and if $A_{nk}^{n'k'}$ be the probability of transition from the state nk to state $n'k'$, then the number of electrons which will leave state nk and go to $n'k'$ in time dt is given by

$$-dN_{nk}^{n'k'} = A_{nk}^{n'k'} N dt$$

Thus the total number of electrons which will leave the state nk per unit time, is

$$\frac{-dN}{dt} = \sum_{n'k'} -dN_{nk}^{n'k'} = \sum_{n'k'} A_{nk}^{n'k'} N$$

where the summation is to be extended over all the possible states to which the electron can jump. Therefore, the population N of the nk level at any time t is given by

[2] Joseph Valasek, J.O.S.A. **17**, 102 (1928).

[3] L. and E. Bloch, Jour. d. Physique **4**, 333 (1923).

$$N=N_0\exp-\left[\left(\sum_{n'k'}A_{nk}^{n'k'}\right)t\right]$$

where N_0 is the number of atoms with an electron in the nk state at the time $t=0$.

The energy emitted per unit time at time t by the jumping of electrons from state nk to $n'k'$ is $A_{nk}^{n'k'}\,h\nu_{nk}^{n'k'}N$, where $\nu_{n'k}^{n'k'}$ is the frequency of the emitted light. Therefore, the intensity of the spectral line is given by the following after replacing N by its value from the above equation,

$$I_{nk}^{n'k'}=A_{nk}^{n'k'}\,h\nu_{nk}^{n'k'}N_0\exp-\left[\left(\sum_{n'k'}A_{nk}^{n'k'}\right)t\right] \tag{13}$$

The average life τ of the excited state nk is given by

$$\tau=\left(\sum_{n'k'}A_{nk}^{n'k'}\right)^{-1}$$

We see from this equation that all of those lines due to electrons jumping from the same level should give the same value for the mean life. This simply means that the life of an excited state can be measured by using any line which originates from that particular level. The intensity of the lines, however, will depend upon the value of $A_{nk}^{n'k'}$ as shown by Eq. (13).

Since the lines given in the above table have not been classified as to their electron transitions it is not possible at present to correlate the above results for the mean lives with the electron jumps. The two lines 3312 and 4797 of Hg III, however, have the same mean life so that we conclude that they must originate from the same energy level.

Kerschbaum[4] has determined the mean life of a number of lines employing the canal ray method of Wien. He has found in general that not only those lines starting from a particular level give the same mean life but all of the arc lines of a given element have the same mean life. Since we have shown above that the mean life is equal to the reciprocal of the sum of the transition probabilities for all possible jumps from the level concerned it is not to be expected that the mean life should be the same for all of the levels of the atom, as Kerschbaum's results seem to indicate. For the spark lines of singly ionized barium, he found that the two lines 4554 and 4934 which originate from the same level (i.e. two lines of the principal series of Ba^+) gave different mean lives, 2.7×10^{-8} and 1.2×10^{-8} sec, respectively. This result is not in agreement with the above considerations.

The writer wishes to thank the National Research Council for its support and the Bartol Research Foundation for providing the facilities used in this work. The writer also desires to thank Professor James Barnes for the privilege of using the densitometer at Bryn Mawr College, and Dr. A. Bramley for helpful discussions.

[4] H. Kerschbaum, Ann. d. Physik **83**, 287 (1927).

ROTATIONAL STRUCTURE OF THE RED BANDS OF SODIUM

By W. R. Fredrickson
Syracuse University

(Received May 23, 1929)

Abstract

Three bands of the red band system of sodium photographed at high dispersion have been measured. Two strong series of lines run through the bands and from the combination relations it is quite certain that these series are bona fide P and R branches. From the combination relations we find $B_0''=0.15435$, $D_0''=-5.89\times10^{-7}$ and $B_0'=0.10846$. The final state values are in close agreement with those of the final state of the blue green system and the constant for the upper state yields $I_0'=255.3\times10^{-40}$ gm cm^2 and $r_0'=3.52\times10^{-8}$ cm. Search is made for other branches but none are found. From a discussion of the possible electronic transitions it is concluded that the electronic transition is the $^1S-{}^1S$ type.

THE absorption spectrum of molecular sodium consists of two band systems, one in the red and the other in the blue-green. Loomis[1] has analyzed the vibrational structure of the blue-green system from a study of Wood's[2] magnetic rotation spectrum of sodium and the writer and Watson[3] have analyzed the vibrational structure of both the red and the blue-green systems from the absorption spectrum. The agreement of the final state coefficients of the vibrational formulas for the two systems shows that the systems have a common final electronic state. By means of this vibrational data and a study of the heats of dissociation of Na_2 Loomis[1] has shown that the molecules in the common lower energy state dissociate into 3^2S atoms while the molecules in the excited state of both the red and the blue-green bands dissociate into a 3^2S atom and a 3^2P atom. Furthermore, Loomis and Wood[4] have worked out the rotational structure of the blue-green bands and have proved conclusively that the electronic transition for this system is $^1P-{}^1S$.

Since the excited molecules of both systems dissociate into a 3^2P and a 3^2S atom, the theoretically possible molecular states[5] for the upper state are ^3P, ^3S, ^1P, and ^1S. From the similarity of the sodium molecule and the CO molecule and by analogy with the Mg atom,[6] one would be inclined to assign the red system to a $^3P-{}^1S$ transition. Thus the red bands would be similar to the Cameron CO bands. These latter bands, however, show triple heads while the sodium bands show only single heads.[7] Mulliken[5] states that no

[1] Loomis, Phys. Rev. **31,** 323 (1928).
[2] Wood, Astrophys. J. **30,** 339 (1909).
[3] Fredrickson and Watson, Phys. Rev. **30,** 429 (1927).
[4] Loomis and Wood, Phys. Rev. **32,** 223 (1928).
[5] Mulliken, Phys. Rev. **32,** 396 (1928).
[6] Mulliken, Phys. Rev. **28,** 493 (1926). Na_2 and CO are similar in that they have the same number of outer electrons.
[7] Ritschl and Villars, Naturwiss. **16,** 219 (1928).

reason is evident for such a contrast between the systems and suggests the possibility that the upper molecular state for the red bands is a ^1S state instead of a ^3P. It is with reference to the question of electronic transition that the following analysis is concerned.

The photographic plates of the spectrum were taken at the Ryerson Laboratory, The University of Chicago, using the twenty-one foot Rowland concave grating in the second order. The (6,0), (5,0) (4,0) bands were measured because they are among the most intense and show the least overlapping.

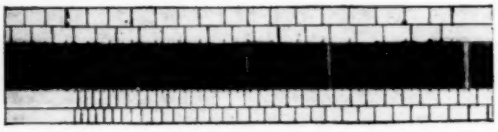

Fig. 1. The (5, 0) band of red Na_2 band system.

An enlargement of the (5,0) band is shown in Fig. 1. The ink lines at the bottom show two series which are of the same intensity and converge at the head of the band. At the top are shown two series which proceed through the band and converge at the head of the preceding band,—the (6,0). In each of the three bands measured two series are found,—the data being given in Table I.

The two series in each band were taken to be P and R branches and the determination of which was P and which was R was made with the aid of the combination relations. According to the band spectrum theory, the combination relations are

$$2\Delta F'(j) = R(j) - P(j) = 4B'(j+\tfrac{1}{2}) + 8D'(j+\tfrac{1}{2})^3$$
$$2\Delta F''(j) = R(j-1) - P(j+1) = 4B''(j+\tfrac{1}{2}) + 8D''(j+\tfrac{1}{2})^3$$

The method of assigning the various series in each band to R and P branches was to apply the last relation above to the series in the three bands measured and to shift the series until the best agreement between the final state combinations was obtained. When the assignment of the series to the P and R branches was once made, the B'' and D'' values were calculated. It is unfortunate that one could not apply the initial state combinations between bands but no two bands with the same initial state could be analyzed because of the overlapping of other bands. However, the initial state combinations for these bands were taken and from them the B' and D' values were calculated.

The following is a summary of the constants:

$B_0'' = 0.15435$	$B_6' = 0.10555$	$D_6' = -3.59\times10^{-7}$
$D_0'' = -5.89\times10^{-7}$	$B_5' = 0.10611$	$D_5' = -3.36\times10^{-7}$
	$B_4' = 0.10664$	$D_4' = -2.61\times10^{-7}$.

Assuming the formula $B'_n = B'_0 - \alpha_1 n' - \alpha_2 n'^2$ we find that $B'_0 = 0.10846$, $\alpha_1 = 0.000395$, and $\alpha_2 = 0.000015$.

TABLE I. *Lines in the red Na_2 bands.*

	6−0		5−0		4−0	
j	*R*	*P*	*R*	*P*	*R*	*P*
10½					15458.02	15453.60
11½					57.20	52.10
12½					56.00	50.60
13½	15677.69	15671.83	15566.62	15560.78	55.10	49.50
14½	76.52	70.39	65.50	59.24	53.78	47.71
15½	75.31	68.75	64.26	57.67	52.63	46.00
16½	73.90	66.98	62.80	56.00	51.24	44.18
17½	72.46	65.11	61.75	54.22	49.89	42.42
18½	70.98	63.10	60.16	52.18	48.30	40.35
19½	69.24	61.12	58.52	50.33	46.71	38.49
20½	67.56	58.92	56.86	48.29	44.65	36.49
21½	65.74	56.64	55.03	45.98	43.08	34.10
22½	63.89	54.30	53.21	43.63	41.25	31.40
23½	61.79	51.86	51.12	41.24	39.10	29.10
24½	59.58	49.38	49.16	38.82	37.09	26.75
25½	57.49	46.77	46.99	36.17	34.90	24.13
26½	55.30	44.12	44.61	33.47	32.60	21.57
27½	52.73	41.16	42.27	30.61	30.22	18.60
28½	50.32	38.27	39.77	27.77	27.82	15.73
29½	47.68	35.25	37.19	24.81	25.45	12.74
30½	44.82	32.14	34.60	21.72	22.69	9.60
31½	42.18	28.92	31.78	18.54	20.38	6.85
32½	39.34	25.61	29.06	15.25	17.84	3.35
33½	36.30	22.27	26.00	11.96	15.00	15400.62
34½	33.31	18.84	23.03	8.44	12.14	15397.32
35½	30.04	15.19	19.93	4.87	9.02	94.00
36½	26.80	11.52	16.66	1.34	5.88	90.49
37½	23.44	7.81	13.43	15497.69	2.66	86.70
38½	19.96	3.89	9.96	93.77	15399.30	82.89
39½	16.48	0.00	6.43	89.77	95.80	79.00
40½	12.84	15595.94	2.88	85.80	92.40	75.25
41½	9.07	91.74	15499.20	81.71	88.68	71.22
42½	5.31	87.57	95.47	77.55	85.00	67.05
43½	1.35	83.15	91.63	73.34	81.03	62.71
44½	15597.47	78.82	87.54	68.94	77.22	58.51
45½	93.19	74.29	83.54	64.47		
46½	89.05	69.69	79.30	59.82		
47½	84.75	65.04	75.07	55.36		
48½	80.25	60.15	70.77	50.51		
49½	75.90	55.32	66.40	45.84		
50½	71.27	50.33	61.95	40.77		
51½	66.62	45.27	57.24	35.80		
52½	61.92	40.17	52.63	30.76		
53½	57.00	34.90	47.80	25.45		
54½	52.18	29.59	43.10	20.38		
55½	46.99	24.03	37.98	15.00		
56½	41.80	18.64	33.00	9.54		
57½	36.84	13.03	27.82	3.94		
58½	31.34	7.35	22.59	15398.34		
59½	26.09	1.34	17.19	92.72		
60½	20.62	15495.47	11.59	86.87		

It is interesting to compare the final state values of the red system with those of the blue-green.[4]

(blue green)	$B_0''=0.15431$	$D_0''=-5.86\times10^{-7}$
(red)	$B_0''=0.15435$	$D_0''=-5.89\times10^{-7}$.

This agreement is as close as can be expected. When the $2\Delta F''$ values are calculated from the above constants and then compared with the experimental values, one cannot say which set better fits the data.

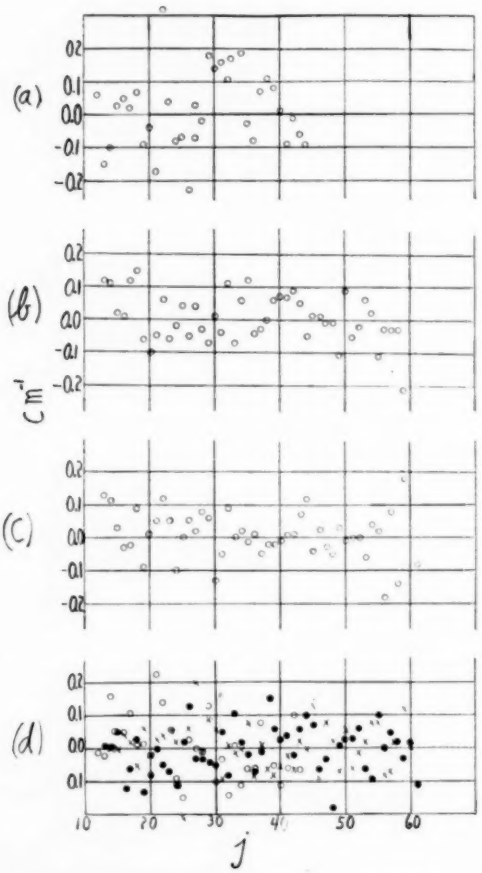

Fig. 2. Differences between the calculated and observed $2\Delta F$ values. (a), (b), (c) give the $2\Delta F'$ values for the (4, 0), (5, 0), (6, 0) bands and (d) gives the $2\Delta F''$ values for the three bands, crosses are the (6, 0), dots are the (5, 0) and circles are the (4, 0).

As to the initial state constants, they agree fairly well with those predicted by Loomis[8]. If we take our values and apply them to the empirical relations of Mecke and Birge which Loomis used in making his predictions we find that B_0/ω_0 which should remain constant in any transition has the values $B_0''/\omega_0''=0.00097$ and $B_0'/\omega_0'=0.00091$, and the value $R=2\times B_0/\alpha$

[8] Loomis, Phys. Rev. **32**, 875 (1928).

which also should remain constant in a transition has the values $R''=1.73$ and $R'=1.83$. With the value of $B'_0=0.10846$ we find the moment of inertia $I'_0=255.3\times10^{-40}$gm cm^2, and the radius of the molecule $r'_0=3.52\times10^{-8}$ cm.

The deviations of the $2\Delta F$ values from the calculated values are shown in Fig. 2. It can be seen from the figure that practically all the deviations are within 0.1 wave-number which is as good as can be expected. The (4,0) band shows the greatest deviations. This band, however, also has the most overlapping.

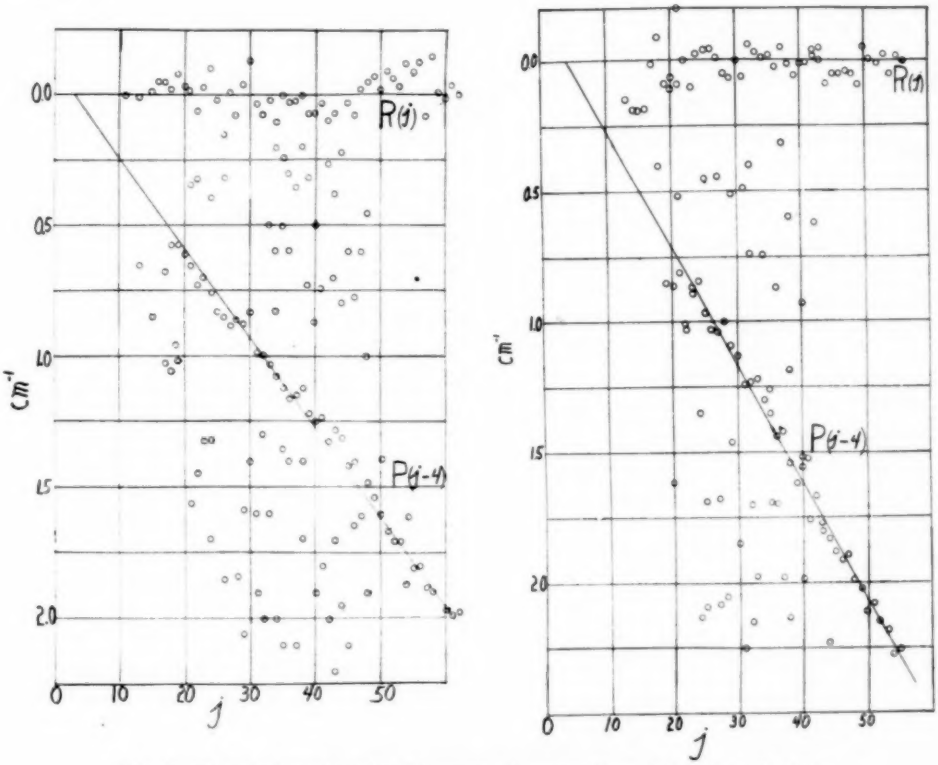

Fig. 3. The circles give the differences between lines in bands and their adjacent calculated R lines for the (5, 0) and (6, 0) bands.

From the agreement of the final state combinations and the agreement of the final state coefficients with those of the blue-green system, it seemed reasonable to suppose that the two branches are bona fide P and R branches. It was desired, however, to determine whether any other branches could possibly be present. Following a method used by Loomis and Wood[4] the R branches for the (5,0) and (6,0) bands were calculated from the formula

$$\nu=A+2B'(j+\tfrac{1}{2})+(B'-B'')(j+\tfrac{1}{2})^2+4D'(j+\tfrac{1}{2})^3+(D'-D'')(j+\tfrac{1}{2})^4$$

where the B and D values are those given above and the A was determined by equating the right hand of the above equation to the frequency of some

one line in the band. The difference in frequencies of every line and its adjacent R line is plotted. Figure 3 shows the situation for the (5,0) and (6,0) bands.

It is seen that most of the points group themselves along two lines, the (0,0) line which represents the R branch and the inclined line which represents the P branch. Should any other branches be present, one would expect the other points to group themselves along other lines. Some of the points scattered throughout the graphs are due to branches from the preceding band. Figure 4 shows the (5,0) band after the lines belonging to the (6,0) band have been removed. From these graphs one would conclude that in

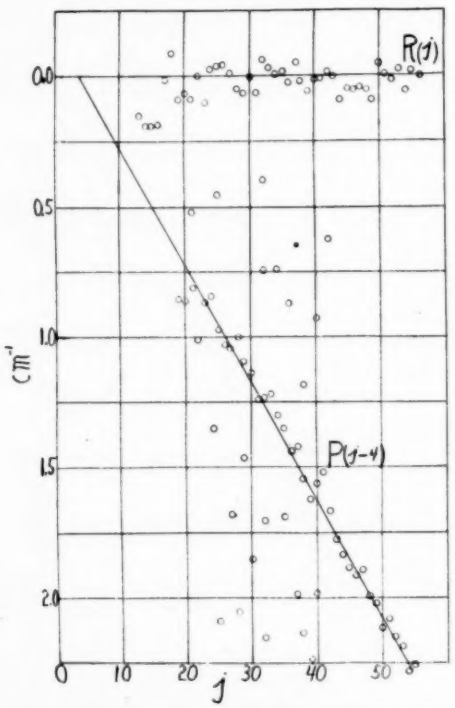

Fig. 4. Same as the (5, 0) band in the preceding figure except that known (6, 0) lines are omitted.

the region of quantum numbers higher than 13 in each band only two branches appear. In the region below quantum number thirteen we are unable to say because the lines are too close together and too weak in intensity.

The presence of only two branches appears to confirm the assignment of electronic transition to the $^1S-{}^1S$ type. If the electronic transition was of the $^3P_1-{}^1S$ type, one would probably expect the same structure and intensity distribution as for the $^1P-{}^1S$ type—single P, Q, R branches with the Q branch the most intense.

In conclusion the writer wishes to thank Dr. W. W. Watson and Dr. R. S. Mulliken for their interest and advice in the work.

RADII AND COLLISION PROBABILITIES OF MESTASTABLE NEON AND MERCURY ATOMS

By M. W. Zemansky*
Palmer Physical Laboratory, Princeton, N. J.

(Received April 17, 1929)

Abstract

The problem of the life-time of metastable atoms was treated on the basis of the assumptions that (1) metastable atoms diffuse to the walls of the containing vessel and give up their energy there, and (2) metastable atoms perform impacts with other atoms and are either lowered to the normal state or raised to a higher state. The result was obtained that, for large values of the time elapsing after the cut-off of the excitation, the average number of metastable atoms per cc decays exponentially with the time, with an exponential constant equal to $A/p+Bp$ where p is the pressure and A and B are constants containing the radius of the metastable atom and the probability of dissipative impact. The experimental results of Meissner and Graffunder, Eckstein, Zemansky and Pool are treated according to the theory, and values of the radius and probability are found. The radius in each case comes out smaller than the normal value, and the values of the probability are shown to substantiate the view that, in impacts between metastable atoms and either normal atoms of the same kind or foreign gas atoms whose first excitation potential is higher than the energy of the metastable atom, the metastable atom is raised to a state of higher energy.

IN A paper by Meissner and Graffunder[1] a critical survey is given of all the various methods that have been used to measure the lifetime of the neon atom in the metastable $^3P_2$ state, and new data are given that are the most reliable up to date. The method employed was briefly this: An absorption tube containing neon is electrically excited for a while, and then the excitation is cut off. After t seconds have elapsed, the absorption of the neon for $\lambda=6402$ ($2^3P_2-3^3D_3$) is measured. (See Fig. 1a) Keeping the pressure of the neon constant and varying t, a curve is obtained where the ordinates represent percentage absorption, and the abscissas time in seconds. Curves of this character are given for neon pressures ranging from 0.50 mm to 5.60 mm. Since the degree to which $\lambda=6402$ is absorbed depends upon the number of atoms capable of absorbing it, the authors assume that

$$1-I/I_0 \propto N' \qquad (1)$$

where I_0 is the incident intensity of $\lambda=6402$, I the transmitted intensity of $\lambda=6402$, N' the average number of metastable 2^3P_2 neon atoms per cc traversed by the beam of light. The curves just described are therefore taken to represent the way in which the metastable neon atoms decrease with the time and the time necessary for the metastable neon atoms to decrease

* National Research Fellow.

[1] K. W. Meissner and W. Graffunder, Ann. d. Physik **84**, 1009 (1927).

to one-half their original number is taken to be the lifetime of the metastable state at the particular pressure. It was found that the lifetime varied with the neon pressure, being a maximum at about 1 mm.

The experiment was performed with a cylindrical absorption tube of known dimensions, and consequently the number of absorbing metastable neon atoms could be computed approximately as a function of the time on the basis of the assumption that the decrease in the number of metastable neon atoms was due to two factors, namely, (1) diffusion to the walls, and (2) dissipative impacts with normal neon atoms. It was necessary to solve the

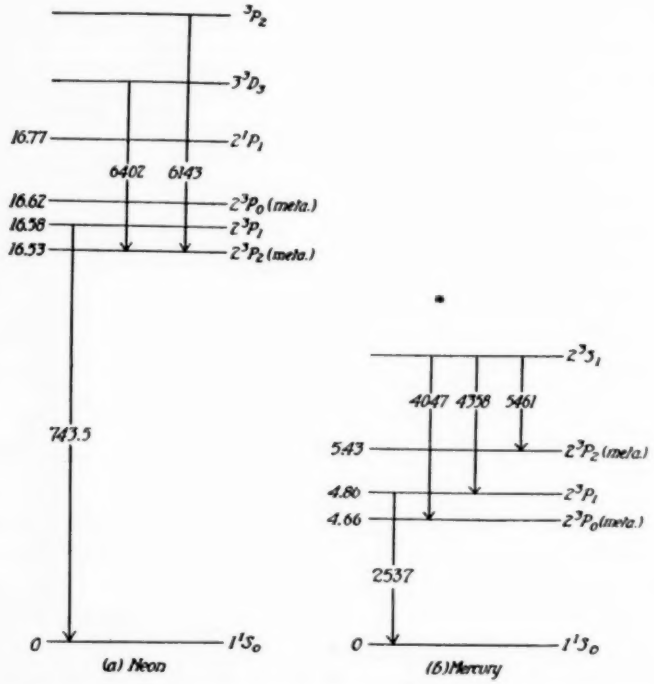

Fig. 1. Energy levels for neon and mercury. The lower metastable state is the one referred to in this paper.

diffusion equation for an infinite cylinder with a dissipative term in it, subject to the condition that, when $t=0$, the distribution of metastable atoms is uniform, and finally to integrate over a cylinder whose length is the length of the absorption tube, and whose radius is the radius of the light beam. The final result was expressed in the form of a series whose numerical value was found to depend very markedly on the ratio of the radius of the absorption tube to the radius of the absorbed light beam. Using a gas-kinetic value of the diffusion coefficient of neon, and assuming a probability of dissipative impact equal to 1.46×10^{-4}, the series was evaluated for various values of t, and the half-life was obtained for a number of pressures. The theoretical curve showing the relation between half-life and pressure did not agree well with the experimental one.

In view of the accuracy of Meissner and Graffunder's experiments, as well as the presence of reliable data on mercury, it was thought worth while to attack the general problem of the diffusion of metastable atoms in a way that would promise a better interpretation of existing experimental results in this field.

The Problem

Let us consider a cylindrical tube of length l and radius c placed with its center at the origin of cylindrical coordinates. Suppose that the tube is filled with a gas or vapor which either optically or electrically has been excited for a while, and that metastable atoms have been formed either in the presence of or without some foreign gas. Let the exitation be cut off and let a cylindrical beam of light of radius b which the metastable atoms are capable of absorbing traverse the tube.

We shall make the following assumptions:—(1) After the excitation is cut off, there is no further resultant rate of formation of metastable atoms. (2) Metastable atoms diffuse to the walls where they either become normal or are raised to a higher stationary state. (3) Metastable atoms perform impacts with normal atoms (and, if a foreign gas is present, with the molecules of the foreign gas, too) which either lower the metastable atoms to the normal state, or raise them to a higher state. (4) The rate at which metastable atoms are being raised to a higher state by the absorption of the light is negligible compared to the rate at which (2) and (3) go on.

The number of metastable atoms per cc, n will then be given by

$$\partial n/\partial t + kn = D(\partial^2 n/\partial r^2 + \partial n/r\partial r + \partial^2 n/\partial x^2) \tag{2}$$

where D is the diffusion coefficient for metastable atoms and k is the number of dissipative impacts per second per metastable atom.

From kinetic theory:—

$$D = \frac{(3R\theta(1/m+1/M))^{1/2}}{3\pi\sigma^2 N} = \frac{\theta(3R\theta(1/m+1/M))^{1/2}}{3\pi\sigma^2 \times 9.71\times 10^{18} p} \tag{3}$$

where R is Boltzmann's constant, θ the absolute temperature, m the mass of metastable atom in gm, M the mass in gm of atom of gas, p the pressure in mm, N the number of atoms per cc of gas and σ the distance between centers at impact in cm and

$$k = 2\gamma\sigma^2 N\left[2\pi R\theta\left(\frac{1}{m}+\frac{1}{M}\right)\right]^{1/2} = 2\gamma\sigma^2 p/\theta \times 9.71\times 10^{18}\left[2\pi R\theta\left(\frac{1}{m}+\frac{1}{M}\right)\right]^{1/2} \tag{4}$$

where γ is the probability that an impact shall raise or lower the metastable atom to a different stationary state.

It is necessary to solve Eq. (2) subject to the conditions that:

$$\text{at } t=0, \quad n=f(r,x)$$
$$\text{at } t>0, \quad n=0 \text{ at } r=c \qquad \text{at } t>0, \quad n=0 \begin{cases} \text{at } x=-l/2 \\ \text{at } x=+l/2. \end{cases}$$

The solution is found to be:—

$$n=\sum_{\nu=1}^{\infty}A_\nu J_0\left(\frac{\mu_\nu}{c}r\right)\cos\left[\left(\frac{\beta_\nu-k}{D}-\frac{\mu_\nu^2}{c^2}\right)^{12/}\cdot x\right]e^{-\beta_\nu t} \tag{5}$$

where $\mu_\nu=\nu^{th}$ root of the equation $J_0(\mu)=0$,

$$\beta_\nu=\left[(2\nu-1)^2\frac{\pi^2}{l^2}+\frac{\mu_\nu^2}{c^2}\right]D+k \tag{6}$$

and the A's are such that

$$\sum_{\nu=1}^{\infty}A_\nu J_0\left(\frac{\mu_\nu}{c}r\right)\cos\left[(2\nu-1)\frac{\pi}{l}x\right]=f(r,x).$$

Let N' be the average number of metastable atoms per unit volume through which the beam of light has passed. Then

$$N'=\frac{1}{\pi b^2 l}\int_0^b\int_{-l/2}^{+l/2}2\pi nr\,dr\,dx$$

$$=\sum_{\nu=1}^{\infty}C_\nu e^{-\beta_\nu t}$$

where the C's are constant coefficients.

From Eq. (6) we have

$$\beta_1=\left(\frac{\pi^2}{l^2}+\frac{5.81}{c^2}\right)D+k,\quad \beta_2=\left(9\frac{\pi^2}{l^2}+\frac{30.5}{c^2}\right)D+k,\qquad \text{etc.}$$

and consequently it is seen that, no matter what values l and c have, the exponential constants in the higher series terms increase very rapidly. If, therefore, we limit ourselves to large values of the time, we may discard all except the first term of the series, and obtain the result,

$$N'=C\,e^{-\beta t} \tag{7}$$

where

$$\beta=\left(\frac{\pi^2}{l^2}+\frac{5.81}{c^2}\right)D+k. \tag{8}$$

I. Neon

The experiments of Meissner and Graffunder give us the percentage absorption of $\lambda=6402$ as a function of the time for different neon pressures. If we adopt their attitude, as expressed by Eq. (1), then Eq. (7) tells us that the latter portions of the curves of $1-I/I_0$ against t ought to be exponential. Upon replotting these curves, this is found *not* to be the case. The reason is that Eq. (1) is not applicable to the experimental set-up of Meissner and Graffunder. They used a long narrow absorption tube, such as to warrant the use of the exponential law of absorption, namely

$$I = I_0 e^{-\alpha N' l} \tag{9}$$

where α is the atomic absorption coefficient of metastable neon atoms for $\lambda = 6402$, N' the average number of metastable neon atoms per cc traversed by the light beam, and l the length of the absorption tube. It is readily seen that Eqs. (1) and (9) agree for small values of $\alpha N' l$ but are quite different for large values. It is a simple matter to compute N' (in arbitrary units) from values of $1-I/I_0$ on the basis of Eq. (9), and upon plotting the logarithm of these new values of N' against the time, the portions of the curves corresponding to $t > 2\times10^{-4}$ sec are all straight lines. The slopes of these straight lines give the exponential constants. The exponential constants are given in Table I.

TABLE I.

Neon pressure in mm	Exponential constant	Neon pressure in mm	Exponential constant
0.50	0.384×10^4	2.15	0.276×10^4
1.02	$.234\times10^4$	3.02	$.345\times10^4$
1.42	$.214\times10^4$	5.60	$.556\times10^4$

From Eqs. (3), (4) and (8),

$$\beta = \left(\frac{\pi^2}{l^2} + \frac{5.81}{c^2}\right) \frac{\theta(6R\theta/m)^{1/2}}{3\pi\sigma^2\times9.71\times10^{18}} \left(\frac{1}{p} + \frac{4\gamma\sigma^2(R\theta/m)^{1/2}}{\theta}\right) \times 9.71\times10^{18} p.$$

In Meissner and Graffunder's experiments: $l = 12$ cm, $c = 1.8$ cm, $\theta =$ about 300°K, $m = 33.3\times10^{-24}$ gm and $R = 1.37\times10^{-16}$, whence

$$\beta = 5.15\times10^{-13}/\sigma^2 p + 8.00\times10^{21}\gamma\sigma^2 p. \tag{10}$$

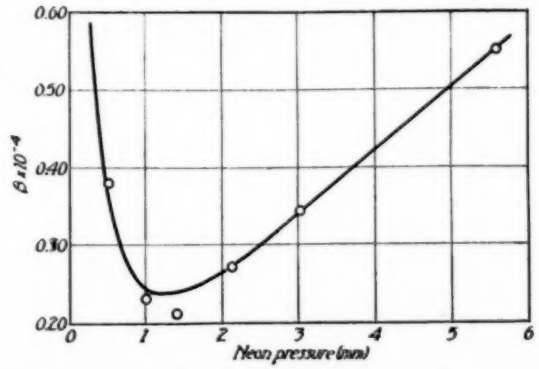

Fig. 2. Exponential constants of Table I as function of neon pressure. The curve is a plot of $\beta = 0.15\times10^4/p + 0.095\times10^4 p$.

In Fig. 2 the exponential constants of Table I are shown as points, and they are seen to lie quite well on the curve

$$\beta = 0.15\times10^4/p + 0.095\times10^4 p. \tag{11}$$

From Eqs. (10) and (11) we obtain: $\sigma = 1.85\times10^{-8}$ cm and $\gamma = 0.00035$.

From viscosity measurements, the radius of a normal neon atom is found to be 1.17×10^{-8} cm. Subtracting this value from the value of σ just found, we get for the radius of a metastable neon atom 0.68×10^{-8} cm, which is about 0.6 the normal value. This will be discussed later along with the interpretation of γ.

The recent work of Eckstein[2] provides a check on the experiments of Meissner and Graffunder. Eckstein measured the absorption of $\lambda=6402$ and $\lambda=6143$ (See Fig. 1a) in a cylindrical column of electrically excited neon in the steady state at various neon pressures and at constant current. Translating his values of percentage absorption into values of N' by means of Eq. (9) and plotting these values of N' against the neon pressure we get the dotted curve shown in Fig. 3. The circles represent the values obtained

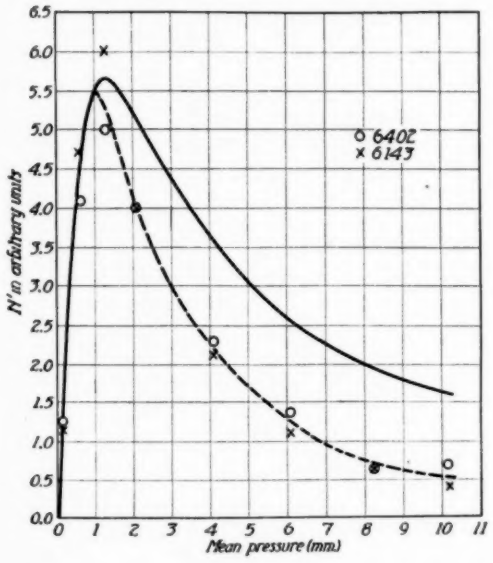

Fig. 3. Values of N' from Eckstein's measurements of absorption of λ6402 and λ6143 in neon. Dotted curve—experimental; full curve—Eq. (12).

by measuring the absorption of $\lambda=6402$ and the crosses refer to $\lambda=6143$ with the scale changed.

A theoretical expression can be obtained for the relation between N' and p on the basis of the same assumptions that were made in the beginning, except that, in place of assumption (1) we shall suppose that, in the steady state, with the current in the absorption tube constant, the rate of formation of metastable atoms is constant. Also, no appreciable error is introduced in regarding the absorption tube used by Eckstein as an infinite cylinder. We have, then, merely to solve the equation for the steady state

$$D(\partial^2 n/\partial r^2+\partial n/r\partial r)=kn-P$$

[2] L. Eckstein, Ann. d. Physik **87**, 1003 (1928).

where D and k have the same meaning as before and P is the constant rate of formation of metastable atoms. The boundary conditions are: when $r=c$, $n=0$, and when $r=0$, $n=$ finite. The solution is found to be

$$n=\frac{P}{k}\left[1-\frac{J_0(i(k/D)^{1/2}r)}{J_0(i(k/D)^{1/2}c)}\right]$$

and the average number of metastable atoms per cc traversed by the light beam (which completely filled the absorption tube), N', is

$$N'=\frac{P}{k}\left[1-\frac{2}{c(k/D)^{1/2}}\,\frac{-iJ_1(ic(k/D)^{1/2})}{J_0(ic(k/D)^{1/2})}\right]. \tag{12}$$

Everything in Eq. (12) is known except P which we have assumed constant. D and k are obtained from Meissner and Graffunder's experiments and $c=1.8$ cm. Table II gives the numerical values. Eq. (12) is plotted in Fig. 3 as a heavy curve. It is seen that the agreement for small neon pressures is quite good. For large neon pressures where N' is approximately equal to P/k, the curve is too high, indicating that k in Eckstein's experiments is larger than in Meissner and Graffunder's. This is not surprising since the light beam, filling the absorption tube must have had an effect in removing metastable atoms comparable to the other effects. We shall regard, in what is to follow, that the values of k that fit Meissner and Graffunder's experiments represent a lower limit to the values of k that are correct for Eckstein's experiments.

TABLE II.

Pressure of neon in mm	D from M. & G.	k from M. & G.	N' (Arbitrary units) from absorption of 6402 and 6143	N' (Arbitrary units) from Eq. (12)
0.2	4060	190	1.60	1.30
0.3	2700	285	2.60	2.73
0.5	1620	475	3.85	3.80
0.7	1160	665	4.80	4.81
1.0	811	950	5.50	5.50
1.5	540	1430	5.00	5.57
2.0	406	1900	4.10	5.21
3.0	270	2850	3.05	4.28
5.0	162	4750	1.75	3.02
7.0	116	6650	1.00	2.27
10.0	81.1	9500	.50	1.67

If a foreign gas is present at a very low pressure then D remains unchanged but k is the sum of the k for neon alone and the k representing the number of dissipative impacts per sec per metastable neon atom with the foreign gas. If therefore, the pressure of the foreign gas is varied while the neon pressure remains constant, the new k will equal the old $k+k'p$ where $p=$ pressure of foreign gas in mm, and

$$k'=2\gamma\sigma^2\times 9.71\times 10^{18}\left[2\pi R\theta\left(\frac{1}{m}+\frac{1}{M}\right)\right]^{1/2}/\theta \tag{13}$$

We will have then

$$J=\frac{N' \text{ without foreign gas}}{N' \text{ with foreign gas}}$$

$$=\frac{\frac{P}{k}\left[1-\frac{2}{c(k/D)^{1/2}}\cdot\frac{-iJ_1[ic(k/D)^{1/2}]}{J_0[ic(k/D)^{1/2}]}\right]}{\frac{P}{k+k'p}\left[1-\frac{2}{c[(k+k'p)/D]^{1/2}}\cdot\frac{-iJ_1\{ic[(k+k'p)/D]^{1/2}\}}{J_0\{ic[(k+k'p)/D]^{1/2}\}}\right]}$$

and to a sufficient approximation at the neon pressures employed by Eckstein

$$J=1+k'p/k.$$

Table III gives Eckstein's results for a mixture of Ne and H_2, the neon pressure remaining constant at 2.18 mm.

TABLE III.

Pressure of H_2 in mm	% abs. of 6402	N'	J	% abs. of 6143	N'	J
0	61.4	4.14	1.00	48.3	2.85	1.00
1.4×10^{-3}	46.0	2.68	1.54	33.5	1.78	1.60
2.7×10^{-3}	17.9	0.86	4.81	12.2	0.56	5.09
3.7×10^{-3}	14.0	0.66	6.28	11.2	0.51	5.58
5.2×10^{-3}	10.0	0.46	9.00	8.7	0.40	7.13

In Fig. 4 J is plotted against the hydrogen pressure and a straight line is drawn. The slope yields a value of 1.37×10^3 for k'/k. Taking as a lower

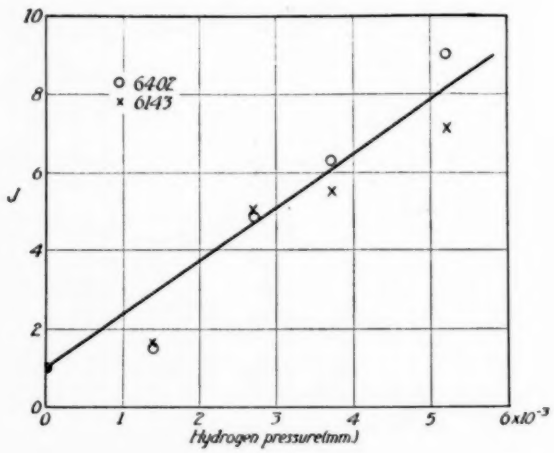

Fig. 4. Values of J as a function of pressure of hydrogen.

limit for k the value 2.07×10^3 obtained from Meissner and Graffunder's experiments for the neon pressure 2.18 mm, we get as a lower limit for k' the value 2.84×10^6, and finally, using Eq. (13), we get $\gamma=0.48$. It is quite

likely that k in Eckstein's experiments is twice as large as in Meissner and Graffunder's and therefore it is possible that γ is unity, which would be expected in virtue of the large amount of energy that a metastable neon atom has compared with the small amount required by a hydrogen molecule for dissociation or excitation. Treating Eckstein's results for N_2 and He in the same way, we obtain, very approximately the values: γ for $N_2 = 0.06$ and for He, $\gamma = 0.0002$.

II. Mercury Vapor

Several years ago the author performed a series of experiments[3] to determine the lifetime of the radiation imprisoned within a cylindrical mass of Hg vapor, and attempted to apply to the results the theory of the diffusion of imprisoned resonance radiation extended to include impacts of the second kind. The exponential constants which are given in Table IV were all very much larger than those calculated according to radiation diffusion and it was concluded that the discrepancy was due to absorption line broadening. Recently, experiments have been performed by Ramsauer[4] and Asada[5,6] which suggest a more satisfactory explanation of the results. According to these writers, metastable $^3P_0$ Hg atoms can give evidence of their presence by being raised to the excited $^3P_1$ state and then radiating $\lambda = 2537$. (See Fig. 1b).

Table IV

No. of Hg atoms per cc $\times 10^{-15}$	Exponential constant $\beta \times 10^{-4}$ for large cell	$\beta \times 10^{-4}$ for small cell
0.77	2.66	
1.40	1.42	2.81
2.50	0.881	1.93
4.40	0.707	1.21
7.26	0.689	0.947
11.8	0.772	0.900
18.8	0.964	1.06
29.0	1.32	1.35

This was shown conclusively by the following experiment: Mercury vapor at the saturation pressure corresponding to room temperature was mixed with nitrogen at a few millimeters pressure and was excited for a while by $\lambda = 2537$. The excitation was then cut off, and the persistence of 2537 was noted for almost 10^{-2} sec after the cut-off. This persistence can not be accounted for on the basis of the diffusion of the radiation, for on this basis the time [7] should be of the order of 10^{-6} sec. The only conclusion that can be drawn is that the metastable atoms which are known to be produced by impacts between excited Hg atoms and N_2 molecules decay partly by dif-

[3] M. W. Zemansky, Phys. Rev. **29**, 513 (1927).
[4] G. Ramsauer, Naturwiss. **16**, 576 (1928).
[5] T. Asada, Phys. Zeits. **29**, 708 (1928).
[6] T. Asada, R. Ladenburg, and W. Tietze, Phys. Zeits. **29**, 549 (1928).
[7] H. W. Webb and H. A. Messenger, Phys. Rev. **33**, 319 (1929).

fusing to the walls and partly by being raised to the $^3P_1$ level from which they either radiate 2537, or become metastable again. Asada, in a footnote suggests that this may be the explanation of the persistence of 2537 in pure Hg vapor at high vapor pressures. The author had arrived at this same conclusion before the papers of Ramsauer and Asada appeared, and the following is the result of the calculation with this point of view.

Since we are supposing now that the radiation emitted is proportional to to the number of times per sec that metastable Hg atoms are raised to the excited level, the radiation emitted should decay with the same exponential constant as the number of metastable atoms per cc. This exponential constant is given by Eq. (8). In these experiments, l = 2.0 cm for the large cell and 1.3 cm for the small cell; c = 2.54 cm; θ = about 350°K in the region where diffusion plays the main role, and about 390°K where impacts become important; $m = 331 \times 10^{-24}$ gm, whence, from Eq. (8), for the large cell

$$\beta = 3.4 \times 3.14 \times 10^3/\sigma^2 N + 9.04 + 10^4 \gamma \sigma^2 N \tag{13}$$

and for the small cell

$$= 6.8 \times 3.14 \times 10^3/\sigma^2 N + 9.04 \times 10^4 \gamma \sigma^2 N. \tag{14}$$

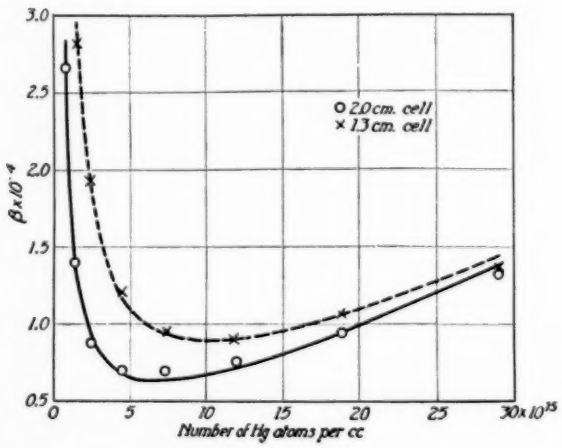

Fig. 5. Exponential constants of Table IV as function of mercury vapor pressure. Full curve—Eq. (15); dotted curve—Eq. (16).

Fig. 5 shows that the experimental points fit curves of this type very well, the points for the larger cell lying on the curve

$$= 2.0 \times 10^{19}/N + 4.6 \times 10^{-13} N \tag{15}$$

and those for the smaller cell, on the curve

$$= 4.0 \times 10^{19}/N + 4.6 \times 10^{-13} N. \tag{16}$$

From either Eqs. (13) and (15) or Eqs. (14) and (16), we get that $\sigma = 2.30 \times 10^{-8}$ cm and $\gamma = 0.0096$. Subtracting from σ the radius of the normal

Hg atom, 1.80×10^{-8} cm, we get, for the radius of the metastable Hg atom, 0.50×10^{-8} cm which is about 0.3 the normal value.

The diffusion of metastable Hg atoms through Hg vapor at different densities has been studied also by Coulliette.[8] He does not, however, give sufficient data to allow his curves to be treated by the methods of this paper. He found for σ the value 4.5×10^{-8} cm and for γ 0.00077. His value of σ yields a radius for the metastable Hg atom 1.5 times the normal value.

In a recent paper, Pool[9] measured the absorption of $\lambda=4047$ ($2^3P_0-2^3S_1$) in a cylindrical cell containing a mixture of mercury vapor at room temperature and nitrogen, as a function of the time elapsing after the excitation of the mercury vapor. The percentage absorption of 4047 gives the same information about the average number of metastable $^3P_0$ Hg atoms as the absorption of 6402 gives concerning the average number of metastable $^3P_2$ neon atoms, and in the same way. (See Fig. 1b). That is, using Eq. (9), Pool's values of $1-I/I_0$ enable us to obtain curves of N' against t for all nitrogen pressures. These were found to be exponential, and the exponential constants are given in Table V.

TABLE V.

Pressure of nitrogen (mm)	$\beta\times10^{-4}$	Pressure of nitrogen (mm)	$\beta\times10^{-4}$
2.5	0.791	16	0.364
4.8	.276	38	.545
6.8	.253	63	1.08
8.7	.274		

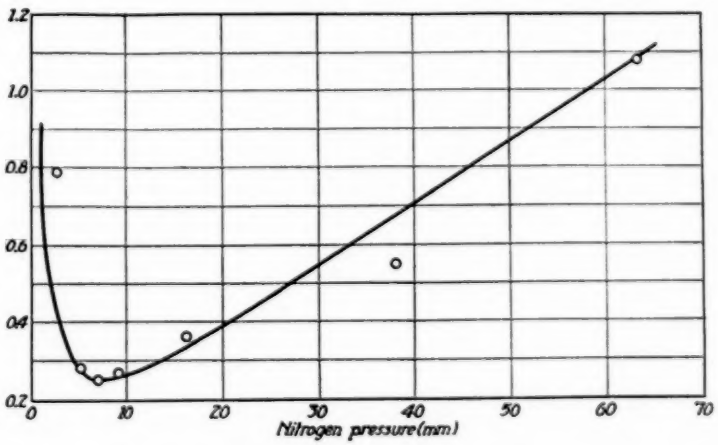

Fig. 6. Exponential constants of Table V as function of nitrogen pressure. Curve is a plot of $\beta=1.0\times10^4/p+0.017\times10^4p$.

In Fig. 6 the exponential constants are shown as points, and they are seen to lie fairly well on the curve

$$\beta=1.0\times10^4/p+0.017\times10^4p.$$

[8] J. H. Coulliette, Phys. Rev. **32**, 636 (1928).
[9] M. L. Pool, Phys. Rev. **33**, 22 (1929).

In Pool's experiments, $l=10$ cm, $c=0.75$ cm, $\theta=293°$K, $M=46.2\times10^{-24}$ gm (N_2), and $m=331\times10^{-24}$ gm (Hg). Substituting these values in Eq. (8), we get

$$\beta=1.81\times10^{-12}/\sigma^2p+0.522+10^{22}\gamma\sigma^2p$$

from which we get $\sigma=1.35\times10^{-8}$ cm and $\gamma=0.00018$. The value of 1.35×10^{-8} cm for σ is astonishing since it is smaller than the gas-kinetic value of the radius of the nitrogen molecule, which is 1.58×10^{-8} cm.

The life of metastable Hg atoms was measured by Asada[6] by a very ingenious method, in which the emission of the green line 5461 was used to provide a measure for the rate at which metastable Hg atoms were raised from the $^3P_0$ level to the $^3S_1$ level by the absorption of 4047. (See Fig. 1b). The metastable Hg atoms were formed in a mixture of Hg vapor at room temperature and nitrogen at various pressures, and the life was found to depend on the nitrogen pressure. It has not been possible, as yet, to obtain the relation between exponential constant and N_2 pressure, and consequently σ and γ cannot be found. Asada's complete results will provide an interesting check on Pool's experiments.

Discussion

The results of all these calculations are collected in Table VI. Column three gives the value of σ calculated from the experimental data, and column four the value of σ obtained from viscosity measurements on normal atoms. The radius of the metastable atom, given in column five, is obtained by subtracting the radius of the normal atom from the experimentally determined value of σ. The most striking result that appears is that, in all cases but

Table VI.

Combination	Author	Exp. $\sigma\times10^8$	Normal $\sigma\times10^8$	Radius of met. atom $\times10^8$	γ	ϵ	Nearest energy difference
Ne Ne_m	Meissner and Graffunder	1.84	2.34	0.67	0.00035	0.26	0.24
H_2 Ne_m	Eckstein	1.76	2.26	.67	$>.48$		
N_2 Ne_m	Eckstein	2.25	2.75	.67	$>.06$		
He Ne_m	Eckstein	1.67	2.17	.67	$>.0002$	$<.28$	.24
Hg Hg_m	Zemansky	2.30	3.60	.50	.0096	.22	.20
Hg Hg_m	Coulliette	4.50	3.60	2.7	.00077	.31	.20
N_2 Hg_m	Pool	1.35	3.35	0	.00018	.28	.20

one, the radius of the metastable atom comes out less than its normal value. (Strictly speaking, Eckstein's experiments merely show that they are consistent with the value of σ found by Meissner and Graffunder). It is hard to say what this means. It is usually assumed that an atom has a larger radius in an excited state than in the normal state, and calculations of the radius of atoms in excited non-metastable states seem to verify this supposition. It is rather interesting, however, to note that the more refinements

that are used in treating the experiments on the excited $^3P_1$ Hg atom, the smaller the radius is taken to be. For example, Stuart[10] assumed for this radius a value 3.4 times the normal, Foote[11], a value 1.2 times the normal and Gaviola[12] a value equal to the normal in some cases and larger than the normal in others. It is the opinion of the author that none of these values is reliable because the calculations that give rise to them are not refined enough to take account of the experimental conditions under which Stuart worked. There seems to be no reason *a priori* why an excited atom cannot have a radius smaller than the normal value, inasmuch as the whole conception of a radius is such an indefinite one. The value of σ yielded by Pool's experiments is very baffling. Perhaps it is connected with a sort of resonance between the $^3P_1$ and $^3P_0$ states of the Hg atom and the nitrogen molecule suggested by Cario and Franck[13] to account for the inability of nitrogen to quench Hg resonance radiation at high temperatures.

The values of γ are not quite as perplexing as the values of σ. In an impact between a metastable atom and a foreign gas molecule, the metastable atom may either give up some or all of its energy, or it may receive energy and be raised to a higher state. It is quite possible that in the case of impacts between metastable neon atoms and hydrogen and nitrogen, the metastable neon atom gives up some of its energy (16.5 volts) in dissociating the hydrogen and nitrogen molecules. Since the hydrogen molecule requires only 4.3 volts and the nitrogen molecule only 9.0 volts for dissociation, one would expect rather high impact probabilities. The values of 0.48 and 0.06 (these values being only lower limits) seem to corroborate this point of view.

On the other hand, when a metastable atom collides with a normal atom of the same kind, or with an atom whose first excitation potential is higher than the energy of the metastable atom, one would expect either nothing at all, or the lifting of the metastable atom to the next state of higher energy. On this basis γ ought to be equal to or less than that fraction of all the collisions in which the mutual kinetic energy is sufficient to raise the metastable atom to a higher level. Let ϵ represent this energy. Then, from kinetic theory

$$\gamma \leqq [(\epsilon/R\theta)+1]e^{-\epsilon/R\theta}.$$

In column seven of Table VI is given the value of ϵ corresponding to the value of γ in column six. It is seen that in the case of metastable Hg atoms the value of ϵ agrees fairly well with the difference in energy between the 2^3P_0 and 2^3P_1 states which is 0.20 volts. This is in agreement with the statement made before: that the persistence of 2537 in Hg vapor can be due to the raising of metastable 2^3P_0 atoms to the 2^3P_1 state and consequent radiation. A difficulty arises, however, in the case of metastable neon atoms dif-

[10] H. A. Stuart, Zeits. f. Physik **32**, 262 (1925).
[11] P. Foote, Phys. Rev. **30**, 288 (1927).
[12] E. Gaviola, Phys. Rev. **33**, 309 (1929).
[13] G. Cario and J. Franck, Zeits. f. Physik **37**, 619 (1926).

fusing through Ne and He. Here one would expect an impact probability corresponding to the difference in energy between the 2^3P_2 and 2^3P_1 states which is 0.05 volt. The experimental values of γ however, correspond to a much higher energy difference, —in the neighborhood of the energy difference between the 2^3P_2 and the 2^1P_1 states (0.24 volt). The only explanation of this that suggests itself is that perhaps when a metastable neon atom is raised to the 2^3P_1 or to the 2^3P_0 level it is not lost permanently. Since these two states lie so close to the 2^3P_2 state, neon atoms are probably going up and down among the states continually and in large numbers, and, although strictly speaking, this should be taken into account in the mathematical treatment, a crude way of looking at the state of affairs is to consider the rate at which metastable atoms are being raised to the 2^3P_1 and 2^3P_0 states equal to the rate at which they are entering the metastable level from these two states. On this point of view, the only way to get rid of a metastable atom is to raise it all the way to the $^1P_1$ state from which it radiates, before it can be knocked down.

It is a pleasure to acknowledge my indebtedness to the National Research Council and to Professors K. T. Compton and L. A. Turner for the opportunity to discuss this paper with them.

THE PHOTOELECTRIC THRESHOLD OF A DOUBLY EVAPORATED FILM

By Roderick Bissell Jones*
Sloane Physics Laboratory, Yale University

(Received January 11, 1929)

Abstract

A method is described whereby a platinum, a nickel, and a "double" platinum-nickel film were obtained by evaporation, simultaneously and under the same conditions. The threshold wave-lengths were first found from saturation photoelectric currents obtained with monochromatic light of different wave-lengths. These values, which were confirmed and determined more precisely by retarding-potential, photocurrent curves, are for Ni 3333A, for Pt 2804A and for the double Ni-Pt 3318A. A similar investigation with tungsten and platinum gave the thresholds of the Pt and the double Pt-W film at 2831A and 2804A respectively, almost 500A above the threshold of W which was 2338A. The threshold of each double film is, therefore, practically the threshold of the constituent which, when pure, has the longer wave-length threshold.

Introduction

IN GENERAL, when light of a frequency ν is incident upon a metallic surface electrons are emitted with velocities ranging from zero up to a definite maximum velocity v. In the equation usually given,

$$(V-K)e=h\nu-h\nu_0, \tag{1}$$

where K is the contact difference in potential between the film and the opposing electrode, h, the Planck constant, $h\nu_0$ is the energy lost in passing from a system where the photoelectron starts to a point just outside the surface.

It is not known what fraction of this energy is spent in separating the electron from the original atom and what work is done to take the electron through the outer surface. It was thought that some light might be thrown on this question by finding the photoelectric thresholds of three metal films formed under the same conditions by evaporation, two of these being made of two different metals and a third of a mixture of the two. This has been done in the experiments to be described and the interesting result found that the photoelectric threshold of the mixture of two metals(in the two different sets of metals used) is the same as that of the constituent having the threshold of lower frequency.

Experimental Arrangement

Figure 1 gives a diagrammatic representation of the apparatus used in the present experiment. The apparatus was made of Pyrex glass. Q is a quartz

* This communication is a part of a dissertation presented in partial fulfillment of the requirements for the degree of Doctor of Philosophy in Physics at Yale University.

plate to admit the ultra-violet light. *D* is a cylinder to collect the photo-electrons. It was constructed of oxidized copper, the threshold wave-length of which is below that part of the spectral region in which the work was to be done. *B* are two filaments of different metals for the purpose of depositing films by evaporation. Evaporation was the method selected to be used because of the greater homogeneity and freedom from gas in the case of films prepared in this way as compared with those obtained by sputtering.[1] In this case where the nature of the surface was to enter into the problem so intimately it was deemed advisable to do away with the presence of gases as much as possible. The three thin glass plates *H*, upon which the films were laid, were held vertically by three iron containers, which were in turn supported by the vertical aluminum shaft *E*. This vertical support was slotted to run through a keyed passage in the aluminum throat piece *F* and, since this latter was secured by device in the glass, the plates throughout all the vertical motion faced on the same direction, rotation being prevented. This was necessary to maintain the plates perpendicular to the beam of light entering *Q* in order that the reflected light should not strike the cylinder, for in spite of the fact that the cylinder is insensitive, it is naturally desirable to avoid all possibility of a spurious source of photoelectrons. The aluminum rod was secured at the top to a hollow iron cylinder. The vertical motion of this latter was produced by means of a solenoid on the outside of the glass. (Not shown.) A cam gave the suspended solenoid a uniform up and down motion. By means of this vertical oscillation it was secured that the uppermost plate was subjected only to the influence of the upper filament, the lowest plate was subjected only to the influence of the lower filament, while the middle plate was subjected to both filaments. It will thus be seen that one of the films deposited by evaporation was of one pure metal, a second was of a second pure metal and that the third film was a mixture of these two metals. The temperatures of the two filaments were so regulated as to give approximately equal rates of deposition and the speed of the up and down motion of the plates was such as to give intimate mixing of the metals on the middle glass disk. Judging from a comparison of opacity with films of known thickness, the films were about twenty molecules deep, which means, if the total number of exposures is taken into account, that each layer of molecules was formed by exposure alternately to the one evaporation and then to the other, seventy-five times before each layer was complete. This insured the presence of an equal number of molecules of both kinds in

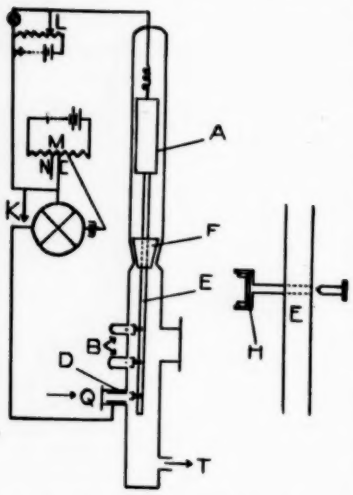

Fig. 1. Diagram of apparatus.

[1] C. Cha, Phil. Mag. **49**, 262 (1925).

the surface layer and each layer underneath. After the deposition of the films larger displacements of the solenoid placed any one of the films behind the Faraday cylinder and in the path of the light.

In order to secure proper electrical connections to very thin films, it is desirable that the external mechanical connections be made to a thick boundary of the film of the same material, which tapers off at its edges into the main thin film, whose properties are being investigated in the experiment. Stuhlmann and Compton[2] found that they secured results for films on glass or quartz, practically as good as their best, by using a sputtered contact and this method was adopted here. The sputtering was done before the formation of the films was begun. Iron spring rings served both to retain the glass plates in their holders and to form the electrical connection between the sputtered edge and the iron holder. The connection to the source of the retarding potential is shown in the diagram at L.

A two stage mercury diffusion pump, backed by a Cenco oil pump maintained a vacuum of 10^{-5} mm of mercury while the films were being made and studied. Pressures were measured with a McLeod gauge and a liquid air trap was used to keep mercury vapor from the rest of the apparatus. The quadrant electrometer used in this experiment had a sensitivity of 3700 mm/volt.

The quadrant electrometer was provided with a subsidiary condenser whose central member was attached to its insulated quadrant. The outer member of this condenser was connected to the point C on a megohm resistance. The midpoint of this megohm was connected to the case of the electrometer, and a point N on the other side of the megohm was connected to the needle of the electrometer. The ends of the megohm were connected to a battery, and the capacity of the condenser was adjusted so that on throwing on the battery, no deflection was obtained in the needle when the quadrant was disconnected from the case. By this method, the influence of fluctuations of the potential of the needle during the measurements was avoided. The source of light was an iron arc used in conjunction with a Gaertner monochromatic illuminator.

PHOTOELECTRIC THRESHOLDS

The photoelectric currents, with varied wave-length of exciting light, were taken for all films, the voltage being sufficient to obtain saturation current. Proper alignments were necessary to prevent disturbing reflections.

The pure platinum photocurrent vs. wave-length curve, Fig. 2, shows the usually accepted platinum threshold with reasonable certainty at 2800A. The pure nickel gives 3320A for the threshold wave-length. This latter value was further confirmed when the retarding potential vs. photocurrent curves were taken, since it was found impossible to get any photocurrents at any voltage with wave-lengths above 3300A. The point of interest is the fact that the threshold for the double nickel-platinum film is approximately the

[2] O. Stuhlmann, Jr. and K. T. Compton, Phys. Rev. **2**, 209 (1913).

same as for the pure nickel, which is the one of the two pure films which has the longer wave-length threshold.

Another pair of metals used was tungsten and platinum. The curves for these are shown in Fig. 3. They are not as easy to interpret as those in Fig. 2. The "foot" attributable to scattered light in the monochromator in the case of W joins the main curve more gradually than does that for Pt in Fig. 2. A reasonable extrapolation of the main curve gives for the threshold a wave-length of about 2340A which is somewhat above 2300A, the value obtained by Hagenow.[3] These curves are consistent with Fig. 2 in that the threshold of the double film is again equal, or nearly equal, to that of the constituent whose threshold wave-length is the longer. The Pt threshold obtained from

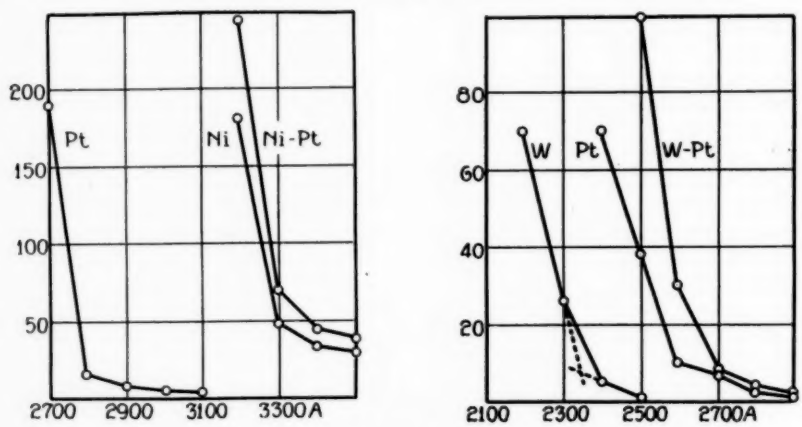

Figs. 2 and 3. Saturation photoelectric current vs. wave-length.

Fig. 3 does not agree with that obtained from Fig. 2, probably owing to some variation in one of those unknown factors which seem to govern so largely the position of photoelectric thresholds. This method not being entirely satisfactory in this regard, it appeared best to try a retarding potential method.

Retarding Potential vs. Wave-length

To find the maximum velocity of photoelectron emission for any wave-length the routine was not to try to find the exact retarding potential experimentally which would just stop the departure of the photoelectrons, "a very uncertain procedure at best"[4] but rather to plot the photocurrent, retarding-potential curve. Should the least amount of radiation of frequencies somewhat greater than that being considered enter the apparatus, as was unavoidable, the voltage requisite completely to hinder a negative discharge would not be the value sought. In all the retarding potential curves obtained there were evidences of the presence of light coming from the monochromator of a frequency greater than the indicated frequency. The current curve,

[3] Hagenow, Phys. Rev. **13**, 422 (1919).
[4] Millikan, Phys. Rev. **7**, 18 (1916).

for any indicated frequency of light being used, approached the potential axis at a constant slope until just before it reached that axis when it would approach the axis asymtotically.

In studying the films by the retarding potential method it was found that the slope of the curves giving the variation of photo effect with retarding

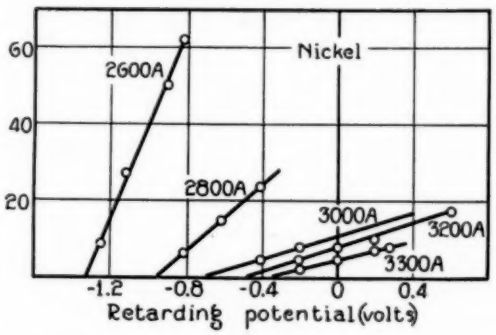

Fig. 4. Photo-electric current vs. retarding potential.

potential for light of different given frequencies decreased rapidly as the threshold frequency was approached. Naturally with light of threshold frequency there would be no current no matter what the value of the retarding potential, i.e., the slope would be zero.

An example of one set of curves as obtained for a nickel film is given in Fig. 4, the individual wave-length curves of which are as yet uncorrected for changes of light intensity and of slit width used in the monochromator.

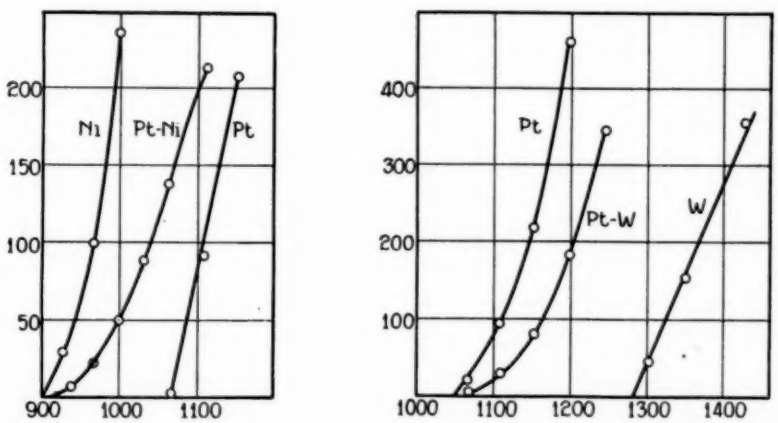

Figs. 5 and 6. Arctan (photocurrent retarding potential) vs. frequency $\times 10^{-12}$.

The intensity of the lines used in the Fe spectrum was measured with a photoelectric cell under the conditions of the research, corrected with the cell's sensitivity factor. The data so taken, when properly corrected for the two variations just mentioned, formed the basis for the curves of the various films which are represented in Figs. 5 and 6. Each point on these curves has for

its ordinate the angle of slope of one of the curves examples of which are given in Fig. 4. As stated above, these angles are expressed as variations of photo current with change of retarding potential. The object of plotting the results in this way is to find the frequency for which there would be no photo-current with any potential, without actually attempting experimentally to realize this limiting condition.

An examination of the curves in Figs. 5 and 6 shows, as was found in the first part of the work, that for both sets of films the threshold frequency of the double film is approximately that of the component having the lower frequency threshold. The actual values of the wave-length thresholds obtained from these curves are for Ni 3333A, for Pt 2864A, for W 2338A, for the double Ni-Pt 3318A and for the Pt-W 2804A.

Conclusions

The threshold of the double film agrees with that of the component having the upper wave-length threshold in each case to within a small percentage although the threshold difference between the pure metals in each of the pairs studied is about 500A.

It will be noted that in the platinum and tungsten case, platinum, having a higher threshold than tungsten, was the deciding factor in the new threshold; but in the case of nickel and platinum it was not the platinum but the nickel which was effective.

The investigation described in this paper was carried out under the direction of Professor W. F. G. Swann of the laboratory and the writer desires to convey his thanks to Professor Swann for the very kind advice and encouragement which he extended through the course of the work. For his continued interest in the problem appreciation is expressed to Professor John Zeleny, Chairman of the Physics Department.

THE PHOTO-IONIZATION OF THE VAPORS OF CAESIUM AND RUBIDIUM

By Ernest O. Lawrence and N. E. Edlefsen
University of California at Berkeley

(Received June 6, 1929)

Abstract

A modification of Foote and Mohler's space charge method for the measurement of photo-ionization was devised which compensated out spurious effects due to fluctuations of temperature and increased the useful sensitivity of the space charge to positive ions about one hundred fold. By measuring simultaneously photo-ionization and light intensities the following results have been obtained. In caesium, the ionization per unit light intensity B_ν varies with frequency ν (over the range 2200A to 3130A) according to the equation

$$B_\nu = \frac{\text{const}}{\nu^3(\nu - \nu_0)}$$

This relation also represents fairly well the experimental observations of B_ν in rubidium. Thus, the continuous absorption resulting in ionization decreases with wave-length much more rapidly than the analagous absorption beyond the Lyman and Balmer series limits as calculated on the wave mechanics by Sugiura, Oppenheimer, and Reiche. The results, moreover, are not even qualitatively similar to Hargreaves' calculation of the variation with frequency of B_ν for lithium. Assuming the principle of detailed balance it follows from these experiments that the effective collision capture cross-sections of caesium and rubidium ions for electrons vary inversely as the square of the energy of the electrons relative to the ions. This is the Thomson recombination law and has been derived on the wave mechanics by Oppenheimer for the recombination of protons and electrons. The existence of photo-ionization by absorption of principal series lines in caesium, so clearly exhibited by Mohler, Foote and Chenault, has been confirmed and also has been observed in rubidium.

EXPERIMENTAL difficulties have hampered studies of photo-ionization of the alkali vapors and results obtained have been somewhat meagre and apparently inconsistent. For example, Samuel[1] observed appreciable ionization of potassium vapor only by wave-lengths near the head of the principal series while on the other hand Williamson[2] and Lawrence[3] have concluded from their experiments that the probability of ionization increases rapidly as one passes to shorter wave-lengths. Further, in caesium vapor Kunz and Williams[4] found ionization setting in exactly at the series limit while Foote and Mohler[5] have obtained convincing evidence that caesium is ionized by wave-lengths considerably longer, the ionization efficiency being only a maximum at the series limit. There are several rather cogent argu-

[1] Samuel, Zeits. f. Physik **29**, 209 (1924).
[2] Williamson, Proc. Nat. Acad. Sci. **14**, 793 (1928).
[3] Lawrence, Phil. Mag. **50**, 345 (1925).
[4] Kunz and Williams, Phys. Rev. **22**, 456 (1923).
[5] Foote and Mohler, Phys. Rev. **26**, 195 (1925).

ments leading to the conclusion that the ionization probability should indeed have a maximum value at the limit and moreover should decrease monotonically on passing to shorter wave-lengths. Mohler, Foote and Chenault[6] do not confirm the latter inference, however, for they find that the ionization probability has a minimum value in the region of 2700A and rises rapidly with decreasing wave-lengths attaining a magnitude of 40 percent of the series limit value in the region of 2536A. Little[7] has confirmed qualitatively their observations. It has been suggested that the ionization by wave-lengths on the long wave-length side of the minimum may be of caesium atoms only while the setting in of molecular ionization by shorter wave-lengths may be responsible for the subsequent rise of the ionization probability curve. It appears on this view that molecular ionization should predominate in potassium vapor since relatively many more molecules are always present and therefore the probability of ionization should be observed as a quantity which increases to shorter wave-lengths from a threshold value itself of wave-length shorter than the series limit—very much as observed by Lawrence.

The lack of agreement of the experimental observations of the various investigators however does not permit one to deduce with confidence the experimental laws governing the several photo-ionization processes. It is of importance to establish these laws because the alkalis are hydrogen-like and are readily susceptible to theoretical treatment. Contributions to this end are contained in the present paper and in another to follow on the photo-ionization of potassium vapor.

The Experimental Method

The experimental difficulties involved in studies of the photo-ionization of the alkalis were largely overcome by Foote and Mohler's[5] ingenious application of Kingdon's[8] observations of the neutralization of space charge around a filament by spiralling positive ions. Their method possesses great inherent sensitivity, for one ion in the course of time effectively neutralizes the space charge of as many as a million electrons. In order to achieve the greatest sensitivity possible using Foote and Mohler's method, which involves balancing out the thermionic emission by a potentiometer arrangement, it is clearly necessary to maintain the total electron emission constant to better than one part in a million—admittedly a difficult experimental feat. We have modified their arrangement so as to compensate out fluctuations of the thermionic emission due to changes in temperature of the filament and thereby have increased the useful sensitivity of the space charge method probably one hundred fold.

Figure 1 shows diagrammatically the arrangement. A 5 mil tungsten filament extended concentrically through two cylinders P_1, P_2 15 mm in diameter and 25 mm in length. Adjacent ends of the cylinders were closed

[6] Mohler, Foote and Chenault, Phys. Rev. **27**, 30 (1927).
[7] Little, Phys. Rev. **30**, 109 (1927).
[8] Kingdon, Phys. Rev. **21**, 408 (1923).

excepting for 2 mm holes while the other ends were open. P_1 and P_2 were attached to adjustable resistances R_1 and R_2 of about 10,000 ohms. A sensitive galvanometer G was connected across the cylinders and resistances as the diagram indicates. The cylinders were approximately symmetrical relative to the filament and therefore received nearly equal portions of the electron emission. A battery maintained them about one volt positive to the filament so that the thermionic current was limited by space charge. The heating current through the filament and the potential difference between filament and cylinders were adjusted to give the maximum sensitivity to positive ions. Usually under such conditions the thermionic current was about $5(10^{-5})$ amps. The resistances R_1 and R_2 were adjusted so as to have across them equal differences of potential arising from the thermionic current, a condition indicated by a null deflection of the galvanometer. Under these circumstances fluctuations in the electron emission due to changes of

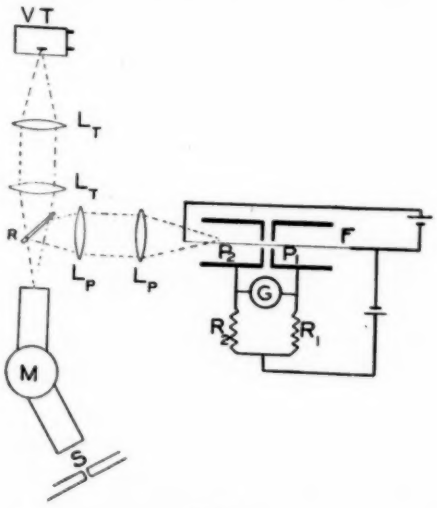

Fig. 1.

temperature of the filament produced approximately equal changes in the voltage drops across the resistances, causing thereby no sensible deflection of the galvanometer. The galvanometer responded only when the percentage changes of the currents through the resistances were not equal. This occurred when the region of P_2 was irradiated by light forming ions in the vapor which were drawn towards the filament and, spiralling around, increased the space charge limited electron emission to P_2. For small current changes due to neutralization of space charge by the ions, the galvanometer deflections were proportional to the rate of ionization of the vapor.

This compensation scheme was so effective that with quite ordinary precautions to keep conditions constant the galvanometer zero remained within the same millimeter scale reading for considerable periods of time. In most of the work a deflection of 0.2 mm of a galvanometer having a sensitivity of 2 (10^{-10}) amps per mm could be detected with certainty.

Thus, since the total thermionic emission was usually about 5 $(10)^{-5}$ amps, it was possible to detect changes in the thermionic emission due to photo-ionization of the vapor of about 1 part in 10^6.

This arrangement eliminated any remaining difficulty in measuring photo-ionization in the alkalis—even in potassium vapor—and reduced the problem of accurately determining the law of variation of ionization with frequency in caesium to finding a steady source of continuous ultra-violet light which after resolution into narrow bands of wave-lengths would be sufficiently intense to be measured by a thermopile. To this end a water-cooled hydrogen discharge tube able to carry 5 amps at 3000 volts was developed.* The tube had a diameter of 7 mm and, as far as we know, produced current densities about 10 times greater than anyone has used before in a similar type of discharge. The discharge proved to be a highly steady source of ultra-violet light, giving bands from twenty to forty angstroms wide of sufficient intensity to be measured by a vacuum thermopile in conjunction with photoelectric amplification of the galvanometer deflections and was used for the experimental study of caesium. An iron arc was used in the observations of photo-ionization of rubidium.

Light from the source S, resolved by a Bausch and Lomb monochromator M into wave-length bands (slits 0.2 mm) passed to a quartz plate R where a portion was reflected and another portion passed through. The transmitted portion was collimated and focused on a vacuum thermopile VT by the lenses L_1. Similar lenses focused the reflected portion in the cylinder P_2 of the photo-ionization tube. An additional quartz plate was inserted in the optical path to the photo-ionization tube which made the two optical paths (from R to VT and P_2) through quartz as well as air very nearly equal. Frequent tests insured that the lenses focused all of the light on the thermopile and in the region of P_2. Clearly this optical arrangement allowed simultaneous measurement of photo-ionization and light intensities, leading to values for the relative ionization per unit light intensity free from serious systematic errors.

It was found in preliminary experiments that the presence of a trace of mercury vapor gave rise to very large photo-ionization by light of wave-length 2536A, being evidently due to absorption of the light by the mercury atoms and collisions of the second kind. To eliminate such spurious effects care was taken to reduce to a minimum the presence in the tube of gases and vapors other than the alkali under investigation. The tube was of Pyrex with a quartz window joined to it by a graded seal. It was carefully baked out at 500°C and the metal parts were glowed till all traces of gases were removed. Caesium—or rubidium—introduced into a side tube by heating calcium filings with its chloride, was successively distilled into a series of constricted tubes which had received the baking at 500°C and finally into the photo-ionization tube which then was sealed off from the side tubes and the pump.

* A description of this ultra-violet source will be submitted for publication elsewhere.

RESULTS

Caesium. Figure 2 exhibits the dependence of the relative probability of ionization of caesium vapor on wave-length. The ordinates record the ionization per unit light intensity produced by wave-length bands (20 to 40A) from the monochromator set at wave-lengths given by the abscissas. The ordinates are in arbitrary units because the nature of the method of observation of the photo-ionization does not allow direct determination of absolute values. The circles and dots represent two sets of data taken by

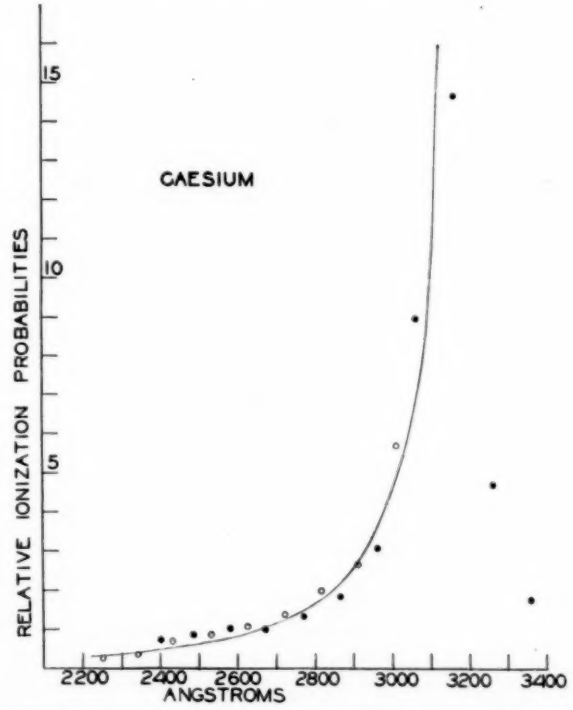

Fig. 2. The wave-length dependence of the ionization per unit light intensity B_ν in Cs. The circles and dots record two sets of observations while the curve represents $B_\nu = \text{const.}/\nu^3(\nu-\nu_0)$.

different observers during the same evening with the photo-ionization tube at a temperature of 180°C. These data indicate that the probability of ionization B_ν decreases rapidly with wave-length from the series limit along the curve of Fig. 2 which is a plot of the relation

$$B_\nu = \frac{\text{const}}{\nu^3(\nu-\nu_0)}$$

ν_0 being the series limit frequency. There is apparently a very slight deviation of the data from the curve in the region of 2500 to 2700A and in the preliminary experiments the deviation was more pronounced, some of the results showing an actual rise in the probability of ionization having a

maximum near 2500A. However, at no time was there observed a probability of ionization at 2500A which was greater than 1/8 of the series limit value. It now seems probable that the earlier observations were due to the presence of impurities in the caesium vapor. There remains, however, always the possibility that the quartz window of the photo-ionization tube possessed throughout the experiments an invisible film which absorbed ultra-violet light, introducing thereby a systematic error. We regard this possibility as highly improbable.

The study of caesium was concentrated on the region of wave-lengths well beyond the series limit where the observations of Mohler, Foote and Chenault and Little indicated a minimum in the ionization probability curve. However, several runs throughout the spectral range were made confirming the existence of ionization by wave-lengths longer than the series limit which Mohler, Foote and Chenault exhibited so well. The results presented here differ from the previous observations—in addition to showing no minimum in the probability of ionization curve—in that the decrease of the ionization probability B_ν beyond the limit is definitely more rapid. This discrepancy between the present work and the observations of Mohler, Foote, and Chenault is not surprising when it is recalled that in their work the light intensities were not measured simultaneously with the observation of ionization but were estimated from knowledge of the spectral energy distribution in the source and the probable transmission characteristics of the optical system. We cannot reconcile satisfactorily, however, Little's results with the present data.

Though the space charge method does not allow measurement of absolute values of ionization it may be useful to record the general order of magnitude of the various quantities involved in the experiments. A current of three amps passing through the hydrogen discharge tube gave a continuous spectrum of ultra-violet light of such intensity that when resolved by the monochromator into bands of 20A in the region of 2200A produced a deflection of the thermopile galvanometer of 0.1 mm. These rather small deflections were readily amplified one hundred fold by a photoelectric cell arrangement similar in principle to thermo-relay devises now widely used. These wave-length bands produced deflections of the photo-ionization galvanometer of about 1 cm corresponding to a change in the thermionic current of 2 (10^{-9}) amp. In the region of 2500A the thermopile galvanometer deflections were about 3 times as great.

Rubidium. Two independent sets of observations of the ionization of rubidium are shown in Fig. 3. The crosses represent data taken at a temperature of 197°C while the circles record observations taken with the photo-ionization tube at a temperature of 245°C. The good general concordance of the two sets of observations attests to the trustworthiness of the results and show rather definitely that the ionization probability function is independent of the vapor pressure and temperature over this range. An iron arc source was here used which because of its unsteadiness gave rise to the rather large, as compared to the caesium observations, fluctuations of

the experimental observations. The dependence on wave-length of the ionization probability B_ν in rubidium clearly is very much the same as in caesium. On the long wave side of the series limit ionization by line absorption is evident, merging into the continuous absorption at the limit where B_ν is a maximum. The successive peaks in the probability curve correspond to lines of the principal series (indicated in the Fig. along the abscissa axis) excepting the peak at 3490A which is of unknown origin. Though the plot of the experimental data suggests that ionization by absorption of light of frequency of one of the principal series lines near the limit is less probable

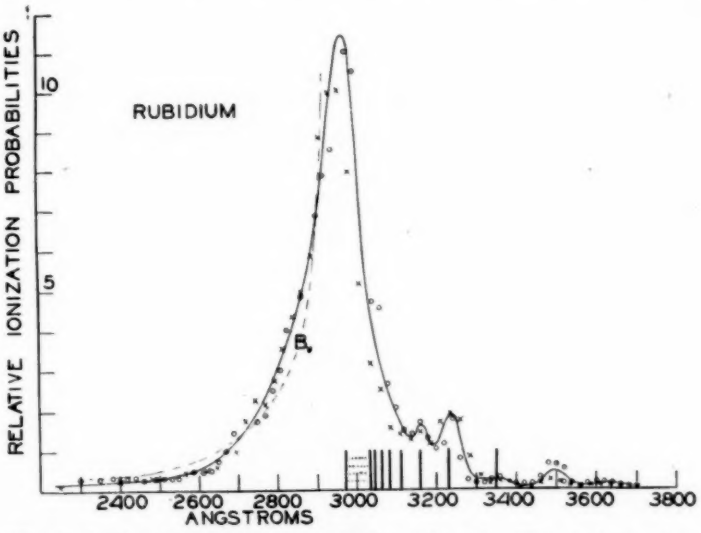

Fig. 3. The ionization in Rb per unit light intensity B_ν. The circles and crosses record observations at temperatures of 197°C and 245°C respectively. The broken curve represents the equation $B_\nu = \text{const.}/\nu^3(\nu-\nu_0)$. The principal series lines converging to the limit are represented along the abscissas.

than ionization by light of slightly greater frequency than the series limit, it is to be borne in mind that the converse is probably true. The reason for this is evident when it is realized that on the long wave-length side of the series limit the ionization is produced by only a very small part of the band of wave-lengths whose total intensity is measured. Beyond the limit the ionization probability decreases with wave-length possibly slightly less rapidly compared to the corresponding variation in caesium. The dotted curve B_ν represents again

$$B_\nu = \frac{\text{const}}{\nu^3(\nu-\nu_0)}$$

where ν_0 is the series limit frequency. The experimental observations of B_ν show a slight deviation from this curve. The data are hardly accurate enough, however, to warrant concluding definitely that this deviation is real.

Discussion

Until recently formulae expressing the variation with wave-length of absorption coefficients were derived by statistical reasoning from the principle of detailed balance. Sugiura,[9] Oppenheimer,[10] and Reiche[11] have now obtained independently from the quite different standpoint of the wave mechanics expressions for the dependence on wave-length of the continuous absorption beyond the Lyman and Balmer series limits in hydrogen. They agree in finding that the continuous absorption decreases with wave-length but are not in precise accord as to the rate of decrease. Sugiura and Reiche find beyond the Lyman limit a λ^5 law obtaining while Oppenheimer finds a $\lambda^{4.3}$ decrease. The alkalies are hydrogen-like and therefore it appears that their regions of continuous absorption should resemble the continuous absorption of hydrogen atoms in various stages of excitation. Thus for example the absorption by lithium should take a course similar to the absorption beyond the head of the Balmer series and caesium atoms should have absorption characteristics like those of hydrogen atoms in the $6S$ level. Now the ionization probability in caesium decreases with wave-length much more rapidly than the fourth or fifth power of the wave-length, being more closely represented by a twelfth power law. It is interesting to observe, however, that Sugiura finds for the absorption beyond the Balmer limit a more rapid decrease with wave-length (λ^6) compared to the Lyman continuous absorption (λ^5) suggesting that the wave mechanics would predict for the continuous absorption by hydrogen in the $6S$ level a much more rapid decrease resembling more closely the caesium absorption.

Hargreaves[12] has carried through a calculation of lithium absorption probabilities using Hartree's approximation method of self-consistent fields and obtains a quite surprising result, for he finds that continuous absorption increases to a maximum value at a very considerable distance beyond the head of the series (about 1.3 equivalent volts) where a continuous decrease sets in which is somewhat less rapid than a λ^4 law. The present experimental results, which one has every reason to believe should be qualitatively similar to the absorption law for lithium, are clearly not in agreement with Hargreaves' predictions.

Returning to the older theories of transition probabilities based on the principle of detailed balance it may be recalled that such theories yield directly the variation with frequency of the ratio B_ν/q_ν namely,

$$B_\nu/q_\nu = \text{const}\ (\nu-\nu_0)/\nu^3 \qquad (1)$$

where B_ν is the probability that an atom will be ionized by light of unit intensity and frequency ν in unit time and q_ν is the effective collision capture cross-section of the corresponding ion for an electron moving with the velocity v relative to the ion specified by

[9] Sugiura, Jour. de Physique **8**, series 6, 113 (1927).
[10] Oppenheimer, Zeits. f. Physik **41**, 268 (1927).
[11] Reiche, Zeits. f. Physik **53**, 168 (1929).
[12] Hargreaves, Proc. Camb. Phil. Soc. **25**, 75 (1929).

$$\tfrac{1}{2}mv^2 = h\nu - h\nu_0$$

$h\nu_0$ being the ionization energy.

Various expressions for q_ν have been either postulated or given a more or less reasonable justification and have been used together with the above relation to evaluate the frequency dependence of B_ν. Milne[13] assumed that the probability that an electron will be captured by an ion varies inversely as the square of its velocity relative to the ion and thereby got a λ^3 law for B_ν. Kramers[14] obtained a λ^4 law. Becker[15] derived the above relation between B_ν and q_ν and to illustrate the usefulness of the relation in getting B_ν he assumed that q_ν depends on electron velocity in the same manner that the probability that a canal ray will pick up an electron from a rest gas molecule depends on its velocity—as observed by Rückardt.[16] Becker recognized that one could hardly expect such a probability law to be applicable to the recombination of ions and electrons and attached little importance to his expression for B_ν. Nevertheless, his expression is the right one for the photo-ionization of caesium up to within about fifty Angstroms of the series limit. The curve of Fig. 3 represents

$$B_\nu = \text{const}/\nu^3(\nu - \nu_0) \tag{2}$$

which is equivalent to Becker's expression, viz.

$$B_\nu = \frac{\text{const}}{(\nu-\nu_0)\nu^3}\left[1 - \frac{(\nu-\nu_0)^2}{4\nu_0^2}\right]$$

within the experimental error since the second term is negligible over the range involved.

If, instead of taking Rüchardt's expression for q_ν, one assumes the Thomson recombination law, which is that recombination varies inversely as the square of the energy of the electron relative to the ion one obtains Eq. (2) which the present experimental data so accurately confirm. The experimental observations are quite free of serious systematic errors and the accuracy of the probability law established experimentally compares with the fluctuations of the experimental points about the smooth curve. Mohler, Foote and Chenault pointed out that their results were consistent with Becker's evaluation of B_ν and the Thomson recombination law as well over the spectral range 3050A to 2700A. The present results indicate that the laws are applicable over a much wider range 3100A to 2200A.

Thus, assuming the validity of the principle of detailed balance these experiments may be regarded as establishing, in addition to the variation of B_ν with frequency, that the effective collision capture cross-section of caesium and rubidium ions for electrons vary inversely as the square of the energy of the electrons relative to the ions. It is significant that Oppen-

[13] Milne, Phil. Mag. **46**, 836 (1923).
[14] Kramers, Phil. Mag. **46**, 836 (1923).
[15] Becker, Zeits. f. Physik **18**, 325 (1923).
[16] Rüchardt, Ann. d. Physik **71**, 377 (1923); Zeits. f. Physik **15**, 164 (1923).

heimer[17] using the wave mechanics has derived the same law for the recombination of protons and electrons, for it is rather to be expected that alkali ions and protons should exhibit such similar properties. There occurs the difficulty pointed out by Mohler and Boeckner,[18] namely, that Oppenheimer's expressions for B_r and q_r do not fulfill the requirement of the principle of detailed balance as embodied in Eq. (1). The present results favor his evaluation of q_r and therefore suggest that there may be an error in the derivation of B_r. Such an inference is questionable, for indeed, the opposite would be deduced from the experiments of Mohler and Boeckner on the continuous spectrum of caesium vapor.

[17] Oppenheimer, Phys. Rev. **31**, 349 (1928).
[18] Mohler and Boeckner, Bur. Stan. Jour. Res **2**, 489 (1929).

ON THE ASYMMETRICAL TOP IN QUANTUM MECHANICS[1]

By S. C. Wang*
Department of Physics, University of Wisconsin

(Received May 1, 1929)

Abstract

An elaboration and a more complete analysis of Witmer's work on the asymmetrical top treated as a perturbation of the symmetrical one show that one can deduce the rigorous solution of the problem from those of the algebraic equations of degree $2j+1$ or less. Without actually solving such equations, we find the terms divisible into even and odd groups just as in the case of the sigma-type doubling in diatomic molecules treated by Kronig, Van Vleck and others. For the case where the asymmetry is slight, an explicit expression for the separation of such similar doublets is obtained. The selection rules, which are rigorous for any degree of asymmetry, consist of the following: (a) Kronig's rule; (b) $\Delta j=0, \pm 1; \Delta m=0, \pm 1$; and (c) rule for the quantum number sigma, $\Delta\sigma=$even for electric moment in z direction and $\Delta\sigma=$odd for moment in $x-y$ plane. The effect of the electronic motions on the rotation of a polyatomic molecule as a whole is also briefly discussed.

THE problem of the asymmetrical top has been treated in the old quantum theory by many authors[2] and in the new quantum theory by Witmer[3] and very recently also by Kramers and Ittmann.[4] Witmer regarded the problem as a perturbation of that of the symmetrical top, the solution of which is well known.[5] He thus obtained the energy values as power series in what we may call the parameter of dissymmetry. In the present paper, using a method which is an elaboration of Witmer's, we shall show that the exact solution of this problem is reducible to the solving of an infinite set of algebraic equations of finite degree and the characteristic functions are thus expressible as linear combinations of a finite number of those for the symmetrical top.

Before the work presented below was undertaken, Professor Kramers suggested[6] to the author the possibility of attacking the problem by a method of separation of variables analogous to that used by Reiche[2] in the old quantum theory. In a short note[7] presented to the American Physical Society,

* National Research Fellow.

[1] A preliminary report of this paper was presented to the New York Meeting of the American Physical Society, Dec. 31, 1928; see Phys. Rev. **33**, 289 (1929).

[2] Epstein, Phys. Zeits. **20**, 289 (1919); Verh. d. D. Phys. Ges. **17**, 398 (1916); Reiche, Phys. Zeits. **19**, 394 (1918); Kramers, Zeits. f. Physik **13**, 343 (1923); Witmer, Proc. Nat. Acad. **12**, 602 (1926); Luetgemeier, Zeits. f. Physik **38**, 251 (1926).

[3] Witmer, Proc. Nat. Acad. **13**, 60 (1927).

[4] Kramers and Ittmann, Zeits. f. Physik **53**, 553 (1929).

[5] Reiche and Rademacher, Zeits. f. Physik **39**, 444 (1926); **41**, 453 (1927); Kronig and Rabi, Phys. Rev. **29**, 262 (1927); also Dennison, Phys. Rev. **28**, 318 (1926).

[6] I take this opportunity to thank Prof. Kramers for this kindness.

[7] Wang, Phys. Rev. **33**, 123 (1929). Unfortunately the writer made an algebraic mistake in the abstract as printed in the Bulletin of the American Phys. Soc., Vol. **3**, No. 5. This was

the present author reported that the Schroedinger's equation for the asymmetrical top is separable in the same set of elliptical coordinates and under under the same conditions as Reiche[2] found in the old quantum theory. The resulting differential equations are exactly of the form of Lamé's equation. Due to an oversight in interpreting the boundary conditions, the writer did not pursue further the solution of the problem by integrating Lamé's equation.

Instead of using Lamé's equation, we shall use an elaboration of Witmer's method[3] which is more closely akin to the standard perturbation technique. At first thought, it might be presumed that the use of the ordinary differential equation might be preferable to a perturbation theory. But, on closer examination, it can be seen that the solution of Lamé's equation involves the use of identically the same algebraic equations met here. Perhaps, the use here of the term perturbation theory is somewhat misleading. One might construe this as some approximate method of obtaining numerical results. Actually our method is an accurate one; all we mean is the use of an orthogonal transformation whereby the matrix representation of the Hamiltonian, generally non-diagonal, in one scheme is transformed into a diagonal one in some other scheme.

The first part of our work consists largely of transferring Witmer's work into orthodox matrix symbolism and removing his restriction $m=j$. Witmer's results on the energy values are correct in the main except for neglecting the sigma-doubling.[8] We now proceed to obtain the matrix elements of the Hamiltonian of the asymmetrical top, referred to the scheme of the set of characteristic functions for the symmetrical top.

The Matrix hamiltonian for the asymmetrical top. By applying Shroedinger's rule to the classical Hamiltonian of a free asymmetrical top, we readily obtain, using the notation of Witmer, the following wave equation:

$$H\Phi \equiv -(A+b\cos 2\phi)\frac{1}{\sin\theta}\frac{\partial}{\partial\theta}\left(\sin\theta\frac{\partial\Phi}{\partial\theta}\right)-\frac{A-b\cos 2\phi}{\sin^2\theta}\left[\frac{\partial^2\Phi}{\partial\psi^2}-2\cos\theta\frac{\partial^2\Phi}{\partial\phi\delta\psi}+\frac{\partial^2\Phi}{\partial\phi^2}\right]-(1+b\cos 2\phi)\frac{\partial^2\Phi}{\partial\phi^2}-\frac{2b\sin 2\phi}{\sin\theta}\left[\frac{\partial^2\Phi}{\partial\theta\partial\psi}-\cos\theta\frac{\partial^2\Phi}{\partial\theta\partial\phi}\right] \tag{1}$$

corrected when the abstract was reprinted in the Phys. Rev., except for a purely typographical error (the correct equation is of the exact Lamé form and should be $f(\lambda)^{1/2}d/d\lambda[f(\lambda)^{1/2}dU/d\lambda]+(a+b\lambda)U=0$). Kramers and Ittmann saw only the abstract in its first form when they wrote their paper.

[8] Witmer's formulas (16) and (17) are valid for $\sigma>4$ (Witmer calls them n). For $\sigma<4$, the corrected formulas, inclusive of the terms of the order b^3, are as follows:

$\sigma=0)$ $W-W_0=-F(2)b^2$;

$\sigma=1)$ $W-W_0=\pm F(1)b+8F(3)b^2/F(1)\mp F(3)b^3$;

$\sigma=2)$ $W-W_0=[F^2(1)+3F(1)-9\pm 6F(2)]b^2/6$;

$\sigma=3)$ $W-W_0=[F^2(1)+8F(1)-54]b^2/16\pm F(3)b^3$;

$\sigma=4)$ $W-W_0=[F^2(1)+15F(1)-180]b^2/30$;

where W_0 is the energy for the symmetrical top and $F(k)$ is abbreviation for $(j+k)!/2^{\sigma^2}(j-k)!$. The plus and minus signs correspond to the sigma doublets. For $\sigma=4$, the formula is, $W-W_0=\lambda_2 b^2+b^4[\lambda_4\pm 16F(4)/9]$, where λ_2 and λ_4 are those quantities given by Witmer.

$$+2b\cos 2\phi\cot\theta\frac{\partial\Phi}{\partial\theta}-b\sin 2\phi(1+2\cot^2\theta)\frac{\partial\Phi}{\partial\phi}+2b\sin 2\phi\cot\theta\csc\theta\frac{\partial\Phi}{\partial\psi}$$

$$=\frac{8\pi^2}{h^2c}E\Phi$$

where θ, ϕ, ψ are the Eulerian angles of the system of principal axes of the top, E is the energy and A_x, A_y, A_z are the three principal moments of inertia. Also we have used the following abbreviations:

$$c=\frac{1}{A_z}-\frac{1}{2}\left(\frac{1}{A_x}+\frac{1}{A_y}\right),\quad A=\frac{1}{2c}\left(\frac{1}{A_x}+\frac{1}{A_y}\right),\quad b=\frac{1}{2c}\left(\frac{1}{A_x}-\frac{1}{A_y}\right). \tag{2}$$

We also assume that A_y lies between the other two in magnitude so that $-1\leqq b\leqq 0$.

The characteristic functions for the symmetrical top have been obtained by several authors already mentioned. We shall adopt here the following expression given by Reiche and Rademacher[5] (multiplied by a proper normalization factor):

$$u_{j\sigma m}(\theta,\phi,\psi)\equiv u_{dsp}(t,\phi,\psi)$$
$$=\left[\frac{(d+s+p)!\,(1+d+s+\rho+p)!\,(d+p)!\,t^d(1-t)^s}{d!^2\,p!(s+p)!\,4\pi^2}\right]^{\frac{1}{2}} \tag{3}$$
$$F(-p;\,1+d+s+p;\,1+d;t)\,e^{i\sigma\phi+im\psi}$$

where $t=\frac{1}{2}(1-\cos\theta)$, $s=|m+\sigma|$, $d=|m-\sigma|$, $j=p+\frac{1}{2}(d+s)$ and we have, following the nomenclature of Van Vleck,[9] used the quantum numbers σ and m in place of the τ and τ' used by Reiche. For the sake of convenience, we also introduce a function defined by the equation:

$$2\pi u_{dsp}(t,\phi,\psi)=U_{dsp}(t)e^{i\sigma\phi+im\psi}.$$

As usual, we now apply the operator H, as given by Eq. (1), to the function $u_{j\sigma m}$.[10] After some simplification, particularly by using the fact that $U_{j\sigma m}(\cos\theta)$ satisfies the differential equation

$$d^2U/d\theta^2+\cos\theta\,dU/d\theta-[((m-\sigma\cos\theta)\csc\theta)^2-j(j+1)+\sigma^2]U=0,$$

we get

$$Hu_{j\sigma m}=[Aj(j+1)+\sigma^2]u_{j\sigma m}-be^{\pm 2i\phi}\{\tfrac{1}{2}[\pm\sigma(1\pm\sigma)-j(j+1)]u_{j\sigma m}$$
$$+\csc\theta(\pm m-(1\pm\sigma)\cos\theta)[(du_{j\sigma m}/d\theta)+\csc\theta(\pm m\mp\sigma\cos\theta)u_{j\sigma m}]\} \tag{5}$$

The matrix elements $H(j',\sigma',m';j,\sigma,m)$ are then just the coefficients in the expansion of the right hand member of (5) in the form

$$\sum_{j'\sigma'm'}H(j',\sigma',m';j,\sigma,m)\,u_{j'\sigma'm'}.$$

[9] Van Vleck, Phys. Rev. **33**, 467 (1929).

[10] From the definitions of d, s, and p given in Eqs. (4), corresponding to any given set of values for j, σ, m, there is one and only one set of d, s, p although the converse is not unique.

The first term of (5) is already in the form of constant $\times u$. We shall next consider the second term with the upper sign. It now becomes necessary to distinguish between the four separate cases governed by the following explicit relations between σ, m, and d, s: (a) $\sigma-m=d$, $\sigma+m=s$; (b) $\sigma-m=d$, $\sigma+m=-s$; (c) $\sigma-m=-d$, $\sigma+m=s$; (d) $\sigma-m=-d$, $\sigma+m=-s$. For all the four cases, this second term of (5) is of the form $g(t)dU/dt+h(t)U$ and we find that the following recursion formulas reduce that expression to a single term for the respective cases:[11]

$$(a)\quad \left[(-d+1+(s+d+2)t)\frac{d}{dt}+\frac{1}{2}\left(\frac{s}{1-t}-\frac{d}{t}\right)-p(p+d+s+1)\right]U_{dsp}$$
$$=[p(p-1)(p+d+s+1)(p+d+s+2)]^{1/2}U_{d+2,s+2,p-2};$$

$$(b)\quad \left[(-d-1+(d-s+2)t)\frac{d}{dt}+\frac{1}{2}\left(-\frac{s}{1-t}-\frac{d}{t}\right)-(p+s)(p+d+1)\right]U_{dsp}$$
$$=[(p+s)(p+s-1)(p+d+1)(p+d+2)]^{1/2}U_{d+2,s-2,p};$$

$$(c)\quad \left[(d-1+(s-d+2)t)\frac{d}{dt}+\frac{1}{2}\left(\frac{d}{t}+\frac{s}{1-t}\right)-(p+d)(p+s+1)\right]U_{dsp}$$
$$=[(p+d)(p+d-1)(p+s+1)(p+s+2)]^{1/2}U_{d-2,s+2,p};$$

$$(d)\quad \left[(d-1+(-s-d+2)t)\frac{d}{dt}+\frac{1}{2}\left(\frac{d}{t}-\frac{s}{1-t}\right)-(p+1)(p+s+d)\right]U_{dsp} \tag{6}$$
$$=[(p+d+s)(p+d+s-1)(p+1)(p+2)]^{1/2}U_{d-2,s-2,p+2}.$$

It must be mentioned, however, that there are, in addition, five exceptional cases for which special recursion formulas different from those above must be used; these five cases are: (i) case (*b*) when $s=1$, (ii) case (*d*) when $s=1$, (iii) case (*c*) when $d=1$, (iv) case (*d*) when $d=1$, and (v) when $d=1$, $s=1$, We shall not reproduce the formulas here, which are quite similar to those in (6). But, collecting the results, we find that the second term of (5) with the upper sign reduces in all cases to the following single term:

$$-\tfrac{1}{2}b[(j-\sigma-1)(j-\sigma)(j+\sigma+1)(j+\sigma+2)]^{1/2}u_{j,\sigma+2,m} \tag{7}$$

except that the sign should be plus instead of minus whenever $m-\sigma=1$. This irregularity of sign is removed if we redefine the characteristic functions u' as done by Van Vleck;[12] namely, by putting $u'=(-1)^{\sigma}u$ for $m\geqq\sigma$ and $u'=(-1)^{m}u$ for $\sigma\geqq m$, where u is defined as in (3).

The second term of (5) with the *lower* sign can be reduced to the one with the *upper* sign by the substitution $\sigma=-\bar{\sigma}$, $m=-\bar{m}$, and evaluated accordingly. But since the latter contributes exclusively to matrix elements

[11] To derive these recursion formulas, we find it most convenient to make use of the relations between contiguous hypergeometric functions given explicitly by Gauss (Ges. Werke, III, 123 ff., 207 ff.).

[12] Van Vleck, reference 9, especially footnote 25.

of the type $H(j', \sigma+2, m'; j, \sigma, m)$ while the former to those of the type $H(j', \sigma-2, m'; j, \sigma, m)$, we see that we can readily deduce the one from the other by using the Hermitian property of the H-matrix.

As a result, the entire expression (5) simplifies to

$$Hu_{j\sigma m} = [Aj(j+1)+\sigma^2]u_{j\sigma m} + bf(j,\sigma+1)u_{j,\sigma+2,m} + bf(j,\sigma-1)u_{j,\sigma-2,m} \quad (8)$$

where

$$f(j,\sigma) \equiv -\tfrac{1}{2}[(j-\sigma)(j-\sigma+1)(j+\sigma)(j+\sigma+1)]^{1/2}$$

Eq. (8) shows that the H-matrix is diagonal both in j and in m; it is in fact independent of m. The diagonality with respect to j could have been suspected from the constancy of the square of the angular momentum vector of a free body while the complete independence of (8) ofthe magnetic quantum number m is, of course, due to the arbitrariness of orientation in space.

The infinite secular determinant constructed in accordance with (8) consequently factors into finite determinants, each having the two fixed indices j and m and the running index sigma. Since sigma extends from $+j$ to $-j$, these factored determinants have the order $2j+1$ in every case. Explicitly the corresponding secular equations are of the form:

$$\begin{vmatrix} j^2-W & & & & & & & \\ & \cdot & & & & & & \\ & & \cdot & 0 & bf(j,\sigma+1) & & & \\ & & \cdot & (\sigma+1)^2-W & 0 & bf(j,\sigma) & & \\ & & \cdot & 0 & \sigma^2-W & 0 & \cdot & \\ & & & bf(j,\sigma) & 0 & (\sigma-1)^2-W & \cdot & \\ & & & & bf(j,\sigma-1) & 0 & \cdot & \\ & & & & & \cdot & & \\ & & & & & & \cdot & j^2-W \end{vmatrix} = 0, \quad (9)$$

where we have included the constant term $-Aj(j+1)$ in the quantity W, which is the energy measured in units of $h^2c/8\pi^2$;[13] the actual energy E would be

$$E = (h^2c/8\pi^2)[Aj(j+1)+W] \quad (10)$$

It is at once evident that the determinant in (9) can be at least factored into two, one connected with the even sigmas and the other the odd ones. In addition, the determinant is symmetrical not only about its main diagonal (Hermitian) but also about the other diagonal owing to the fact $f(j,\sigma) = f(j,-\sigma)$; this enables one to factor the determinant once more and this is closely connected with the possibility of dividing the terms according to the type of Kronig symmetry first pointed out by him in two papers.[14] We shall discuss this division of terms a little more in detail in a later section.

[13] The constant c, not to be confused with the velocity of light, has been defined in Eq. (2).

[14] Kronig, Zeits. f. Physik **46**, 814; **50**, 347 (1928). See also Wigner and Witmer, Zeits. f. Physik **51**, 859 (1928).

Because of the above simplification, Eq. (9) reduces, for the cases $j=1,2,3.$ to quadratic equations at most; the resulting energy values we thus obtained agree with those given in the paper of Kramers and Ittmann and will not be repeated here. In this connection, it may be mentioned, however, that in their work using elliptical coordinates and obtaining Lamé's equation, these four factored algebraic equations are those belonging to four separate types of Lamé's functions; but here we find that these separate equations, when combined, could be embodied in the single symmetrical form (9).

We may also point out the relation between the characteristic functions given in the two papers. Our result in Eq. (9) shows that in general the characteristic function for the asymmetrical top can be written:

$$\Phi_{j\sigma m}=e^{im\psi}\Sigma_{\sigma'}S_{\sigma\sigma'}U_{j\sigma' m}(\cos\theta)e^{i\sigma'\phi} \tag{11}$$

where the $S_{\sigma\sigma'}$'s are the orthogonal sets of solutions of the system of homogeneous equations whose eleminant is (9). Kramers and Ittmann treat the case $m=0$ and obtain as characteristic functions the products of Lamé's functions of the two elliptical coordinates; these products can be also expressed, as they have pointed out, as linear combinations of ordinary tesseral harmonics (in which θ and ϕ are regarded, however, as two of the Eulerian angles used here). Now Eq. (11) reduces just to this latter form when we put $m=0$ because the U's reduce to the associated Legendre functions when $m=0$. From the arbitrariness of the spatial orientation, one can get all the energy values by considering some special cases, like $m=0$ (Kramers and Ittmann) or $m=j$ (Witmer). Also the intensities could be obtained because of the resulting independence of the coefficients $S_{\sigma\sigma'}$ in (11) of m. It seems, however, to be a satisfying check to have shown explicitly this independence of m.

Sigma-type doubling phenomena. In the problem of the symmetrical top there is the degeneracy with respect to m and also with respect to the pairs of states $(j,+\sigma),(j,-\sigma)$. In the case of an asymmetrical top this latter degeneracy is removed i.e., for given j and m there are $2j+1$ distinct states. For cases where the departure from the symmetrical case is small, the terms will appear as doublets (except the term sigma $=0$, which always remains single), each grouped around the $\pm\sigma$ term of the symmetrical top. Borrowing the terminology of Mulliken[15] for a similar splitting up of sigma terms in diatomic molecules, we shall call this the sigma-type doubling in the asymmetrical top.

We shall now seek an explicit formula for this doublet separation on the assumption that the dissymmetry factor $|b|\ll 1$. Perhaps the most straightforward way of calculating this is to follow the procedure of Van Vleck[9] in an analogous calculation for the sigma doublet in diatomic molecules. In that paper, he extended Born, Heisenberg and Jordan's perturbation technique to systems where the degeneracy is removed only after one reaches a

[15] Mulliken, Phys. Rev. **28**, 1202 (1926). The theory of sigma-type doubling in diatomic molecules has been worked out by Kronig,[14] Hill and Van Vleck, Phys. Rev. **32**, 250 (1928) and Van Vleck.[9]

higher order of approximation than the first. Using Van Vleck's formula (41), we find the doublet separation in our case is

$$h\Delta\nu = b^{\sigma}[h^2c(j+\sigma)!]/[2^{3\sigma}\pi^2(j-\sigma)!(\sigma-1)!^2] \qquad (12),$$

which appears first in the sigma-*th* order of approximation. Since the quantity b measures the departure from the case of the symmetrical top, the experimental detection of this separation would furnish a useful method of estimating the magnitude of molecular dissymmetry. We note here that the separation should be large for low sigmas and should disappear as sigma increases.

From the secular Eq. (39) in Van Vleck's paper, we also find that the proper linear combination of the functions $u_{j,\sigma,m}$ and $u_{j,-\sigma,m}$ to be used as the zero order characteristic functions for the asymmetrical case are:[16]

$$v_+(j,\sigma,m) = (u_{j,\sigma,m} + u_{j,-\sigma,m})/2^{1/2} \qquad (13)$$

and

$$v_-(j,\sigma,m) = (u_{j,\sigma,m} - u_{j,-\sigma,m})/2^{1/2} \qquad (14)$$

From here on we shall call states of the type (13) the plus sigma states and (14) the minus sigma states. We then find that the $2j+1$ states of same j and m, arranged in the order of increasing or decreasing energy (according as $A_z < A_x$, or vice versa), run as follows: $\sigma = 0+, 1-, 1+, 2-, 2+$, and so on.

Rules of combination. Theoretically, once the Eq. (9) is solved, the matrix elements $S_{\sigma\sigma'}$ can be computed and the characteristic functions are given by (11). The intensity for any transition $(j', \sigma', m'; j'\sigma, m)$ can then be calculated from the already known results for the symmetrical top and the total intensity for the actual transition $(j', \sigma'; j, \sigma)$ can be calculated by summing over all possible Zeeman components. We shall not attempt to make any calculation in this direction. Instead, we shall draw from Eq. (9) some conclusions about the selection rules that are quite general in nature and do not depend on any particular solution of (9).

In the series of papers on band spectra in diatomic molecules, Kronig[14] pointed out that since the wave equation is invariant to a reflection of all particles about the x-z plane, which he represents by his transformation (15) in his second paper, the characteristic functions should also be transformed into their own multiples by such a reflection; or, if all functions are normalized, they should merely be multiplied by $+1$ or -1. Kronig calls such functions "even" or "odd" respectively. In the present case of an asymmetrical top, we have the same invariance of the wave equation, hence we expect each of the states is also either even or odd in the Kronig sense. To verify this, we first note that all the $v_+(\sigma)$'s for given j and m have the same Kronig symmetry and also the $v_-(\sigma)$'s.[17] If now we use in our representation of the Hamiltonian as a matrix these v functions as our fundamental set instead

[16] The state $\sigma = 0$ is an exception; it will have $v_+(0) = u_{j0m}$ and there will be no states $v_-(0)$.

[17] Functions having the same sigma (with regard to sign also) but different j's have the same or opposite Kronig symmetry according as the difference in j is even or odd. See Fig. 1.

of the u's we find that the secular equation corresponding to (9) factors into two, with the one factor involving only the positive sigmas (including zero) and the other the negative ones. This means that the new characteristic functions will be linear combinations of the v's having the same Kronig symmetry and hence will themselves also have the property of being either even or odd in the Kronig sense.

Since the electric moment operator is odd with respect to Kronig transformation, the Kronig rule of combination holds in our case; namely, transition can occur only between states of different Kronig symmetry.

In the case of symmetrical top we have the additional selection rules $\Delta j=0, \pm 1$; $\Delta m=0, \pm 1$; $\Delta\sigma=0, \pm 1$. Clearly the first rwo rules remain

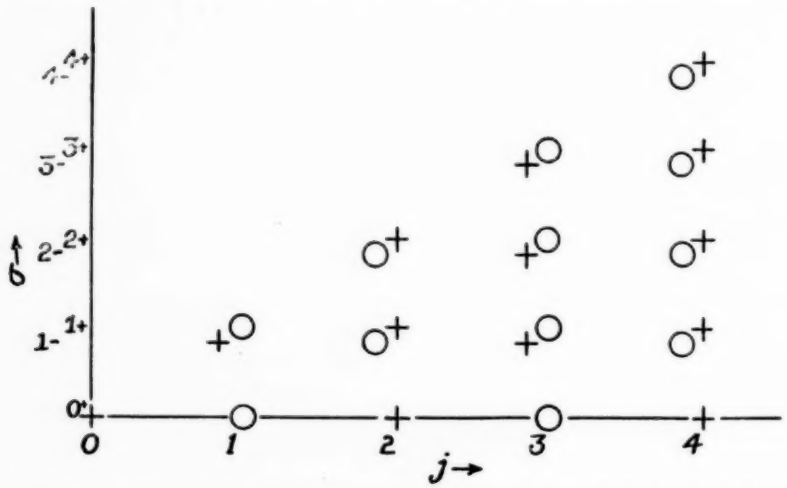

Fig. 1. Kronig rule: ○ states combine only with + states. Rule for j: Only states in same column or adjacent columns combine. Rule for σ: Corresponding to a $\frac{z}{x-y}$ component of the electric moment, the only transitions are those with an $\frac{\text{even}}{\text{odd}}$ number of jumps in the rows $(\Delta\sigma=\frac{\text{even}}{\text{odd}})$.

unchanged in passing to the present problem. As for the last one, from the fact mentioned before that the determinant (9) factors into two, separating the even and the odd sigmas,[18] we readily find the following rule concerning the sigmas:

(a) Corresponding to an electric moment in the z direction in the top, transition can occur only between states both with even sigmas or both with odd ones, and

(b) Corresponding to an electric moment in the x-y plane, transition can occur only from a state with even sigma to one with an odd sigma or vice versa.

The accompanying diagram gives a summary of all the essentials about the rules discussed above.

[18] These are even and odd in the ordinary sense of the words and are not to be confused with the "even" and "odd" in the Kronig sense.

Polyatomic molecules. In an important paper on moleculer spectra, Born and Oppenheimer[19] showed that in the wave equation of a polyatomic molecule, the predominant rotational term is the operator for an asymmetrical top. In addition, due to the coupling of the electronic and the nuclear vibrational motions to the rotation of the molecule, correction terms enter which are in general complicated if explicit expressions are desired (except in the case of diatomec molecules, for which see the papers of Konig[14] and Van Vleck[9]). However, if we consider the ideal case where the nuclear vibrational effects are vanishingly small ("frozen nuclei"), a calculation similar to that of the last two authors can be made for the general polyatomic molecule. It is found that the following elements should then be added to the H-matrix given in (9)[20]

$$H_1(n', j, \sigma, m\ ; n, j, \sigma, m) = \frac{1}{2}\left(\frac{M_x^2}{A_x}+\frac{M_y^2}{A_y}+\frac{M_z^2}{A_z}\right)(n'; n) - (h/2\pi)\frac{\sigma M_z(n'; n)}{A_z} \quad (15)$$

$$H_1(n', j, \sigma \pm 1, m; n, j, \sigma, m) = (h/4\pi)(M_y \pm iM_z)(n'; n)\left[(j \mp \sigma)(j \pm \sigma + 1)\right]^{1/2} \quad (16)$$

where M_x, M_y etc. are the ordinary angular momentum matrices or their squares for the stationary molecule and where n or n' designates the totality of the electronic quantum numbers.

The most important parts of (15) and (16) are obtained, however, by taking an average over the electronic frequencies i.e. taking $n' = n$. Then the first term of (15) merely shifts the energy scale by a constant amount and it corresponds to the results obtained by Kramers and Pauli[21] in the old quantum theory. The second term[22] of (15) will change the spacing of the different sigma terms belonging to the same j. As for the elements (16), they will vanish when the molecule has a regularity around an axis of symmetry (symmetrical top). That this is so can be seen as follows: These matrix elements are $I = \int V^*_n (M_y \pm iM_z) V_n dv$, where V_n is the characteristic function of the stationary molecule. The operators $(M_y \pm iM_z)$, when transformed in terms of those in cylindrical coordinates about the axis of symmetry, will involve the angle ϕ only through the factors $e^{\pm i\phi}$; and, if the nuclear distribution in the molecule has a periodicity in ϕ of modulus $w = 2\pi/k$ (k an integer), the product $V^*_n V_n$[23] will be simply periodic in ϕ with period w. Now since we can evaluate the integral I equally well after making the tranformation in ϕ given by $\phi' = \phi + a$, we shall evaluate it k times with $a = w, 2w, 3w \cdots kw$, and add them up. We get

$$kI = I\Sigma_{l=1,2,k}\, e^{2\pi i l/k}\ ;\ \therefore I = 0.$$

[19] Born and Oppenheimer, Ann. d. Physik **84**, 457 (1927).

[20] We must mention that the H's in (15) and (16) are measured in absolute units, while in (9) it is in units of $h^2c/8\pi^2$.

[21] Kramers and Pauli, Zeits. f. Physik **13**, 351 (1923).

[22] The average of M_z will vanish if the characteristic function is invariant with respect to a reflection about some plane passing through the axis of symmetry.

[23] Although the product $V_n^* V_n$ is invariant after the rotation, the separate functions V_n and V_n^* may be multiplied by some kth root of unity after such a rotation.

To take all the averaged terms in (15) and (16) into account in the more general case of polyatomic molecules, one can proceed in two ways; if the new perturbation elements are small compared to those in (9), one can first solve the asymmetrical top problem and consider (15) and (16) as perturbations of the latter; on the other hand, if both are of the same order of magnitude, one has to solve the combined problem obtained by adding the H and H_1 matrices. In the latter case, the presence of the elements of the type (16) in particular will invalidate most of our previous statements concerning the division of the secular determinant according to even and odd sigmas and the selection rule for sigma.

I am deeply indebted to Professor J. H. Van Vleck for much encouragement and very helpful suggestions and criticisms throughout the course of the work.

ON THE SATURATION OF THE ELECTRIC AND MAGNETIC POLARIZATION OF GASES IN QUANTUM MECHANICS

By K. F. Niessen
Department of Physics, University of Wisconsin

(Received June 1, 1929)

Abstract

The calculations of dielectric and magnetic susceptibility in quantum mechanics previously made by Van Vleck are extended to include higher powers of the field strength. This is necessary in fields so strong that the moment is not linear in the field strength.

Electric polarization. As noted by Debye the electric polarization of a gas results from two effects: (a) a change in the spacial orientation of the rigid or permanent moment of the molecule, (b) the inducing of an elastic polarization or deformation of the molecule.

1. *Rigid molecules.* The effect of (a) is calculated in §2 to all powers of the field strength and yields exactly the classical Langevin function

$$L(\mu, F, T)=\mu[\text{cotgh}(\mu F/kT)-kT/\mu F]$$

provided only the (rotational) energy changes in "allowed" transitions are small compared to kT. Here μ is the permanent moment of the molecule.

2. *Deformable molecules.* The part of the moment resulting from the effect (b) (induced polarization, described with matrix elements whose frequencies are large compared to kT/h), and the part arising from the superposition of (a) and (b) is calculated in §3 to terms of the third order in the field F. The complete formula for the moment is to this order:

$$m_F=\left(\frac{\mu^2}{3kT}+p_0\right)F+\left(q_0+\frac{q_1}{kT}+\frac{q_2}{k^2T^2}-\frac{\mu^4}{45k^3T^3}\right)F^3$$

where p_0, q_0, q_1, q_2 are constants whose explicit expressions in terms of the individual matrix elements are rather complicated. The expression is of the same type form as that of Debye's, except for addition of the term q_0 and reduces identically to his type form if, following Debye, we specialize the model by supposing the restoring forces to be simple harmonic.

Magnetic polarization of atoms. Brillouin showed that if we neglect the "spin," the magnetic polarization per atom in a monatomic gas is

$$m_H=\beta\left[\frac{le^{l\beta H/kT}+(l+1)e^{-(l+1)\beta H/kT}}{e^{l\beta H/kT}-e^{-(l+1)\beta H/kT}}-\frac{1}{e^{\beta H/kT}-1}\right]=B(l,\beta,H,T)$$

where $l+1$ is the azimuthal quantum number of the old quantum theory and β the Bohr magneton. We show that the reason this "Brillouin" function differs from that of Langevin is because the various Cartesian components of the angular momentum matrix do not commute in multiplication, a complication not found in the electric case. The appearance of a Brillouin function (which is expressible as the difference of two Langevin functions) instead of a single L-function obviates Debye's objection that the classical Langevin theory yields infinite entropy at $T=0$ in contradiction to the Nernst heat theorem.

Magnetic polarization of atoms with spin. When now the spin is included two limiting cases can conveniently be considered; viz. those in which the spin multiplets

are very small or very large compared to kT. In the first case the magnetic polarization is the sum $B(l, \beta, H, T)+B(s, 2\beta, H, T)$ of two Brillouin functions representing the orbital and spin effects respectively. In the second case we need consider only the component of the magnetic moment parallel to the total angular momentum associated with the inner quantum number j. The polarization per atom then becomes $B(j, g\beta, H, T)$ where g is the Landé-factor.

Magnetic polarization of diatomic gases. With narrow multiplets ($\Delta\nu<<kT/h$) the polarization is $L(\sigma_l\beta, H, T)+B(s, 2\beta, H, T)$ while with wide multiplets the formula is instead $L((\sigma_l+2\sigma_s)\beta, H, T)$ where σ_l and σ_s have their usual spectroscopic meaning. The reason that the Langevin function appears whereas the Brillouin function alone was encountered in the atomic case, is that now only the component of orbital angular momentum parallel to the axis of figure is of the important low frequency type and with only one effective Cartesian component no questions of non-commutability can arise.

§ 1 Introduction

THE dielectric constant ϵ is connected with the average molecular electric moment $\bar{\bar{m}}_z$ in the direction of the field F, according to the relation

$$\epsilon-1=4\pi N\bar{\bar{m}}_z/F, \tag{1}$$

where N is the number of molecules per 1 cm^3 of the gas. In the usual calculations of dielectric constants, it is assumed that the electric moment $\bar{\bar{m}}_z$ can be taken proportional to the field strength. This is an adequate approximation in fields of ordinary magnitude, but in strong fields one should differentiate $\bar{\bar{m}}_z$ with respect to F instead of dividing by F in order to obtain the most convenient definition of the dielectric constant. Furthermore higher order terms in the development of $\bar{\bar{m}}_z$ in F must be considered, thus giving a dependence of dielectric constant on field strength and a tendency to saturation, whereby the electric moment approaches a finite value instead of increasing linearly with F, when F becomes very large. Actual dielectrics usually exhibit only a very small tendency toward saturation at any field strength obtainable experimentally so that only the terms in $\bar{\bar{m}}_z$ which are proportional to F and F^3 come within the range of observation. The correction term in F^3 is calculated for the general molecule in § 3, but first in § 2 we calculate $\bar{\bar{m}}_z$ correct to all powers of F for a rigid molecule with only a permanent moment, as with this restricted type of molecule the extension to all powers of F occasions no difficulty.

Similar calculations of the saturation effect will also be made for the case of magnetic rather than electric polarization, as there is considerable similarity between the electric and magnetic cases, although some important differences arise from the non-commutativeness of the angular momentum matrices involved in the magnetic case. The magnetic saturation is experimentally much easier to detect than the electric.

Throughout this paper we follow substantially the method of Van Vleck,[1] which has the advantage of freeing one from special models of atoms or molecules. He showed that the Langevin-Debye formula $N\alpha+N\mu^2/3kT$ for the susceptibility in fields too weak for saturation could be obtained by

[1] J. H. Van Vleck, Phys. Rev. **29**, 727 (1927); **30**, 31 (1927); **31**, 587 (1928).

assuming only that the energy levels of the molecule can be separated into two categories: the "low levels" which are characterized by the fact that the spacings between them are small compared to kT, and "high levels" whose excess of energy above the normal states is large compared to kT. For greater detail in discussing these two categories of states, we refer to p. 730 of Van Vleck's[1] paper I.

Notation. In the present paper small letters $a, b, \cdots$, will be used for the "low" states and capital ones $A, B, \cdots$, for the excited states. Greek letters $\alpha, \beta, \gamma, \cdots$, will be used to denote collectively states of both types. Thus symbolically we may write $\sum_\alpha = \sum_a + \sum_A$ where $\sum_a$ means a summation over the low states $a, b, c, \cdots$, and $\sum_A$ that over the excited ones. A frequency of the type ν_{ba} is a low frequency, while one of the type ν_{Ba} is high and $\nu_{\beta a}$ can be either. Van Vleck used three indices (n, j, and m) for one state and sometimes we shall use this notation too. The index n then represents the entire group of quantum numbers whose effect on the energy is large compared to kT, m is the axial quantum number quantizing the angular momentum about the axis of the field, while j signifies all the quantum numbers (except m) such that an "allowed" change in them causes only a change in energy small compared to kT. Commonly j symbolizes one or more quantum numbers associated with the rotational fine structure. In low levels n is to have the value n_0 and for the excited ones $n > n_0$. A state a in our notation would be the same as n_0jm in the Van Vleck notation $b, c, \cdots$, similar to $(n_0j'm')$, $(n_0j''m'') \cdots$, while A or B would mean njm or $n'j'm'$ (or $n'jm$) etc.

§2. The Quantum-mechanical Derivation of the Complete Formula for the Electric Polarization of Gases of Rigid Molecules with a Permanent Electric Moment

In the present section, we are concerned with molecules having only a permanent electric moment, and we neglect the "high frequency" part of the moment involved in transitions to excited states, so that the matrix elements of M^z will all be of the type (ab) and none of the type (aB). We choose the electric field F along the z-axis and $W_a(F)$ denotes the energy of a molecule in the state a and in the presence of the field F. Such a molecule has then along the z-axis an electric moment, whose time average[2] is $\bar{m}_z = -\partial W_a^{(F)}/\partial F$. We assume in the calculation of the susceptibility that the molecules are concentrated practically entirely in the low states. For their distribution over these states we use the Boltzmann distribution law, so that we obtain for the average of $\bar{m}_z$ over all molecules:

$$\bar{\bar{m}}_z = \frac{\sum_a -\partial W_a^{(F)}/\partial F \cdot e^{-W_a^{(F)}/kT}}{\sum_a e^{-W_a^{(F)}/kT}} = kT\frac{\partial Z}{\partial F} \tag{2}$$

with
$$Z = \log \sum_a e^{-W_a^{(F)}/kT} \tag{2a}$$

Let us expand the exponentials as a power series in $(W_a^{(F)} - C)/kT$ about

[2] Cf, J. H. Van Vleck, Phys. Rev. **31**, 585 (1928), footnote 21.

some common origin C for the energy. The choice of C is not important, but should presumably be chosen so as to make the convergence as good as possible, and C might therefore conveniently be taken as the average value of W^0 for the low levels; i.e., $C=\sum_a W_a : N_a$ in which N_a denotes the total number of low states. We find then

$$Z=-C/kT+\log N_a+\log\,[1-\pi_1+\pi_2-\pi_3+\cdots], \tag{3}$$

where

$$\pi_p=\sum_a (W_a^{(F)}-C)^p/p!k^pT^pN_a. \tag{4}$$

In these π_p we could substitute the development

$$W_a^{(F)}-C=W_a^0-C+FW_a^{(1)}+F^2W_a^{(2)}+\cdots.$$

Explicit formulas for W_a^1, W_a^2, $\cdots$, could be obtained by the perturbation theory of Born, Heisenberg and Jordan, but the convergence of this development might not be good for such high powers (all powers are here required!). Such explicit formulas however are fortunately unnecessary in the present special case of only low frequency matrix elements $M^z{}_{ab}$. The sum in π_p namely can here be evaluated by means of the general theorem that

$$[W_a^{(F)}]^p=\sum_{\beta\gamma} S_{a\beta}[(H^{(F)})^p]_{\beta\gamma}S^{-1}_{\gamma a}.$$

In the presence of an electric field the Hamiltonian function is

$$H^{(F)}=H^0-FM^z.$$

therefore
$$\sum_a (W_a^{(F)}-C)^p=\sum_{\beta\gamma}[(H^0-C-FM^z)^p]_{\beta\gamma}\sum_a S^{-1}_{\gamma a}S_{a\beta}$$

In the absence of excited states the indices β and γ can only indicate low levels $b, c, \cdots$. Thanks to this restriction we now have:

$$\sum_a S^{-1}_{ca}S_{ab}=\sum_\alpha S^{-1}_{c\alpha}S_{\alpha b}=\delta_b{}^c$$

therefore
$$\sum_a (W_a^{(F)}-C)^p=\sum_b[(H^0-C-FM^z)^p]_{bb}=\sum_a[(H^0-C-FM^z)^p]_{aa} \tag{5}$$

Let us now for a moment neglect the rotational energy which is just what Langevin did in his classical theory. We shall then derive the Langevin formula for $\overline{\overline{m}}_z$. Actually this neglect is not legitimate. Therefore we shall afterwards take the rotational energy into account and show the reason why the final result remains the same. Neglecting first the rotational energy, and throughout the whole section also the spin, we may put $W_a^0=W_b^0=\cdots=C$, so that the matrix H^0-C now becomes identically zero. We then have from (4) and (5)

$$\pi_p=(-1)^pF^p\sum_a (M_z{}^p)_{aa}/p!k^pT^pN_a. \tag{6}$$

Here N_a is the number of levels in which n always equals n_0, so that we have

$$N_a = \sum_j N_j p_j = \sum_j (2j+1) N_j$$

where p_j denotes the weight of a low state; i.e., the number of possible values of m when j and $n = n_0$ are given; and where further N_j is the number of possible indices j with $n = n_0$. Therefore $N_j = 1$ if we neglect the electron spins. A summation over the low levels a can be split up into $\sum_a = \sum_j \sum_m$ In accordance with the meaning of statistical weights, we evaluate the quantum mechanical average $\sum_a (M_z^p)_{aa}/N_a$ by averaging first over the m's and then the answer over j, indicated by a bar with j attached. Hence

$$\sum_a (M_z^p)_{aa} : N_a = \overline{\left[\sum_m (M_z^p)_{(n_0 j m, n_0 j m)} : p_j \right]}^j \tag{7}$$

Now a quantum mechanical average of $(M_z^p)_{(nojm, noim)}$ over the axial or so-called magnetic quantum number m, which involves a discrete summation, yields the same results as a continuous classical average by means of an integration over a continuous distribution of axes. Thus:

$$\frac{\sum_m (M_z^p)_{(n_0 j m, n_0 j m)}}{p_j} = \frac{\mu_j^p \int \cos^p \theta d\omega}{\int d\omega} \tag{8}$$

Here μ corresponds to the value of the electrical moment of the molecule in the classical theory, while θ is the angle between μ and the z-axis, so that on the right side m_z^p has been averaged classically over all possible orientations of the molecule in space. This theorem which has been already proved by Van Vleck for $p = 2$ holds for every value of p, as is shown in the appendix, but only on the assumption that the moment is not substantially changed by the rotation, in agreement with the fact that we deal here with rigid molecules. Consequently μ_j can be taken independent of j and so we obtain from (7) and (8)

$$\sum_a (M_z^p)_{aa} : N_a = \overline{\mu^p \cos^p \theta}^{cl},$$

where the bar with cl denotes a classical average. Substituting these values in (6) we find:

$$1 - \pi_1 + \pi_2 - \cdots = \overline{(e^{F\mu \cos \theta / kT})}^{cl}$$

from which and (2), (3) the Langevin formula

$$\overline{m}_z = \mu \left[\operatorname{cotgh} \frac{\mu F}{kT} - \frac{kT}{\mu F} \right] = L(\mu, F, T). \tag{9}$$

is derived in a well known way.

Correction for rotation. Let us now include the rotational energy in our calculation. Then we have to go back to (5) where H^0-C does not vanish any longer. The procedure is best explained by evaluating the sum (5) for a definite value of p. For $p=5$ we have:

$$\sum_a [(H^0-C-FM^z)^5]_{aa} = \sum_{a,b,c,d,e} G_{(ab)}G_{(bc)}G_{(cd)}G_{(de)}G_{(ea)} \tag{10}$$

where $$G_{(ik)} = (W_i{}^0-C)\delta_k{}^i - FM^z{}_{(ik)},$$

since H^0 is a diagonal matrix with elements $W_a{}^0, W_b{}^0, \cdots$. Let us first consider a definite term of the sum; e.g.:

$$[(H^0-C-FM^z)^5]_{kk} = \sum_{l,m,n,0} G_{(kl)}G_{(lm)}G_{(mn)}G_{(n0)}G_{(0k)}. \tag{11}$$

When we write the right hand side as a polynomial in F, the highest power of F that occurs is F^5, namely in:

$$\sum_{l,m,n,0} (-1)^5F^5M^z_{kl}M^z_{lm}M^z_{mn}M^z_{n0}M^z_{0k} = (-1)^5F^5(M_z{}^5)_{kk}$$

which we get by taking from the five G-factors each time the term $-FM^z$. To build up the term with F^4 in the polynomial we have to take from four G-factors the term $-FM^z$ and from the remaining one the term $(W_i{}^0-C)\delta_j{}^i$, where i, j mean kl, lm, or ok, depending upon the place of the "remaining" G factor. Since this last term is zero unless $i=j$, the summation will not be extended over four indices l, m, n, o, but only over three, the missing one again depending on the place of the remaining G factor. So there are five possibilities, two of which are:

$$\begin{aligned} &(-1)^4F^4\sum_{mn0}(W_k{}^0-C)M^z_{km}M^z_{mn}M^z_{n0}M^z_{0k} = (-1)^4F^4(W_k{}^0-C)(M_z{}^4)_{kk} \\ &(-1)^4F^4\sum_{ln0}M^z_{kl}(W_l{}^0-C)M^z_{ln}M^z_{n0}M^z_{0k} \sim (-1)^4F^4(W_k{}^0-C)(M_z{}^4)_{kk}. \end{aligned} \tag{12}$$

The last equation does not hold rigorously but only if we neglect the difference between $W_l{}^0$ and $W_k{}^0$. If now all matrix elements with two low indices were different from zero, we should have to put all low energy levels equal to $W_k{}^0$, since we have to sum over l, i.e., over all low levels, and that would be the same as neglecting the rotational energy entirely, so that our approximation would be as poor as the previous one. Using note 26 of Van Vleck's paper[1] I, we remark however that the number of intermediate[3] levels (here denoted by l, m, n, o) will be very small, if we start from some initial level k, to which we have to return again as a final state after a few transitions.

[3] The name intermediate level is chosen for those levels which belong to the intermediate indices in the range of indices occurring in products as $M_{ab}{}^z\ M_{bc}{}^z\ M_{cd}{}^z\ M_{da}{}^z$ etc. They lie therefore between the initial and final state, not with respect to energy but with respect to place in the matrix product.

There are namely selection principles for the rotational quantum number in virtue of which all matrix elements vanish which relate to two levels which do not lie close together (or at least nearly vanish in case the selection principles for some reason do not hold vigorously). All we need to assume is therefore that the energy levels in the *neighborhood* of W_k^0 may be taken equal to W_k^0. So the five possibilities will give us a term of order F^4 in (11)

$$5\cdot(-1)^4F^4(W_k^0-C)(M_z^4)_{kk}$$

and the same assumption enables us to calculate the terms with F^3, etc., the numerical coefficients being of course the binomial coefficients belonging to the fifth power:

$$10(-1)^3F^3(W_k^0-C)^2(M_z^3)_{kk}, \qquad 10(-1)^2F^2(W_k^0-C)^3(M_z^2)_{kk} \text{ etc.}$$

We only considered the term $[\quad]_{kk}$ in the sum (10). To evaluate the *sum* itself we have therefore to suppose that the very few energy levels in the neighborhood of W_a^0 may be taken equal to W_a^0, those around W_b^0 to W_b^0, in general those around an arbitrary level W_k^0 equal to W_k^0. This assumption is by no means so drastic as our previous one which includes putting *all* low levels equal to one another. Only when we chose instead of $p=5$ for example $p=50$, we might encounter an intermediate level bound to the initial one by a range of non-vanishing matrix elements and yet far away from it. There our assumption would be very likely about as bad as our previous one, but terms with a great value of p contribute very little, since they belong to the outermost part of the development which we assumed to converge. Changing our special case $p=5$ into that of an arbitrary power, we find thus in a fair[4] approximation, from which one could obtain our previous approximation by omitting the term W_a^0-C. Instead of (6) we now obtain

$$\pi_p=\overline{\left\{\sum_m\left[(W^0{}_{n_0j}-C-FM_z)^p\right]_{(n_0jm,n_0jm)}:p_j\right\}}:p!k^pT^p. \tag{13}$$

Here we have written $W_{n_0j}^0$; instead of $W_{n_0jm}^0$ for W_a^0 since it signifies the energy in the absence of an external field and therefore does not depend on m. This fact is very important for the next transformation, as it permits us after the development of the p*th* power to bring $W_{n_0j}^0-C$ in each term before the summation sign $\sum_m$. The expression $\{\cdots\cdots\}$ in (13) is therefore a collection of quantum mechanical averages instead of the one (6) which appeared previously. But on each one our theorem (8) can be applied, taking there $p=0,\ 1,\ 2,\cdots p$ so that we obtain a *collection* of classical averages, giving us:

[4] The degree of approximation is still higher than it is merely because of the fact that only evels lying close together had to be taken equal. If we namely assume their energy values to vary linearly, i.e. to show constant differences λ, this λ would only appear as λ^2 and higher powers in the final result the term with λ cancelling o.t on account of symmetry.

$$\{\cdots\}=\overline{(W^0_{n\,oj}-C-F\mu_j\cos\theta)^p}^{cl}$$

where the bar of course refers to θ. This had further to be averaged over j to find π_p in formula (13). For such a double average we use a bar with indices cl, j. We find then:

$$1-\pi_1+\pi_2-\pi_3+\cdots=\overline{(e^{-(W^0_{noj}-C-F\mu_j\cos\theta)/kT})}^{cl,j}$$

Since we assumed that μ was not appreciably affected by the centrifugal force and therefore independent of j, we have

$$\log(1-\pi_1+\pi_2-\pi_3+\cdots)=\log\overline{(e^{-(W^0_{noj}-C)/kT})}^{j}+\log\overline{(e^{F\mu\cos\theta/kT})}^{cl}$$

The function Z defined in (2a) (the logarithm of the so-called "Zustandsumme") thus separates into two parts, a purely rotational part independent of F and a "magnetic" part which is the same as the Langevin value of Z we previously obtained when we neglected the molecular rotations. The first part is the same as the value of Z in the absence of a magnetic field and by (2) contributes nothing to the polarization. The inclusion of the rotation thus does not impair the validity of the Langevin formula for the polarization provided the temperature is high enough so that the quantum frequencies of rotation are small compared to kT/h.

§3 The Electric Polarization of a Gas of Deformable Molecules in a Strong Field

Deformations due to rotation, i.e. to a centrifugal force, will be neglected. Only those owing to the static electric field will be considered, so that we shall give here the quantum mechanical analog of the well known classical corrections which Debye added to the Langevin function in the case of electric polarization. Since the molecules are no longer rigid, we have here also to do with high frequency matrix elements which describe the deformation in the matrix language. This fact complicates our calculations very much. We again have here to use the equations (2), (3), (4) for $\overline{m}_z$, Z and π_p but the evaluation of π_p in the fashion of §2 was only possible in the absence of excited levels (in the derivation of Eq. 5) i.e., in the absence of high frequency matrix elements. We must therefore find another way here. We shall be content with a development of the polarization in powers of F exact through terms in F^3. At the same time, we assume that the temperature is large enough to make an expansion of the polarization in powers of $h\nu/kT$ legitimate. Calculating with Debye only the terms with F and F^3 we see immediately from the form of the Boltzmann law that we can omit in the polarization all terms with $(kT)^{-4}$ and higher negative powers. We need therefore for the logarithms in Z an expansion exact in terms with $(kT)^{-4}$ on account of Eq. (2). Since π_p contains $(kT)^{-p}$ we write:

$$\log(1-\pi_1+\pi_2-\pi_3+\cdots)$$
$$=-\pi_1+\left(-\frac{\pi_1^2}{2}+\pi_2\right)+\left(-\frac{\pi_1^3}{3}+\pi_1\pi_2-\pi_3\right)+\left(-\frac{\pi_1^4}{6}+\pi_1^2\pi_2-\pi_1\pi_3-\frac{\pi_2^2}{2}+\pi_4\right)$$

From the above we have to develop the π's in a power series of F but need not go beyond F^4, again on account of Eq. (2). Therefore we substitute:

$$W_a^{(F)}=W_a^0+FW_a^{(1)}+F^2W_a^{(2)}+F^3W_a^{(3)}+F^4W_a^{(4)} \tag{14}$$

in the right side of (4) and find thus

$$\pi_p p!k^pT^pN_a=\sum_a(W_a^0-C)^p+\sum_{k=1,2,3,4}F^k\sum_a K_a^{(k,p)}, \tag{15}$$

introducing $K_a^{k,p}$ as the coefficient of F^k in the expansion of $(W_a^{(F)}-C)^p$. It can be shown that $\sum_a K_a^{k,p}$ vanishes for an odd value of k, so that π_p will become an even function of F. The proof is based upon the fact that:

$$M^z_{(njm,n'j'm')}=-M^z_{(n,j,-m',n',j',-m')}$$

the ground of which is that a change of the magnetic (or axial) quantum number both in the initial and final state can be interpreted as a reversing of the direction of z. From this and from the fact that m ranges symmetrically over negative and positive values, it follows that:

$$\sum_{m'm''m'''}M^z_{(njm,n'j'm')}M^z_{(n'j'm',n''j''m'')}\cdots M^z_{(\cdots,njm)} \tag{16}$$

is multiplied by $(-1)^k$, k being the number of matrix elements in each product, when we replace m (i.e. the axial quantum number in the initial *and* final state) by $-m$ From its definition we know that K_a^{kp} contains only terms which can be written as

$$CW_a^{(j)}W_a^{(j')}W_a^{(j'')}\cdots W_a^{(l)} \text{ with } j+j'+j''+\cdots l=k. \tag{17}$$

From the theory of Born, Heisenberg and Jordan (compare also the explicit formulas for W_a^1, W_a^2, W_a^3, and W_a^4 in (22a)) we know that W_a^j consists only of terms with j matrix elements arranged as in (16) and summed in the same way over the indices m', m'' $\cdots$ and over other indices which do not play a role in our proof. Therefore the term (17) and consequently also $K_a^{k,p}$ is multiplied with $(^-1)^{j+j'\cdots l}=(-1)^k$ if we choose instead of a $(=n_0,j,m)$ another state $n_0,j,-m$. Now in the summation $\sum_a K_a^{k,p}$ each state n_0j, m may be combined with another $n_0,j,-m$ so that all terms cancel out if $p=$odd, and thus we have proved

$$\sum_a K_a^{(kp)}=0 \quad \text{for} \quad k \text{ odd}. \tag{18}$$

Let us for the present neglect the rotational energy since we may expect from our results in §2 that this part of the energy would only affect the value of

the "Zustandsumme" Z but not that of the polarization itself. Afterwards we shall correct our result again for the omission of the rotational terms. We now have

$$K_a^{(kp)}=0 \quad \text{for} \quad k<p, \tag{19}$$

since in its terms there occurs always at least one factor (W_a^o-C) which vanishes by taking $W_a^0=W_b^0=\cdots=C$. From (15), (18) and (19) we obtain:

$$\left.\begin{aligned} \pi_1 N_a kT &= F^2\sum_a K_a^{(21)}+F^4\sum_a K_a^{(41)} \;;\; \pi_3 N_a 3!k^3T^3=F^4\sum_a K_a^{(43)} \\ \pi_2 N_a 2!k^2T^2 &= F^2\sum_a K_a^{(22)}+F^4\sum_a K_a^{(42)} \;;\; \pi_4 N_a 4!k^4T^4=F^4\sum_a K_a^{(44)} \end{aligned}\right\} \tag{20}$$

The quantities $\sum_a K_a^{kp}$ now become also very simple, thanks to the assumption $W_a^0-C=0$. These are the coefficients of F^k in the expansion of $\sum_a(FW_a^1+F^2W_a^{(2)}+\cdots)^p$ and we have

$$\left.\begin{aligned} K_a^{(41)} &= W_a^{(4)} \;; & K_a^{(43)} &= 3W_a^{(1)}W_a^{(1)}W_a^{(2)} \\ K_a^{(42)} &= 2W_a^{(3)}W_a^{(1)}+W_a^{(2)}W_a^{(2)} \;; & K_a^{(44)} &= W_a^{(1)}W_a^{(1)}W_a^{(1)}W_a^{(1)} \end{aligned}\right\} \tag{20a}$$

So we need now to calculate W_a^1, W_a^2, W_a^3 and W_a^4. As is known, Born, Heisenberg and Jordan have developed a general method for the calculation of W_a^k from the matrices H^0, H^1, H^2 $\cdots$ occurring in the perturbed Hamiltonian and they gave explicitly the formulas for W_a^1, W_a^2, and W_a^3. Since in our case $H^{(2)}=H^{(3)}=\cdots=0$ it may be useful to follow another method which, although substantially equivalent, is perhaps a bit more lucid. We denote the eigen-functions and eigen-values of the Schroedinger equation in the absence of the field by u_n^o, W_n^0 and in its presence by u_n, W_n. On account of the assumed completeness of the u_n^0 we can make the expansion:

$$u_n=\sum_m(\delta_n{}^m+Fc_{mn}^{(1)}+F^2c_{mn}^{(2)}+\cdots)u_m^0 \tag{21}$$

so that u_n reduces to u_n^0 when $F=0$. Substituting this, together with the expansion (14) for W_n into the Schroedinger equation:

$$(H^0+FH^{(1)})u_n=W_nu_n \tag{22}$$

and equating the coefficients of equal powers of F in the left and right hand side, we obtain several relations in which the operators H^0 and H^1 work upon u_1^0 u_2^0 u_3^0 $\cdots$ etc. The effect of the operator H^o is simply given by the Schroedinger equation $H^0u_n^0=W_n^0u_n^0$ and if we introduce matrix elements by means of

$$H^{(1)}u_n^0=\sum_m H_{mn}^{(1)}u_m^0$$

then our relations (22) become merely linear forms in the u_n^0 themselves. Because of the linear independence of these u_n^0 the coefficient of each u_n^0 must vanish, yielding us the following equations:

$$W_m^0 c_{mn}^{(1)} + H_{mn}^{(1)} - c_{mn}^{(1)} W_n^0 = \delta_n^m W_n^{(1)}$$

$$W_m^0 c_{mn}^{(3)} + \sum_k H_{mk}^{(1)} c_{kn}^{(2)} - c_{mn}^{(3)} W_n^0 - c_{mn}^{(2)} W_n^{(1)} - c_{mn}^{(1)} W_n^{(2)} = \delta_n^m W_n^{(3)}$$

$$W_m^0 c_{mn}^{(4)} + \sum_k H_{mk}^{(1)} c_{kn}^{(3)} - c_{mn}^{(4)} W_n^0 - c_{mn}^{(3)} W_n^{(1)} - c_{mn}^{(2)} W_n^{(2)} - c_{mn}^{(1)} W_n^{(3)} = \delta_n^m W_n^{(4)}$$

originating respectively from the terms with F, F^2, F^3 and F^4 in the development of equation (22).

Putting $m=n$ in the first equation we find $W_n^1 = H_{nn}^1$ since the unknown c_{nn}^1 then cancels out. For $m \neq n$, it gives $c_{mn}^1 = H_{mn}^1/(W_n^0 - W_m^0) = H_{mn}^1/h\nu_{nm}$. Putting $m=n$ in the second equation we are able to find W_n^2 since c_{nm}^1 has been found already and c_{nn}^1 and c_{nn}^2 cancel out. So we get successively the values for W_a^1, W_a^2, W_a^3, and W_a^4. The calculation goes on very easily since we always get rid of many terms, when we collect each time those with c_{nn}^i. These coefficients only play a role in the normalization of the new eigen-functions, but the energy is of course independent of them. We thus find, on writing $H_{nm}^{(1)} = -M_{nm}^z$

$$W_a^{(1)} = -M_{aa}^z, \quad W_a^{(2)} = \sum_\beta{}' \frac{M_{a\beta}^z M_{\beta a}^z}{h\nu_{a\beta}}$$

$$W_a^{(3)} = -\sum_{\beta\gamma}{}' \frac{M_{a\beta}^z M_{\beta\gamma}^z M_{\gamma a}^z}{h^2 \nu_{a\beta}\nu_{a\gamma}} + \sum_\beta{}' \frac{M_{aa}^z M_{a\beta}^z M_{\beta a}^z}{h^2 \nu_{a\beta}^2} \tag{22a}$$

$$W_a^{(4)} = \sum_{\beta\gamma\delta}{}' \frac{M_{a\beta}^z M_{\beta\gamma}^z M_{\gamma\delta}^z M_{\delta a}^z}{h^3 \nu_{a\beta}\nu_{a\gamma}\nu_{a\delta}} + \sum_\beta{}' \frac{M_{aa}^z M_{aa}^z M_{a\beta}^z M_{\beta a}^z}{h^3 \nu_a{}^3{}_\beta}$$

$$- \frac{1}{2}\sum_{\beta\gamma}{}' \frac{2M_{a\beta}^z M_{\beta\gamma}^z M_{\gamma a}^z M_{aa}^z + M_{a\beta}^z M_{\beta a}^z M_{a\gamma}^z M_{\gamma a}^z}{h^3} \frac{\nu_{a\beta} + \nu_{a\gamma}}{\nu^2{}_{a\beta}\nu^2{}_{a\gamma}}$$

where a dash above a summation sign denotes that β, γ, δ always must be unequal to a. When we now exclude the rotational terms, the indices β, γ, δ $\cdots$ can only indicate excited states and have to be replaced by B, C, D $\cdots$ and the dash is no longer necessary. These equations permit us to calculate the $K_a^{k,p}$ of (20a) and so also the functions π_p in (20). Substituting the last ones in the development of the logarithms in Z and applying the relation (2) between $\overline{m}_z$ and Z, we find:

$$\overline{m}_z = pF + qF^3$$

$$q = -\frac{p^2}{2kT} + \frac{4}{N_a}\left[-P_0 + \frac{P_1}{2kT} - \frac{P_2}{6k^2T^2} + \frac{P_3}{24k^3T^3}\right]. \tag{23}$$

Introducing the abbreviation:

$$(a\beta\gamma\delta a)^z = M^z_{a\beta} M^z_{\beta\gamma} M^z_{\gamma\delta} M^z_{\delta a} \tag{23a}$$

we have for P_0, P_1, P_2 and P_3 the following values:

$$\left.\begin{aligned} P_0 &= \sum_{aBCD} \frac{(aBCDa)^z}{h^3 \nu_{aB}\nu_{aC}\nu_{aD}} + \sum_{aD} \frac{(aaaDa)^z}{h^3 \nu^3_{aD}} \\ &\quad - \frac{1}{2} \sum_{aCD} \frac{2(aCDaa)^z + (aCaDa)^z}{h^3} \frac{\nu_{aC}+\nu_{aD}}{\nu_a{}^2{}_C \nu^2{}_{aD}} \\ P_1 &= 2 \sum_{aCD} \frac{(aaCDa)^z}{h^2 \nu_{aC}\nu_{aD}} - 2 \sum_{aD} \frac{(aaaDa)^z}{h^2 \nu^2_{aD}} + \sum_{aCD} \frac{(aCaDa)^z}{h^2 \nu_{aC}\nu_{aD}} \\ P_2 &= 3 \sum_{aD} \frac{(aaaDa)^z}{h \nu_{aD}}, \qquad P_3 = \sum_a (aaaaa)^z \end{aligned}\right\} \tag{24}$$

We could also express p explicitly in $K_a{}^{k,2}$ or in summations over matrix elements, but this can be omitted since p has already been calculated by Van Vleck. His result reads in our notation:

$$p = \frac{\mu^2}{3kT} - \frac{2}{3h} \sum_{n'} \frac{M_{(n_0 n')} M_{(n' n_0)}}{\nu_{(n_0 n')}} \tag{25}$$

where the summation over j and m has already been carried out. The first term containing the permanent molecular moment μ represents the rotational terms (those with low frequency matrix elements), while the second term, contains the high frequency elements of the matrix M defined by

$$|M_{(n_0 n')}|^2 = |M_{x(n_0 n')}|^2 + |M_{y(n_0 n')}|^2 + |M_{z(n_0 n')}|^2$$

The diagonal elements of the square of the low frequency part of the matrix M are assumed to be equal ($=\mu^2$) (cf. Eq. (33) below).

Since the rotational terms of p are already included in Van Vleck's value, we have only to examine what corrections are occasioned in $P_0 \cdots P_3$ if we will no longer neglect the rotational terms. We have then to build up the quantities $K_a{}^{kp}$ with the aid of $W_a{}^1 \cdots W_a{}^4$ in which β, γ, $\delta \cdots$ now can denote both the "low" indices b, c, d, $\cdots$ for the rotational terms and B, C, D, $\cdots$ for the deformation terms and furthermore can denote partly "low", partly "high" indices for the interaction between rotation and deformation. Also we may no longer neglect terms with $W_a{}^o - C$ in $K_a{}^{kp}$ (cf. 20a) and we have at the same time to take into account the quantities $K_a{}^{kp}$ with $k<p$, which in (19) only vanished by neglecting the rotational energy. The calculation is therefore very complicated, but for the case that low frequencies such as ν_{ab}, ν_{bc} etc. may be considered as very small[5] compared with high frequencies as ν_{aB} the final result can be put in a comparatively simple form. We find:

[5] Of course also small with respect to kT/h since only then the development has a meaning.

$$
\left.\begin{aligned}
P_0 &= \sum_{aBCD} \frac{(aBCDa)^z}{h^3 \nu_{aB}\nu_{aC}\nu_{aD}} + \sum_{abcD} \frac{(abcDa)^z}{h^3 \nu^3{}_{aD}} \\
&\quad - \frac{1}{2} \sum_{abCD} \frac{2(aCDca)^z + (aCbDa)^z}{h^3} \; \frac{\nu_{aC} + \nu_{aD}}{\nu^2{}_{aC}\nu_{aD}} \\
P_1 &= 2 \sum_{abCD} \frac{(abCDa)^z}{h^2 \nu_{aC}\nu_{aD}} - 2 \sum_{abcD} \frac{(abcDa)^z}{h^2 \nu_a{}^2{}_D} + \sum_{abCD} \frac{(aCbDa)^z}{h^2 \nu_{aC}\nu_{aD}} \\
P_2 &= 3 \sum_{abcD} \frac{(abcDa)^z}{h\nu_{aD}} \; ; \quad P_3 = \sum_{abcd} (abcda)^z
\end{aligned}\right\} \tag{26}
$$

Comparing this result with that of (24) we could find a rule as to how to construct (26) from (24). As we said already, the derivation is very complicated and laborious and will therefore not be given here, since the result is already obvious enough, when compared with that of (24) Still we might derive some equations needed in the proof and giving an idea about the way in which to reach the final result.

We shall first prove the relation:

$$
L = \frac{1}{\nu_{ab}\nu_{ac}\nu_{aD}} + \frac{1}{\nu_{ba}\nu_{bc}\nu_{bD}} + \frac{1}{\nu_{ca}\nu_{cb}\nu_{cD}} = \frac{1}{\nu_{aD}\nu_{cD}\nu_{bD}} = \frac{1}{\nu^3{}_{aD}} \tag{27}
$$

neglecting $\nu_l/\nu_H{}^4$ in comparison with 1, where ν_l denotes a low frequency and ν_H some high one. On account of $h\nu_{aD} = W_a{}^0 - W_D{}^0$ there will occur many negative frequencies. We write more cyclically:

$$
L = \frac{-(\nu_{bc}\nu_{cD}\nu_{Db}) + (\nu_{cD}\nu_{Da}\nu_{ac}) - (\nu_{Da}\nu_{ab}\nu_{bD})}{-\nu_{ab}\nu_{bc}\nu_{ca}\nu_{aD}\nu_{bD}\nu_{cD}} = \frac{u}{v} \, . \tag{28}
$$

The nominator U vanishes if we assume $W_b{}^0 = W_a{}^0$ or $W_c{}^0 = W_a{}^0$ or $W_c{}^0 = W_b{}^0$ and U can therefore be factored into

$$
u = f\nu_{ab}\nu_{bc}\nu_{ca}
$$

introducing a function f which we now will determine without any calculation. Although contrary to the physical meaning of $W_D{}^0$ we may still mathematically determine the value of U for one of the assumptions

$$
W_D{}^0 = W_a{}^0 \quad \text{or} \quad W_D{}^0 = W_b{}^0 \quad \text{or} \quad W_D{}^0 = W_c{}^0 \, . \tag{29}
$$

For each of these assumptions we find immediately $U = -\nu_{ab}\nu_{bc}\nu_{ca}$ and from that we suspect that for an arbitrary value of $W_D{}^0$

$$
U = -(\nu_{bc}\nu_{cD}\nu_{Db}) + (\nu_{cD}\nu_{Da}\nu_{ac}) - (\nu_{Da}\nu_{ab}\nu_{bD}) = -\nu_{ab}\nu_{bc}\nu_{ca} \, .
$$

To prove that this equation holds identically, we consider it first as a quadratic equation for the determination of $W_D{}^0$. From the above we already know three solutions: namely, the values (29). But a quadratic equation with three different roots must be an identity. Using this value for U we get for L the second value in (27) and in an allowed approximation the third value.

This relation (27) is a typical one and we shall show how it is used to oust the low frequencies from the denominators containing both low and high ones. This of course is always very important since our final result consisted solely of terms with only high frequencies in the denominator. From §2 we know, that we do not need to pay attention to terms which contain entirely low frequencies and corresponding matrix elements, since they may affect Z only by a

constant and have no influence on the polarization. Let us therefore consider some "mixed" terms, such as[6]:

$$\sum_{\alpha\beta\gamma\delta}{}' \frac{M^s_{a\beta}M^s_{\beta\gamma}M^s_{\gamma\delta}M^s_{\delta a}}{h^3\nu_{a\beta}\nu_{a\gamma}\nu_{a\delta}} = \sum_{\alpha\beta\gamma\delta} \left\{ \begin{matrix} a & \beta & \gamma & \delta & a \\ & \neq & \neq & \neq & \\ a & a & a & a & \end{matrix} \right\}^s \tag{30}$$

occurring among others in $W_a{}^4$ and so in P_0 and of whose indices β, γ, δ we will take only one "high." It contains then among other terms:

$$\left\{ \begin{matrix} a & b & c & D & a \\ & \neq & \neq & & \\ a & a & a & & \end{matrix} \right\}^s + \left\{ \begin{matrix} a & b & C & d & a \\ & \neq & & \neq & \\ a & & a & a & \end{matrix} \right\}^s + \left\{ \begin{matrix} a & B & c & d & a \\ & & \neq & \neq & \\ & a & a & a & \end{matrix} \right\}^s$$

Since we have to sum over the indices a, b, c, d, A, B, C, D, we can arbitrarily change the name of the indices in the three terms independently. This means only that we arrange the terms in the entire group in another way, gathering each time three others together.

We take now:

b, c, D, a instead of a, b, C, d in the second term
c, D, a, b " " a, B, c, d " " third "

This alteration of names is so chosen that the symbols then appearing denote the same product of matrix *elements*, so that e.g.

$$(abcDa)^s = (bcDab)^s = (cDabc)^s .$$

This only means that $M_{ab}{}^s M_{bc}{}^s M_{cD}{}^s M_{Da}{}^s = M_{bc}{}^s M_{cD}{}^s M_{Da}{}^s M_{ab}{}^s$, etc. and has nothing to do with commutativeness of matrices. Our sum so becomes:

$$\sum \left\{ \begin{matrix} a & b & c & D & a \\ & \neq & \neq & & \\ a & a & a & & \end{matrix} \right\}^s + \sum \left\{ \begin{matrix} b & c & D & a & b \\ & \neq & & \neq & \\ b & & b & b & \end{matrix} \right\}^s + \sum \left\{ \begin{matrix} cD & a & b & c \\ & \neq & \neq & \\ c & c & c & \end{matrix} \right\}^s$$

Although the "arguments" $\{ \cdots \}^s$ contain the same product of matrix elements, we cannot yet combine these three sums together into a single one, on account of the various secondary conditions of inequality between some of the lower indices. Therefore we make a division in the following way:

$$\left\{ \begin{matrix} a & b & c & D & a \\ & \neq & \neq & & \\ a & a & a & & \end{matrix} \right\}^s = \left\{ \begin{matrix} a & b & c & D & a \\ \text{all unequal} & & & & \end{matrix} \right\}^s + \left\{ \begin{matrix} a & p & p & D & a \\ & & \neq & & \\ & & a & & \end{matrix} \right\}^s$$

and similarly for the other arguments. Thus we obtain for our entire sum:

$$\sum_{abcD} \frac{(abcDa)^s}{h^3} \left(\frac{1}{\nu_{ab}\nu_{ac}\nu_{aD}} + \frac{1}{\nu_{bc}\nu_{bD}\nu_{ba}} + \frac{1}{\nu_{cD}\nu_{ca}\nu_{cb}} \right)$$

$$+ \sum_{apD} \left\{ \begin{matrix} a & p & p & D & a \\ & & \neq & & \\ & & a & & \end{matrix} \right\}^s + \sum_{bpD} \left\{ \begin{matrix} b & p & D & p & b \\ & \neq & & & \\ b & & & & \end{matrix} \right\}^s + \sum_{cpD} \left\{ \begin{matrix} c & D & p & p & c \\ & & & \neq & \\ & & & c & \end{matrix} \right\}^s$$

We see now how the first part of it can be transformed with our relation (27) into a sum of terms with only high frequencies, which one might recognize in the expression for P_0 in (26). For the transformation of the second part we need to combine it with other terms of $W_a{}^{(3)}$. Even the terms with $W_a{}^0 - C$ as a factor can be treated in some analogous way. A typical relation we need then is

$$\frac{\nu_{a0}}{\nu_{ab}\nu_{ac}\nu_{aD}} + \frac{\nu_{b_0}}{\nu_{ba}\nu_{bc}\nu_{bD}} + \frac{\nu_{c_0}}{\nu_{ca}\nu_{cb}\nu_{cD}} = -\frac{1}{\nu^2{}_{aD}}$$

when $\nu_l/\nu_H{}^3$ is neglected in comparison to 1. Then we wrote only mathematically without thinking of a real absorption or emission frequency $W_{a0} - C = h\nu_{ac}$. The above relations and transformations are, we hope, enough to give an idea of the proof.

[6] The new symbol is related to the old one of (23a) in the following way

$$\{a\beta\gamma\delta a\}^s = (a\beta\gamma\delta a)^s / h^3 \nu_{a\beta}\nu_{a\gamma}\nu_{a\delta}$$

Let us now return to our formula (26) for $P_0 \cdots P_3$. In our q-formula (23) we need only these quantities divided by N_a, i.e. we need there several quantum mechanical average values and we showed in § 2 how to transform these into classical ones. Still there is a difference on account of the presence of high energy levels. The summation over the low intermediate levels will lead to a function of the molecular moments in the unexcited states, that over the high ones will remain in our answer as a sum. For the details we refer to the appendix; only some important points will be given below.

The $x'y'z'$ axes are fixed in the molecule and their positions with respect to the xyz axes (fixed in space) are indicated by the Eulerian angles $\theta\varphi\psi$. Since we have for the classical moments:

$$M^z = -M^{x'} \sin\theta \cos\psi + M^{y'} \sin\theta \sin\psi + M^{z'} \cos\theta,$$

and since we have to consider for the q-formula only matrix-products of four factors M^z, it will be clear that the application of our rule for the calculation needs the classical averages:

$$\begin{aligned} &\overline{\sin^4\theta \cos^4\psi} = \overline{\sin^4\theta \sin^4\psi} = \overline{\cos^4\theta} = 1/5 \\ &\overline{\sin^4\theta \cos^2\psi \sin^2\psi} = \overline{\sin^2\theta \cos^2\theta \cos^2\psi} = \overline{\sin^2\theta \cos^2\theta \sin^2\psi} = 1/15 \end{aligned} \qquad (31)$$

while many other averages vanish. The first three values will be connected with the terms containing four elements of the matrix $M^{z'}$ or four of $M^{y'}$ or of $M^{x'}$ and the last three with each of the terms of the right side of

$$(\alpha\beta\gamma\delta\alpha)^{i,i'} = M^i_{\alpha\beta} M^i_{\beta\gamma} M^{i'}_{\gamma\delta} M^{i'}_{\delta\alpha} + M^i_{\alpha\beta} M^{i'}_{\beta\gamma} M^i_{\gamma\delta} M^{i'}_{\delta\alpha} + M^i_{\alpha\beta} M^{i'}_{\beta\gamma} M^{i'}_{\gamma\delta} M^i_{\delta\alpha} \qquad (32)$$

This new symbol will be useful further on. Here and throughout the whole paper we suppose *always* $i' \neq i$ and both can denote x' or y' or z'. Since the other average values besides those in (31) vanish, the matrices M^i and $M^{i'}$ are always represented by an even number of elements in the remaining terms.

These classical averages replace only quantum mechanical averages over the axial quantum number (m) so that our rule gives e.g.

$$15 \sum_{abcd} (abcda)^z : N_a = \left[3 \sum_i \sum_{a'b'c'd'} (a'b'c'd'a')^i + \sum_{ii'} \sum_{a'b'c'd'} (a'b'c'd'a')^{ii'} \right] : N_{a'}$$

where the dash on a, b, $\cdots$ indicates that the summation is to extend over all quantum numbers originally involved in a, b, $\cdots$ except over the axial quantum numbers. Consequently we had in the right hand side to divide by N_a' instead of N_a. If at the beginning we had described the state of a molecule by means of its $x'y'z'$ system, we should have had no axial quantum number entering into our formulas and so in some respects the indices $a'b'c' \cdots$ may be related to the states described in the $x'y'z'$ system.

Now if we neglect the deformation of a molecule by rotation, the sum

$$\sum_{b'} M^i_{a'b'} M^i_{b'c'} = \mu_i^2 \delta^{c'}_{a'} \qquad (33)$$

must be a diagonal matrix, which we may suppose in accordance with our assumption as constant, i.e. the same for each of the $N_{a'}$ states a'. Since i can denote x', y' or z', terms such as (33) correspond classically to the squares of the electric moments of the molecule along the principal axes, when $x'y'z'$ are properly chosen in the molecule, e.g. symmetrically in a diatomic one. So we have:

$$\sum_{abcd}(abcda)^2 : N_a = \sum_i \mu_i^4 + \sum_{i,i'} \mu_i^2 \mu_{i'}^2 = \mu^4 .$$

To obtain the last term in the second expression, we used the fact that M^i and $M^{i'}$ commute with one another:

$$(M^i M^i M^{i'} M^{i'})_{a'a'} + (M^i M^{i'} M^i M^{i'})_{a'a'} + (M^i M^{i'} M^{i'} M^i)_{a'a'} = 3(M^i M^i M^{i'} M^{i'})_{a'a'}$$

This was permitted for *electric* moments, since they are proportional to coordinates and all coordinates commute; but for magnetic moments this would not have been allowed.

More complicated is the calculation of:

$$\sum_{abcD} \frac{(abcDa)^2}{h^{p_\nu p}{}_{aD}} : N_a = \sum_{a'b'c'D'} \left[\frac{1}{5} \sum_i \frac{(a'b'c'D'a')^i}{h^{p_\nu p}{}_{a'D'}} + \frac{1}{15} \sum_{i,i'} \frac{(a'b'c'D'a')^{i,i'}}{h^{p_\nu p}{}_{a'D'}} \right] : N_{a'} \qquad (34)$$

There the first sum in the right side is transformed as follows:

$$\sum_{a'b'c'D'} \frac{(a'b'c'D'a')^i}{h^{p_\nu p}{}_{a'D'}} : N_{a'} = \mu_i^2 \sum_{a'D'} \frac{M^i_{a'D'} M^i_{D'a'}}{h^{p_\nu p}{}_{a'D'}} = \mu_i^2 \sum_{n'} \frac{|M^i_{(n0n')}|^2}{h^{p_\nu p}{}_{(n0n')}}$$

where we assumed in accordance with the sum rule (cf. Van Vleck for $p=1$) that the fraction in the middle part of the above equation when summed over D' is independent of the choice of a' from the low states. This fraction depends therefore only on the indices n. Further, we used the fact that $M_{n0n'}{}^i$ and $M_{n',n_0}{}^i$ are complex conjugate so that their product is the square of their absolute value, indicated by $|\ \ |$. For the other term in the right side of Eq. (34) we have the result

$$\sum_{a'b'c'D'} \frac{(a'b'c'D'a')^{i,i'}}{h^{p_{na'D'}}} : N_{a'} = \mu^{i2} \sum_{n'} \frac{|M^i_{(n0n')}|^2}{h^{p_\nu p}{}_{(n0n')}} + 2\mu_i \mu_{i'} \sum_{n'} \frac{|M^i_{n0n'} M^{i'}_{n'n0}|}{h^{p_\nu p}{}_{n0n'}}$$

as follows from the definition of the symbol $(\ \ )^{ii'}$ in (32) and also from the further relation:

$$\sum_{b'} M^i_{a'b'} M^{i'}_{b'c'} = \mu_i \mu_{i'} \delta^{c'}_{a'}$$

Thus the whole right side of (34) has now been found. The result is

$$\sum_{abcD} \frac{(abcDa)^2}{h^{p_\nu p}{}_{aD}} : N_a = -\frac{1}{30} \sum_{i\,i'} \{\mu_i^2 (3a_p{}^{ii} + a_p{}^{i'i'}) + 2\mu_i \mu_{i'} a_p{}^{ii'}\}$$

if we introduce the abbreviations:

$$-2\sum_{n'} \frac{|M^i_{n0n'}|^2}{h^{p_\nu p}{}_{n0n'}} = a_p{}^{ii}; \qquad -2\sum_{n'} \frac{|M^i_{n0n'} M^{i'}_{n'n0}|}{h^{p_\nu p}{}_{n0n'}} = a_p{}^{ii'} = a_p{}^{i'i}$$

Still another kind of transformation is necessary for:

$$\sum_{abCD} \frac{(aCbDa)^2}{h^2 \nu_{aC} \nu_{aD}} : N_a = \frac{1}{5} \sum_i \sum_{n'n''} \frac{M^i_{n0n'} M^i_{n'n0} M^i_{n0n''} M^i_{n''n0}}{h^2 \nu_{n0n'} \nu_{n0n''}}$$

$$+\frac{1}{15}\sum_{i'i''}\sum_{n'n''}\frac{M^{i}_{n_0n'}M^{i}_{n'n_0}M^{i'}_{n_0n''}M^{i''}_{n''n_0}+M^{i}_{n_0n'}M^{i''}_{n'n_0}M^{i}_{n_0n''}M^{i'}_{n''n_0}+M^{i}_{n_0n'}M^{i'}_{n'n_0}M^{i'}_{n_0n''}M^{i}_{n''n_0}}{h^2\nu_{n_0n'}\nu_{n_0n''}}$$

$$=\frac{1}{20}\sum_{i}(a_1{}^{ii})^2+\frac{1}{60}\sum_{i'i'}(a_1{}^{ii}\cdot a_1{}^{i'i'})+\frac{1}{30}(a_3{}^{iii'})^2.$$

The first two terms in the last member will be found immediately from the definition of $a_1{}^{ii}$ where one also may use n'' instead of n'. The last term results from the fact that.

$$\frac{1}{15}\sum_{ii'}\left[\sum_{n'}\frac{M^{i}_{n_0n'}M^{i}_{n'n_0}}{h\nu_{n_0n'}}\right]\left[\sum_{n'}\frac{M^{i}_{n_0n'}M^{i'}_{n'n_0}+M^{i'}_{n_0n'}M^{i}_{n'n_0}}{h\nu_{n_0n'}}\right]$$

$$=\frac{1}{30}\sum_{ii'}\left[\sum_{n'}\frac{M^{i}_{n_0n'}M^{i'}_{n'n_0}+M^{i'}_{n_0n'}M^{i}_{n'n_0}}{h\nu_{n_0n'}}\right]^2=\frac{1}{30}(a_1{}^{ii'})^2$$

Where the second expression follows from the preceding one by dividing this by 2 and counting the indices i and i' in the first factor twice, combining a term i, i' with a term i', i for which the second factor is the same. Dividing the following sum into two others which can be treated in a similar way to the preceding one, we find

$$\sum_{abCD}\frac{(aCbDa)^2}{h^3}\frac{\nu_{aC}+\nu_{aD}}{\nu_{aC}^2\nu_{aD}^2}:N_a=\frac{1}{10}\sum_{i}(a_1{}^{ii}\cdot a_2{}^{ii})+\frac{1}{30}\sum_{i_1i'}(a_1{}^{ii}a_2{}^{i'i'})+\frac{1}{15}\sum_{ii'}a_1{}^{ii'}a_2{}^{ii'}$$

In order to throw the other averages in our g-formula into a compact form, we introduce a new symbol for the sum of two others already defined in (23a) and (32):

$$(\cdots)^{3i+i,i'}=3(\cdots)^{i}+(\cdots)^{i,i'} \tag{34a}$$

and find then after a classical averaging:

$$\sum_{aBCD}\frac{(aBCDa)^2}{h^3\nu_{aB}\nu_{aC}\nu_{aD}}:N_a=\frac{1}{15}\sum_{ii'}\sum_{n'n''n'''}\frac{(n_0n'n''n'''n_0)^{3i+i,i'}}{h^3\nu_{n_0n'}\nu_{n_0n''}\nu_{n_0n'''}}=I$$

$$\sum_{abCD}\frac{(abCDa)^2}{h^2\nu_{aC}\nu_{aD}}:N_a=\frac{1}{15}\sum_{ii'}\sum_{n'n''}\frac{(n_0n_0n'n''n_0)^{3i+i,i'}}{h^2\nu_{n_0n'}\nu_{n_0n''}}=II$$

$$\sum_{abCD}\frac{(aCDba)^2}{h^3}\frac{\nu_{aC}+\nu_{aD}}{\nu_{aC}^2\nu_{aD}^2}:N_a=\frac{1}{15}\sum_{i'i'}\sum_{n'n''}\frac{(n_0n_0n'n''n_0)^{3i+i,i'}}{h^3}\frac{\nu_{n_0n'}+\nu_{n_0n''}}{\nu_{n_0n'}^2\nu_{n_0n''}^2}=III$$

All quantum mechanical averages in our q-formula (23) have now been calculated. Using these and the value (25) of p, which can be written in the form:

$$p=\frac{\mu^2}{3kT}+\frac{1}{3}\sum_{i}a_1{}^{ii}$$

we find at last:

$$\overline{m}_z=\left(p_0+\frac{\mu^2}{3kT}\right)F+\left(q_0+\frac{q_1}{kT}+\frac{q_2}{k^2T^2}-\frac{\mu^4}{45k^3T^3}\right)F^3$$

with

$$3p_0=\sum_{i}a_1{}^{ii}$$

$$15q_0=\sum_{i,i'}\left[a_1{}^{ii}(3a_2{}^{ii}+a_2{}^{i'i'})+2\mu_i{}^2(3a_3{}^{ii}+a_3{}^{i'i'})\right]$$

$$+\sum_{i,i'}4\mu_i\mu_i{}'a_3{}^{ii'}-60(I-III)$$

$$45q_1=(a_1{}^{x'x'}-a_1{}^{y'y'})^2+(a_1{}^{y'y'}-a_1{}^{z'z'})^2+(a_1{}^{z'z'}-a_1{}^{x'x'})^2 + \sum_{i,i'}[6\mu_i{}^2(3a_2{}^{ii}+a_2{}^{i'i'})+12\mu_i\mu_{i'}a_2{}^{ii'}]+180II$$

$$(45/2)q_2=(\mu_{x'}{}^2-\mu_{y'}{}^2)(a_1{}^{x'x'}-a_1{}^{y'y'})+(\mu_{y'}{}^2-\mu_{z'}{}^2)(a_1{}^{y'y'}-a_1{}^{z'z'}) +(\mu_{z'}{}^2-\mu_{x'}{}^2)(a_1{}^{z'z'}-a_1{}^{x'x'})+3\sum_{i,i'}\mu_i\mu_{i'}a_1{}^{ii'}.$$

The terms with p_o, q_o, q_1 and q_2 would vanish for rigid molecules, since then the high frequency elements involved in $a_p{}^{ii}$, $a_p{}^{ii'}$ would not exist.

In the special case considered by Debye in which the deformation can be described by means of harmonically bound particles, our formulae for W would not have contained third and higher powers of the field strength, i.e. all quantities whose first power possesses two or more frequencies in the denominator would not have appeared. So we would have to omit in our general answer the quantities I, II, III, $a_2{}^{ii}$, $a_2{}^{i'i'}$, $a_2{}^{ii'}$, $a_3{}^{ii}$, $a_3{}^{i'i'}$, $a_3{}^{ii'}$.

Further we have $a_1{}^{i,i'}=0$ if the $x'y'z'$ system is so chosen in the molecule that corresponds with the axes of the deformation ellipsoid in the classical theory.

Thus q_0 and the second line of q_1, q_2 would vanish and the result would have been exactly the formula of Debye[7] in which his coefficients a_{11}, a_{22}, a_{33} have to be replaced by our $a_1{}^{x'x'}$, $a_1{}^{y'y'}$, $a_1{}^{z'z'}$ the latter being therefore the quantum mechanical interpretation of the classical binding coefficients.

Magnetic Saturation in Quantum Mechanics

The calculation of the magnetic saturation differs from the electric in two respects: (a) in the non-commutativeness of the magnetic moment or angular momentum matrices, and (b) the presence of a term in the Hamiltonian function E which is quadratic in the magnetic field H. It is well known that the commutation rules for the components of the angular orbital momentum are:

$$L^{y'}L^{z'}-L^{z'}L^{y'}=L^{x'}ih/2\pi \qquad (35)$$

and those obtained by a cyclic interchanging of the indices.

According to Van Vleck and others the Hamiltonian[8] function in the presence of a magnetic field H is:

$$E=E^0+HE^{(1)}+H^2E^{(2)}$$

with

$$E^{(1)}=(e/2mc)\sum_i(p_{\phi i}+2p_{\psi i})\ ;\quad E^{(2)}=(e^2/8mc^2)\sum_i R_i{}^2.$$

Here p_{ϕ_i} and p_{ψ_i} are the components of orbital and spin angular momentum of the ith electron in the direction of the applied magnetic field, which we assume lies along the z axis. The factor 2 multiplying p_ψ is of course due to the anomaly in the spin magnetic moment. The generalized momenta p_ϕ

[7] Debye, Handbuch der Radiologie, Vol. VI, p. 779.

[8] We indicate the Hamiltonian here with E to avoid confusion with the magnetic field strength H.

and p_ψ are conjugate to azimuth angles ϕ and ψ specifying the motion[9] of the electron and its spin axis respectively around the z axis. This specification of the spin axis by means of Eulerian angles would, of course, presumably imply some kind of mechanical model for the electron spin, but fortunately the results are the same if we use Dirac's recent relativistic theory which frees us from using a model. The differences (a) and (b) tend to make the calculation more difficult than in the electric case, but these difficulties are usually offset by the fact that in paramagnetic terms the effect of the high frequency elements in the magnetic moments is negligible. The term proportional to H^2 is that responsible for diamagnetism and is negligible in comparison with the paramagnetic terms in paramagnetic atoms or molecules. Consequently we shall disregard this term in the balance of this section. We may mention, however, that a long calculation shows that if we neglect the spin, the influence of the diamagnetic term E^2 on the magnetic moment is, to terms in H^3:

$$-(e^2/6mc^2)(\xi+\eta+\zeta)H+(e^2/90mc^2k^2T^2)\left[(\xi-\eta)(\boldsymbol{\mu}_1^2-\boldsymbol{\mu}_2^2)\right.$$
$$\left.+(\eta-\zeta)(\boldsymbol{\mu}_2^2-\boldsymbol{\mu}_3^2)+(\zeta-\xi)(\boldsymbol{\mu}_3^2-\boldsymbol{\mu}_1^2)\right]H^3$$

where ξ, η, ζ are the time averages of $\sum_i x_i'^2$, $\sum y_i'^2$, $\sum_i z_i'^2$ respectively, the primed axes being fixed in the molecule, *e.g.* coinciding with its principal axes of inertia. Also $\boldsymbol{\mu}_1$, $\boldsymbol{\mu}_2$, $\boldsymbol{\mu}_3$ have been used to denote the components of magnetic moments along these three principal axes.[10]

Paramagnetic atoms without spin. Here $p_\psi=0$ and $\sum p_\phi$ is a diagonal matrix whose elements are $mh/2\pi$ where m is the usual magnetic quantum number. If we neglect the diamagnetic effect, the energy is given rigorously to all powers of H by:

$$W_a=W_a^0+m\beta H$$

where $\beta=he/4\pi mc$ denotes the Bohr magneton.

Brillouin[11] has shown that then the magnetic moment is

$$\overline{m}_z=\beta\left[\frac{le^{l\beta H/kT}+(l+1)e^{-(l+1)\beta H/kT}}{e^{l\beta H/kT}-e^{-(l+1)\beta H/kT}}-\frac{1}{e^{\beta H/kT}-1}\right]=B(l,\beta,H,T) \tag{36}$$

as he shows this is the same as

$$\overline{m}_z=\beta\sum_{m=-j}^{m=+j}me^{m\beta H/kT}:\sum_{m=-j}^{m=+j}e^{m\beta H/kT} \tag{37}$$

The right hand side of (36) we shall call a "Brillouin function" and denote it by $B(l, \beta, H, T)$.[12] As the square of the magnetic moment is $l(l+1)\beta^2$ one might at first thought expect $B(l, \beta, H, T)$ to be the same as $L((l^2+l)^{\frac{1}{2}}\beta,$

[9] R_i is the radius vector from the ith electron to the nucleus.

[10] Bold face letters denote always magnetic moments.

[11] Brillouin, J. de Physique **8**, 74 (1927).

[12] The introduction of the constant β parameter in this formula might appear superfluous here but will be very useful afterwards.

H, T) where $L(\mu, H, T)$ is the Langevin function defined in Eq. (9) now with H instead of F. Actually this is not the case, as one easily verifies that

$$B(l,\beta,H,T)=L((l+\tfrac{1}{2})\beta,H,T)-L(\tfrac{1}{2}\beta,H,T). \tag{38}$$

The difference is due to the non-commutativeness of the various components of the angular momentum matrices. This can be seen as follows. If one follows a method analogous to that used in the electric case, rather than Brillouin's simple method, one finds that to terms in H^3:

$$\overline{m}_z=\mathfrak{P}H+\mathfrak{Q}H^3 \tag{39}$$

where

$$\mathfrak{P}=\frac{\sum_a(\mathfrak{M}^z\mathfrak{M}^z)_{aa}}{N_akT},\quad \mathfrak{Q}=\frac{\sum_a(\mathfrak{M}^z\mathfrak{M}^z\mathfrak{M}^z\mathfrak{M}^z)_{aa}}{6N_ak^3T^3}-\frac{\mathfrak{P}^2}{2kT} \tag{40}$$

Here $\mathfrak{M}$ denotes the magnetic moment matrix. If one could perform the spacial averaging in the same way as in the electric case, Eq. (39) would become:

$$\overline{m}_z=H\mathfrak{y}^2/3kT-H^3\mathfrak{y}^4/45k^3T^3$$

the first terms of a Langevin function, whereas actually it will be shown to give:

$$\overline{m}_z=H\mathfrak{y}^2/3kT-H^3[\mathfrak{y}^4+\tfrac{1}{2}\mathfrak{y}^2\beta^2]/45k^3T^3 \tag{41}$$

being the first terms of $B(l, \beta, H, T)$ if we set $\mathfrak{y}^2=l(l+1)\beta^2$. The term with β in (41) is due to the non-commutativeness of angular moment matrices, as will now be shown. Neglecting the spin, we have

$$\mathfrak{M}^z=-eL^z/2mc \tag{42}$$

where the matrix L corresponds to the total orbital impulse moment of the electrons and L^z to its component $\sum_i p_{\phi_i}$ along the z-axis. Using again an $x'y'z'$ system fixed in the molecule we find by averaging over the Eulerian angles and following the same procedure as in the appendix:

$$15\sum_a(L^zL^zL^zL^z)_{aa}:N_a=\sum_{i,i'}(LLLL)^{3i+i,i'} \tag{43}$$

where i and $i'\neq i$ again denote $x'y'z'$ and the symbol in the right hand side is defined in (34a). Here we reach the point from which calculations of the electric and magnetic polarization no longer parallel each other. For the L^i and $L^{i'}$ the commutation rules (35) are valid. By applying these and using (32) one finds

$$(LLLL)^{x'y'}_{aa}=(L^{x'}L^{x'}L^{y'}L^{y'})_{aa}+(L^{x'}L^{y'}L^{x'}L^{y'})_{aa}+(L^{x'}L^{y'}L^{y'}L^{x'})_{aa}$$

$$=3(L^{x'}L^{x'}L^{y'}L^{y'})_{aa}-(2L^{x'}L^{x'}L^{y'}+L^{x'}L^{y'}L^{x'})_{aa}ih/2\pi.$$

According to the commutation rules we may interchange x' and y' if we reverse at the same time the sign of $ih/2\pi$. Adding the resulting $(LLLL)^{y'z'}$ to $(LLLL)^{x'y'}$ and replacing the indices $x'y'$ in this sum in a cyclic way we find by summing

$$\sum_{ii'}(LLLL)_{aa}^{ii'}=3\sum_{ii'}(L^iL^iL^{i'}L^{i'})_{aa}-[L^{x'}(L^{x'}L^{y'}-L^{y'}L^{x'})+L^{y'}(L^{x'}L^{x'}-L^{x'}L^{x'})$$
$$+L^{z'}(L^{y'}L^{x'}-L^{x'}L^{y'})]_{aa}ih/2\pi$$
$$=3\sum_{ii'}(L^iL^iL^{i'}L^{i'})_{aa}-(h^2/4\pi^2)\sum_i L^iL^i.$$

Adding $3\sum_i(L^iL^iL^iL^i)_{aa}$ we obtain

$$\sum_{ii'}(LLLL)_{aa}^{3i+i,i'}=(3L^4-(h^2/4\pi^2)L^2)_{aa}. \tag{44}$$

Furthermore we have still in $\mathfrak{P}$:

$$\sum_a(LL)_{aa}:N_a=\sum_i L^iL^i:3=(L^2)_{aa}:3, \tag{45}$$

Using (40), (42), (43), (44), (45) and setting $(L^2)_{aa}\,(e/2mc)^2=\mathfrak{y}^2$ one obtains at last Eq. (4) so that the ground for the difference between L and B is explained. It will be noted that the complication in the space averaging from the non-commutativeness arises only when the terms in the moment of order H^3 and higher are included. It did not appear in Van Vleck's work, as he considered only the part of the moment which is linear in H and here we have only to find the average $\mathfrak{P}$ where no "mixed" terms $(L^iL^{i'})_{aa}$ appear after the classical averaging (cf. 45).

From the above it follows that as soon as we deal in the following with non-commutative or commutative matrices, we expect in the answer for the polarization always respectively a Brillouin or Langevin function as their contributions.

Still in another respect is the relation (38) instructive. It gives the answer to an objection of Debye[13] against the Langevin function for the magnetic polarization. Debye finds for the entropy S per cc of a gas in a magnetic field:

$$S=(S)_{H=0}-\int x(d\sigma/dx)dx$$

where $x=H/T$ and σ is the polarization per cc. Taking $\sigma=NL(\mu, H, T)$ where N is the number of molecules per cc he finds (written in our notation)

$$S=(S)_{H=0}-Nk[\log(2\mathfrak{y}x/k)-1+(1+2\mathfrak{y}x/k)e^{-2\mathfrak{y}x/k}+\cdots]$$

making $S=\infty$ for $T=0$ contrary to the theorem of Nernst requiring a finite entropy for $T=0$. Using for σ not one Langevin function, but the difference of two of them (according to 38) one finds instead of the fatal $\log(2\mu x/k)$ now $\log[(2l+1)\beta x/k]-\log(\beta x/k)$ which remains finite for $T=0$ and $x=\infty$.[14]

[13] P. Debye Ann. der Phys. **81**, 1154 (1926).

[14] At first thought it would appear as though the validity of the Langevin formula in the electric case would lead us into Debye's difficulty of infinite entropy at $T=0$, when an electric field is applied. However in our analysis of the electric case, we supposed the intervals in the

Atoms with spin. We must now seek to incorporate the spin, which was not included by Brillouin. First of all, we consider a gas of *atoms* with spin. Here we must deal with two limiting cases, viz. multiplet structures narrow and wide compared to kT. The intermediate case is too intractable to be readily treated and will not be considered here. Let us first consider:

Narrow multiplets. From the quantum mechanical theorem of spectroscopic stability, we know that by an increase of field strength the magnetic polarization only increases on account of the increase of H, not on account of a change in the structure of the formula. In other words, a Paschen-Back effect may change the type of quantization or the formula for an *individual* Zeeman component but not the expression for the susceptibility. The reason that this is possible is that the susceptibility is always a statistical thing, involving a summation over all possible states rather than the properties of one particular state. To find the polarization formula, we can therefore choose the field strength so that the calculations become as simple as possible, i.e. in the case of a field so strong that it overpowers the coupling between L and S (the spin moment) and gives separate spacial quantization of L and S. The components $\sum p_\phi$ and $\sum p_\psi$ of orbital and spin moments parallel to the axis of figure are then diagonal matrices of elements $m_l h/2\pi$ and $m_s h/2\pi$. In the several states the quantum numbers m_l and m_s range from $-l$ to $+l$ respectively from $-s$ to $+s$, where $L=lh/2\pi$ and $S=sh/2\pi$. We have now rigorously to all powers of H:

$$\overline{m}_z=\beta\frac{\sum_{ml}\sum_{ms}(m_l+2m_s)e^{(m_l+2m_s)\beta H/kT}}{\sum_{m_l}\sum_{m_s}e^{(m_l+2m_s)\beta H/kT}}$$

Since

$$\sum_{m_l}\sum_{m_s}m_l e^{(m_l+2m_s)\beta H/kT}=\left[\sum_{m_l}m_l e^{m_l\beta H/kT}\right]\left[\sum_{m_s}e^{m_s\beta H/kT}\right]$$

and analogous formulae hold for the other double sums we always can cancel one sum in the denominator against one in the numerator and find using the expression (37) for the Brillouin function:

$$\overline{m}_z=B(l,\beta,H,T)+B(s,2\beta,H,T).$$

Here the use of β as parameter, (see footnote 12) will become clear since the last term could not be written as B(2s,β, H, T) this corresponding to a sum over $4s+1$ terms instead of $2s+1$.

Wide multiplet structure. If on the other hand, the multiplet structure is wide compared to kT, i.e., $h\Delta\nu\gg kT$ the interaction between L and S is very strong and these cannot be quantized separately. L and S form always the same resultant J around which they rotate very rapidly. J itself rotates

---

rotational fine structure small compared to kT, a condition not fulfilled in the vicinity of $T=0$. Instead, special formulae for the susceptibility are required at low temperature. These have been given by Mensing and Pauli, VanVleck, and Kronig in the special case of rigid non-gyroscopic diatomic molecules. Such formulae make the entropy finite at $T=0$ as will indeed any quantum formula involving a discrete succession of energy states rather than a continuous classical distribution.

slowly around H and gives us therefore low frequency matrix elements. Now the low frequency matrix elements play the most important role in our answer as in the magnetic case the effect of the high frequency elements is usually negligible. Neglecting therefore the matrix elements corresponding with rotations around J, we can treat J as we should have treated L in an atom without spin. There is still a difference, $jh/2\pi$ being the value of the mechanical impulse moment J the corresponding magnetic moment is not $j\beta$ but $gj\beta$ on account of the anomaly of the spin, which contributes also to J. Therefore is the answer here:

$$\overline{m}_z = B(j, g\beta, H, T).$$

Diatomic molecules. We consider first those with *narrow* multiplet structure ($h\Delta\nu \ll kT$). Since the multiplet structure is due to the different possible orientations of the spin, we know that in this case $S^{z'}, S^{y'}$ and $S^{z'}$ are all of low frequency and since they do not commute, the spin will give the contribution $B(s, 2\beta, k, T)$ to the final result. To find that of L we can confine ourselves to its low frequency elements, namely the components $L^{z'}$ of L parallel to the axis of symmetry of the diatomic molecule. The components $L^{z'}$ and $L^{y'}$ perpendicular to this axis consist entirely of matrix elements of the unimportant high frequency type. The reason for this is that a change of the quantum number σ_l in $L^{z'} = \sigma_l h/2\pi$ gives always a large difference in energy as appears from the spectroscopic data. This is equivalent to the statement that the vector L precesses rapidly about the axis of figure. So we have only to deal with $L^{z'}$ and this commuting with itself, will give a Langevin function, so that the polarization for molecules with narrow multiplets will be:

$$\overline{m}_z = L(\sigma_l\beta, H, T) + B(s, 2\beta, H, T).$$

In the remaining case, that of *wide* multiplet structure, also $S^{z'}$ and $S^{y'}$ consist exclusively of high frequency elements, while those of $S^{z'}$ are only of low frequency and are to be added to the elements of $L^{z'}$ in order to give the total effective moment. Since all components along one axis commute, we have here

$$\overline{m}_z = L((\sigma_l + 2\sigma_s)\beta, H, T).$$

APPENDIX

Equivalence of Quantum Mechanical and Classical Spacial Averages

In the derivation of the Langevin formula for the electric polarization of a gas of rigid molecules in § 2 we needed the theorem (8).

$$\sum_m (M_z^p)_{(n_0 jm, n_0 jm)} : p_j = \mu^p \int \cos^p \theta d\omega : \int d\omega$$

On account of the assumed rigidness we had to deal only with low levels, so that we could throughout take $n = n_0$ in the "intermediate"[3] levels which

appear in writing out the element of a matrix product when $p>1$. Still we prefer to give a more general theorem holding also for elastic molecules, where $n \neq n_0$ is possible in the intermediate levels. This will include the first theorem as a special case. The statement of this generalization can better be given when we have found the analytical expression for it. We make use of this extension in § 3 for the derivation of Debye's correction terms.

Our theorem now is based upon considerations analogous to those of Van Vleck[1] on the principle of spectroscopic stability, where he considered the second power of the moment. As already mentioned the x, y, z and the x', y', z' systems of axes are fixed respectively in space and in the molecule, the relative position being determined by means of the well known Eulerian angles θ, ϕ, ψ. The wave function $U_{njm}(x_1 \cdots x_f, y_1 \cdots y_f, z_1 \cdots z_f)$ for a molecule with f different particles (electrons and protons) can be written very approximately (i.e. neglecting rotational distortion of electronic motions) in the form:

$$U=\psi_{njm}(x_1' \cdots z_f', \theta, \phi, \psi)=u_n(x_1'y_1'z_1' \cdots x_f'y_f'z_f')f_{njm}(\theta, \phi, \psi) \quad (46)$$

where u_n is independent of j on account of the assumed rigidness of the molecule with respect to the centrifugal force. The matrix elements in the xyz system are defined by.

$$M^z{}_{(njm, n'j'm')}=\int \psi_{njm} M^z \psi_{n'j'm'} dx_1 \cdots dz_f \quad (47)$$

where

$$M^z=\sum_k e_k z_k=\lambda_{x'z}M^{x'}+\lambda_{y'z}M^{y'}+\lambda_{z'z}M^{z'}.$$

In this equation $M^{x'}$ etc. are not matrices but the classical moments $\sum_k e_k x_k'$ etc. k ranging from 1 to f and $\lambda_{x'z}$, $\lambda_{y'z}$ $\lambda_{z'z}$ denote the ordinary direction cosines connecting the z axis with the $x'y'z'$ axes and are functions of θ, ϕ, ψ.

Now
$$dx_1 \cdots dz_f = dV d\omega \quad (48)$$

where dV and $d\omega$ denote the phase elements for the coordinates occurring respectively in u_n, f_{njm}. We will use q, q', q'' $\cdots$ to denote arbitrarily and independently from each other the axes x',y',z'. (The indices i and i' did not fit, since we assumed always $i' \neq i$). We find then by substituting

$$M^z{}_{(njm, n'j'm')}=\sum_q \int u_n M^q u_{n'} dV \int f_{njm}\lambda_{qz} f_{n'j'm'} d\omega = \sum_q M^q{}_{nn'}\lambda_{qz(njm, n'j'm')} \quad (49)$$

Using this substitution for each of the factors in, for example

$$\sum_m [(M^z)^3]_{(n_0jm, n_0jm)}$$

$$= \sum_m \sum_{n'j'm', n''j''m''} M^z{}_{(n_0jm, n'j'm')} M^z{}_{(n'j'm', n''j''m'')} M^z{}_{(n''j''m'', n_0jm)}$$

we obtain.

$$\sum_m [(M^z)^3]_{(n_0jm,n_0jm)} = \sum_{qq'q''} a_{qq'q''} \left\{ \sum_{n'n''} M^{q}_{n_0n'} M^{q'}_{n'n''} M^{q''}_{n''n_0} \right\} S_{qq'q''} \tag{50}$$

where the coefficients $a_{qq'q''}$ are numerical values and further

$$S_{qq'q''} = \sum_m \sum_{j'm'} \sum_{j''m''} \lambda_{qz}(n_0jm, n'j'm') \lambda_{q'z}(n'j'm', n''j''m'') \lambda_{q''z}(n''j''m'', n_0jm).$$

To evaluate S we need the rules of multiplication for the λ-elements. These, defined in (49) by an integral can be regarded as defined equally well by the expansion

$$\lambda_{qz} f_{n'j'm'} = \sum_{jm} \lambda_{qz(njm,n'j'm')} f_{njm}$$

where it is to be particularly noted that unlike the usual definition of matrix elements the index n, which is not here an index of summation, has different values n, n' on the right and the left hand side, i.e. the f on the left hand side belongs to a different set of orthogonal functions than that on the right.

To derive first the multiplication rules for *two* λ-elements we take

$$\lambda_{qz}\lambda_{q'z} f_{n''j''m''} = \sum_{jm} (\lambda_{qz}\lambda_{q'z})_{(njm,n''j''m'')} f_{njm} \tag{51}$$

We develop the left hand side again, but now in two steps, in each of which we use a different constant value of n', n'' of the index n

$$\lambda_{qz}(\lambda_{q'z} f_{n''j''m''}) = \lambda_{qz} \sum_{j'm'} \lambda_{q'z(n'j'm',n''j''m'')} f_{n'j'm'}$$

$$= \sum_{j'm'j''m''} \lambda_{q'z(n'j'm',n''j''m'')} \lambda_{qz(njm,n'j'm')} f_{njm}.$$

Comparing this answer with (51) we find the multiplication rule

$$(\lambda_{qz}\lambda_{q'z})_{(njm,n''j''m'')} = \sum_{j'm'} \lambda_{qz(njm,n'j'm')} \lambda_{q'z(n'j'm',n''j''m'')}$$

from which we see easily the extension to the case of a product of more than two λ's. We have therefore

$$S_{qq'q''} = \sum_m (\lambda_{qz}\lambda_{q'z}\lambda_{q''z})_{(n_0jm,n_0jm)} = \sum_m \int \lambda_{qz}\lambda_{q'z}\lambda_{q''z} \left| f_{n_0jm} \right|^2 d\omega.$$

Now $\sum_m |f_{n_0jm}|^2$ is independent of the choice of the system $x'y'z'$, i. e. independent of θ, ϕ, ψ according to the spectroscopic stability principle previously mentioned, so that it can be replaced by a constant C_{n_0j} giving

$$S_{qq'q''} = C_{n_0j} \int \lambda_{qz}\lambda_{q'z}\lambda_{q''z} d\omega. \tag{52}$$

Substituting (52) in (50) the left hand side of (50) will contain $C_{n_0 j}$. To get rid of this constant we divide (50) by the statistical weight p_j. Now we have, using the normalization of the f's

$$p_j = \sum_{m=-j}^{m=+j} 1^m = \sum_m \int |f_{n_0 jm}|^2 d\omega = C_{n_0 j} \int d\omega$$

so that the above mentioned division leads to

$$\frac{1}{p_j} \sum_m [(M^z)^3]_{(n_0 jm, n_0 jm)}$$

$$= \sum_{qq'q''} \frac{\int a_{qq'q''} \lambda_{qz} \lambda_{q'z} \lambda_{q''z} d\omega}{\int d\omega} \left[\sum_{n'n''} M^q_{n_0 n'} M^{q'}_{n'n''} M^{q''}_{n'' n_0} \right]. \quad (53)$$

This analytical statement of the theorem for the special case of a third order expression in $(M^z)^p$ can immediately be extended to any other power. In words, the general theorem reads as follows: *The average of the diagonal elements of $(M^z)^p$ taken over the axial quantum numbers m with a given value of j and n can be calculated by resolving the matrices in a geometrical way along the principal axes of the molecule and averaging the resulting terms classically over all orientations of the molecule.* If there are no excited states possible, the sum inside the square brackets in (53) becomes simply $\mu^q \mu^{q'} \mu^{q''}$ and the whole right side of (53) is then classically built. If we can reckon with these $\mu^q, \mu^{q'}, \mu^{q''}$ classically, i.e. if the M's commute in multiplications (as they do in the electric case) the right side of (53) is then of course equivalent to the classical average $\overline{\mu^3 \cos^3 \theta^{cl}}$ and we obtain for an arbitrary power our relation (8). In the magnetic case μ^q and $\mu^{q'}$ would not commute for $q' \neq q$ so that our relation (8) does not hold for Magnetic Moments (cf. the example in 42, 43, 44) whereas (53) is still valid as it did not require the different components of the M's to commute.

I am indebted greatly to Professor Van Vleck for valuable guidance in this research and to the International Education Board for its financing.

THE TEMPERATURE DEPENDENCE OF ELECTRICAL CONDUCTIVITY

By William V. Houston
California Institute of Technology

(Received May 6, 1929)

Abstract

To explain the fact that the resistance of a pure metal becomes zero at the absolute zero of temperature it is necessary to take into account the restrictions placed upon the electron scattering by the quantum statistics. When these are included as a probability of transition, the Brillouin treatment of wave scattering gives a very satisfactory law of the temperature dependence of resistance.

IN A previous paper it was shown that electrical resistance is caused by the diffraction of the electron waves.[1] The waves of the electrons which contribute essentially to the conductivity are so long that if the ions of the crystal were regularly arranged and stationary, they would pass freely through the lattice without retardation. The irregular motion due to temperature energy, however, causes a general scattering in all directions. This general scattering produces a resistance which increases with the temperature. For the computation of this increase, the work of Debye on the scattering of x-rays provided a convenient method.[2] This served admirably to show the validity of the fundamental idea, but it is not quite correct at very low temperatures. Frenkel and Mirolubow[3] have avoided this difficulty by using the work of Brillouin[4] on the scattering of light, and they find that the resistance should increase with the third power of the temperature for very low temperatures. In their work, however, the mean free path is not introduced in quite the same way as in the work of Sommerfeld, who followed Lorentz.[5] A treatment by the method of Lorentz gives a slightly different law of variation with temperature.

When account is taken of the fact that an isolated ion does not scatter uniformly in all directions, the properties of the ion are found to affect the temperature coefficient of conductivity as well as the value of the conductivity itself. This is in accord with the experiments which have shown that no single function can represent exactly the temperature dependence of the conductivity for all metals.

However, all of these treatments are based upon the idea that the resistance of a metal is due wholly to the temperature motion of the ions in the crystal lattice. Hence, if the resistance becomes zero at the absolute zero

[1] W. V. Houston, Zeits. f. Physik **48**, 449 (1928).
[2] P. Debye, Ann. d. Physik **43**, 49 (1914).
[3] Frenkel and Mirolobow, Zeits. f. Physik **49**, 885 (1928).
[4] Brillouin, Ann. de Physique **17**, 88 (1922).
[5] H. A. Lorentz, Theory of Electrons; A. Sommerfeld, Zeits. f. Physik **47**, 1 (1928).

of temperature, it must be assumed that the temperature motion of the ions also becomes zero at this point. But it is almost certain that this is not the case. On the one hand, the quantum theory in its present form indicates that a harmonic oscillator in its lowest state possesses a half unit of energy, i.e. $E_0 = \frac{1}{2}h\nu$ and therefore, presumably a considerable amount of motion. (If every standing wave which can exist in a crystal is present with $\frac{1}{2}h\nu$ of energy, the ions must be far from a state of rest.) On the other hand, the experiments which have been made to determine the intensity of the x-ray diffraction pattern as a function of the temperature seem to point rather clearly to the existence of zero point energy and a zero point motion of the system.[6]

The solution of this difficulty also is to be found in the work of Brillouin, when it is combined with the Fermi statistics. According to Brillouin, the light reflected from an elastic wave has a frequency equal to the sum or the difference of the frequencies of the incident light wave and the elastic wave. Since the frequency of an electron wave is proportional to its energy, it is evident that this means that the electron impacts are all inelastic, and that the electron either loses or gains an energy equal to $h\nu$ where ν is the frequency of the elastic wave.[7] But the electron can gain energy only when two conditions are fulfilled. First, there must be a vacant state of higher energy to which the electron can jump; and second, the elastic wave must be able to lose the energy which the electron gains. This means that the elastic wave cannot be in its lowest energy state before the impact. On the other hand, the electron can lose energy only when there is a vacant state of lower energy to which it can jump. In this case, the state of the elastic vibration is not important since the elastic oscillator can always absorb energy.

It is not difficult to derive an expression for these restrictions. Sommerfeld has shown that only electrons whose velocities are close to the critical velocity $\bar{v}$ need be considered in computing the conductivity. $\bar{v}$ is given by $m\bar{v}^2/2kt = \log A$, where A is the constant in the distribution function of the Fermi statistics. After an impact these electrons will have the energy $(\frac{1}{2})m\bar{v}^2 \pm h\nu$. Thus the probability that there is a place of higher energy to which the electron can jump is

$$P' = 1 - 1/\left\{(1/A)e^{[(m\bar{v}^2/2)+h\nu]/kT} + 1\right\} = 1/(1+e^{-h\nu/kT}). \qquad (1)$$

But at the same time the elastic vibration must be able to lose energy. The probability that an oscillator is not in its state of lowest energy, i.e. that $E = (n+1/2)h\nu$ where $n > 0$ is

$$P'' = e^{-h\nu/kT}. \qquad (2)$$

For these two conditions to be satisfied at the same time, there is the probability

[6] James, Waller and Hartree, Roy. Soc. Proc. **A118,** 334 (1928).

[7] This fact and its consequences were first recognized by Bloch, Zeits. f. Physik **52,** 555 (1928). However, he did not explicitly develop the law of temperature dependence which results from it in the simple way given here.

$$P_1 = P'P'' = 1/(e^{h\nu/kT}+1). \tag{3}$$

The probability that the electron can lose energy is given by

$$P_2 = 1 - 1/\{(1/A)e^{[(m\bar{v}^2/2)-h\nu]/kT}+1\} = 1/(e^{h\nu/kT}+1) \tag{4}$$

Then the probalility that one or the other of these processes can take place is merely half the sum of the two probabilities

$$P = (1/2)(P_1+P_2) = 1/(e^{h\nu/kT}+1). \tag{5}$$

For $T=0$, $P=0$, so that no scattering can take place regardless of the motion of the crystal lattice.

We may now briefly outline the application of this restriction to the computation of the electrical resistance. Frenkel and Mirolubow have given a concise presentation of the theory of Brillouin so we may use the equations as given by them. When account is taken of the zero point energy, the intensity per unit solid angle scattered in a given direction is given by

$$S = S_1 n^2 w h Q \kappa V \{1/(e^{hwQ/kT}-1)+\tfrac{1}{2}\} \tag{6}$$

V is the volume of the crystal which does the scattering, and Q is the reciprocal of the wave-length of the elastic wave which does the scattering. Q satisfies the relation

$$Q = 2q \sin(\theta/2) \tag{7}$$

where q is the reciprocal of the wave-length of the incident electron wave and θ is the angle of scattering. w is the velocity of the elastic wave in the crystal, n is the number of atoms per unit volume, and κ is the compressibility. S_1 is the intensity scattered by a single atom in the given direction. Frenkel and Mirolubow treat this as independent of the direction.

As usual, we write the expression for the distribution function when a current is flowing in the x direction, as

$$f(\xi,\eta,\zeta) = f_0(\xi,\eta,\zeta)+\xi\chi(v) \tag{8}$$

where ξ, η, ζ are the velocity components and f_0 is the function when no current is flowing. The expression for $\chi(v)$ then is

$$-8\chi n^2 w h \kappa V \int S_1\{1/(e^{hwQ/kT}-1)+\tfrac{1}{2}\}\{1/(e^{hwQ/kT}+1)\}(\xi'-\xi)Q\sin\theta d\theta d\phi = \frac{eF}{m}\frac{\partial f}{\partial \xi}+\xi\frac{\partial f}{\partial x}. \tag{9}$$

In Eq. (9), ν is replaced by wQ, and ξ' is the x component of the velocity to which the electron is scattered by the impact. In this equation the small change of total velocity, due to the exchange of energy, may be neglected. ξ' can then be expressed terms of ξ, θ, ϕ. If the integration is carried out with respect to ϕ and the result is expressed in terms of $\theta/2$, we may use Eq. (7) to express the integral as follows:

[8] Reference 1, Eq. (6).

$$\frac{8\pi\chi n^2 whV}{q^4}\int S_1\left\{\frac{1}{(e^{2h\omega Q/kT}-1)}+\frac{1}{2(e^{h\omega Q/kT}+1)}\right\}Q^4dQ=\frac{eF}{m}\frac{1}{\xi}\frac{\partial f}{\partial \xi}+\frac{\partial f}{\partial x} \tag{10}$$

If we now assume that S_1 has the form given by Wentzel[9] and again use Eq. (7) and simplify, we have:

$$\frac{2\pi\chi Z^2e^4n^2wh}{m^2v^3}\int\frac{Q^4dQ}{(e^{h\omega Q/kT}-1)(Q^2+4q^2c)^2}=\frac{eF}{m}\frac{1}{v}\frac{\partial f}{\partial v}+\frac{\partial f}{\partial x}. \tag{11}$$

In this equation, $c=\lambda^2/16\pi^2b^2$, where b is a measure of the extent of the ion, and $q^2=1/\lambda^2$, so that $4q^2c=1/4\pi^2b^2=aQ_1^2$. If we let $h\omega Q/kT=x$, and $h\omega Q_1/k=x_0$, we may write for the reciprocal mean free path, which is proportional to the resistance:

$$l^{-1}=\frac{2\pi Z^2e^4n^2\kappa\Theta k}{m^2v^4}\frac{1}{x_0}\int_0^{x_0}\frac{x^4dx}{(e^x-1)(x^2+ax_0^2)^2}. \tag{12}$$

The upper limit of this integration, at least for monovalent metals, may be taken as Θ/T where Θ is the characteristic temperature of Debye. For metals where the wave-length of the electrons considered is less than twice the minimum wave-length of the elastic vibrations, the upper limit may have to be modified. However, the limit is always uncertain since the shortest elastic vibrations are certainly not sinusoidal.

Eq. (12) shows that the resistance should become zero with the temperature even when the zero point energy is considered. This is due entirely to the restriction imposed by Pauli's principle and the fact that all scattering is with change of wave-length. This restriction is expressed by P in Eq. (5). Above the zero point, the rate of change of resistance depends upon the factor a. When a is large, that is, when the scattering of a single ion is the same in all directions, the resistance should increase with the fifth power of the temperature for very low temperatures, and with the first power of the temperature for temperatures large compared with θ. When a is very small, the resistance is proportional to T for low temperatures. The observed variation lies, of course, somewhere between these limits.

The integral in Eq. (12) can be expanded for values of x_0 which are not too large, and then integrated. The result is:

$$\frac{1}{x_0}\int_0^{x_0}\frac{x^4dx}{(e^x-1)(x^2+ax_0^2)^2}=\frac{A}{x_0}-\frac{B}{2}+\frac{Cx_0}{12}-\frac{Dx_0^2}{720}+\cdots \tag{13}$$

where

$$\begin{aligned}
A&=\tfrac{1}{2}\{\log(a+1)/a-1/(a+1)\}\\
B&=\{(3a+2)/2(a+1)-(3a)^{1/2}/2)\tan^{-1}(1/a^{1/2})\\
C&=\tfrac{1}{2}\{(2a+1)/(a+1)-2a\log(a+1)/a\}\\
D&=\tfrac{1}{2}\{(a+1)^2/2-3a(a+1)+3a^2/2+a^3/(a+1)+3a^2\log(a+1)/a\}
\end{aligned} \tag{14}$$

[9] G. Wentzel, Zeits. f. Physik **40**, 590 (1926); Reference 1, Eq. (14).

The resistance can be found by inserting the value of l in Sommerfeld's equation. This gives for the resistance of gold 1.45×10^{-18} if a is taken as 0.1. The observed value is 2.28×10^{-18}. With this value of a, the resistance as a function of temperature is given in Table I. The values of R/R_0 for high temperatures are determined from Eq. (13), and for low temperatures by a rough graphical integration. The agreement with the observed values could be improved by adjusting the constant a.

TABLE I. *R/R_0 for gold with $a=0.1$ and $\theta=190$.*

T	20.4	68	90	169	273	573	773
R/R_0 cal.	0.007	0.15	0.23	0.56	1.00	2.34	3.25
R/R_0 obs.	0.006	0.177	0.270	0.592	1.00	2.24	3.16

We may, also, write the expression for the variation of resistance with pressure in a simple form. The resistance itself may be written:

$$R=E\kappa f(\Theta/T) \tag{15}$$

where E is independent of the pressure. We then have the expression:

$$\frac{1}{R}\frac{dR}{dp}=\frac{1}{\kappa}\frac{d\kappa}{dp}-\frac{T}{f\Theta}\frac{df}{dT}\frac{d\Theta}{dp}. \tag{16}$$

Since

$$\Theta=\text{const}/\rho^{1/6}\kappa^{1/2}$$

this may be written

$$\frac{1}{R}\frac{dR}{dp}=\left(1+\frac{2T}{f}\frac{df}{dT}\right)\frac{1}{\kappa}\frac{d\kappa}{dp}+\frac{\kappa T}{6\rho f}\frac{df}{dT}. \tag{17}$$

This gives the correct order of magnitude for the effect.

We may then conclude that the restriction of the transition probabilities on account of the degeneration of the electron gas, not only explains why the resistance goes to zero at the absolute zero, but when combined with the scattering equations of Brillouin, gives a very satisfactory law of the temperature variation of the resistance.

ON THE ANALYSIS OF ELECTRONIC VELOCITIES BY ELECTROSTATIC MEANS

By A. Ll. Hughes and V. Rojansky
Washington University, St. Louis, Missouri

(Received April 19, 1929)

Abstract

In magnetic analysis of electronic velocities the plane containing the receiving slit is placed at the angle $\Phi_m = 180°$ to the plane containing the entrance slit. The "resolution," at Φ_m, between two electrons of velocities V and v, both entering normally to the plane of the entrance slit, is $d_m = 2\beta r_0$, where $\beta = (V-v)/V$. The "departure from perfect re-focussing," at Φ_m of two electrons of velocity V, one entering normally to the plane of the entrance list and the other at an angle α to the normal, is $s_m = \alpha^2 r_0$. Since in some experiments the use of a magnetic field is a disadvantage, it is of interest to investigate the analyzing possibilities of electrostatic fields. In the present paper the radial, inverse first power, electrostatic field is considered in this connection. It is found that by a proper construction of the apparatus it should be possible to analyze velocities almost as well as by magnetic means. The plane of the receiving slit should be placed at the angle $\Phi_e = 127°17'$ to the plane of the entrance slit. The resolution at this angle is given by $d_e = (2\beta - 4\beta^2)r_0$, and the "departure from perfect re-focussing" by $s_e = 4\alpha^2 r_0/3$. It is also found that the 180° and 90° positions of the plane of the receiving slit are highly unsatisfactory. These results are obtained from approximate solutions of the equation of the electronic orbits, and are checked by numerical integration.

I. Introduction

IT IS well known that an electron, projected into a uniform magnetic field in a direction perpendicular to the lines of magnetic force, describes a circle whose radius depends on the velocity of the electron and on the strength of the magnetic field. If electrons enter the field in directions making but small angles with QP (see Fig. 1, the plane of which is perpendicular to the lines of force), it is the geometrical property of their circular paths that good re-focussing of the electrons of a given velocity occurs at the angle $\phi = 180°$. This property has been taken advantage of in many investigations, notably in the case of β-rays, as it enables one to compensate for the feebleness of a source of electrons by using a beam spread over an appreciable angle.

In certain types of experiments it is more convenient to use electrostatic rather than magnetic fields. A type of electrostatic field which, in its effect on an electron path, closely resembles a magnetic field, is the radial, inverse first power, electrostatic field. Such a field has occasionally been used in experimental work, but inasmuch as the conditions for best re-focussing and best resolution do not appear to have been worked out, it has always been necessary to limit the beam of electrons entering the field to a very small angle in order to secure sufficient resolution between electrons of different velocities.

The present investigation shows that in a radial, inverse first power, electrostatic field, good re-focussing and good resolution are to be found at the angle $\Phi = 127° 17'$, which, in fact, plays the same part for this type of an electric field as does the 180° position for the magnetic field. The problem

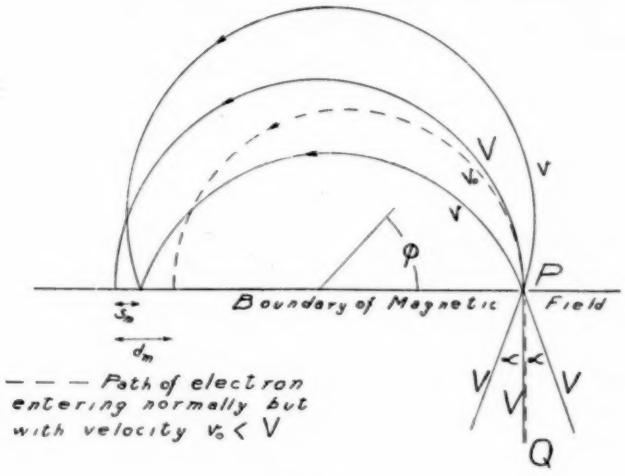

Fig. 1.

was solved by obtaining approximate solutions of the equation of the orbit. The results were checked for particular cases by numerical methods of solving the equation of the path without any approximations other than arithmetical ones.

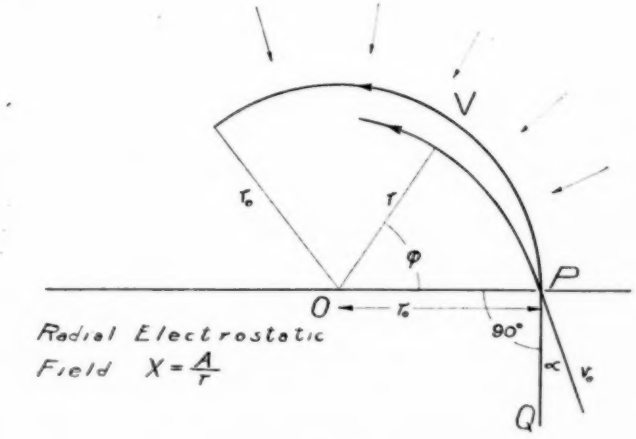

Fig. 2.

2. Approximate Solution of the Equation of the Orbit. Re-focussing and Resolution

Let us consider a two dimensional, radial, electrostatic field of intensity $X = -A/r$, Fig. 2, and investigate the orbit of an electron, of mass m and charge $-e$, projected into the field at the point P with an initial velocity v_0.

The differential equation of the orbit, in polar coordinates r and ϕ, is

$$h^2u^2\left(\frac{d^2u}{d\phi^2}+u\right)=\frac{Ae}{m}u, \tag{1}$$

where $u=1/r$, and h is the angular momentum per unit mass.[1] If α denote the angle between QP and the initial direction of motion, then $h=r_0v_0\cos\alpha$. Introducing a new variable $y=u/u_0$, and a parameter c defined by $c^2=Ae/mv_0^2\cos^2\alpha$, we now transform (1) into

$$\frac{d^2y}{d\phi^2}+y=\frac{c^2}{y} \tag{2}$$

which must be solved subject to the initial conditions:

$$\text{at } \phi=0,\ y=1,\ \text{and } \frac{dy}{d\phi}=-\tan\alpha.$$

As (2) cannot be solved in terms of the elementary functions[2], we can either seek an approximate solution in terms of the parameters c and α, or evaluate particular solutions by numerical methods. Both lines of attack are carried out below for the cases of interest in the application of this theory to experimental devices.

Before proceeding further it is advantageous to evaluate the velocity which an electron entering at P must have in order that it shall describe a circular path. It is seen that a circular orbit is possible only if the initial direction of motion is along QP, i.e., normal to OP, and if the velocity, which we denote by V, satisfies the relation $mV^2/r_0=-Xe=Ae/r_0$, or

$$mV^2=Ae.$$

This relation shows, first, that by varying the constant A of the field, it is possible to make any velocity to be that appropriate to circular orbits; secondly, that V is independent of r_0; and, thirdly, that the parameter c in (2) is given by $V/v_0\cos\alpha$.

For the practical problem of ascertaining the position of best re-focussing and the degree of resolution between different velocities, we need to know the paths of electrons entering the radial electrostatic field at but a small angle to QP, and having a velocity deviating but slightly from the velocity V appropriate to a circular path. Let us consider two orbits, which we may call twin orbits, deviating from perpendicular entrance into the field by angles $+\alpha$ and $-\alpha$, respectively, and in which the velocities at entrance are, in each case, v_0. Applying a method of successive approximations described by Routh,[3] we now find that, to a first approximation, the equations of the respective twin orbits are:

[1] See, for example, A. G. Webster, The Dynamics of Particles, and Rigid, Elastic, and Fluid Bodies, (Teubner, 1912), p. 39.

[2] E. T. Whittaker, Analytical Dynamics, (Cambridge, 1927), p. 81.

[3] E. J. Routh, A Treatise on Dynamics of a Particle, (Cambridge, 1898), p. 236.

$$y_1 = c + (1-c)\cos (2)^{1/2}\phi - (\tan \alpha \sin (2)^{1/2}\phi)/(2)^{1/2},$$
$$y_2 = c + (1-c)\cos (2)^{1/2}\phi + (\tan \alpha \sin (2)^{1/2}\phi)/(2)^{1/2}. \quad (4)$$

The twin orbits, therefore, cross each other whenever $y_1 = y_2$, i.e., whenever the last term in each expression vanishes. Hence they cross for the first time after entrance when $(2)^{1/2}\phi = \pi$. Denoting the corresponding value of ϕ by Φ_e, we have

$$\Phi_e = \pi/(2)^{1/2}, \text{ or } \Phi_e = 127°17'. \quad (5)$$

As this angle is independent of α, it denotes, to the first approximation, the position of best re-focussing.

To investigate the *resolution*, i.e., the separation between the paths of two electrons, both entering normally at P but with slightly *different* velocities, we put $\alpha = 0$ in (4), differentiate with respect to ϕ, and obtain: $y_1' = y_2' = -(2)^{1/2}(1-c)sin\ (2)^{1/2}\phi$. This vanishes at $\phi = \Phi_e$, and it therefore follows that at this angle the resolution is at a maximum. Thus Φ_e besides being the angle at which the best re-focussing occurs, is also the angle at which the resolution is best. From (4) it follows that, at Φ_e,

$$y = 2c - 1. \quad (6)$$

We now define the *resolving power*, d_e, to be $r_0 - r$, where r_0 is the radius of the circular path in which an electron of velocity V will travel, while r is the radius vector (at $\phi = \Phi_e$) of the path of an electron entering along QP with velocity v_0. We recall the definitions of y and c (in which we set $\alpha = 0$), introduce a new symbol $\beta = (V - v_0)/V$, and, neglecting higher powers of β, obtain from (6)

$$d_e = (2\beta - 4\beta^2)r_0. \quad (7)$$

It is also important to evaluate the *departure from perfect re-focussing*, s_e, which is the separation, at Φ_e, of the twin paths of the electrons entering the electric field at angles $\pm\alpha$ with QP from the path of the electron entering along QP, all electrons having one and the same velocity V. As a satisfactory result cannot be obtained by the use of (6), it is necessary to use in place of (4) the *second* approximation to the solution of (2). The analysis cannot be summarized effectively, and so only the final result will be given: the departure s_e is toward the inside of the circle of radius r_0, and when α is expressed in radians and its powers higher than the second are neglected,

$$s_e = 4\alpha^2 r_0/3. \quad (8)$$

The *third* approximation to the solution of (2) reveals the result that the angle Φ_e, at which the twin orbits cross, decreases with increasing α, but to an extent which is negligibly small in any case likely to occur in an experimental arrangement.

For purposes of comparison, we give the values of the *resolution*, d_m of the *departure from perfect re-focussing*, s_m, in the familiar magnetic case, in which the best re-focussing occurs at $\Phi_m = 180°$. These values are:

$$d_m = 2\beta r_0, \tag{9}$$

$$s_m = \alpha^2 r_0. \tag{10}$$

3. Numerical Integration of the Equation of the Orbit

To check the formulas for s_e and d_e obtained above, numerical determination of several particular orbits was effected. As is well known, numerical calculation of a particular solution of an ordinary differential equation can, except in singular instances, be carried out to any desired degree of approximation even though the equation may not admit of explicit integration. Two different methods were used in this work.

One method was to integrate Eq. (2), subject to the initial conditions, once, getting

$$\frac{1}{2}\left(\frac{dy}{d\phi}\right)^2 = (1-\beta)^2 \sec^2\alpha \log y - \frac{1}{2}y^2 + \frac{1}{2}\sec^2\alpha,$$

from which it follows that

$$\phi = \int_1^y [2(1-\beta)^2 \sec^2\alpha \log y - y^2 + \sec^2\alpha]^{-1/2} dy.$$

Particular numerical values were then assigned to α and β, and the values of the integrand were calculated for closely spaced values of y ($y = 1.01, 1.02,$

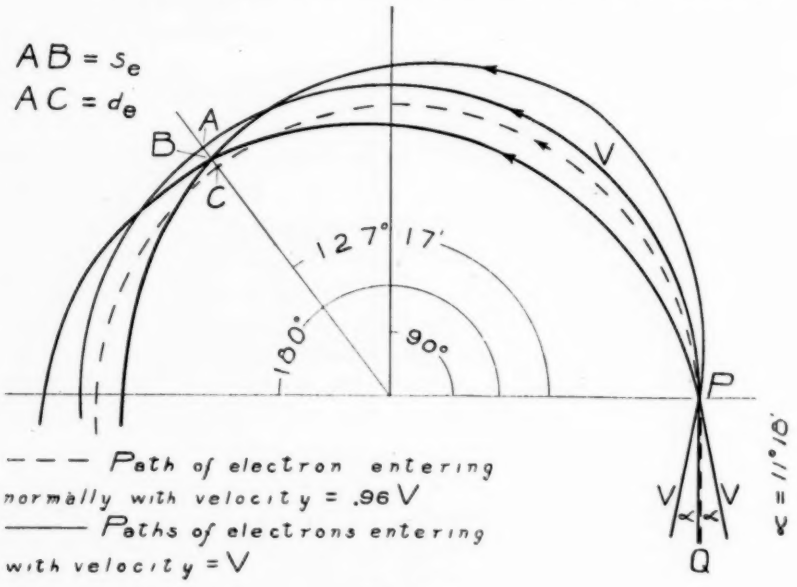

Fig. 3.

$\cdots$, for an inner orbit, $y = 0.99, 0.98, \cdots$, for an outer orbit; near an apse closer spacing was necessary). From these the values of the definite integral, and therefore of ϕ were obtained by *calculating* "the area under the curve."

The fact that an orbit is symmetrical about the apsidal lines was also used in mapping out the orbits. This method was applied to the cases $\alpha = \pm 11°18'$, $\beta = 0$ and $\alpha = \pm 5°42'$, $\beta = 0$ to study re-focussing, and to the cases $\alpha = 0$, $\beta = 0.02$ and $\alpha = 0$, $\beta = 0.04$ to study resolution. Fig. 3 represents some of the orbits calculated in this manner. The full lines PA and PB correspond to the cases $\alpha = \pm 11°18'$, $\beta = 0$, and the dotted line to the case $\alpha = 0$, $\beta = 0.04$, i.e., when the electron enters perpendicularly with a velocity 0.96 V. It is seen that the "resolution" between electrons of slightly different velocities, but all entering the field perpendicularly, is considerably poorer at 90° and at 180° than at 127°. Moreover, this resolution can be detected easily at 127°, even if the entering beam of electrons is spread over an angle $\pm 11°18'$, but it is hopelessly obliterated at the 90° or 180° position by the wide "spread" of the electron beam at these positions.

Another method of numerical integration used here was that due to Milne.[4] Its technique is quite simple, and in the present instance only the four operations of arithmetic were involved. The cases $\alpha = \pm 5°42'$, $\beta = 0$ and $\alpha = \pm 11°18'$, $\beta = 0$ were investigated in this manner, the calculations being carried out to five places of decimals.

The results of the numerical work lead to the conclusion that the formulas for s_e and d_e are correct, for the ranges considered, to the order to which they were derived, as the discrepancy between (7) and the true value of d_e was found to be of the order of β^3, and that between (8) and the true value of s_e, of the order of α^4.

4. Conclusions

From a practical experimental point of view, it is important to know how good the re-focussing is for the paths of two electrons, one entering the electrostatic field with just the right velocity to describe a circular path, and the other, having the same velocity, but entering at an angle $\pm\alpha$. Hence we plot the values of s_e, the departure from perfect re-focussing at 127°17′, as a function of the angle α (Fig. 4). (For the sake of comparison, we plot also the values of s_m, at 180°, the corresponding quantity in the magnetic case.) On the same diagram, we also record the values of d_e and d_m, which measure the electric and magnetic resolutions, respectively, for electrons entering the field *perpendicularly*, but with velocities $0.99V$, $0.98V$ and $0.97V$, (which correspond to $\beta = 0.01$, 0.02, and 0.03). As to scale, the values of s and d are given directly in centimeters, when the radius of the circular path, taken by an electron entering perpendicularly with the velocity V is just one centimeter.

So long as the existence of the re-focussing property of an inverse first power, radial, electrostatic field is unsuspected, the position of the receiving slit (or photographic plate) in any particular experimental arrangement in which electrons are deflected by such a field, is largely a matter of experimental convenience. Under such conditions, one would perhaps naturally put the receiving slit (or photographic plate) at 90° or 180°. It is therefore

[4] W. E. Milne, American Math. Monthly **33**, 455 (1926).

instructive to tabulate the spread of the electron beam at each of these positions together with the much smaller departure from perfect re-focussing

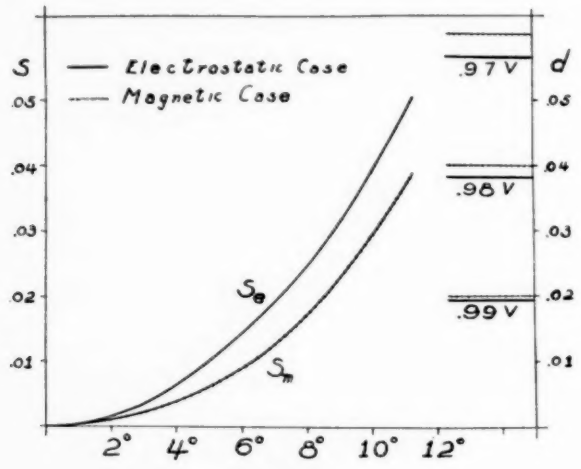

Fig. 4.

at 127°17′ for different values of α. For purposes of comparison, the maximum possible spread is included.

Angle	s_e at 127°17′	Spread at 90°	Spread at 180°	Max. Spread at 63°
11° 18′	0.0501	0.202	0.258	0.270
5° 40′	.0129	.111	.132	.134
2° 51′	.0032	.057	.066	.067

(The last line is an interpolation. Note that while s_e diminishes as the *square* of the angle, the other spreads diminish only as the *first power* of the angle.) It is seen from this table that to place the receiving slit (or photographic plate) in the 90° or 180° position, gives almost the worst departure from perfect re-focussing that the apparatus is capable of. This conclusion also follows from an inspection of Fig. 3.

In the analysis given above, just as in the usual derivation of the re-focussing properties of a magnetic field, some of the complications arising in experiment, such as a finite entrance slit, etc., were disregarded.[5] An account of an experimental test of the conclusions reached here is given in the following paper.

[5] It may be remarked that in the electrostatic case the velocity of a given electron varies with the radius vector.

RE-FOCUSSING OF ELECTRON PATHS IN A RADIAL ELECTROSTATIC FIELD

By A. Ll. Hughes and J. H. McMillen
Washington University, St. Louis, Missouri

(Received April 19, 1929)

Abstract

The method which utilises a uniform magnetic field is the one customarily employed for the analysis of electronic velocities. As the presence of a magnetic field is objectionable in certain investigations, analysis by an electrostatic field was considered. The theoretical considerations for a two-dimensional, inverse first power, radial electrostatic field (given in the preceding paper) show re-focussing at 127°17′ of the same order as that in the magnetic case at 180°. The present paper describes the apparatus and procedure used in verifying the predicted re-focussing at 127°17′. A radial electrostatic field was produced by a difference of potential between two coaxial cylindrical surfaces. Three oxide coated filaments allowed electrons to enter the field either normally or in directions making 5° with the normal. Satisfactory re-focussing and resolution were found.

IN THE preceding paper[1] it has been found that a two-dimensional, inverse first power, radial electrostatic field has a hitherto unsuspected re-focussing property for electron orbits, provided that these orbits satisfy certain conditions. If an electron is moving from a certain point in this field, perpendicularly to the radius passing through that point, with just the right velocity, so that under the influence of the electric field, it will describe a circular path concentric with the axis of the field, then all other electrons having the same velocity and starting from the same point, but moving initially in slightly different directions from that of the first electron, will describe orbits which re-focus at the point which is 127° 17′ from the starting point. As this result may be useful in a variety of experiments for studying electron velocities, or for sorting out electrons of one and the same velocity, it is desirable to investigate whether or not re-focussing can be obtained easily in an apparatus designed to realize the theoretical conditions.

Apparatus

The main part of the apparatus was machined out of an aluminum alloy casting (Fig. 1) and closed back and front by two flat thick plates of aluminum alloy. The electrostatic field was produced between accurately machined cylindrical surfaces of brass A and B. The radii of curvature were 50.0 mm and 60.0 mm respectively. These cylindrical surfaces extended to within 0.5 mm of the inside walls of the casting C at each end. The angle of the casting at D was made 127°. The entrance slit, S_1, for the electrons was 0.3 mm wide, and the exit slit, S_2 leading into the Faraday cylinder was 1.0 mm wide. The lengths of the slits were 10 mm. As the length of the cylinders perpendicu-

[1] A. Ll. Hughes and V. Rojansky, Phys. Rev. **34**, 284 (1929).

lar to the plane of the diagram was 30 mm, the field over the central 10 mm may be considered to be free from distortion. The slits S_1 and S_2 were placed as symmetrically as possible between the cylindrical plates. The deflecting field between the cylindrical plates was produced by connecting A and B to a source of potential. A and B were also connected to the ends of a 10,000 ohm resistance, the middle point of which was grounded to the casting C, which insured that the zero equipotential surface between the deflecting plates A and B was always on the circle passing through the slits.

To secure beams of electrons passing through the slit S_1 making small angles with the perpendicularly entering beam, three oxide coated filaments were mounted in positions indicated by P, Q, and R. Electrons emitted from any one of these filaments were accelerated to full speed by a field applied

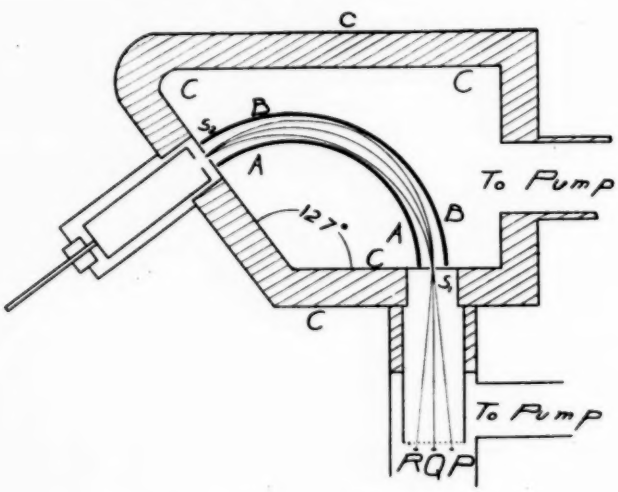

Fig. 1. Diagram of apparatus.

between the filament and the nearby grid, after which they travelled in a field free space towards the slit S_1. Since the distances between the positions P and Q and between Q and R were both about 7 mm, and the distance from any one of them to S_1 was 70 mm, the angles PS_1Q and QS_1R were between 5° and 6°. As it is conceivable that slight differences of contact potential could exist between the three different filaments P,Q and R and so make the actual accelerating potentials differ slightly, we devised an arrangement whereby one and the same filament could be shifted into any one of the three positions. The results with the latter arrangement were somewhat more consistent than with the three separate filaments. The electron currents into the Faraday cylinder F were measured by an electrometer, shunted by a suitable high resistance (a conducting glass) so that currents between 10^{-13} and 10^{-11} amp. could be readily measured. The vacuum was produced by a fast Gaede Steel Diffusion Pump with liquid air traps to intercept mercury vapor. Pressures were always below 10^{-5} mm.

Results

The velocity v which an electron must have on entering the field perpendicularly at the slit S_1, in order to describe the circle joining S_1 and S_2 is given by $mv^2/r_0 = Xe/r_0$, where r_0 is the radius of the circular path, and X the intensity of the electric field. Expressing X in terms of the potential difference, V_2, between the cylindrical surfaces, and mv^2 in terms of the potential difference, V_1, accelerating the electrons into the deflecting field, we have

$$2V_1e/55 = V_2e/55 \ \log(60/50).$$

Hence the deflecting potential $V_2 = 0.365\ V_1$. For 99.1 volt electrons, the deflecting potential should therefore be 36.1 volts. We found experimentally that, for 99.1 volt electrons, the deflecting potential necessary to bring the electron beam (from the filament Q alone) on to the slit was 35.8 volts. The discrepancy may no doubt be attributed to the difficulty of securing experi-

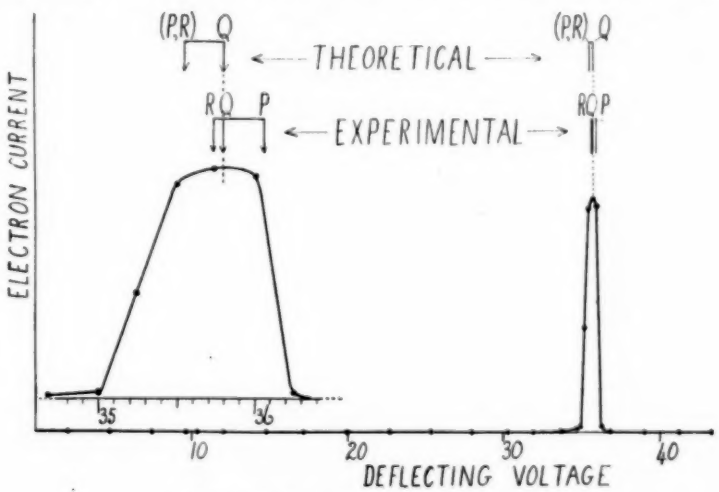

Fig. 2. Velocity distribution curve.

mentally precisely the ideal conditions postulated in the theory. Thus the deflecting field does not maintain its full value in the region close to the slits. It was very satisfactory to find that the *proportionality* between the voltage accelerating the electrons from the filament and the deflecting voltage held constant to about 0.7 percent for all the accelerating voltages tried, viz. 200, 100, and 50 volts. (To get better constancy, it would no doubt be necessary to substitute potentiometer methods for measuring the voltages in place of the voltmeters.)

The resolving power of the experimental arrangement may be inferred from the typical velocity distribution curve given in Fig. 2, in which electron currents entering the Faraday cylinder are plotted against the deflecting voltages. The electrons were accelerated from the filament Q by 99.1 volts. The shape of the peak is shown enlarged in the inset. The width of the peak may be accounted for, in part, by the finite width of the slits S_1 and S_2. Taking the width of the slits to be 0.3 mm and 1.0 mm respectively, it is

easy to show that this accounts for a spread of 0.43 volts in the deflecting voltage. The remainder, 1.2−0.43, may be attributed to the small potential drop along the filament, finite distribution of velocities of emission of electrons, and possibly to a departure from exact parallelism of the slits. Two peaks whose maxima are separated by a deflecting voltage of 1.2 volts could easily be resolved, when the total deflecting voltage is 36 volts. We may estimate the smallest difference in deflecting voltage, which would just indicate the presence of two distinct peaks, to be about half this, 0.6 volt. This means that the apparatus would just separate 99.1 volt electrons from 100.7 volt electrons.

The main purpose of this research was to investigate the re-focussing property of the electrostatic field. This was done by studying the exact values of the deflecting potentials necessary to bring the maximum electron current from the filaments P, Q, and R (or from the same filament moved from P to Q to R) into the Faraday cylinder. The results for the 99.1 volt electons may be taken as typical. It was found that electrons from P (leading to the *inner* path in the deflecting field) always required slightly *more* deflecting potential than the electrons from Q to bring them into the slit S_2.

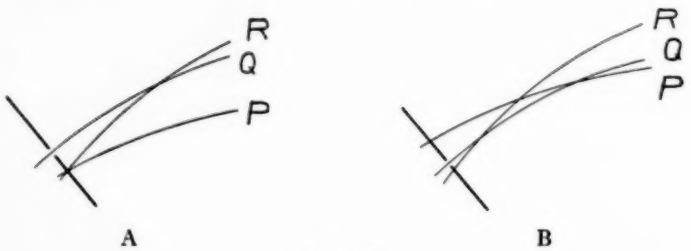

Fig. 3.

It was also found that electrons from R (leading to the *outer* path in the deflecting field) always required slightly *less* deflecting potential than the electrons from Q. The average deflecting voltages necessary to bring the peaks of the electron currents from Q, P, and R, into the Faraday cylinder, were 36.08, 35.80, and 35.74 volts respectively. These values are indicated in Fig. 2, just above the peak. The theoretical value of the departure from perfect re-focussing, the s_e of the previous paper, is also indicated. The inference is that the paths of the electrons just before entering the slit S_2 form a pattern shown in Fig. 3B, while that predicted in the previous paper should be as in Fig. 3A. Not only is there re-focussing, but it is evident that there is, what we may call, slight over-re-focussing. This state of affairs may no doubt be attributed to the fact that the experimental arrangements do not accurately satisfy the conditions specified in the theory.[2] For instance, while the cylin-

[2] With the thought that the results pictured by Fig. 3B might possibly be due to some asymmetry of the positions of the slits with respect to the deflecting plates, we tried the effect of making the potentials of A and B with respect to the grounded casting take several values, while maintaining the total difference equal to V_2. No closer approach to the theoretical pattern, Fig. 3A, could be obtained in these trials than had been obtained when the potentials of A and B were equally above and below that of the ground.

drical surfaces A and B (Fig. 1) were machined accurately to less than 0.1 mm it is not certain that, because they had to be supported by insulators, they were concentric and parallel to say 0.2 mm. The important fact however is that, even when the electron beam has a *total* width of as much as 11° or 12°, the electron beam is re-focussed so well at the second slit that the *total* departure from perfect re-focussing is less than one-third of the width of the experimental distribution of energy curve obtained for (nominally) uni-velocity electrons in a negligibly narrow beam. For a beam, half as wide, the experimental departure from perfect re-focussing would probably too small to measure. It is instructive to consider what would be the order of the deflecting voltages necessary to bring electrons from P, Q, and R, respectively on to the slit S_2, if the field had no re-focussing property. A rough calculation shows that, if the electron beams from P, Q, and R, keep diverging at the same rate as the average rate of separation in the first 63°, then deflecting voltages of the order of 38.6, 36.0, and 33.4 volts would be required to bring the beams from P, Q, and R, respectively on to the slit S_2. It is very evident then that excellent re-focussing has been obtained experimentally.

This investigation shows that a re-focussing magnetic field may be replaced by a re-focussing electrostatic field in the analysis of the energy distribution in electron beams. It is clearly possible to use the same method for isolating a uni-velocity beam of electrons without restricting the angle to an indefinitely small value.

ON THE ABSENCE OF CHANGE IN MAGNETIC SUSCEPTIBILITY WITH CRYSTALLIZATION IN STRONG MAGNETIC FIELDS

By L. A. Welo
Rockefeller Institute for Medical Research and Princeton University

(Received April 25, 1929)

Abstract

Lead, tin, bismuth, nickel chloride and potassium ferricyanide were crystallized in strong magnetic fields and examined for changes in the magnetic susceptibilities. The changes, if any, were not more than 0.16 percent in Pb, 0.29 percent in Sn, 0.32 percent in Bi, 0.42 percent in $NiCl_2$ and 0.04 percent in $K_3Fe(CN)_6$.

THIS paper describes attempts to alter the magnetic susceptibilities of some diamagnetic and paramagnetic substances by crystallization in fairly strong magnetic fields. The substances were lead, tin, bismuth, nickel chloride and potassium ferricyanide. The choice of the metals was determined partly by their conveniently low melting points and partly by the fact that they represent, according to Honda,[1] three types of susceptibility changes at the melting point. The susceptibility of lead changes very little (-0.12×10^{-6} to -0.07×10^{-6}); that of tin changes sign although the absolute value of the change is small ($+0.025\times10^{-6}$ to -0.038×10^{-6}) while that of bismuth exhibits a large discontinuity (-1.00×10^{-6} to -0.07×10^{-6}). $NiCl_2$ is a typical paramagnetic salt and in working with it one is less likely to meet with chemical complications than with, say, a salt like $FeCl_3$. $K_3Fe(CN)_6$ represents salts showing the magnetic anomalies often observed when a transition element appears in a complex ion.

Preparation of the Material

The metals were cast as thin disks 7 mm in diameter and 1 mm thick in a special form of graphite mould. The central part of the mould where the disks were formed had walls only 1 mm thick, so that it was possible to work with gaps of 3 mm. The pole face diameter was 8 mm. When lead and tin were cast the fields were 25100 gauss. After the completion of the work with lead and tin, the pole tips were found to be partly hollow, the bolts not having been completely turned up. New pole tips were made before the final work on bismuth was done and fields of 28900 gauss were obtained.

The disks for comparison (cast without field) were formed in the same mould and with the mould mounted between the pole pieces.[2] This insured

[1] K. Honda, Ann. d. Physik **32**, 1027 (1910).

[2] This procedure has raised the question as to the magnitude of the residual fields and the possibility that they might produce as much effect as the maximum fields applied. The residual fields were 298 gauss in the work with bismuth and 91 gauss in the work with the salts. The

that the rates of cooling were the same and that the only difference was the presence or absence of the magnetic field. A pile of 10 disks was used when comparing the susceptibilities. Both sets of 10 disks were made from the same melt. To eliminate any possible non-homogeneity of the melt the disks were cast alternately, with field, without field, with field, etc. until the required number of 20 were secured. The magnetic field was turned on before pouring and left on until the mould had cooled to about 100°C. The castings were trimmed with broken pieces of glass instead of a file.

$NiCl_2$ was crystallized out of an alcoholic solution by the circulation of dry, dust-free air above the solution at the bottom of a small test tube. $K_3Fe(CN)_6$ was crystallized out of an aqueous solution in the same way. The gap and the pole faces were larger than when casting the metals. The fields were 18500 gauss. $NiCl_2$ came down as a fine powder. The $K_3Fe(CN)_6$ crystals were powdered before measuring.

No attempts were made to grow single crystals.

The Method of Comparison

For the measurements a torsion balance was constructed, following, in the main, the design of Terry.[3] With this balance the susceptibility is proportional to the product of the two currents necessary for compensation; I, the current in the fixed coils and i the current in the suspended coil. In the general case the observed value

$$(Ii)=(Ii)_s+(Ii)_c+(Ii)_f+(Ii)_a$$

where the subscripts s, c, f and a refer, respectively, to the substance being studied, the container, the stray field and the air correction.

The last three terms are not altered by replacing the ten disks cast in a magnetic field by the ten cast without the field. Also, the two sets of disks can be adjusted to equal masses. Then the condition that crystallization in magnetic fields has no effect on the susceptibility is

$$(Ii)_m=(Ii)_{nm}, \tag{1}$$

the subscript m referring to the set cast with magnetic field and nm to the set cast with no field.

With the powdered salts it was more practicable to determine the masses as M_m and M_{nm} instead of adjusting to equality. The correction for the container, for the stray field and for the air having already been made we have as condition for absence of effect

$$\frac{(Ii)_{sm}M_{nm}}{(Ii)_{snm}M_m}=1 \tag{2}$$

---

pole pieces that were used in the study of lead and tin were destroyed so that the residual fields could not be determined, but they were certainly less than 298 gauss because of the cavities. The present negative results do not, therefore, exclude possible effects within the range 0–300 gauss in the metals and within the range 0–90 gauss in the salts.

[3] E. M. Terry, Phys. Rev. 9, 394 (1917)

Results

Lead. The first observations gave the result $(Ii)_m < (Ii)_{nm}$. A second double set (10 disks cast with magnetic field and 10 without) showed an inequality in the same direction but of smaller amount. The absolute values of (Ii) were larger in the second double set which indicated that paramagnetic or ferromagnetic contaminations were present in the first. Their absence from the second double set was not certain so that still a third double set was cast, with more rigid precautions against the entrance of dust while melting and pouring, and while handling the finished castings. With this third double set $(Ii)_m = (Ii)_{nm}$ within the limits of the errors of measurement.

Measurements were made with the disk axes both parallel and perpendicular to the field. In all, 16 determinations of $(Ii)_m$ were obtained, the disks being piled in the container and mounted in the balance 4 times and measurements made for each mounting at 4 different positions in the field. In the same way 16 determinations of $(Ii)_{nm}$ were made. These measurements yielded 16 values of $(Ii)_m - (Ii)_{nm}$ for which the mean was $+0.00011$. The mean value of $(Ii)_s$ (not (Ii)) was 0.06934 so that the diamagnetic susceptibility of lead cast with the magnetic field was not increased by more than

$$\frac{0.00011}{0.06934} \times 100 = 0.16 \text{ percent}.$$

Tin. Three double sets of tin castings were made of which two gave $(Ii)_m = (Ii)_{nm}$ within the limits of error. For one of these, comparisons were made with the disk axes parallel to the field with readings at 5 different positions. A similar comparison was made with the disk axes perpendicular The mean of 10 values of $(Ii)_m - (Ii)_{nm}$ was -0.000024. The mean value of $(Ii)_s$ was -0.00838 so that the increase in susceptibility of the paramagnetic tin cast with a magnetic field of 25100 gauss was not more than

$$\frac{0.000024}{0.008380} \times 100 = 0.29 \text{ percent}.$$

In the work with tin difficulties were expected because of magnetic anisotropy since it is not cubic but tetragonal in structure. They did not appear so that the crystals were either small and numerous enough to be oriented at random or else, tin is magnetically isotropic. I am not aware of any studies on magnetic susceptibilities of single tin crystals as a function of the orientation.

Bismuth. In bismuth the difficulty of magnetic anisotropy[4] did appear. With the disk axes parallel to the field I observed $(Ii)_{sm} = 0.1836 = N_1$ and $(Ii)_{snm} = 0.1902 = N_2$ as the means of 5 measurements on each set, repiling and remounting in the balance each time. The means of 9 measurements with the disk axes perpendicular were, repiling and remounting each time:

[4] C. Nusbaum, Phys. Rev. **29**, 905 (1927).

$(Ii)_{sm}=0.1890=N_3$ and $(Ii)_{nm}=0.1848=N_4$ (The adjustment to equal values of $\int H(dH/dx)\,dv$ was made).

It can be shown, if there is no effect while crystallizing in a magnetic field and if enough measurements are made, repiling each time so that the disks are oriented at random, that the identity

$$N_1+2N_3=N_2+2N_4$$

should exist. This identity is satisfied by the foregoing values of N_1, N_2, N_3 and N_4 to within 0.32 percent, the change in diamagnetic susceptibility, if any, being an increase.

Nickel chloride. Only one sample of $NiCl_2$ was prepared with a magnetic field and one without it. Also, only one measurement was made on each of these samples, the value of $(Ii)_s$ taken being the maximum as the position of the sample was changed with respect to the field. Placing the observed values of $(Ii)_s$ and M in Eq. (2) there was obtained

$$\frac{0.2024\times0.2515}{0.1730\times0.2930}=1.0042$$

so that crystallizing $NiCl_2$ in a magnetic field of 18500 gauss did not increase the susceptibility by more than 0.42 percent. Care was taken that the comparison was made at the same temperature.

Potassium ferricyanide. As with $NiCl_2$, only one set of samples was prepared and only one measurement made with each. It was found that

$$\frac{0.08964\times0.3408}{0.09064\times0.3369}=1.0004$$

so that the effect, if any, was very minute.

Professor E. P. Adams suggested these experiments and I am indebted to him for much helpful advice.

A NEW METHOD FOR MEASURING THE DIELECTRIC CONSTANTS OF CONDUCTING LIQUIDS

By Allen Astin
New York University, University Heights

(Received March 12, 1929)

Abstract

A modified resonance method for determining the dielectric constants of conducting liquids is described in which no correction is necessary for the conductivity of the dielectric. The circuit contains an inductance in parallel with two series condensers, one of which is either shunted by a resistance or contains the conducting liquid as its dielectric. The vacuum tube voltmeter is found a more sensitive resonance indicator than a thermocouple and is connected to measure the p. d. across the shunted condenser. It is shown theoretically and experimentally, that the capacity of the condenser for maximum p. d. across it is independent of the parallel resistance. A preliminary curve is given showing the variation of the dielectric constants of weak KCl solutions with concentration. The dielectric constant decreases, reaching a minimum at a concentration of 0.0005 mols per liter. The average activity coefficient of the ions calculated by means of Hückel's equation is 1900. This result is checked by using two condensers of different size and shape. Readings from the two condensers agree only when the coupling with the oscillator is extremely loose. The lowering obtained is much greater than that reported by any other observers. However, results very similar to those of other experimenters are obtained when the coupling is increased slightly, but then readings from the two condensers do not check. The frequency employed is 3×10^6, the highest value at which lead wire effects are negligible. No change of the dielectric constant with different applied fields is found for a 0.0005 normal KCl solution. This investigation was prompted by earlier results of Furth. Previous values for sugar solutions are checked. Standardization of the condensers is with benzene. The dielectric constant of benzene is determined by a method devised for non-conducting liquids which gives directly absolute values. The dielectric constant for benzene is 2.239 ± 0.005 at 25°C. The dielectric constant of water obtained from a comparison with benzene is 79.5 ± 0.5 at 25°C.

Introduction

RESEARCHES on the dielectric constants of conducting liquids have increased greatly in number since the appearance of the Debye-Hückel theory of solutions. There is, however, almost no agreement in the results of the investigators, especially from those employing resonance methods. For example, determinations of the average activity coefficients for KCl ions by use of Hückel's equation[1] give results varying from 810 as reported by Walden, Ulich and Werner,[2] to 0 as reported by Voight,[3] and for NaCl from 600 as reported by Sommer[4] to 30 as reported by Hellman and Zahn.[5]

[1] E. Hückel, Phys. Zeits. **26**, 93 (1925).
[2] Walden, Ulich and Werner, Zeits. f. Phys. Chem. **115**, 177; **116**, 261 (1927).
[3] B. Voight, Zeits. f. Physik **44**, 70 (1927).
[4] S. Sommer, Berlin Dissertation, 1923 data from Bluh Phys. Zeits. **27**, 226 (1926).
[5] H. Hellman, and H. Zahn, Ann. d. Physik **81**, 711 (1926).

Values falling almost anywhere between these limits are obtained from the data of other observers. Perhaps the best agreement between two experimenters is in the works of Pechold[6] and Carman and Schmidt.[7] The results in each case were obtained by a force method.

The purpose of the investigation discussed in this paper was to determine the factors which might account for the discrepancies in results of resonance methods and to eliminate as many of them as possible. The undesirable factors can be readily summarized.

A condenser containing a conducting dielectric may be considered as a pure capacity in parallel with a resistance. In order to investigate the capacitive properties of the dielectric, the impedance of the pure capacity to an alternating current should be at least of the same order of magnitude as that of the resistance. This can be accomplished only by increasing the frequency of the current employed. The frequency has been increased to the limit; modern vacuum tube technique, making it possible to exceed 10^8 cycles per second. At such high frequencies however, complications are introduced which more than neutralize the advantage of decreased capacitive impedance. First, is the effect of lead wires because at very high frequencies they constitute the major part of the inductance of the circuit. Accurate determinations of the capacity changes involved in dielectric constant measurements require the evaluation of the lead effects. Some observers such as Walden, Ulich and Werner have used an arrangement, at frequencies around 10^8, in which a standard condenser is placed in parallel with the one containing the liquid under investigation and in their calculation have neglected the inductance of the leads between the two condensers. From the dimensions of the apparatus a consideration of this would certainly alter the results. Furthermore, if the leads are considered the evaluation process is difficult and uncertain, especially since the change which they introduce is not a constant change but one which varies as the capacity ratio varies. This has been mentioned by Lattey.[8] To eliminate the lead correction, the frequency in the present research was kept below 3×10^6 where the leads, by actual test, had a negligible effect.

The maintenance of constant frequency presents another problem when working in the radio range. The variations of frequency of the oscillator were found much less in simple resonance circuits than in bridge circuits so that the former type was considered preferable and has been used in this work. Detection of resonance with a thermocouple circuit, the method used by most investigators in this field, was not satisfactory because the reaction of the thermocouple circuit on the secondary, at such coupling as gave measurable deflections, could not be accurately interpreted. Likewise, resonance indicated by a dip in the grid current of the oscillator was sufficiently sensitive only when the coupling was too close to be sure of no frequency variation at resonance. A vacuum tube used as an electrostatic

[6] R. Pechold, Ann. d. Physik **83,** 427 (1927).
[7] A. P. Carman, and C. C. Schmidt, Phys. Rev. **30,** 925 (1927).
[8] R. T. Lattey, Phil. Mag. **41,** 829 (1921).

voltmeter was found to be the most sensitive resonance indicator. Furthermore, its effect on the circuit can be made capacitive only, the magnitude of which can be determined if necessary.

The simplest resonance circuit which has been used in this type of work is shown in Fig. 1, where x represents the resistance of the dielectric in the condenser C. The value of C for maximum current in the circuit under an induced emf of constant frequency is

$$C=(C_0/2)(1+(1+4L/C_0x^2)^{1/2})$$

where C_0 is the value of C at resonance when x is infinite. It should be observed that this equation involves a correction for the conductivity of the liquid which increases as the conductivity increases. The conductivities of liquids at high radio frequencies are not accurately known so that definite limitations are placed on the method. Lattey has devised a circuit of greater possibilities by placing an air condenser in series with the conducting condenser. He has shown that by a proper choice of circuit constants the resistance correction can be made more accurately than in the other circuit. It was found, however, that by adapting the vacuum tube voltmeter to the type of circuit used by Lattey an arrangement could be found in which the resistance correction could be entirely eliminated.

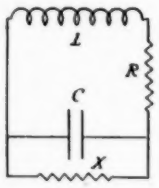

Fig. 1. Simple resonance circuit containing conducting dielectric.

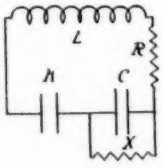

Fig. 2. Resonance circuit with conducting condenser in series with non-conducting condenser.

Description of the Circuit

The series circuit is shown in Fig. 2. The tube voltmeter is connected to indicate the maximum potential drop across C rather than across L. The conditions for this maximum p. d. when an emf E_0 of constant frequency is induced in the circuit are obtained as follows. The impedance Z of the the circuit to an alternating currrent of angular frequency ω is

$$Z=j\omega L+R-\frac{j}{\omega k}+\frac{1}{j\omega C+1/x} \qquad [j=(-1)^{1/2}]$$

or

$$\frac{|E_0|^2}{|I|^2}=|Z|^2=\left(R+\frac{x}{1+x^2\omega^2C^2}\right)^2+\left(\omega L-\frac{1}{\omega k}-\frac{x^2\omega c}{1+x^2\omega^2C^2}\right)^2.$$

If E_c is the p.d. across C, then

$$\frac{|E_c|^2}{|I|^2}=\frac{x^2}{1+x^2\omega^2C^2}$$

Eliminating I^2 and replacing $(1+x^2\omega^2C^2)$ by B

$$|E_c|^2=|E_0|^2\left(\frac{x^2\omega^2k^2B}{(BRk\omega+kx\omega)^2+(B\omega^2Lk-B-x^2\omega^2kC)^2}\right).$$

The maximum value of E_c obtained by varying C corresponds to the minimum value of the denominator providing it does not become zero. The value of C corresponding to the maximum value of E_c is

$$C=k\frac{(\omega^2Lk-1)}{R^2k^2\omega^2+(\omega^2Lk-1)^2}$$

If (ω^2Lk-1) is positive, C corresponds to a finite maximum of E_c.

Since x is missing from this last equation it means that the resistance of the electrolyte will have no effect on the value of C for the maximum deflection of the voltmeter. Furthermore C is a function of terms which can be kept constant so that changes in C can be measured directly by the change in a standard condenser placed in parallel with C.[9]

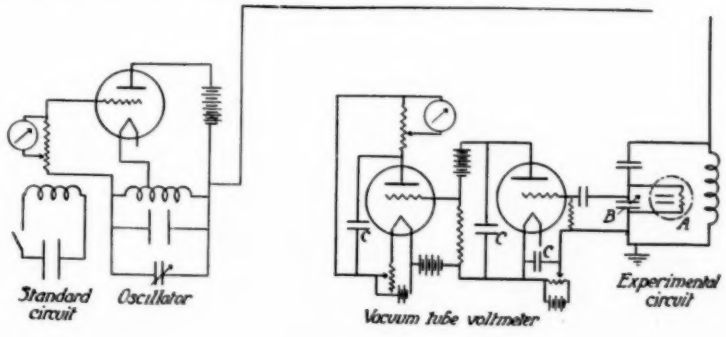

Fig. 3. Diagram of the experimental circuits. A is the test condenser containing conducting liquid, B is the standard variable condenser, CCC low impedance by-pass condensers.

The experimental arrangement used to obtain preliminary data as test of the circuit is shown in Fig. 3. The oscillator was a simple Hartley circuit adjusted to a frequency 2.7×10^6. The frequency was regulated by closing the switch in the standard circuit and varying a vernier condenser on the oscillator for minimum deflection of the grid galvanometer. The vernier

[9] This advantage, of a resonance setting independent of the resistance, can be obtained in a more simple circuit. If an alternating p. d. is applied across the coil in Fig. 1 instead of being induced in the circuit, the condition for minimum current from the source is independent of the parallel resistance. Experimentally, however, this condition could not be obtained at radio frequencies because it was impossible to keep the frequency of the source constant with such coupling.

condenser was controlled by a long glass rod to remove the body capacity of the operator. The grid galvanometer was of high sensitivity and had a coil of low moment of inertia to give quick response. The galvanometer suspenpension was twisted so that the normal grid current gave zero reading on the scale. This greatly magnified the amount of any variations which were observed by a lamp and scale arrangement, the scale being about 15 feet from the galvanometer.

The oscillator and resonance circuits were about 15 feet apart and were coupled through a long horizontal antenna from the oscillator and a short vertical one from the other. The strength of the coupling could be varied by changing the distance between the ends of the two antennae. The coupling was made so loose that the secondary circuit produced no detectable effect on the grid current of the oscillator. Such loose coupling was found quite necessary as will be shown later.

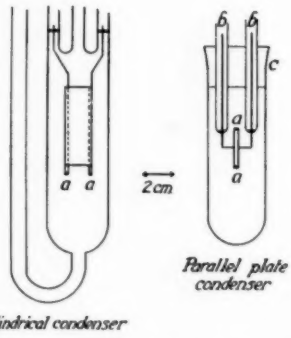

Fig. 4. Diagram of the test condensers drawn to scale. *aa*—glass spacers, *bb*—capillaries, *c*—rubber stopper.

The inductance of the coil and antenna in the secondary circuit was about seven microhenries.[10] A mica condenser of about 700 $\mu\mu$f served as the series condenser. A G. R. C. precision condenser was used as the standard variable condenser. This was also operated by a long arm to remove body capacity. Two condensers were used for the liquids tested and diagrams of them are shown in Fig. 4. The electrodes of each were of platinum. The effective

[10] This experimental arrangement did not conform exactly to the conditions assumed in developing the theory of the circuit because here the emf was induced in the antenna instead of in the coil. It was assumed that the effect of the antenna, whose capacity was very small was of an added inductance and that the emf was induced in the circuit, which would then give the same result as obtained above for the resonance condition. The reason for this assumption was that the resonance observed was series resonance which results from an emf induced in the circuit. If the effect of the antenna had been to apply a p. d. across the coil, i.e., between the antenna terminal and the grounded side of the coil, parallel resonance would have been obtained which was not the case experimentally. It is possible that the use of the antenna may have caused a small error; it was used in the preliminary work of this paper because it provided a convenient arrangement for securing coupling variations and at the same time proper shielding. It has been eliminated in an improved form of the apparatus for more extensive work now in progress.

capacity in air of the parallel plate condenser was 2.6 $\mu\mu$f and of the cylindrical condenser 14.1 $\mu\mu$f.

The grid and filament were connected to the terminals of the variable condenser with as short leads as the dimensions of the apparatus permitted. The blocking condenser in the grid circuit prevented a leak current flowing through the conducting liquid. The various low impedance by-pass condensers made the effect of the voltmeter on the secondary circuit that of a small capacity in parallel with a high resistance. Neither of these effects as seen from the theory of the circuit would have any bearing on the changes to be measured. The potentiometer on the C battery permitted adjustment of the bias to give the maximum change in the plate current for a given p. d. impressed on the grid. The second tube in the voltmeter circuit served as a direct current amplifier. The galvanometer in the plate circuit of this tube was of the same type as that in the grid circuit of the oscillator. Its suspension was likewise twisted to give zero reading when normal plate current was flowing. All tubes used were of the 201-A type.

It was found that steadier readings were obtained by grounding one side of the system as shown in the diagram. The test condenser was immersed in a constant temperature water bath which was kept at 25.0°C.

Benzene was used as a standard liquid and the dielectric constants of of water and water solutions were determined with respect to the dielectric constant of benzene. This latter was determined by a method devised to give directly the absolute value of the dielectric constants of non-conducting liquids. The method, in brief follows.

Standardization of Benzene

A condenser of gold plated parallel plates, separated by small glass spacers was placed in parallel with a coil of 2 henries inductance. The natural period of this system was measured by Hubbard's arrangment of the drop chronograph.[11]

If L is the inductance of the circuit and C the capacity, excluding that between the plates, A the area of one of the plates, d the thickness of the glass spacers, the natural period of the system is given by

$$T=2\pi(L(C+kA/4\pi d))^{1/2}$$

The period as obtained from the chronograph readings is

$$T=s/(2gh)^{1/2}$$

where s is twice the distance in cm between two successive nodes on the discharge curve, h the average distance the projectile has fallen as it strikes the levers and g the acceleration of gravity. Then

$$s^2=8\pi^2ghL(C+kA/4\pi d)$$

[11] J. C. Hubbard, Phys. Rev. **9**, 529 (1917).

If d is changed to d_1 by using a new set of glass spacers and s_1 is the new value of s then

$$s_1^2 - s^2 = Bk(1/d_1 - 1/d)$$

where B is a constant. If the dielectric is now changed from k to k_1 and the readings repeated, s' and s_1' being the new nodal intervals the relation between the dielectric constants is

$$k_1 = k(s_1'^2 - s'^2)/(s_1^2 - s^2)$$

The intervals are measured directly from a micrometer screw and if k for air is taken as unity the absolute value of the dielectric constant of the liquid results directly. This method of using glass spacers of different thicknesses to eliminate lead corrections was first used by Powers and Hubbard in a resonance method.[12]

Four sets of glass spacers gave four independent values for the dielectric constant of benzene. The average value was 2.239 ± 0.005. The measurements were taken at a frequency of 7.7×10^3 and temperature 25°C. It was assumed that there was no change in this value between this frequency and 2.7×10^6, an assumption which seems justified because of the non-polar nature of benzene. This result is in good agreement with recent determinations of this constant. Sayce and Briscoe[13] give 2.2389 and Harriss[14] 2.2482, at 25°C. These values are about two percent lower than those generally accepted by handbooks prior to 1925.

The conductivity of water was too high to permit its use as a dielectric in this circuit.

Results

The dielectric constant of water was determined with respect to that of benzene using the resonance circuit. The calculation was made from the equation

$$(k_1 - 1)/(k_2 - 1) = c_1/c_2$$

where k_1 and k_2 are the dielectric constants of water and benzene, and c_1 and c_2 the changes made in the setting of the standard condenser for maximum reading of the voltmeter caused by introducing each liquid into the test condenser. The average value for water obtained by using both condensers shown in Fig. 4 was 79.5 ± 0.5. The average conductivity of the water was 2×10^{-6} mhos per cm, but variations one-half to five times this value made no measurable change in the dielectric constant.

The values for methyl alcohol and glycerine were found to be 34.0 and 50.6. These values are slightly lower than those generally listed in handbooks. Kahlbaum c. p. materials were used.

[12] Powers and Hubbard, Phys. Rev. **15**, 535 (1920).
[13] L. A. Sayce and H. V. H. Briscoe, Chem. Soc. J. **127**, 315 (1925).
[14] H. Harriss, Chem. Soc. J. **127**, 1049 (1925).

Tests of the method with sugar solutions gave the results in Table I. These values agree very closely with those reported by Harrington[15] but are higher than those published by Furth.[16] At a concentration of one mol per liter Furth's result is about 10 percent higher, this difference decreasing in the weaker solutions.

The method was next tested with KCl solutions and the results obtained are also shown in Table I. With solutions stronger than 0.003 N in the parallel plate condenser and 0.0005 N in the cylindrical condenser the p. d. across the standard condenser was too small to be measured. The resistance

TABLE I. *Dielectric constants of KCl and sugar solutions.*

KCl			Sugar	
Conc. mols/l	Ratio—k of solution to k of water		Conc. mols/l	K_s/K_w
	parallel plate condenser	cylindrical condenser		
0.00025	0.988	0.989	0.10	0.978
0.0005	0.978	0.978	0.25	0.967
0.001	0.989	—	0.50	0.943
0.002	1.001	—	0.75	0.915
0.003	1.019	—	1.00	0.887

of the solution in each condenser in this limiting case was about 100 ohms. The probable error of the results was about one-half of one percent for water, the sugar solutions and the most dilute KCl solutions and about one and one half percent for the strongest solutions.

The agreement of the two readings from the larger condenser with those of the smaller is considered as evidence that the condition for maximum p. d. across the condenser is independent of the parallel resistance. The resistance of a solution in the cylindrical condenser was about one-fifth the resistance of the same solution in the other condenser. A direct test of this point was not possible because a variable resistance without some capacitive or inductive effect could not be found. For example, a General Radio "non-inductive" resistance box in parallel with the standard condenser changed the setting for maximum deflection 82 $\mu\mu$f when the resistance was one 100-ohm coil and 132 $\mu\mu$f when the resistance was ten ten-ohm coils.

In 1924 Furth[17] published data from a force method showing a dependence of the dielectric constant of NaCl solutions on the applied field. Although he corrected this data in 1927[18] a test of the point seemed interesting because measurements of the strengths of applied fields could be made readily with the tube voltmeter. Furthermore a change in the dielectric constant of polar substances is expected in strong fields although not likely in the small fields which were used in this work. No change was found in the dielectric constant

[15] E. A. Harrington, Phys. Rev. **8,** 581 (1916).
[16] R. Furth, Ann. d. Physik **70,** 64 (1923).
[17] R. Furth, Phys. Zeits. **25,** 676 (1924).
[18] R. Furth, Zeits. f. Physik **44,** 256 (1927).

of water in fields varying between 58 volts per cm and one-half volt per cm and no change was found in a 0.0005 N KCl solution in fields from three to one-fourth volts per cm. These field values were the maximum or peak values. The different fields were obtained by varying the output of the oscillator.

When the coupling between the oscillator and secondary circuit was increased to give a small, sharp dip in the grid galvanometer of the former at resonance, quite different results were obtained. The readings from the two condensers no longer agreed. A typical example of this disagreement is shown in the curves *I* and *J* in Fig. 5. *I* was obtained with the parallel plate condenser and *J* with the cylindrical condenser. Curve *A* is the graph of the

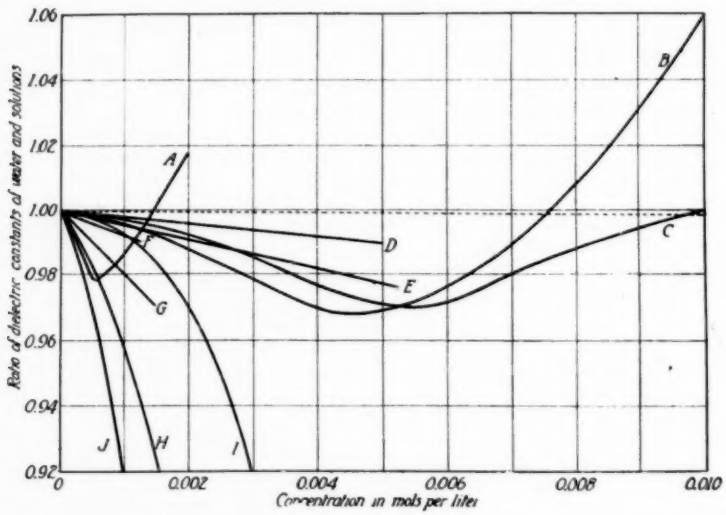

Fig. 5. Dielectric constants of KCl solutions as reported by different observers. *A*—Astin, resonance method at 3×10^6. *B*—Carman and Schmidt, force method at 500; *C*—Pechold, force method at 50; *D*—Schancke and Schreiner, Nernst bridge method at 10^6; *E*—Sommer, Nernst bridge method at 10^6; *F*—Sach, Nernst bridge method at 10^6; *G*—Walden, Ulich and Werner, resonance at 10^8; *H*—Lattey, resonance method at 10^7; *I* and *J*—Astin, same method as curve *A* with closer coupling. *I*—with parallel plate condenser, *J*—with cylindrical condenser. The dotted line indicates the lowering predicted by Hückel.

data in Table I. The other curves are the dielectric constants of KCl solutions as reported by other experimenters. The conditions under which *I* and *J* were obtained were such that the additional transfer of energy between the primary and secondary circuits gave measurable deflections of the voltmeter at concentrations twice the highest obtained in curve *A*.

Conclusions

An estimate of the average activity coefficient of KCl ions obtained from the data in Table I and Hückel's equation

$$k = k_0 - 2\delta\gamma$$

gave $\delta = 1900$. k and k_0 are the dielectric constants of the solution and pure solvent and γ the concentration in mols per liter. That this value is higher than those obtained from the data of other observers is evident from a glance at Fig. 5. The lowering of the dielectric constant predicted by Hückel is shown by the dotted line. In spite of the wide variety of results which have been reported none agrees even as to order of magnitude with this predicted lowering. Voight reports no lowering but since his result consists of a single reading at 0.0013 N it bears little weight.

Since it was possible to make the curve *I* agree more or less closely with *F*, *G* and *H* (*I* is merely a typical curve, it could be made to take different shapes and positions by additional changes in coupling) it is suggested that perhaps some of these results are in error because of coupling effects. Hellman and Zahn[19] have already criticised the work of Walden, Ulich and Werner because of tight coupling between the resonance and thermocouple circuits. None of the observers using resonance and bridge methods whose curves are listed records tests as to the constancy of the frequency of the a.c. source; it has merely been assumed constant. A more extensive test of this point is under way using heterodyne methods to note frequency variations and using crystal control to insure a certain degree of stability. The use of the vacuum tube voltmeter in the present work made it possible to work at looser coupling than if a thermocouple had been used. Other experimenters have used thermocouples as resonance indicators.

Hellman and Zahn use a decrement method and eliminate many of the difficulties which are present in resonance methods. They are able to measure much stronger solutions than has been hitherto possible but their method does not apply to very dilute solutions. With NaCl (they have not worked with KCl) the most dilute solution they could measure was 0.05 N. Since the interesting region, or at least the region where results will be most easily interpreted, is the very dilute region where ionization is complete, they extrapolated their results to cover solutions weaker than 0.05 N. Their results decrease slightly at first, reach a minimum, and then increase. Because of the initial decrease they assume a linear lowering from zero concentration to their initial concentration. In view of the many discrepant results in this region through which they extrapolate, their assumption seems unwarranted. The results for NaCl differ as widely as for KCl, even the two force methods yield very different data for the former salt.

Since it was possible to extend the limiting concentration of the present method twofold by a slight increase in coupling it is believed that the useful range can be considerably extended by using sources of much stronger output. This work together with a study of the effect of frequency changes is already under way.

Appreciation is expressed to Professor W. A. Lynch for his frequent and valuable counsel and to Professor J. C. Hubbard of Johns Hopkins University for suggesting the problem.

[19] H. Hellman, and H. Zahn, Phys. Zeits. **26,** 680 (1925).

THE DISTRIBUTION OF MOBILITIES OF IONS IN MOIST AIR*

By John Zeleny
Sloane Physics Laboratory, Yale University

(Received March 22, 1929)

Abstract

A search was made in undried air for groups of ions having different mobilities and no such distinct groups were found among ions two or more seconds after their formation. A critical study was made of the effects of diffusion upon the distribution of ions moving in an electric field. Experimental results obtained for N, the volume density of ions which after a time t are located at a distance r from the origin agree fairly well with the theoretical formula

$$N=\frac{N_0}{(4\pi Dt)^{3/2}}\epsilon^{-r^2/4Dt},$$

where D is the coefficient of diffusion. The mobilities and the spreading of the ions were measured by a modification of the author's method in which ions passing between two concentric cylinders under an electric field are simultaneously carried axially by a slow, non-turbulent current of air of known velocity. The ions entered the air stream through small openings in the walls of the outer cylinder and their distribution at the central cylinder was measured by catching them on a narrow insulated section of that cylinder which was connected to an electrometer. The ions were found to be confined to one group covering a range of mobilities in which the fastest ions have mobilities about 45 percent larger than the slowest for positive ions and about 30 percent larger for negative ions. The distribution would be explained if a number of unresolved permanent distinct groups exist, but a more probable explanation rests on the assumption that the ions are clusters which change in size under the influence of molecular bombardment, the life of each stage being sufficiently long so that the number of changes occurring during the time of passage of the ions is not very great. No certain change in the distribution was noted for changes of the time of passage of the ions between 0.05 sec. and 0.67 sec. The mobilities of the ions were determined under widely different conditions in air ranging in water content between 1.5 mg/liter and 7.6 mg/liter. Without weighting the observations, the average mobility found for the negative ions is 2.00 cm/sec·volt/cm for an average water content of 3.2 mg per liter of air, and the average for the positive ions is 1.22 cm/sec·volt/cm for an average water content of 2.7 mg per liter of air, the most probable error in each case being about one percent.

SOME observers have in recent years reported results on the mobility of ions in air which point to the existence of several distinct types of ions of each sign.

Nolan[1] using the blast method found indications in moist air of eight unique mobilities for both positive and negative ions. Later he and Harris[2] using both the blast method and the alternating field method found still

* Read before the American Physical Society on Dec. 30, 1928. A report on the first part of the work was made at the April Meeting, 1928.

[1] J. J. Nolan, Proc. Roy. Irish Acad. **35**, 38 (1920).

[2] J. J. Nolan and J. T. Harris, Proc. Roy. Irish Acad. **36**, 31 (1922).

more types of ions both in saturated air and in dried air. The interpretation of the observations was questioned by Blackwood[3] and Loeb[4] who in attempts to verify the results found no positive evidence of more than one unique mobility for ions of each sign. Nolan[5] repeated the observations taken with the alternating field method and obtained now about 20 groups of ions which according to a computation are progressively made up of 15 to 36 molecules each. C. T. R. Wilson[6] found by his cloud method that ions formed by an alpha-ray were separated by an electric field into four groups.

Erikson[7] discovered that the positive ion in air soon after formation has the same mobility as the negative ion but in a very short time undergoes changes so that its mobility assumes the lower value which has usually been assigned to it. No other types of ions were found. This result was verified by Wahlin[8] and by Tyndall and Grindley.[9] After aging the ions for a longer time Wahlin[10] later found six distinct types of positive ions in air.

Busse[11] interprets results he obtained by a blowing method as showing that the ions produced in air by rays from radioactive substances have mobilities spread over a wide range whose magnitude depends on the sign and age of the ions and on the humidity of the air. Laporte[12] in an extensive research by a new method involving the passage of ions between two rotating disks obtains well defined distribution curves which he also interprets as showing that the ions of each sign are not all alike but that they differ among themselves by such small steps that their mobilities appear to cover continuously a large range of values whose limits differing by more than 100 percent depend upon the sign of the ions and upon the humidity of the air.

Briggs[13] obtained a similar though less extended band of mobilities in air for recoil atoms of radioactive substances, the largest value being 50 percent larger than the smallest.

Schilling[14] using extreme precautions for getting pure air not only confirmed the large effect of traces of impurities but also showed that "aging" of ions does not occur in pure or in saturated air but only for intermediate states, when the mobilities of both kinds of ions diminish with age, between 0.05 sec. and 1.2 sec.

Mahoney[15] found only the final ions in dry or fairly dry air. These showed no change in mobility for ions of either sign for a range of age from

[3] O. Blackwood, Phys. Rev. **20,** 499 (1922).
[4] L. B. Loeb, Jour. Franklin Inst. **196,** 537 (1923).
[5] J. J. Nolan, Phys. Rev. **24,** 16 (1924).
[6] C. T. R. Wilson, Proc. Camb. Phil. Soc. **21,** 408 (1922–23).
[7] H. A. Erikson, Phys. Rev. **20,** 117 (1922).
[8] H. B. Wahlin, Phys. Rev. **20,** 267 (1922).
[9] A. M. Tyndall and G. C. Grindley, Proc. Roy. Soc. **A110,** 358 (1926).
[10] H. B. Wahlin, Phil. Mag. **49,** 566 (1925).
[11] W. Busse, Ann. d. Physik. **81,** 277 (1926).
[12] Marcel Laporte, Ann. de Physique **8,** 466 (1927).
[13] G. H. Briggs, Proc. Camb. Phil. Soc. **23,** 73 (1926).
[14] H. Schilling, Ann. d. Physik **8,** 23 (1927).
[15] J. J. Mahoney, Phys. Rev. **33,** 217 (1928).

0.001 sec. to 0.03 sec. He considers the ions of each sign all to have the same mobility. In moist air of 60 percent or 90 percent relative humidity the results of Erikson on aging of the positive ions were confirmed, only that the rate of transformation was found to be somewhat slower than that reported by Erikson.

These various results bear rather conflicting testimony on the structure of gaseous ions and in connection with them must be borne in mind the very large number of other researches on mobilities whose results have been interpreted in terms of a unique mobility for each sign of ion. It seemed highly desirable that more work be done to throw added light on the problem of the distribution of ionic mobilities under conditions where disagreement as to the facts still exists.

A blast method, although more laborious and in some respects of more restricted use than the alternating field method, was chosen for the work being reported because it has the great merit that in its use a steady state exists during the procedure of making a measurement, and this state makes a detailed analysis of results more certain. Moreover in the form used by Erikson and by Tyndall and Grindley different types of ions should indicate themselves by separate peaks in a curve, evidence which for measurements of this kind is generally regarded as more convincing than that given by "breaks" in a curve.

For measurements of the absolute mobilities of ions, and for investigations on the distribution of mobilities within an apparent group it is essential that the air streams used in the experiments be free from all turbulence. In order to eliminate the turbulent motion of the air stream which was doubtless present in researches where high velocity streams were used in tubes of rectangular cross section, I adopted as best suited for the purpose a modified form of the apparatus I used in my early mobility measurements.[16]

Method

In this method a steady stream of gas of known mean velocity is blown through the space between two coaxial cylinders, and the distance measured that the ions are carried down stream by the gas while they are moving the distance between the two cylinders under the influence of the radial electric field. The ions were produced in an outer chamber and introduced into the stream by means of auxiliary air jets passing through small holes in the outer cylinder. The charge carried by those which are caught on a narrow, insulated portion of the inner cylinder was measured. At any point a distance r from the common axis of the cylinders the radial velocity of the ions is given by $[kV/r \log (b/a)]$, k being the mobility of the ions, V the potential of the outer cylinder, b the inner radius of the outer cylinder, and a the outer radius of the inner cylinder. The down stream velocity of the ions at the same point due to the air stream is given by

[16] J. Zeleny, London Phil. Trans. **A195**, 193 (1900).

$$v=\frac{p}{4\mu \log (b/a)}\left[(b^2-r^2)\log\frac{r}{a}-(r^2-a^2)\log\frac{b}{r}\right],^{17} \quad (1)$$

where p is the pressure difference per unit length of the cylinders and μ is the coefficient of viscosity of the gas. The actual path of the ions is a compound curve each terminus of which is normal to one of the cylinders. (See curve A of Fig. 9.)

If U is the mean velocity of the gas stream and X is the distance the ions are carried down stream in crossing between the cylinders, the mobility

$$k=\frac{U(b^2-a^2)}{2VX}\log\frac{b}{a}\cdot \quad (2)$$

The present paper will be confined to an account of the work done on the mobility of old ions in filtered air having its normal water content. It was thought that the presence of water and carbonic acid might be propitious for the formation of ions of different types if such types exist.

Apparatus

The apparatus used is shown diagrammatically in Fig. 1 and consists of two concentric brass cylinders the outer of which is 123 cm long and has

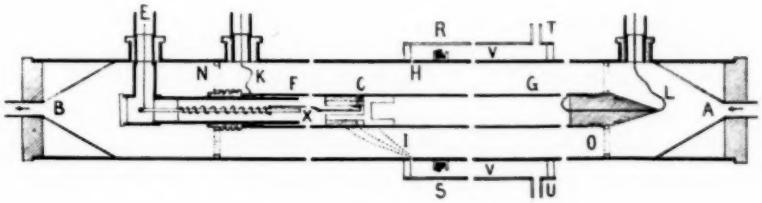

Fig. 1. Diagram of apparatus.

an inner diameter of 7.297 cm while the inner cylinder has an outer diameter of 2.538 cm. The inner cylinder is divided into three main sections, which are insulated from one another. The narrow section, C, to be called the collecting ring, is 1.5 mm wide and is separated from F (15.9 cm long) and from G (70 cm long) by air gaps, 0.38 mm wide. The central cylinder is supported in an exactly coaxial position with the outer cylinder by two wheel supports N and O, each of which has four narrow spokes connecting its hub with its rim. The hubs are insulated from the inner cylinder. The wires K and L permit F and G respectively to be connected either to ground or to an electrometer. The collecting ring, C, is joined by the wire X and a flexible spring and rod arrangement to the wire E leading to the electrometer. This arrangement permits the central electrode to be moved parallel to its axis for changing the position of C relative to the ion inlet openings in the outer cylinder, without disturbing the connections to the electrometer. The quadrant electrometer was used at sensitivities between 1500 and 3000 scale divisions

[17] Leigh Page, Theoretical Physics, p. 231.

per volt, and permitted work with small ion densities to minimize the effects of space charges and of mutual repulsion of the ions.

Distributed uniformly around the circumference of a right section through H of the outer cylinder are 102 holes each 1 mm in diameter, which permit ions produced in the ionization chamber VV, by radioactive material in the tubes RS, to be blown into the space between the two cylinders by a slow auxiliary air stream entering at T and U.

The ions were produced in VV by beta-rays coming from forty small glass tubes (old radon tubes) containing Ra D, E, F. The tubes were fastened around the circumference of a movable metal ring RS and were partially surrounded by a lead collar shield to prevent direct beta-rays striking the chamber walls near the openings at H, in order to reduce to a negligible amount the number of scattered beta-particles entering the main gas stream through these holes. The ring RS was usually placed 1.5 cm from the openings H and with streams of the magnitude used to carry ions into the main apparatus the age of the ions when they entered at H was more than 2.5 sec.

The auxiliary air stream by which the ions were carried into the main stream was supplied by a device which forced a constant measurable volume of air per sec. into the chamber VV. This was done by displacing air in a fixed gasometer by water entering through a pipe under a constant pressure head. Before entering the ionization chamber the air was dried by passage through a tower of calcium chloride[18] and filtered by passage through a cotton filter.

The main gas stream entered the space between the cylinders through a funnel A, provided with a number of gauzes of fine mesh (not shown in Fig. 1) for equalizing the stream as it enters. The air was supplied by the laboratory compressed air system and was filtered by passage through a large cotton filter. Its water content was determined periodically by chemical means. The rate of flow of the air was measured by means of a water manometer placed in parallel with a fixed length of tubing that carried the flow; the arrangement having first been calibrated by aid of a precision gasometer for whose use I am indebted to Professor Yandell Henderson.

Notwithstanding the fact that the stream velocities to be used were well below the limits for which turbulent motion sets in as given by Osborne Reynolds,[19] the steadiness of the gas flow between the two cylinders under the experimental conditions used was investigated by aid of smoke jets. A full size duplicate apparatus was made in which a brass tube was used for the upstream portion of the outer cylinder while the remaining portion was made of a piece of glass tubing of nearly the same diameter to permit observation of the smoke jets. The brass portion was provided with inlet holes around a circumference similar to those used in the actual apparatus for admitting ions.

[18] This might have been omitted to advantage in view of recent work of Erikson (Phys. Rev. **32**, 791 (1928)) showing that some of the final positive ions in dry air are changed to the initial type on entering moist air. [Added in proof. Recent measurements made on positive ions gave the same distribution of mobilities when the calcium chloride tower was removed from the ion bearing air current as was obtained when the tower was present.]

[19] Osborne Reynolds, London Phil. Trans. **A174**, 935 (1883).

Forcing air through these holes at the same rate as was done during the measurements in the original apparatus had no effect on the stability of the main air stream between the concentric cylinders. When smoke was admitted with the air entering these holes the glass part of the system presented the beautiful appearance of a hundred narrow stationary white streaks running the full length of the tube without the slightest mingling, although in such very close proximity to one another. The smoke streamers remained close to the wall of the outer cylinder. Measurements made with a bent wire gauge placed in one of these streamers at a distance of about 5 cm from its point of entrance showed a maximum penetration of but 1.5 mm into the main stream when the velocity of the air entering the inlet holes was 17 cm/sec. and the mean velocity of the main stream was 8.6 cm/sec. In the actual experiments the inlet jet velocities used were somewhat smaller than that given above but due correction will be made for the penetration of these jets into the main streams between the cylinders.

A single smoke jet was used for testing the stability of the central portion of the air stream. The jet entered from the up-stream side of the apparatus through a long narrow glass tube having an opening about 1 mm in diameter. It is essential to have the jet stream enter very slowly. For average stream velocities up to 12 cm/sec. the stream lines remained very steady. Above this velocity the smoke jet began to show a slow irregular side wabble, the excursions of which were larger at right angles to a radius than along it. At a mean velocity of 14.5 cm/sec. the maximum excursions were at times as much as 1 mm and at a velocity of 20 cm/sec. the excursions covered several millimeters at some distance down stream from the jet inlet.

Two methods of procedure were followed in making measurements. In the first, the collecting ring was kept at a fixed distance down stream from where the ions entered, and readings were taken of the charge received by the ring as the potential of the outer cylinder was varied. In the second method the potential of the outer cylinder was kept at a fixed value and the central cylinder was moved so that the collecting ring occupied different positions relative to the ion-inlet openings.

Experiments with Stationary Collecting Ring and Variable Voltage

An example of the results obtained when the center of the collecting ring was kept at a fixed distance of 4 cm from the plane through the centers of the ion inlet holes is given in Fig. 2. The positive ion currents received by the collecting ring are represented in the curves by ordinates corresponding to voltages on the outside cylinder given as abscissas. In curve *A* the average velocity of the air stream was 9.7 cm/sec. and in curve *B* it was 14.7 cm/sec. The auxiliary stream by which the ions were carried into the main stream through the inlet holes delivered 20 cc of air per sec. Allowance for this air volume has been made in the above values of the average air stream velocities. Each curve has considerable breadth but only one peak. The largest voltage for which ions reached the collector in each case is approximately three times

as large as the lowest voltage. This means that for any one voltage the ions reach the central electrode spread over a rather large distance along its length. A part of this spread arises from the physical widths of the ion entrance holes and of the ion collecting ring, the whole distance thus involved being 2.9 mm. This does not account for as much as ten percent of the spread observed. Another part of the spreading arises from the diffusion and mutual repulsion of the ions in their passage between the two cylinders. The magnitude of this effect has been determined experimentally and will be considered in detail in connection with the second method of procedure where the voltage is kept fixed and the collector ring moved, since in that method the correction can be applied more directly. It need only be stated here that when the requisite transformations are made to permit the correc-

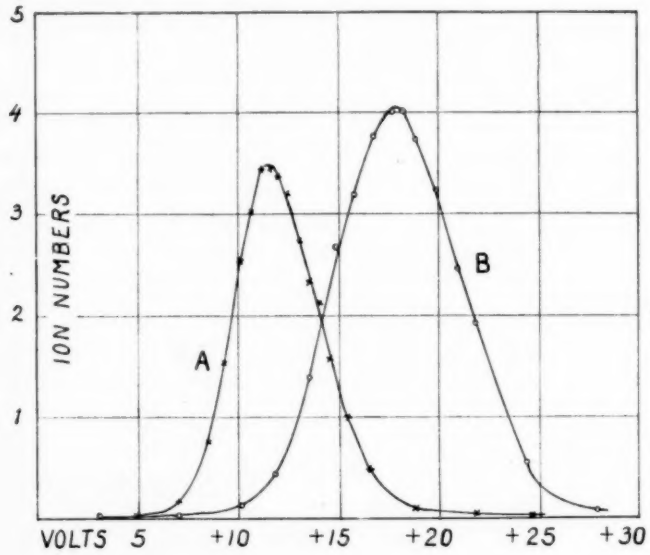

Fig. 2. Positive ion currents for different voltages. Collecting ring distance, $X=4$ cm. Air pressure = 76.9 cm of Hg. Temperature = 23°C. Water content of air = 2.4 mg/liter. Air stream velocity, for curve $A=9.7$ cm/sec; for curve $B=14.7$ cm/sec.

tion to be applied to the results obtained by the procedure now under consideration, the computation shows that a portion of the observed spreading of the ions remains unexplained unless we assume that all of the ions do not have the same mobility. Making this assumption, the continuous nature of the curves points to the conclusion that the ions are not comprised in a few distinct groups having definite but quite different mobilities. More probably, as assumed by Busse[11] and by Laporte,[12] the ions form one statistical group in which the mobility changes more or less gradually from one portion of the ions to the next. If there are permanent groups of ions within the range observed, which differ in mobility among themselves, these have not been resolved. The many curves obtained both with positive and negative ions show no evidence of more than one peak.

The observations recorded in Fig. 3 were made primarily to find electrons or negative ions of high mobility if present. For this purpose the collecting ring was placed only 0.49 cm down stream from the holes through which the ions enter. The gas stream velocity used was 21.4 cm/sec., and the auxiliary ion stream delivered 22.9 cc/sec. Fast ions or electrons should be detected if present with small voltages on the outer cylinder. The many readings taken in this region at small voltage intervals give no indication of the presence of any ions of this character as numerous as one-tenth of a percent of those represented by the peak of the curve.

The whole evidence of all of the experiments both with positive and negative ions is against the existence in moist air of more than one general group of ions of each sign, two or more seconds after the formation of the ions.

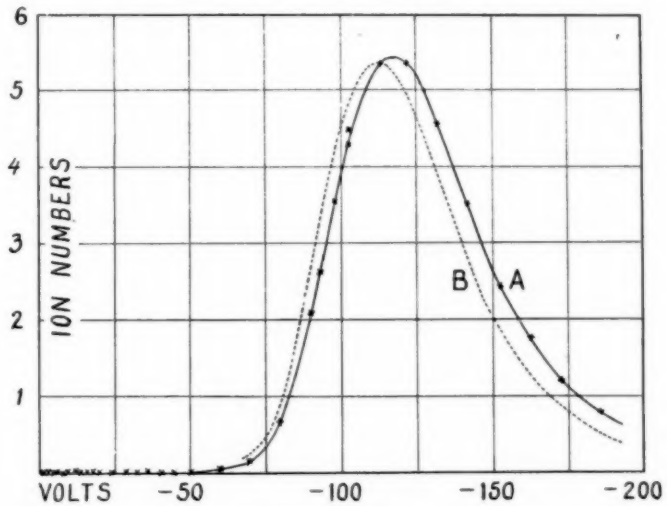

Fig. 3. Negative ion currents for different voltages. Collecting ring distance, $X = 0.49$ cm. Air pressure = 76.1 cm of Hg. Temperature = 21°C. Water content of air = 2.38 mg/liter. Air stream velocity = 19.9 cm/sec. Curve *B* is corrected for variation of spreading with voltage.

The present method of procedure lends itself to the determination of absolute values of mobilities for the ions corresponding to the peaks of the curves. Two correction factors which are involved will first be considered.

Owing to the fact that the collecting ring has a definite width while the total linear spread of the ions received along the length of the central cylinder depends in an inverse manner upon the potential difference between the two cylinders, the curves shown do not give the exact distribution of the ions. When a large voltage is applied and the ions cover but a short length of the inner cylinder those striking the fixed width of the collector ring form a larger fraction of the whole than would have been the case had a smaller voltage been used and the ions been spread over a greater distance along the cylinder. To correct for this variation of dispersion with voltage, the distribution for some one voltage is taken as a standard and the readings for other voltages are adjusted to the scale for the standard voltage by taking the readings to

be inversely proportional to the two voltages concerned. The dotted curve in Fig. 3 is a corrected curve obtained in this way from the main curve, the standard voltage taken being the one for which the two curves cross each other. The peak of the curve is shifted by this correction toward the smaller voltages, usually by about 2 to 3 percent.

The second correction to be considered arises from the fact that the air laden with ions has an appreciable radial velocity as it enters the main gas stream through the small openings in the outer cylinder. The actual distance these jets of ionized air penetrated into the gas stream was determined, as already noted, by aid of smoke, for a case where the jets had a somewhat larger velocity than that used in most of the experiments. For velocities differing from this the distance of penetration of the jets was found by assuming that this distance is directly proportional to the entering velocity of the jets. During nearly all of the measurements made the penetration distance of the jets was approximately 1 mm. In this portion of their path the ions move under the combined action of the electric field and of the jet stream. The contribution which the jet stream makes to the inward displacement of the ions is the part of the penetration distance given by the ratio of the mean velocity of the jet stream to the sum of this mean velocity and the velocity of the ions under the electric field alone. The mean velocity of the jets was taken as one half of their velocity on entrance. The computed distance the ions were carried inward by the action of the jets of air was found for the different cases to be between one and three percent of the total distance between the cylinders. This percentage of the distance thus computed for each case was applied as a first approximation correction to the mobility value obtained by Eq. (2). The effect of the correction was to diminish the mobility values given by the formula.

The contact difference of potential between the collector ring and the outside cylinder was found by experiment to be but 0.05 volt, the ring being negative with respect to the cylinder.

The mobility thus found for the negative ions from the corrected peak of the curve in Fig. 3, when reduced to air under a pressure of 76 cm of mercury and to a temperature of 20°C on the assumption that mobilities vary inversely as gas densities, was 2.10 cm/sec · volt/cm. The water content of the air was 2.38 mg per liter of air. The values obtained similarly for positive ions from the curves of Fig. 2 were in each case 1.21 cm/sec · volt/cm.

A summary of all of the results obtained by this method of procedure for the mobilities of those positive and negative ions which reached the central electrode at the peaks of the corresponding distribution curves is given in Table I. X is the distance the collecting ring was situated down stream from the ion inlet openings, U is the mean velocity of the main stream and S the volume of air entering per sec through the ion inlet holes. The fourth column gives the water content of the air used, in mg per liter, and the last two columns give the mobilities. Owing to the varying water content the results are not directly comparable. The average of the mobilities found by this first procedure is 1.20 cm/sec for the positive ions and 2.00 cm/sec for

the negative ions, corresponding to an average water content of about 3 mg per liter of air. Corrections have been made in all cases for the variation of dispersion with voltage and for the effect of the ion inlet streams as has been explained, and the results have been reduced to normal air pressure and a temperature of 20°C. The average ratio of the voltages marking the beginning and end of each distribution curve (compare Fig. 2) was 2.7 for positive ions and 2.4 for negative ions. These numbers do not indicate the range

TABLE I. *Summary of mobility results; fixed collecting ring method.*

X Down stream distance cm	*U* Velocity main air stream cm/sec	*S* Ionized air vol. cc/sec	Water content mg/liter	Mobility of positive ions cm/sec · volt/cm	Mobility of negative ions cm/sec · volt/cm
3.00	7.43	16.	—	—	1.94
3.00	7.43	16.	—	1.20	—
3.00	7.43	16.	—	—	1.98
3.00	7.43	16.	—	—	2.12
3.00	13.6	17.	4.67	—	2.02
3.00	13.6	16.6	4.07	—	1.94
3.00	13.6	16.	—	1.22	—
3.00	13.5	13.5	1.87	1.19	—
4.00	13.5	12.	5.32	—	2.00
4.00	13.9	27.	5.32	1.20	—
4.00	13.4	20.5	2.51	1.22	—
4.00	13.4	20.	2.51	—	1.97
4.00	5.42	16.	2.40	1.20	—
4.00	15.2	20.	2.35	1.21	—
4.00	9.91	20.	2.35	1.21	—
8.00	11.7	20.	2.35	1.22	—
8.00	11.7	18.	2.14	—	2.03
1.12	11.7	18.	2.38	1.13	—
1.12	11.4	5.5	2.38	1.14	—
1.12	11.4	5.5	2.38	—	1.99
1.12	11.7	20.2	2.38	—	1.97
1.12	11.8	20.3	2.38	—	1.94
1.12	11.9	25.	2.38	—	1.93
.49	21.7	23.	2.39	—	2.10
			Average	1.20	2.00

of mobilities included in each set of ions, but are given to show that the spreading of the positive ions was somewhat greater than that of the negative ions.

A modification of the experimental arrangement may be made by connecting the down stream portion *F* of the inner cylinder as well as the collecting ring *C* to the electrometer. The arrangement is then similar to that which I used originally[16] for mobility measurements except that at that time the ions were produced by x-rays in a narrow section transverse to the cylinders. Curve *A* in Fig. 4 represents the results of an experiment done with this modified arrangement, the ordinates representing in arbitrary units the number of ions carried past the gap *C* for different voltages on the outer cylinder.

For very small values of the voltage the ions are blown out of the apparatus except such as are caught by the wire K. As the voltage is increased the ions eventually all reach the section F of the inner cylinder and the curve remains horizontal until the voltage is sufficiently high for some of the ions to be pulled across to G. This latter number increases with increase of field until none of the ions get past C and the ordinates of curve A vanish. Curve B of the same figure was obtained with the collecting ring C alone connected to the electrometer, the ordinates being on twice the scale of those of curve A. It is seen that with increasing voltages on the outer cylinder, B begins to rise where A begins to fall, it reaches its maximum height where the slope of A is the greatest and the two reach the zero axis at approximately the same voltage. If any unique mobility is to be obtained by use of

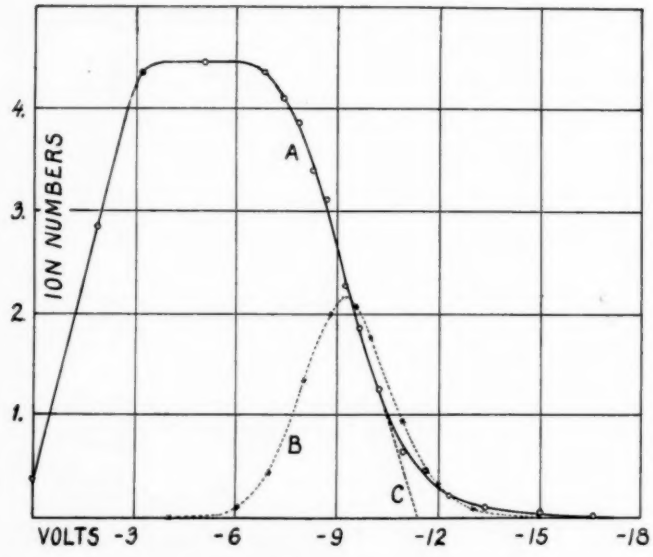

Fig. 4. Negative ion currents for different voltages. Curve B gives currents reaching collecting ring at $X=4$ cm; curve A gives currents from all ions carried down stream 4 cm or more. Air pressure = 74.45 cm of Hg. Temperature = 22.5°C. Water content of air = 5.32 mg/liter. Air stream velocity = 13.0 cm/sec.

a curve like A it should be found from a voltage corresponding to the maximum of curve B, i.e., where curve A has the greatest slope. What was actually done in the early mobility experiments,[16] in which however the ions were introduced differently as already described, was to prolong the slope of a curve similar to A, until it intersected the axis of abscissas and use the intercept voltage thus found for computing the mobility. It is now seen that the mobility so obtained was not that which here corresponds to that of the maximum slope. In the example given in Fig. 4, the mobility obtained from the voltage at the maximum slope is 20 percent higher than that got from the C intercept voltage. Owing to the different way in which the ions were initially distributed this correction may not be applied directly to the old mobility values.

Spread of Ions by Diffusion

It seemed highly important to determine as accurately as possible whether all and if not all what part of the spreading of the ions along the central electrode, shown by the experiments described above, may be explained by the diffusion and mutual repulsion of the ions in their motion between the cylinders. For this purpose it was found advantageous to change the procedure to a more laborious one in which a constant potential difference was maintained between the cylinders and the ion distribution reaching the central one was obtained by moving the collecting ring, *C*, to different distances down stream from where the ions enter the air stream.[20]

The ion distribution was first found in this way in each experiment with no air stream flowing between the electrodes. Examples of the distributions

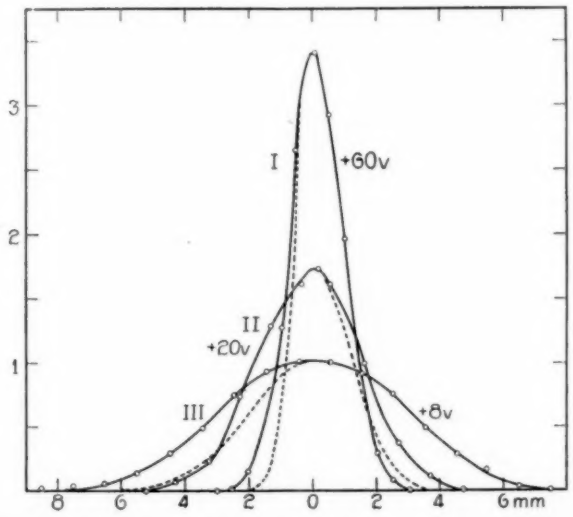

Fig. 5. Distribution of ions along central cylinder for specified positive voltages on outer cylinder when no air stream is flowing. Atmospheric pressure. Broken line curves give theoretical distributions.

of positive ions for three different voltages on the outside cylinder are shown by the full line curves in Fig. 5. Curve I should be slightly displaced to the left of the position shown. A portion of the spreading having a width of 2.9 mm is due to the dimensions of the collecting ring and of the openings through which the ions enter. The remainder arises from the combined effects of lateral diffusion and of mutual repulsion of the ions. It was thought that an appreciable part of the spreading of the ions might be due to the slowing up of the air jets which carry the ions into the space between the two cylinders, but a comparison experiment done in which no jets were used, the ions being produced by alpha-rays entering directly the openings in the outer cylinder, showed that such spreading is negligible in amount.

[20] A similar procedure was used by Erikson and by Tyndall and Grindley in some of their experiments.

It is of some importance to determine whether a considerable part of the observed spreading arises from the mutual repulsion of the ions, even though small ion densities were used with the object of minimizing this effect; since, when the ions are carried down stream in an oblique path, mutual repulsion acts to spread the ions at right angles to this path.

The amount of spreading due to diffusion of the ions alone may be computed as follows. Einstein[21] has shown that the probability of a particle being between two planes dx apart which are a normal distance x from the location of the particle at a time t seconds previously is given by

$$[1/(4\pi Dt)^{1/2}]e^{-x^2/4Dt}dx$$

where D is the coefficient of diffusion of particles of the kind in question. From this expression it may be deduced that if N_0 is the ion density in an elementary volume at any moment the ions from this volume will be so spread by diffusion after a time t that at a distance r from the initial position the ion density will be

$$N=\frac{N_0}{(4\pi Dt)^{3/2}}e^{-r^2/4Dt}. \tag{3}$$

For purposes of comparison it is only necessary to use the numerical values of the exponential term for different values of r.

Since the value of D is intimately connected with the value of the ionic mobility it seemed best to compute the coefficient of diffusion from the mobility k here obtained, by the relation

$$D=\frac{3\times 10^8 k}{1.23\times 10^{10}}. \tag{4}$$

Using for the mobility of the positive ions the value 1.22 cm/sec, the coefficient of diffusion is found to be 0.0298. This value is considerably smaller than the values given by Townsend[22] for positive ions produced by Becquerel rays, these being 0.032 for dry air and 0.036 for moist air.

To compare the values obtained by Eq. (3) with the experimental results shown in Fig. 5 it is only necessary to use for each case the time taken by the ions to cross the space between the two cylinders. It is evident that the lateral spreading of the ions is not influenced by the motion imparted to them by the electric field which is normal to this direction.

The time required for the ions to traverse the distance between the two cylinders is given by

$$t=\frac{(b^2-a^2)}{2Vk}\log_e\frac{b}{a}=\frac{6.18}{Vk} \tag{5}$$

V, being as before the potential difference between the two cylinders and k the ionic mobility. The times of passage of the ions are thus found to be 0.053

[21] A. Einstein, Ann. d. Physik **17**, 558 (1905).

[22] J. S. Townsend, Phil. Trans. **A195**, 259 (1900).

sec for the case represented by curve I, 0.25 sec for curve II, and 0.63 sec for curve III. The dotted curves, Fig. 5, show in each case the theoretical spreading of the ions as computed by Eq. (3). These dotted curves fall in each case inside of the experimental ones. It must be remembered however that to make a direct comparison possible it would be necessary to have the ions start from a region of negligible width and to have their distribution measured by an equally narrow collector. In the experimental procedure the ions originated in an area of 1 mm width and the collector gathered ions from a region almost 1 mm to either side of its middle point. Both of these considerations tend to make the experimental curves broader than the theoretical ones. If full allowance of 1.45 mm is made of half the widths of the ion streams and the collector, the experimental curve III agrees almost exactly at its lower end with the theoretical one, whereas the discrepancy now shown is more than corrected for in the other two curves. Had Townsend's value of the coefficient of diffusion been used for computing the spreading of the ions, the dotted curves would have been still farther from the axis than they now are. It will suffice to say without more detailed dis-

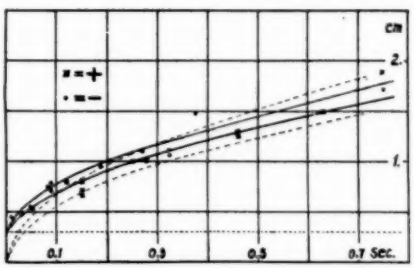

Fig. 6. Variation with time of crossing of total spread of ions in both directions, when no air stream is flowing. Atmospheric pressure.

cussion that diffusion is sufficient to account for all or nearly all of the spreading observed and that therefore mutual repulsion of the ions had at best but little effect. Even if an appreciable amount of the spreading results from mutual repulsion, the method of correction to be used will correct for it in large part.

It is of interest to note that diffusion should be taken into account in making mobility measurements by methods like the Rutherford alternating field method. If the passage of the positive ions should take 0.1 sec, then because of diffusion as computed by Eq. (3), ions of a density of one-quarter of a percent of the maximum density would be found 2.68 mm ahead of the main body of ions. For a time of passage of 0.01 sec. the corresponding distance would be 0.85 mm.

It is seen from Eqs. (4) and (5) that the product Dt of Eq. (3) will for a given voltage have the same values for both positive and negative ions, and that accordingly the ions should be equally spread out on reaching the central electrode. This was found experimentally to be the case. For the same time of passage however the negative ions spread more than do the positive ones.

The experimental values obtained for this spread taken between the extreme limits of the two limbs of each distribution curve (like A of Fig. 2) are given in Fig. 6 for both positive and negative ions, since use is to be made of these values later on. The points on the curves represent all of the values obtained even though in some of the cases the number of observations made on the distribution was not sufficient to determine the limits with much precision. The curves are projected back so that at $t=0$ the ordinate intercept has a value of 2.9 mm, the sum of the widths of the ion inlet holes and of the collecting ring. The ordinates above the horizontal dotted line thus represent the total spreading in both directions. The broken curves in Fig. 6 show the spreading in both directions as computed by Eq. (3) for limits where the ions have a density of one-quarter of a percent of the density at the maximum. For the coefficient of diffusion of the negative ions the value 0.0488 was used as computed from the mobility, 2.00 cm/sec. The upper curve is for negative ions, the lower for positive. These curves are separated by a greater distance than are the experimental curves. If Townsend's values for the coefficients of diffusion are used in Eq. (3) the separation of the two theoretical curves is reduced to about the same amount as that shown for the experimental results. If the experimental curves are lowered to allow for the widths of the ion inlet holes and the collector, the experimental curves do not show as much spreading as do the theoretical ones computed on the supposition that all of the spreading arises from diffusion. Perhaps the full allowance should not be made for the sum of the widths of the inlet holes and collector. Some of the discrepancy remains to be explained but it is quite evident that no effects of mutual repulsion of the ions are discernible.

Experiments with Constant Voltage and Variable Position of Collecting Ring

The actual measurements made with a gas stream flowing and where the distribution of the ions received by the inner cylinder was determined by moving the collecting ring, will now be considered in detail. Two examples of the results are shown in Figs. 7 and 8. In Fig. 7 the applied potential on the outer cylinder was +20 volts. Curve A gives the distribution of the ions along the inner cylinder when no gas was flowing through the apparatus. The ions here are spread over a length of approximately 10.0 mm. Curve B shows the distribution when an air stream of average velocity 6.52 cm/sec was carrying the ions down stream during their passage between the two cylinders. The peak of this curve is displaced 16.5 mm down stream from that of Curve A and the ions are now spread over approximately 17.2 mm, instead of 10.0 mm. This increase of 7.2 mm in the spreading of the ions along the inner cylinder indicates that the ions did not all take the same time in their passage and it remains to find whether this difference of mobility arises from an actual difference among the ions themselves or whether it can be accounted for by some effect which is not included in the allowance of 10.0 mm already made for the spreading of the ions when no air stream was passing through the apparatus.

Any separation of the ions by diffusion which is parallel to the axis of the cylinders does not affect the time taken for the ions to cross between the cylinders nor is this time affected by the motion of the air down stream.

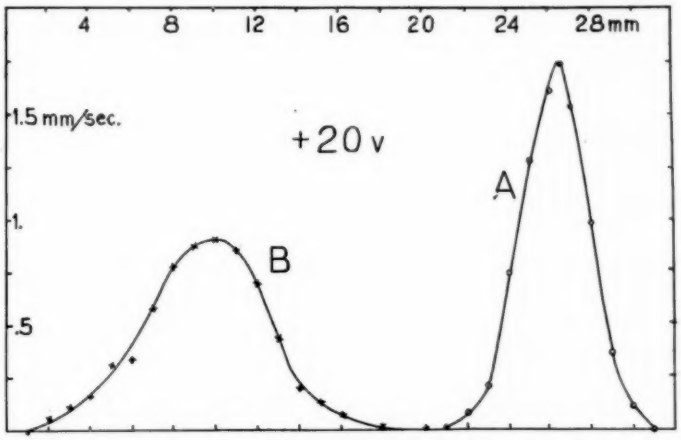

Fig. 7. Distribution of ions along central cylinder with +20 volts on outer cylinder. *A*, without air stream. *B*, with air stream velocity = 6.52 cm/sec. Air pressure = 75.2 cm of Hg. Temperature = 21.3°C. Water content of air = 1.46 mg/liter.

Were this the whole effect of diffusion the spreading along the cylinders of ions having a unique mobility would be the same with the air stream as without. Diffusion however spreads the ions in all directions, and the time of passage of those diffusing against the field is lengthened while for those

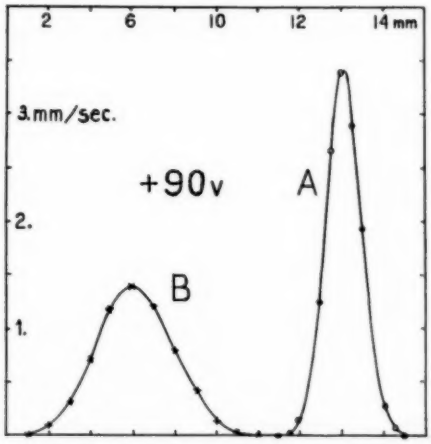

Fig. 8. Distribution of ions along central cylinder with +90 volts on outer cylinder. *A*, without air stream. *B*, with air stream = 18.95 cm/sec. Air pressure = 75.5 cm of Hg. Temperature = 22.4°C. Water content of air = 3.08 mg/liter.

diffusing with the field the time is shortened. This change in the time of passage produces no effect upon the location of the place where the ions will reach the inner electrode when no gas stream is flowing between the cylinders

but in case such a stream is flowing it will do so. It remains to show in any special case how much if any this radial diffusion will carry ions, when they arrive at the inner cylinder, beyond the limits of the axial diffusion observed when no air stream is used.

In considering the results of diffusion of ions from an extended volume of gas it suffices to find the distribution of the ions after a given time from a small element of volume, and then superimposing the distributions from all of the volume elements in question. The final distribution of the ions originating in one volume element is not affected by the presence of other ions from other elements since in diffusion the ions are supposed to have no mutual interaction but to have their wanderings governed solely by chance. In the present arrangement where the ions enter the stream through small openings, a small element of one stream may be followed in its passage and the distribution of its ions on arrival at the central electrode will represent the distribution of all of the other elements.

The ions starting from the outer cylinder in an elementary volume are spread over a larger and larger volume as they approach the inner cylinder. Owing to the radial nature of the electric field, the volume throughout which these ions are distributed as they approach the inner cylinder with increasing speed is not spherical. Its section made by a plane passing through the cylinder axis will be more or less elliptical with the minor axis parallel to the axis of the cylinders and equal in length to the spread of the ions along this axis as determined experimentally when no gas stream is flowing. Moreover owing to the variable velocity of the gas stream through which the ions pass, the major axis of the diffusion volume undergoes a tilt, the forward half of the volume being carried down stream faster than the rear half during the first part of its journey and slower than the rear half during the last part of the passage. A step by step analysis of two examples showed that this tilt which is never large compensates itself almost completely when the volume reaches the inner cylinder so that at that time its major axis is essentially normal to the axis of the cylinder.

The procedure which was followed to find how far beyond the limits of the minor axis of the diffusion ellipsoid any of those ions reached the inner cylinder which had diffused with or against the motion due to the electric field will be illustrated by considering the example represented by Curve *B* of Fig. 7. Without an air stream the ions showed a spread in either direction of one half of 10.0 mm or 5.0 mm. This spread does not all arise from diffusion since without any diffusion owing to the width of the ion stream and of the collecting ring a spread of 1.45 mm in each direction would have been indicated. The net spread due to diffusion alone is thus $5.0-1.45=3.55$ mm. If in a uniform field therefore the central ion of the diffusion volume would have moved 2.38 cm, the distance between the two cylinders of our apparatus, the most forward ion would have gone $2.38+0.355=2.735$ cm while the rearmost ion would have moved but 2.025 cm. The apparent mobilities of these ions would accordingly be respectively 1.40 cm/sec and 1.04 cm/sec, taking 1.22 cm/sec for the mobility of the central ion.

The time taken for the central ion to cross as given by Eq. (5) is 0.253 sec. The distance r from the axis that the slowest ion is situated at this instant is given by

$$t=\frac{b^2-r^2}{2Vk}\log_e\frac{b}{a}=\frac{0.528}{20\times 1.04}(13.31-r^2)=0.253\ ;\ \text{whence}\ r=1.83\ \text{cm}.$$

The ion is therefore still $1.83-1.27=0.56$ cm from the surface of the central cylinder. The elliptical section of the diffusion volume at the moment when the central ion reaches the inner cylinder would have a semi-minor axis of 0.355 cm and a semi-major axis of 0.56 cm. A part of an ellipse B with these values as axes is now constructed (see Fig. 9) with the major axis passing

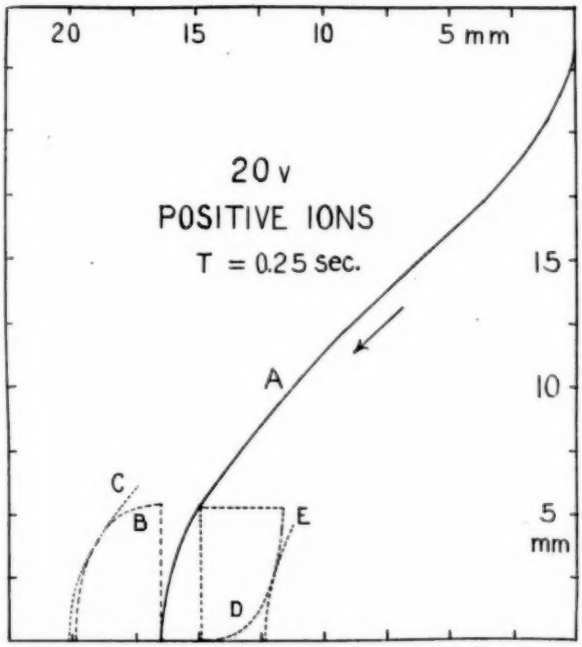

Fig. 9. Curve A shows path of positive ion taking 0.25 sec. to cross. Air stream velocity = 6.52 cm/sec. $BCDE$ illustrate method of correcting spread of ions for upward and downward diffusion. See text.

through the point where the central ion of path A reached the cylinder, in this case, 1.65 cm down stream from the point of entry of the ions into the air stream. Of all the possible ion paths starting from the place of entry the one, C, that is tangent to this ellipse B will give the farthest down stream point that can be reached by any ion in the diffusion volume. This point is obtained most easily by trial on a large scale drawing. To do this the equation of the path of an ion must first be found and this is obtained as follows: The down stream velocity of the ion due to the air current, at a distance r from the axis, is

$$\frac{dx}{dt}=\frac{p}{4\mu\log(b/a)}\left[b^2\log\frac{r}{a}+a^2\log\frac{b}{r}-r^2\log\frac{b}{a}\right]$$

and its radial velocity due to the electric field at the same place is

$$\frac{dr}{dt} = -\frac{kV}{r \log (b/a)}$$

whence the equation of the path becomes

$$x = \frac{p}{16kV\mu}\left[(b^4+r^4)\log\frac{b}{a} - 2b^2r^2\log\frac{r}{a} - 2a^2r^2\log\frac{b}{r} - (a^2-b^2)(r^2-b^2)\right]. \quad (6)$$

The value of p/μ is readily determined for any special case by the equation giving the volume of gas passing per second through the apparatus, i.e.,

$$\text{volume/sec} = \frac{\pi(b^2-a^2)p}{\mu}\left[(b^2+a^2) - \frac{b^2-a^2}{\log\ (b/a)}\right].$$

The actual value of p in the experiment was quite small being of the order of one bar per cm.

After one path curve is drawn on a large scale it becomes comparatively simple to draw from this others which are more or less elongated replicas of it.

It is seen that in this case the tangential path C reaches the cylinder at 2.01 cm which is only a trifle beyond the limits of the diffusion volume and the correction sought is here very small. When the ions are carried much farther down stream and the time of their passage between the cylinders is longer than was the case in this example the correction may assume large values and experimental errors make its exact determination difficult. The correction is doubtless overestimated by this method because as the diffusion volume becomes elliptical fewer ions diffuse to the extreme end of the major axis of this volume than reach the ends of the minor axis.

The up-stream limit on the central cylinder that may be reached by ions which have diffused in the direction of the electric field may be obtained in a manner quite similar to that used above for determining the down stream limit. Thus in the above example the foremost ions of the diffusion volume take 0.22 sec. to traverse the distance between the two cylinders, and at that instant the central ions of the volume are found to be still 0.54 cm from the inner cylinder and the minor axis of the diffusion volume is 0.32 cm, as given by the curve for positive ions in Fig. 6. We next construct the quadrant of the ellipse, D, Fig. 9 and find the ion path which will be tangent to this ellipse. This path reaches the cylinder at 1.22 cm. The limits thus found between which ions all having one mobility should arrive at the central cylinder for the case under consideration are 2.01 cm and 1.22 cm down stream from the ion inlet openings. Owing to the widths of the collecting ring and of the ion inlet openings these limits should be extended in each direction by 0.145 cm, giving 2.15 cm and 1.08 cm as the extreme limits. These distances are to be compared with the observed distances in Fig. 7 between the limbs of curve B and the center of the undisplaced curve A, which are 2.55 cm and 0.83 cm. The observed spreading of the ions is thus seen to be 0.65 cm greater than is accounted for by diffusion on the supposi-

tion of a unique mobility. Assuming that the remnant spread arises from the presence of ions of different mobilities, the values of these mobilities at the two extreme limits are 1.44 cm/ sec. and 0.985 cm/sec., the larger being 46 percent greater than the smaller. A similar analysis of the results shown in Fig. 8 gives for the peak mobility 1.30 cm/sec. and for the two extreme values 1.72 cm/sec. and 1.07 cm/sec., the water content of the air being in this case twice as large as in the preceding one.

A simple consideration shows that the peak of each distribution curve represents very closely the place reached by the central ion of the diffusion volume.

TABLE II. *Results for positive ions.*

1	2	3	4	5	6	7	8	9	10	11	12
Volts on A	Air velocity cm/sec	Water content mg/liter	Crossing time sec	Largest X cm	Largest X corrected	Peak X cm	Smallest X cm	Smallest X corrected	Peak mobility cm/sec	Lowest mobility	Highest mobility
30.15	18.95	3.63	0.16	—	—	2.84	—	—	1.32	—	—
30.1	18.95	—	.16	4.22	3.82	2.94	1.72	2.23	1.29	.98	1.68
15.0	18.95	3.63	.32	7.75	6.82	5.65	3.81	4.68	1.34	1.10	1.60
90.0	18.95	3.08	.05	1.49	1.22	1.00	0.48	0.76	1.27	1.05	1.69
7.0	11.42	4.00	.75	—	—	7.18	—	—	1.27	—	—
9.0	11.11	3.22	.54	7.84	6.29	5.64	3.34	4.50	1.30	1.17	1.61
40.0	12.74	1.65	.13	2.32	1.96	1.57	.90	1.29	1.23	.99	1.49
20.0	6.52	1.46	.27	2.55	2.06	1.65	.83	1.37	1.18	.95	1.42
10.0	3.40	1.99	.58	2.72	1.86	1.85	1.07	1.86	1.09	1.09	1.09
30.0	10.14	1.87	.17	2.52	2.12	1.63	.97	1.40	1.24	.96	1.45
10.0	10.14	1.87	.51	7.05	5.75	4.92	2.77	4.00	1.21	1.04	1.50
8.0	3.40	2.37	.67	3.65	2.69	2.18	1.10	2.06	1.15	.95	1.25
							Averages		1.24	1.03	1.48

TABLE III. *Results for negative ions.*

1	2	3	4	5	6	7	8	9	10	11	12
Volts on A	Air velocity cm/sec	Water content mg/liter	Crossing time sec	Largest X cm	Largest X corrected	Peak X cm	Smallest X cm	Smallest X corrected	Peak mobility cm/sec	Lowest mobility	Highest mobility
30.1	18.95	3.63	0.10	—	—	1.79	—	—	2.12	—	—
30.1	18.95	4.42	.10	—	—	1.93	—	—	1.96	—	—
30.	18.95	—	.10	2.55	2.19	1.94	1.20	1.60	1.97	1.74	2.40
30.	18.95	2.94	.10	2.65	2.29	1.93	1.25	1.65	2.03	1.67	2.33
15.	18.95	3.63	.20	5.15	4.61	3.70	2.55	3.16	2.05	1.63	2.38
9.	11.11	3.22	.34	5.00	4.09	3.62	2.54	3.43	2.04	1.80	2.15
90.	18.95	3.53	.03	1.01	0.78	0.62	0.31	0.56	2.04	1.60	2.25
10.	3.40	1.50	.34	1.83	1.27	1.13	0.53	1.15	1.79	1.58	1.75
30.	10.14	1.50	.10	1.54	1.17	0.97	0.56	0.94	2.10	1.73	2.16
10.	10.14	1.50	.30	4.22	3.52	2.90	1.82	2.56	2.07	1.71	2.35
10.	3.40	7.63	.33	1.74	1.19	1.09	.44	1.07	1.86	1.71	1.90
8.	3.40	2.19	.40	2.29	1.55	1.32	.49	1.22	1.94	1.65	2.10
							Averages		2.00	1.68	2.18

In order to test the method and find the best working conditions, determinations were made with largely different values of the quantities involved. The voltage applied to the cylinder *A* was varied in the ratio of 1 to 13, the time taken for the ions to cross being thus varied over the same range. The velocity of the air stream was varied in a ratio of about 1 to 6. The distances that the ions were carried down stream in crossing between the cylinders were altered in the ratio of about 1 to 7. The ion density was varied several fold. Some of the extreme conditions used were not suitable for high accuracy. Nevertheless the results are all recorded in Tables II and III.

In both tables, column 7 gives the displaced distances of the peaks of the distribution curves and column 10 gives the mobilities computed from these distances, reduced to a pressure of 76 cm of mercury and a temperature of 20°C after correction has been made for the effect of the ion inlet jets discussed in a previous section. In column 6 are given the values of the farthest distance ions were carried down stream after the values of column 5 were corrected for diffusion, etc. as explained on the preceding pages. Column 9 gives similarly corrected values of the shortest distance ions were carried down stream. Columns 11 and 12 give values of mobilities corresponding respectively to the distances in columns 6 and 9, after being reduced and corrected as were those of column 10. The values of the mobilities which correspond to the peaks of the ion-distribution curves are not strictly comparable among themselves owing to the variations in the water content of the air, although these variations did not cover a large range. Those mobilities given in column 10 of Tables II and III for which the water content of the air was determined, are plotted as ordinates in Fig. 10 as disks against the water content of the air as abscissas. Similar values taken from Table I are plotted with crosses.

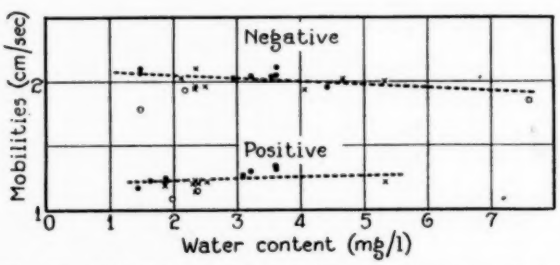

Fig. 10. Mobilities plotted against water content of air.

It must be remembered as was stated above that these results include some observations which were taken to test out the method under extreme experimental conditions where high accuracy was not attainable. Especially noticeable is the somewhat erratic position of the points marked by triangles which represent results obtained with a stream velocity of only 3.4 cm/sec., the lowest that was used. These differ greatly among themselves also as regards the limits of spread of the ions. One of the results for negative ions for a water content of 1.5 mg/liter is so low that some unusual error is suspected. [Added in proof. This has been traced to reading 191 on a scale as 189.] There is some question whether these readings should be considered of equal value with the others. Their omission certainly removes the most discordant of the results.

Most of the values are crowded into so small a range of water content of the air that a very accurate curve of relation cannot be drawn. The negative mobilities show a decrease with increase of water content of the air, the rate being somewhat less than that given by Tyndall and Grindley.[23] The mobili-

[23] A. M. Tyndall and G. C. Grindley, Roy. Soc. Proc. **A110**, 341 (1926).

ties of the positive ions, appear on the whole to increase with increase of water content of the air. The average of the mobilities of the positive ions given in column 10 of Table 2 is 1.24 cm/sec. · volt/cmf or an average water content of 2.7 mg per liter of air. For the negative ions the average of the values given in column 10 of Table III is 2.00 cm/sec. · volt/cm for an average water content of 3.2 mg per liter of air. The results are reduced to a pressure of 76 cm of mercury and a temperature of 20°C. The value for the negative ions is identical with that found by the stationary collecting ring method as given in Table I. The value for the positive ions is here three percent larger.

The determinations of the limits of spread of the ions are necessarily subject to much more error than the location of the peaks of the distribution curves. The limits were taken at points where the ordinates of the curves were about one-quarter of a percent of the maximum ordinate. In a few of the earlier measurements these limits of spread were not determined, as shown by blanks in the Tables. The distance between the limits given in columns 6 and 9 is the spread of the ions along the inner cylinder which is left unaccounted for, after the corrections have been applied for diffusion and for the other causes which have been considered, on the supposition of a unique mobility for all of the ions of each sign. Assuming that this remnant spread of the ions is indicative of the presence of ions of different mobilities, the limiting values of these mobilities have been computed and are given in columns 11 and 12 of the Tables. For the positive ions the mobilities at the upper limit are on the average 45 percent larger than those of the lower limit while for the negative ions they are 30 percent larger. Within the rather large experimental errors of these quantities, there appears to be no systematic change of the relative values of the limiting mobilities with the time of crossing of the ions nor with the water content of the air over the ranges used. It should be pointed out, because the fact may have some significance, that for the positive ions the "peak" mobility is very closely midway between the values of the extreme limits whereas for the negative ions the "peak" value is markedly closer to the higher limit. Laporte's curves for the negative ions in moist air show rather the opposite of this.

Discussion

The only previous results on distribution of mobilities that can be compared directly with those obtained here are those of Laporte,[12] who did not use a blast method. The total spread of mobilities in air as shown by his curves is approximately the same as that given by my curves. Moreover he also finds the spread of the positive ions greater than that of the negative ions. He does not give numerical values for the relative values of the maximum and minimum mobilities but as he estimates the effect of diffusion in his experiments to be much less than that found by me, his ratios should be larger than those given above.

Other observers, who have employed blast methods for measuring mobilities, have used such large stream velocities that owing to the turbulence of the motion it was not possible to ascribe the observed spreading of the

ions definitely to the presence of ions of different mobilities. Nearly all such observers have however remarked upon the breadth of the positive ion distribution curves being greater than that of the negative. There was a question in those cases whether the greater breadth of the positive ion curves did not arise either from the turbulence of the gas stream since these ions for the same field take longer to cross or from the fact that the positive ions are carried down stream farther than are the negative ions. Erikson[24] avoided this dilemma by using different fields for the two ions so that the time taken to cross was the same for both ions. Using old ions, he still finds the spread of the positive ion curve very much greater than that of the negative. Mahoney[15] also used this procedure but he states that the feet of the positive ion curves he obtained are only a little wider than those of the negative curves. However, in his figures, the central portions of the positive ion curves appear much broader than do those of the negative curves. Briggs,[13] as stated, estimates that the mobilities of the recoil atoms of radioactive substances are distributed continuously over a range of values, of which the largest are 50 percent greater than the smallest.

The evidence seems therefore fairly conclusive that the ions under consideration, whether positive or negative, do not all have the same average mobility; it is overwhelmingly so for the positive ions. Two different explanations present themselves to account for the distribution of mobilities which has been found. We may suppose that among aged ions there is present a number of more or less permanent groups of ions which differ in mobility by such small amounts that they have not been resolved by the methods used. Or, what seems more plausible, we may think of the ions as molecular clusters whose size is undergoing changes owing to the continuous bombardment of the molecules of the circumambient gas. The changes in size of the clusters must be considered as taking place at sufficiently long intervals so that in the time of crossing the number of changes is not very great. Busse[25] supposes water molecules alone cluster about the original ion and Laporte[12] postulates further that after the original ion has become surrounded by one layer of water molecules it is possible for molecules of the surrounding gas to become attached also. These hypotheses were both based on the supposed finding by Busse of what he thought were monomolecular ions having a mobility of 14–15 cm/sec. Busse[26] has since withdrawn this result, because the more extensive and more refined experiments of Schilling[14] failed to detect ions of such high mobility. It is therefore not necessary to consider water molecules as essential for cluster building, although other experiments indicate that such molecules occupy a preferential position.

Erikson[7,24] has presented the attractively simple and strongly supported hypothesis that the negative ions and the "initial" positive ions are monomolecular whereas the "final" positive ions consist of two molecules. Recent work has however greatly weakened the full force of the arguments adduced for this view.

[24] H. A. Erikson, Phys. Rev. **33**, 403 (1929).
[25] W. Busse, Ann. d. Physik **81**, 587 (1926).
[26] W. Busse Ann. d. Physik **84**, 327 (1927).

The first argument given by Erikson is that since the ions must initially have been monomolecular we should be able to detect the transition stages if clusters are formed. That this need not be the case is shown by the work of Mahoney[15] who found that in dry air, cleared of condensable vapors by liquid air traps, the final positive ion was fully formed 0.0014 sec. after its creation. This time is too short for the detection of any intermediate stage or stages and hence also a negative cluster may be formed too quickly for the detection of any stage earlier than the final one.

Erikson's most powerful argument for his hypothesis centers about the two distinct peaks obtained during the transition period of the positive ion, and he argues that if several molecules were involved intermediate stages should appear between the initial and final ions. The time involved in this transition period runs into hundredths of seconds whereas Mahoney found the time required for the full formation of the final positive ion in dry air to be less than 0.0014 sec.; it may have been much less. The comparatively long period discovered by Erikson that the "initial" ion takes to transform into the final form may therefore measure something quite different from the time required for the occurrence of a propitious encounter during which a charged molecule may attach itself to a neutral one. According to Valasek[27] and Tyndall and Grindley[9] increase of humidity of the air increases the transformation period of the positive ions, and Mahoney only found this period sufficiently long for measurement in the presence of water vapor. Molecules of water or molecules of some other impurity,[28] are therefore in some way involved in retarding the formation of the final positive ion, and this must arise from a change produced in the nature of the ion first formed by the ionizing process. The ion thus transformed must later undergo another drastic change in some comparatively rare encounter which makes possible the formation of the final ion cluster. This view is essentially the same as that held by Tyndall, Grindley and Sheppard.[26]

The experimental evidence presented in this communication shows that the final ions in moist air, both positive and negative, consist in each case of a group of which the members do not all have the same mobility. As the "initial" positive ions have the same mobility as the negative ions, they too must consist of a group whose individuals are not all alike.

Since Erikson[24] also found the distribution curve for the final positive ions to be much broader than a similar curve for negative ions under a like displacement, he too is forced to assume that the final positive ion is a changing aggregation, varying according to his view between one, two and three molecules.

The changes produced in the mobility especially of the negative ions in air by the addition of small amounts of impurities seem much too large to be accounted for by supposing them due to a diminution of the free paths of the ions caused by the polarization of the molecules of the impurity being greater than that of the molecules of the gas itself. It is therefore natural to

[27] Leila M. Valasek, Phys. Rev. **29**, 542 (1927).

[28] A. M. Tyndall, G. C. Grindley and P. A. Sheppard, Roy. Soc. Proc. **A 121**, 185 (1928).

suppose that the impurity produces the observed changes because it becomes more readily attached to an ion than do the main constituent molecules of the gas.

The method used in these experiments has proved itself well adapted for measuring the absolute values of the mobilities corresponding to the peaks of the distribution curves. Steady motion of the gas stream is realized, the quantities involved can all be obtained accurately, and the effects of diffusion, mutual repulsion of the ions, and effects of space charge can be eliminated. Some improvement on the accuracy of the results reported could be obtained by using only the most favorable values of the quantities measured.

It should be noted that some observers using high fields reduce their results directly by proportion to values for lower fields whereas theory shows that for such high fields the velocities of the ions are not proportional to the fields.

The value of 1.22 cm/sec. obtained for the mobility of the positive ions is considerably smaller than that usually given. The reason for this may be the fact that the positive ions decrease in mobility with age and the ions I used were all over two seconds old. The value given is only a little below 1.24 cm/sec., the value recently obtained by Tyndall, Starr and Powell[29] by a relative method for positive ions 0.25 sec. old.

It is proposed to make measurments with the apparatus described in very dry air and under other conditions. Ions may be produced directly in the main gas stream by allowing alpha-rays to enter for a short distance through the ion inlet openings *H*. Some preliminary measurements already done in this way where the time taken for the ions to cross the space between the cylinders was 0.01 sec., gave almost but not quite identical single peaked distribution curves for both positive and negative ions.

I am greatly indebted to my assistant Mr. R. S. Baldwin for efficient help with the experiments over long hours. Mr. H. Margenau kindly made for me the transformation involved in Eq. (3).

[29] A. M. Tyndall, L. R. Starr and C. F. Powell, Roy. Soc. Proc. **A121**, 172 (1928).

A THEORY OF THE PERMANENT MAGNETIC FIELDS OF THE SUN AND EARTH*

By Ross Gunn
Naval Research Laboratory, Washington D. C.

(Received June 4, 1929)

Abstract

The motion of ions, executing short free paths under the influence of thermal agitation in an inhomogeneous magnetic field, in crossed magnetic and gravitational fields or in crossed magnetic and electric fields are shown to produce drift currents. The ion drifts are found to be opposite in direction to the drifts produced in the analogous cases of long free path. Under the condition of radial symmetry and a closed circuit the magnetic gradient gives rise to circular currents which flow in such a direction that magnetic regeneration takes place. Regeneration is limited by demagnetizing currents arising from the thermal motions of the ions interacting with the resultant magnetic field and an internal electric or gravitational field. The magnetic moments of the sun and earth are calculated from data which are approximately known and the correct magnitudes obtained. The permanent fields arise from the thermal energy of the body and would be maintained if the bodies ceased their rotation. The asymmetry of the earth's magnetic field indicates that the hemisphere embraced by the Pacific Ocean is at a higher mean internal temperature than the rest of the earth.

ONE of the unsolved problems of cosmical physics has been the problem relating to the origin and maintenance of the permanent magnetic fields of the sun and the earth. Many theories[1,2] of the field have been proposed, most of which depend in some manner on the rotation of the body. It is generally accepted that those theories which have been definitely formulated lead to values for the magnetic moments which are far too small to account satisfactorily for the observed facts. It is the purpose of the present paper to outline briefly certain electromagnetic effects which are of such a magnitude as to be able to account for the observed magnetic moments of the earth and sun. The present theory attributes the magnetic field to electrical currents set up in the high temperature regions of the sun and earth as a result of the thermal motion of the ions interacting with a self produced magnetic field and an inhomogeneity of the magnetic field *or* an electric field produced by any one of several phenomena. Analysis of the motions of ions and electrons spiralling about an inhomogeneous impressed magnetic field shows that two important effects are produced,[3,4,5,6] (1), a diamagnetic

* Released for publication by the Navy Department.
* Presented at meeting American Geophysical Union, April 25, 1929.
[1] Dictionary of Physics, Glazebrook, Vol. II.
[2] Handbuch der Physik, Vol. 15.
[3] Schroedinger, Wien, Ber. **66,** 1305 (1912) also Bulletin 16 of Nat'l. Res. Council.
[4] R. Gunn, Phys. Rev. **32,** 133 (1928)
[5] R. Gunn, Phys. Rev. **33,** 614 (1929).
[6] R. Gunn, Phys. Rev. **33,** 832 (1929).

effect dependent on the magnitude of field; (2), a drift velocity dependent on the gradient of the field which gives rise to a steady current under suitable conditions. Expressions have been derived[6] for the current density resulting from the drift velocity imposed on the ions due to thermal agitation and an inhomogeneous magnetic field. The resulting currents that flow in a highly ionized region when the free paths are long have been shown to account for the magnetic fields of sun-spots[7] and to account for a portion of the general solar magnetic field.[6] The extension of the calculations to the case where the free paths of the ions are short leads immediately to a consideration of the currents and resulting magnetic fields which are produced in the interior of the sun and earth.

In the earlier work an expression was given, without formal proof, for the drift current due to an impressed magnetic gradient when the ion free paths were short. It now seems of sufficient interest to carry through the

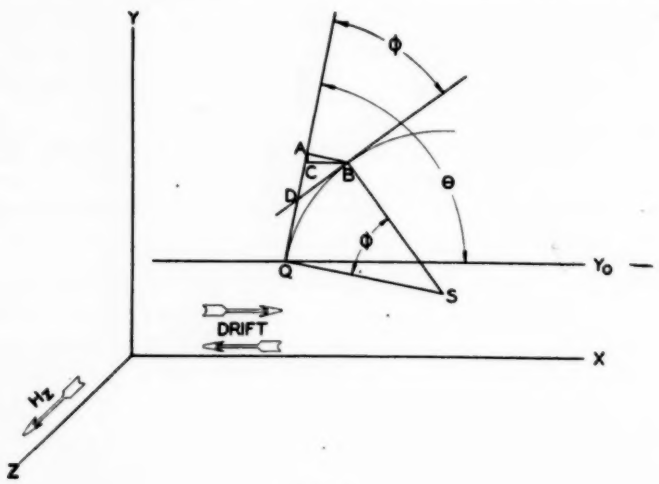

Fig. 1.

calculation somewhat more carefully and take into account the effect of small electric or gravitational fields which may be present. Consider an ionized region having a magnetic field impressed in the positive Z direction and having a uniform magnetic gradient dH_z/dy, a uniform electric gradient E_y, or a uniform gravitational field g_y. An ion after collision at Q (Fig. 1), begins a free path at random, making initially an angle θ with the x axis. In the presence of the magnetic field the ion traces out a portion of a circle in the xy plane and terminates its free path at a point B. The radius of the circle R traced by the ion is given by

$$R=mV/He \tag{1}$$

where m is the mass of the ion, V its velocity, e its charge and H the impressed magnetic field. All quantities are expressed in c.g.s. electromagnetic units.

[7] R. Gunn, Astrophys. J. May (1929).

The departure δ of the ion path from its normal straight line under no magnetic field is given by (AB) or $\delta \doteq \lambda/2 \sin \phi$; where λ is the length of the free path (QB) and ϕ is the angle swept off by the ion between collisions or $\phi = \lambda/R$ so that $\delta = \lambda/2 \sin \lambda/R$. The component δ_x of the departure δ in the x direction represented in the figure by $\overline{BC}$, is the departure effective in producing drift currents and

$$\delta_x = \lambda/2 \sin \lambda/R \sin \theta. \tag{2}$$

Since the magnetic field is non-uniform and an electric or gravitational field is present the instantaneous value of R is a continuous function of y. The path of an ion is approximately a true circle whose radius is determined by the average velocity and the average value of the magnetic and electric field impressed on the ion as it executes a free path. It will be convenient to discuss for the present the velocity of the ion and its impressed magnetic field rather than the electric and magnetic fields. Moreover, we shall assume (correctly) that the change in scalar velocity of an ion between any two collisions is small compared to the thermal velocity of agitation. Let the mean thermal velocity of the ions and their impressed magnetic field at $y = y_0$ be V_0 and H_0 respectively, then the mean value of $1/R$ for a given ion describing a free path λ which originated on y_0 is

$$\frac{1}{R} = \frac{e}{m}\left[\frac{H_0}{V_0} + \frac{\lambda}{2} \sin\theta \frac{d(H_z/V)}{dy}\right] \tag{3}$$

so that the departure in the x direction is

$$\delta_x = \frac{\lambda}{2} \sin\theta \sin\left[\frac{\lambda e}{m}\left(\frac{H_0}{V_0} + \frac{\lambda}{2} \sin\theta \frac{d(H_z/V)}{dy}\right)\right]. \tag{4}$$

In the present discussion we shall confine our attention to the case of short free paths so that $\lambda << R$. If we expand (4) and neglect product terms containing the sines of small angles and set the cosines of the same small angles equal to unity, then (4) becomes

$$\delta_x = \frac{\lambda}{2} \sin\theta \sin\left[\frac{\lambda^2 e}{2m} \sin\theta \frac{d(H_z/V)}{dy}\right]. \tag{5}$$

Expanding again and neglecting second order terms

$$\delta_x = \frac{\lambda^2 e}{4m} \sin^2\theta \frac{d(H_z/V)}{dy} \tag{6}$$

In order to obtain V_x the mean value of the departure per unit time for a typical ion with random distribution in θ we have only to multiply (6) by the number of collisions per second and average the values with respect to θ; thus (6) becomes

$$V_x = \frac{\lambda^2 eV}{8m} \frac{d(H_z/V)}{dy} = \frac{\lambda^2 e}{8m}\left[\frac{dH_z}{dy} - \frac{H_z}{V}\frac{dV}{dy}\right] \tag{7}$$

and the current density $i_x = Ne\,V_x$ is given by

$$i_x = \frac{Ne^2\lambda^2}{8m}\left[\frac{dH_z}{dy} - \frac{H_z}{V}\frac{dV}{dy}\right] \tag{8}$$

where dH_z/dy is the impressed magnetic gradient, N is the number of ions partaking of the thermal motion, e their charge, λ their mean free path and V the scalar velocity of the ion in the xy plane. The second term in equation (8) involving the velocity V is restricted to a *continuous* velocity change; that is, the velocity must change *during* the free path since otherwise the ion drift vanishes.

Inside the sun or earth apparently the only factors which could give rise to a continuous change of velocity along a radial axis are electric and magnetic fields and gravity. In these regions the electric and gravitational forces are small and the thermal velocities are large compared to any change of velocity produced between collisions by the impressed electric or gravitational fields. Remembering that the mobile ion is the electron, Eq. (8) may be transformed to

$$i_x = \frac{Ne^2\lambda^2}{8m}\left[\frac{dH_z}{dy} - \frac{H_z m g_y}{kT} - \frac{eH_z E_y}{kT}\right] \tag{9}$$

where E_y is an impressed electric field, k the Boltzmann constant, T the absolute temperature and g_y by gravitational acceleration. It will be noted that the sign of each term in this equation is opposite to that resulting when the ion paths are long or when it is tacitly assumed that, on the average, an ion executing a short free path starts from rest. The bearing of the present derivation on the anomalous Hall effect, and on drift currents arising from an inhomogeneous magnetic field will be discussed in a future paper. Application of these effects to an explanation of the sun's and earth's magnetic field shows that the first term contributes in such a manner as to magnetize the bodies, the second term tends to demagnetize the bodies and the last term may magnetize or demagnetize according to the direction of the impressed electric field. It will be convenient to treat each of these effects separately and estimate their relative importance in the production of the observed magnetic fields.

Considering first the electric currents arising from direct gravitational action we find that these currents flow in such a direction that they demagnetize the earth. A calculation of the value of the second term of Eq. (9) in the brackets using $H_z = 0.5$ gauss, $m = 10^{-27}$ grams, $g = 10^3$ cm/sec^2, $k = 1.37 \times 10^{-16}$ and $T = 10^4$ degrees, yields a value of 2×10^{-11} gauss/cm which is small compared to the other quantities inside the bracket. We may then conclude that the direct gravitational action on the ion is unimportant and in the following we shall confine our attention to the two more important effects which are due (1) to a magnetic gradient and (2) an electric field.

All the phenomena which have been mentioned depend on the presence of a magnetic field and we must account in some manner for an initial field

which was in the correct direction relative to the direction of rotation of the sun and earth to regenerate and produce the observed fields. Several possibilities present themselves, but perhaps the most reasonable arises from the considerations of Pannekoek,[8] who has considered the gravitational separation of the positive ions and electrons in the sun and calculated the mean volume charge density. A similar calculation shows that the earth, at the time of its formation, possessed a positive charge of 10^{-5} coulombs with an appropriate electron atmosphere which rendered the whole electrically neutral. This separation of charge combined with the rotation of the earth provided a very small magnetic field which was in the correct direction to grow and form our present field.

We shall consider the currents produced inside the sun or earth as a result of thermal motion of the ions and their interaction with an impressed non-uniform magnetic field. Let us suppose for simplicity that when the earth was whirled off the sun by tidal or other forces that its rotation and static charge produced a non-uniform, but radially symmetrical magnetic field that was directed from north to south and parallel to the axis of rotation at all points inside the earth, the field being greater at the center than at the surface. By choosing the direction of the magnetic flux as the positive z axis, applying the first term of Eq. (9) and remembering that everything is symmetrical about the axis of rotation, it is found that a circular current is produced which *increases* the total magnetic flux enclosed by the current. This increase in magnetic flux increases the gradient which in turn increases the current. Thus such a radially symmetrical system is regenerative and can build up large magnetic fields from insignificant beginnings. In order to examine under what condition this type of regenerative action can give rise to steady currents, consider a line integral around a rectangular circuit which lies in a plane perpendicular to the current. Neglecting the contribution of the ends of the rectangle to the integral, we have approximately

$$i_z = \frac{1}{4\pi}\left(\frac{dH_z}{dy}\right)_1 \tag{10}$$

where $(dH_z/dy)_1$ is the magnetic gradient produced by the current i_z as a result of the impressed gradient. If we neglect temporarily the effects of electric and gravitational fields a comparison of Eqs. (10) and (9) shows that to a rough approximation

$$1/4\pi = Ne^2\lambda^2/8m \tag{11}$$

This relation serves to specify the magnitudes of the quantities necessary to produce a current under the assumed conditions. By assuming that the charged particle effective in producing the drift current is the electron, and assuming the number of electrons partaking of thermal agitation at high temperature is equal to the number of free electrons in the region or 10^{23} ions/cm^3 then the substitution of $m = 10^{-27}$ gms, $e = 1.59 \times 10^{-20}$ e.m.u. in

[8] Pannekoek, Bull. Astr. Inst. Netherlands, No. 19 (1922).

Eq. (11) shows that λ the free path of the electron must approximate 3×10^{-6} cm. The requirements are less stringent if the variable permeability of the medium is taken into account, but this factor will redistribute the resulting magnetic field in an unknown manner and will not be considered. Calculations made by Eddington[9] indicate that in the center of Capella the electrons of most atoms are stripped off and mean free path of the ion or electron increases to well over 10^{-2} cm. We cannot estimate exactly at the present time how far the stripping of the atoms progresses, but there is considerable evidence supporting the view that the free paths of the ions within the sun are much longer than 10^{-6} cm, and that the electron density is greater than 10^{23}. Moreover, it is known that the internal temperature of the earth is 10,000° or more, so the assumption of a free path length of 10^{-6} cm in that region also seems warranted.

It seems probable that electric currents rising from the inhomogeneity of the self produced magnetic field are the currents important in the production of the magnetic fields associated with the sun and earth. However, if a theory of the growth of the magnetic field similar to the foregoing is to be accepted, the resulting currents in the steady state must be great enough to account for the observed magnetic moment. A calculation of the magnetic moment is readily made if the effective magnetic gradient and free path length for the ions are known at all points within the earth or sun. Actually such information is lacking and on the earth we must content ourselves by assuming values for the free paths consistent with Eq. (11) and assuming that the average gradient effective in producing currents is nearly the same or slightly larger than that observed at the surface of the earth; namely, 1.6×10^{-9} gauss/cm. The cross sectional area of the solar and terrestrial current sheet is roughly $\pi R^2/2$ where R is the radius of the earth or sun and the mean area of the current circuit is $\pi R^2/4$ so that the total magnetic moment M is given roughly by

$$M=\frac{\pi^2R^4}{8}\cdot i_\theta \tag{12}$$

where i_θ is the mean westward current density. By aid of Eq. (10) this becomes

$$M=\frac{\pi^2Ne^2\lambda^2R^4}{64m}\frac{dH}{dr}. \tag{13}$$

If we assume that the carrier effective in producing the current is the electron and take $N=10^{23}$, $e=1.57\times10^{-20}$ e.m.u., $\lambda=3\times10^{-6}$ cm, $R=6.4\times10^{8}$ cm, $m=10^{-27}$ gms and $dB/dr=1.6\times10^{-9}$, we find that the magnetic moment of the earth is 12×10^{24}. This value is taken to be in agreement with the observed values of 8.24×10^{24}, since as we shall show later, demagnetizing currents may exist which are of the same order of magnitude as the magnetizing currents. It seems probable that the average values taken for dH/dr and R

[9] Eddington, The Internal Constitution of the Stars, p. 222 (1926).

as well as the free path λ will require revision. The regions where the currents become large cannot as yet be specified exactly but it seems reasonable to expect moderate currents to appear when the temperature of the ionized region approaches a few thousand degrees. Geophysicists believe that inside the earth a temperature of 2,500° is attained at 300 km below the surface and we are therefore probably not far in error when we assume that currents circulate through the total volume of the earth.

A calculation of the magnetic moment of the sun cannot be made directly since no data are available regarding the mean gradient. A lower limit to the magnetic moment may be set, however, since the simplest consideration indicates that in the high temperature regions of the sun, the free path and mean gradient will be larger than on the earth. If we assume that the gradients and free paths are the same, then the solar magnetic moment will be larger than that of the earth by the fourth power of the ratio of the diameters. On this basis the minimum possible value of the solar magnetic moment is 5.0×10^{33}. Direct spectroscopic evidence indicates that the moment is roughly 8.6×10^{33}, while the following extrapolation of diamagnetic data into regions well below the photosphere indicates that the solar magnetic moment is several hundred times the smallest allowable value given above. It has been shown[5] that at a certain critical ion density, an ion gas is no longer strongly diamagnetic and as we penetrate deeper and deeper into the sun's atmosphere we find a critical pressure which is such that the outward radial magnetic gradient drops to moderate and normal values. It has also been shown[5] that the outward radial magnetic gradient of the sun could be explained if we assumed that the effective permeability of the diamagnetic medium was nearly zero. This assumption which was shown to agree moderately well with observational data provided a further relation between the magnetic field and the ion density. Moreover, the discussion indicated that the limitation of the solar magnetic field was to be attributed to the high temperature and ionization of the solar atmosphere and not to a special peculiarity of the manner by which the field was produced. We would then expect the solar and terrestrial magnetic fields to arise from the same causes as indicated by the present work. The critical ion density which we have discussed is given by

$$N_{critical}=\frac{4eB}{\pi\sigma^2(2mkT)^{1/2}} \tag{14}$$

where e is the ion charge in e.m.u., B the magnetic field strength, σ the kinetic theory diameter of the ions, m the mass of an electron, k the Boltzmann constant and T the absolute temperature. When the free paths are long, the ion density N is related to the field by

$$N\doteq B^2/4\pi kT. \tag{15}$$

If we restrict ourselves to the critical value of B we may equate (4) and (5) which yields

$$B_{critical}=\frac{16e}{\sigma^2}\left(\frac{kT}{2m}\right)^{1/2} \tag{16}$$

taking $e=1.57\times10^{-20}$; $k=1.37\times10^{-16}$; $T=6{,}000°$; $\sigma=2\times10^{-8}$ cm and $m=10^{-27}$ gm B critical approximates 12,000 gauss. This value of the field is found some distance below the photosphere where the ion pressure is nearly one half an atmosphere. If we calculate the magnetic moment of the sun using the above figures for the equatorial field the magnetic moment turns out to be 4×10^{36} a value nearly 800 times the smallest allowable value which indicates reasonably enough, that the mean magnetic gradient and ion free paths are much larger in the sun than in the earth.

In the foregoing theory no mechanism has been provided to limit the magnetic fields or gradients and the field would be expected to build up to much larger values by regenerative action than are actually observed. In a search for a means to control the final magnetic field we are led to a consideration of effects which could demagnetize the body. We have seen in the development of Eq. (9) that currents can be produced by an electric field of the proper sign which are opposite in direction to the currents produced by magnetic gradients. Several effects within the sun and earth could give rise to radial electric fields which upon interacting with an impressed magnetic field and thermal agitation will produce drift currents. Among those that seem important we may mention temperature gradients, difference in ion concentration due to temperature ionization or non-uniform distribution of radioactive material and gravitational separation of charge such as considered by Pannekoek.[8]

The electric field arising from a temperature gradient assuming that the mobile ion is the electron, is given on classical theory by

$$E_y=\frac{k}{2e}\frac{dT}{dy} \tag{17}$$

where dT/dy is the temperature gradient, k the Boltzmann constant, e the ion charge and E_y the resulting electric field. Similarly the electric field arising from a difference in ion concentration C is given by

$$E_y=\frac{kT}{eC}\frac{dC}{dy} \tag{18}$$

and the electric field arising from the gravitational separation of charge[8] is

$$E_y=(\mu/e)g_y \tag{19}$$

where μ is the average molecular mass and g_y the gravitational acceleration.

Leaving out of consideration ion concentrations due to radioactive material, which may be important, it is possible to calculate the electric fields due to the above effects. Using such data as are available it turns out that the electric field due to the gravitational separation of the ions is the largest and this will be considered in the present discussion for the purpose of illustration. The electric field due to the gravitational separation of charge is non-uniform, drops to zero at the center of the body, and is

always directed radially outward. The mean atomic mass of the particles inside the earth may be taken to be 1.0×10^{-23} grams as compared to 3.7×10^{-24} grams in the sun and the mean gravitational acceleration as 5×10^{2} cm/sec^2. Substitution of these quantities in Eq. (19) gives E_y as 0.3 e.m.u/cm which on substitution in the last term of Eq. (9) gives a value for $eH_z E_y/kT$ of 1.2×10^{-9} if we take $H_z=0.5$ gauss and $T=10{,}000°$. Comparison of this value with the assumed value for the surface magnetic gradient of 1.6×10^{-9} gauss/cm shows that the effects due to the gradients or magnetizing action are larger, but almost identical in magnitude with the demagnetizing action arising from the electric field. We are thus led to conclude that the two effects play a part in the production and maintainance of a steady field and that the absolute value of the resulting magnetic moment will depend on the size and temperature of the body and on the internal distribution of the gravitational, magnetic and electric fields. With an exact knowledge of the internal distribution of the magnetic field of the earth it would be possible to calculate the consequences of the present theory and in this manner study the requirements relating to the internal distribution of the electric field. A complete theory, moreover, must take account of a variable free path which when applied to the sun or earth would tend to reduce the demagnetizing effects and increase the relative magnetization. It seems quite possible that a portion of the magnetic flux directed from north to south near the axis, returns somewhere inside the earth. Such a distribution or a distribution taking into account diamagnetic effects would give rise to a system of currents which would be enormously more complicated than the systems we have just considered.

The eccentricity of the magnetic fields of the earth and sun relative to their rotational axes indicates that the values of the free paths and temperatures are not symmetrical about these axes and the magnetic axis would therefore be expected to be displaced toward the hotter regions as viewed from the axis of rotation. The present theory indicates that at the time of formation of the earth the area now embraced by the Pacific Ocean was much hotter than the other half of the earth and that at great depths this asymmetry still persists today. These considerations are in keeping with the view that the planets were formed as a result of tremendous tides on the sun since such a mechanism readily explains why one side of the planet would be much hotter than the other and would account for the reflected shift in the magnetic poles of the sun which are known to be slightly displaced from the geographic poles.

The theory which has been developed provides a regenerative magnetizing mechanism which is capable of producing internal circulating currents in the sun and earth of a magnitude and distribution suitable for the production of the observed fields. The theory further provides a demagnetizing mechanism which is capable of controlling the regenerative phenomenon and limits the resultant magnetic field to finite values which are dependent on the physical constants of the hot body. It is not to be supposed that the theory is complete and will not need modification for the complete solution to the problem will undoubtedly be very complicated.

ON THE ULTRA-VIOLET LIGHT THEORY OF AURORAE AND MAGNETIC STORMS*

By E. O. Hulburt
Naval Research Laboratory

(Received June 6, 1929)

Abstract

The ultra-violet light theory of aurorae and magnetic storms suggests (1) that because of winds and unusual production of ions the ionized region of the high atmosphere may be in violent agitation during the day of a magnetic storm, that it grows calmer at night and becomes agitated the next day if the storm continues, (2) that there may be auroral displays in polar regions with no magnetic storms in temperate latitudes, (3) that auroral displays in temperate latitudes should as a rule be accompanied by magnetic storms, and (4) that polar aurorae should follow several hours or a day after strong magnetic disturbances observed in temperate latitudes. These inferences are shown to be in agreement with the data from magnetic observatories and observations of aurorae in temperate and polar latitudes.

IT IS the purpose of this paper to develop certain details of the ultra-violet light theory[1] of aurorae and magnetic storms and to bring to attention experimental facts which are in accord with the theory. Briefly, the theory was built on the hypothesis that the sun, when active, emitted an unusual flare of ultra-violet light which produced an unusual number of ions and excited atoms and molecules in the high atmosphere of the earth. The ions by means of their diamagnetism and their gravitational drift currents gave rise to the magnetic storm. Neutral atoms and molecules, upon collision with the excited particles or with ions undergoing recombination, received some or all of the excitation or recombination energy in the form of kinetic energy. This was sufficient to give some of them velocities as high as 10 km sec^{-1}. They moved out to distances of perhaps 40,000 or 50,000 km from the earth in a few hours. At these remote levels they were ionized by the ultra-violet sunlight and were then constrained by the magnetic field of the earth to descend to the polar regions. There in some manner they gave up a part or all of their energy to form the auroral display.

The winds in the upper atmosphere of the earth and the heating of these high levels by solar radiation were discussed for the case of a quiet sun.[2] For an active sun, the activity being assumed to be the emission of an ultra-violet flare, it was shown[1] that the flare caused an unusual ionization and an unusual heating and expansion of the atmosphere in the levels above, say, 50 km which lifted the ionized regions upward as much as 100 km. This gave rise to winds in the upper atmosphere which blew ion clouds about in great

* Published with the permission of the Navy Department.
[1] Maris and Hulburt, Phys. Rev. **33**, 412 (1929).
[2] Maris, Terr. Mag. and Atmos. Elect. **33**, 233 (1928).

turmoil. It is of interest now to pursue a little farther the general idea of "winds and weather" in the high atmosphere. The moving ion clouds because of their magnetic effects will produce an agitation of the earth's magnetic field. The magnetic agitation due to this cause would be expected to become less at night, for at night the winds may quiet down and the ion clouds melt away by the recombination of the ion pairs. Day-time irregularities which decrease at night are conspicuous on the storm curves of certain observatories for example, Cheltenham, Maryland, U.S.A., and Huancayo, Peru. At Cheltenham the day-time storm curve is in general very jagged and irregular with perhaps 5 to 10 irregularities an hour of amplitudes 5 to 10γ (γ is 10^{-5} gauss) for a moderate storm and of greater amplitudes for more intense storms. During the night, and often within an hour of sundown, these short period fluctuations die out to a greater or less extent and set in again at dawn if the storm still continues. This day and night effect was unmistakable on the horizontal magnetic intensity curves of 134 out of 175 storms which occurred in the years 1902 to 1924. It was not evident on the curves of the other 41 storms, for these storms were either too violent or too mild or too short. The short period daylight irregularity was in general superimposed on fluctuations of larger amplitude, roughly 20 to 50γ for a moderate storm, and of longer period, an hour or so, and these in turn on the still larger diurnal and world-wide storm variations which have already been discussed.[1] The daytime ionic turbulence was inferred from the behavior of wireless waves during a magnetic storm.[3] This turbulence of the under surface of the ionized region of the atmosphere should perhaps be compared to the waves of a stormy sea rather than to clouds whipped by a tempest.

Quantitatively the theory seems acceptable. For an ion cloud 20 km square at a height of 100 km, containing 10^{11} ions cm^{-3} in its lower surface, moving with a speed of 200 km $hour^{-1}$ would by its diamagnetism[4] cause at sea level underneath it a change of 3γ in 20 minutes. The equations for this calculation are on page 341, reference 1. A sudden creation or destruction of the ion cloud would of course produce a similar magnetic pulse. It is probable that the complete magnetic effect of such an ion cloud is due to the ion drift currents arising from gravitational action,[5] dynamo action and from magnetic gradients[6] in addition to the diamagnetism caused by the thermal agitation of the ions. To calculate the effect of the drift currents would require exact knowledge of the entire physics of the ion cloud. It may be mentioned that the foregoing explanation of the day-time fluctuations of periods of several minutes does not necessarily apply to the rapid pulsations, consisting of long continuous trains of moderately regular waves, of periods from 10 to 100 or 200 sec. and of amplitudes of the order of 1γ, observed extensively by van Bemmeln and others.[7]

[3] Maris and Hulburt, Proc. Inst. Rad. Eng. **17**, 494 (1929)

[4] Gunn, Phys. Rev. **32**, 133 (1928).

[5] Reference 1, page 426; Page, Phys. Rev. **33**, 553 (1929).

[6] Gunn, Phys. Rev. **33**, 832 (1929).

[7] See Terada, Jour. of the College of Science, Tokyo Imperial Univ. **37**, Art. 9, (1917), nd references *infra*.

A daylight irregularity which becomes less at night is not a characteristic common to all magnetic stations. For example, the effect is not prominent, or is absent altogether, on the magnetic storm curves at Watheroo, Western Australia, and at Honolulu. The curves of these stations, however, are at all times relatively smooth. One may suggest that the meteorological conditions in the high atmosphere above these stations are relatively quiet even during magnetic storms, although of course the disposition of the earth under a station may, through earth currents, etc., have an important effect upon the magnetic characteristics of the station as well as the ionized regions above the station. In polar regions, as at Sitka, Alaska, the storm curve is so violent and irregular that day and night differences are not evident.

In general one would expect the ultra-violet flares emitted by the sun to differ in intensity and in the distribution of energy in the spectrum. In experiments with pulses of wireless waves transmitted from this laboratory Breit, Tuve and Hafstad at their receiving station about 10 km away do not usually receive at all waves of 34 meters in length. The ground wave does not reach them and the electron density in the Kennelly-Heaviside layer, which is supposed to be about 3×10^5 electrons cm^{-3} for a summer day,[8] is not sufficiently great to reflect (refract) the waves downward at nearly normal incidence. If the electron density were increased to 9.7×10^5 the 34 meter wave would be reflected at normal incidence and the signals would be received. Actually the signals were received erratically at various times and on two occasions on the day previous to a magnetic storm.[9] In explanation of these observations one may suppose that the sun emitted relatively feeble ultra-violet flares. A flare of sufficient intensity to increase the normal daytime upper atmospheric ionization by a factor of 3 would not cause a magnetic disturbance great enough to be called a storm, if the calculations, reference 1, page 427, give a correct idea of the amount of ionization necessary to produce a disturbance of storm magnitude. Such a feeble flare might occur at any time or when the flare was warming up to storm intensity.

In the spectrum of the ultra-violet solar flare it is the wave-lengths shorter than the limit of the principle series of a given atom which probably are the most effective in ionizing the atom whereas somewhat longer wave-lengths would be expected to cause excitation of the atom. No theory of the physics of the solar outburst was suggested, but in a general way one would expect various types of solar flares, such as (1) flares containing mainly the excitation wave-lengths, (2) flares which contain both the excitation and ionizing wave-lengths in varying intensity, etc. On the assumption that the spectral energy distribution in the flare is that of a black-body the flare of type 2 might result from a hotter outburst than that of type 1. The black-body assumption can hardly be very approximately true, for the spectrum of the flare is probably some characteristic gaseous bright line and continuous spectrum emission. A flare of type 1 would produce many excited

[8] Hulburt, Phys. Rev. **31**, 1018 (1928).
[9] Hafstad and Tuve, Terr. Mag. and Atmos. Elec., March (1929).

atoms; these give rise to high flying atoms or molecules which when ionized fall to the polar regions and cause the aurora. Since such a flare does not produce many ions there will be no strong magnetic disturbance. Therefore in this case there may be a strong auroral display in high polar latitudes unaccompanied by a magnetic disturbance in temperate latitudes of sufficient intensity to be called a storm. Examples of this were the strong auroral displays seen on April 20 and 27, June 18 to 21, 1908, at Cape Royds[10] on June 3, 1912, and on May 29, June 19 and July 7, 1913 at Cape Denison.[11] Both of the stations were on the Antarctic continent. The magnetic conditions at the Antarctic stations were disturbed at these times,[12] but in temperate latitudes no magnetic storms were recorded on or within a few days of these dates. Many brilliant auroral displays with no temperate zone magnetic disturbances were recorded by the Maud Expedition[13] during the years 1922 to 1925 in the Arctic Sea north of Siberia.

A flare of type 2 would, in addition to producing many ions, give rise to many high flying particles which, because of the unusual intensity of the ionizing wave-lengths, would be ionized quickly before they had time to attain great heights. They would not reach polar areas, but would move along the magnetic lines of force of the earth's field to high temperate latitudes in sufficient concentration to give an auroral display. Therefore strong magnetic storms would be expected to be accompanied by aurorae in high temperate latitudes and the stronger the storm the more spreading of the display into lower latitudes there would be. This spreading effect is in accord with the observations summarized by Røstad.[14] Temperate zone auroral displays were observed by Barnard[15] at the Yerkes Observatory on about 140 nights in the years 1902 to 1909. Magnetic storms accompanied 120 of the displays. On the nights when there were no storms, the auroral manifestations were feeble and it is possible that magnetic disturbances may have occurred which were too weak to be listed as storms.

A particle ejected upward from the atmosphere with a velocity around 10 km sec^{-1} reaches 40,000 km levels in about 3 hours. If it is ionized there by the sunlight it falls to polar regions requiring several hours for the descent, the exact time depending on the pitch of the spirals of its path and on its velocity at the instant of ionization, provided that the only influences which act on the ion are gravity and the magnetic field of the earth. If other agencies are present, such as light pressure, electric fields, etc., their effects should be considered in a complete discussion. If the same ultra-violet flare which causes the polar ion migration and hence the aurora, also causes heavy

[10] Mawson, British Antarctic Expedition 1908, Trans. Roy. Soc. of South Australia **40,** 151 (1916).

[11] Mawson, Australasian Antarctic Expedition 1911–14, Scientific Reports, Series B, **2.** Part 1, (1925).

[12] Webb, Australasian Antarctic Expedition, 1911–14, Scientific Reports, Series B. **1.** March (1925).

[13] Sverdrup, Carnegie Inst. Pub. No. **6,** 175 (1927).

[14] Røstad, Geofysiske Publ. Oslo **5,** 1 (1928).

[15] Barnard, Astrophys. J. **31,** 208 (1910).

ionization in the atmosphere and hence a magnetic storm, the aurora should appear a number of hours after the initiation of the storm. Since the ion migration to the poles is suppressed while the flare is at its greatest intensity one might expect the delay in the appearance of the aurora in high polar regions to be greater for a long continued intense magnetic storm than for a shorter storm. The auroral observations recorded in the journals of the British[10,16] and Australasian[11] Antarctic Expeditions and of the Maud Arctic Expedition[13] furnish data in keeping with these theoretical inferences. The journals give a description of the appearance of the aurora at stations in high polar latitudes at various times throughout the day for many months, except when cloudy weather, daylight and other things interfered with the observations. The general catalogs of aurorae of Rubenson, Fritz, Greely, Lovering, Tromholt and others were on the whole not detailed enough to be useful in the present discussion. The magnetic storm data were taken from the records of the Cheltenham Observatory, Md, and of the Greenwich Observatory. It is conceivable that the solar ultra-violet flare began gradually,

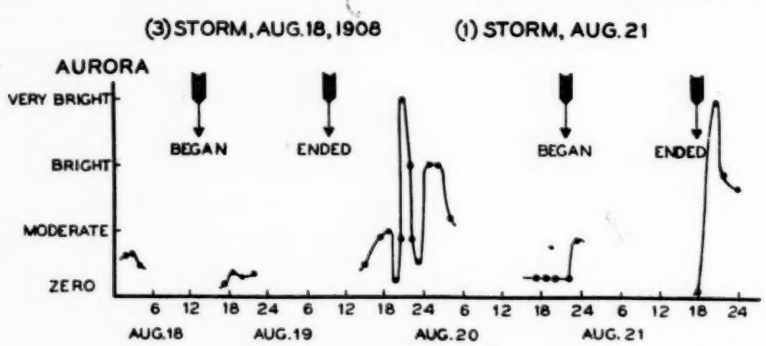

Fig. 1. Aurora intensities at Cape Royds and magnetic storms of August 18 and 21, 1908.

first emitting only the excitation wave-lengths and then later the ionizing wave-lengths. In this case the aurora might begin before the magnetic storm. Therefore one should deal as far as possible with storms which commenced suddenly, on the idea that the flare began to emit both ionizing and exciting wave-lengths at the same time. And, too, there is better agreement between various magnetic observatories as to the time of commencement of a storm if the storm began sharply.

In Fig. 1 are plotted the auroral displays associated with the magnetic storms of August 18 and 21, 1908, of strengths (3) and (1), respectively; (1) means a moderate storm, (2) an intense storm, etc. The ordinates, which are of course qualitative, are plotted from the auroral appearances described by the 1908 expedition.[10] Figs. 2 and 3 give the plots for the (1) storm of August 5, 1912 and the (3) storm of September 17, 1912, respectively, using the auroral data of reference 11. Altogether 11 magnetic storms were found for which

[16] Wright, British (Terra Nova) Antarctic Expedition 1910–13, "Observations on the Aurora," published 1921.

the antarctic and arctic auroral data were sufficiently complete to permit figures similar to Figs. 1, 2 and 3 to be made. The results of these are summarized in Fig. 4, in which the ordinates are the intensities of the magnetic storms and the abscissas are the number of hours from the commencement of the storm to the beginning of the auroral display. The letters along-side of each dot or cross of Fig. 4 give the date of the magnetic storm as follows:

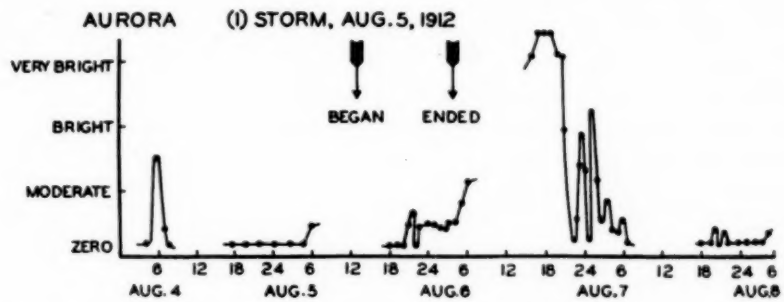

Fig. 2. Aurora intensity at Cape Denison and magnetic storm of August 5, 1912.

A June 3, *B* August 18, *C* August 21, 1908; *D* May 4, *E* June 7, *F* Spetember 7, *G* October 14, 1912; *H* April 9, *I* June 1, 1913; *J* January 20, 1923; *K* October 23, 1924. Of these storms only *B*, *F*, *C* and *I*, shown by the crosses, had sudden commencements. The other seven storms, shown by the dots, set in more or less gradually and should perhaps be given less weight than the first four storms. It is seen from Fig. 4 that the auroral displays began about a day after the commencement of the storm on the average, and, although the data are too few for great certainty, that the time interval between the dis-

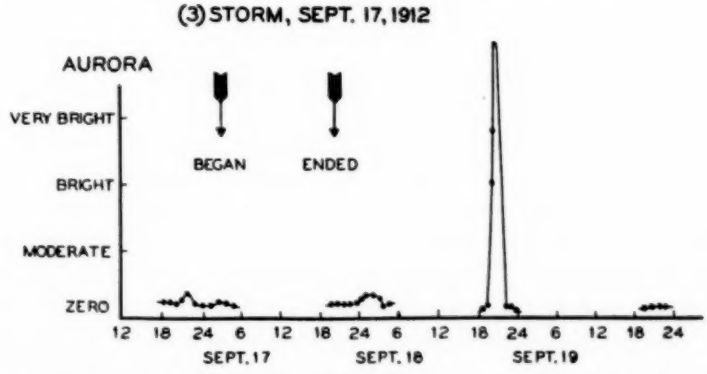

Fig. 3. Aurora intensity at Cape Denison and magnetic storm of September 17, 1912.

play and the storm was longer for the more intense storms. The auroral data of the Maud Expedition contributed only two points in Fig. 4. Their observations were made around 75° north latitude and 160° east longitude which was in the zone of maximum auroral frequency. As a result auroral displays were of such frequent occurrence that it was difficult to say in most cases whether a particular display was associated with a particular magnetic

storm, although in general strong auroral activity occurred at the epochs of strong solar activity.

The matter of the relative frequency of the appearance of the aurora with the time of day deserves further comment. It is true that at certain arctic stations the intense auroral displays occur more often before midnight, local time, than during the early morning hours, although aurorae are common enough at all hours of the night.[17] To explain this the ultra-violet light theory suggested that the high flying ions swing around the earth with an angular velocity equal to or less than the angular velocity of the rotation of the earth on its axis, so that they descend to the earth during the night hours. In spite of the fact that it appeared doubtful some stress was laid on the possibility that the ions might move with the angular velocity of the earth because

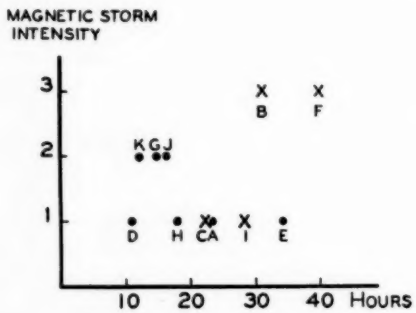

Fig. 4. Ordinates, intensities of magnetic storms; abscissas, time intervals in hours from the commencement of the magnetic storm to the commencement of the auroral display in polar latitudes.

of the following remarkable sequence of numerical facts (reference 1, page 419), namely; that due to the centrifugal force arising from such an angular velocity ions in the equatorial belt at or above 42,200 km will be kept from falling down to the earth, and the magnetic line of force which is at this level at the equator ends at 67° magnetic latitude which is the zone of maximum auroral frequency. Recently Page[18] has shown that in order for the ions to move with the angular velocity of the earth there must exist an electric field such as might be produced by an excess negative charge on the earth distributed in a certain manner over the surface. The existence of such a field can not be definitely denied, for it appears to be too small to be detected by direct experiment, but on the other hand there seems to be no clear reason why it should exist. For the present we must regard the sequence of numerical facts just mentioned as a coincidence and leave the matter unsettled.

Furthermore, the facts as to the appearance of the aurora are on the whole complex. Mawson's[11,12] observations in the antarctic and Sverdrup's[13] observations in the arctic areas indicated two maxima in the frequency of auroral appearance, one before midnight and one in the early morning hours,

[17] Chree, Encyclopaedia Britannica, 13th ed. **2**, 927 (1926).
[18] Page, Phys. Rev. **33**, 823 (1929).

with a somewhat different distribution of occurrence throughout the night for arches, glows and streamers. Barnard's[15] observations indicated a similar tendency. Out of 100 nights for which his record seemed to be fairly complete aurorae were seen on 62 nights between 9 and 11 o'clock, on 52 nights in the early morning hours and on 31 nights around midnight. As far as can be judged from his descriptions great or fairly great auroral displays were witnessed on only five occasions during the years from 1902 to 1909; namely, on August 21, October 30, 1903, February 9, 1907, October 30, 1908 and October 18, 1909. Two of these developed their maximum activity before midnight, two after midnight and the remaining one was active before and after 12 P.M. with a dull period at midnight. Future developments of the theory of the aurora should contemplate these facts and others given in the excellent reports of Mawson, Sverdrup and others, and must perhaps at the same time look to the laboratory to supply further information about the various atomic processes which give rise to the auroral light. For the idea has obtruded itself at all times that the emission of the auroral light may not depend simply upon an energy influx carried by ions, but may require in addition that the atmosphere into which the ions fall be in a suitable and perhaps critical condition, such a condition being an erratic function of wind currents and the states of excitation of the molecules and atoms of the upper atmospheric gases.

THE EXPANSION OF GASES ON MIXING, ESPECIALLY AT VERY LOW PRESSURES. I. ITS RELATION TO THE EMPIRICAL CALCULATION OF THE FUGACITIES IN GASEOUS MIXTURES

By Louis J. Gillespie
Research Laboratory of Physical Chemistry
Massachusetts Institute of Technology*

(Received April 8, 1929)

Abstract

From plots of the expansion of a gas in a mixture, $(\bar{v}_1 - v_1)$, or of the expansion of gases on mixing to form a mole of mixture from the pure gases at constant temperature and pressure, $(\Sigma x_1\bar{v}_1 - \Sigma x_1 v_1)$, as functions of the pressure, it is clear that these quantities do not vanish at zero pressure. These expansions do not vanish for mixtures of ethylene and argon, ethylene and oxygen, nitrogen and hydrogen, and nitrogen and methane, in which cases the limiting values are, according to the existent data, finite and positive. Values for zero pressure can be calculated from a "linear combination of constants" in the equation of state for the mixture, which values in all cases but the first are evidently suitable end-points for the extrapolation to zero pressure. In the case of argon and ethylene the calculated points are not so suitable, but are reasonably good. In this case, the Lorentz formula for the mutual co-volume fits very well and the corrections on the Lewis and Randall rule for argon and ethylene have been calculated to 50 atmospheres from curves drawn according to the Lorentz formula. In a number of cases the corrections differ by 1 percent from those calculated by previous investigators, who assumed the expansions to vanish at zero pressure. The empirical calculation of fugacities from the pressure data of gaseous mixtures is in general improved by, if it does not in fact require, some knowledge of the expansions at zero pressure.

I. Introduction

THE fugacity of a gas, f, is its pressure p corrected for the deviations of the gas from the law of ideal gases, $pv = RT$. One way to exhibit the correction is by means of the equation

$$f = p \exp\left[\int_0^p (\mu - \mu_i)dp/RT\right] \tag{1}$$

where μ is the chemical potential of the gas at the pressure p, and μ_i is the chemical potential which would be calculated for it at the pressure p by assuming the ideal gas law. The unknown function of the temperature is thus eliminated from the μ; it is the principal advantage of the fugacity that it can be calculated from an equation of state.

For phases in isothermal equilibrium f, like μ, is equal for a given component in the different phases to which it is capable of free migration. We shall refer to the fugacity of a gas in a mixture, which will be equal to the fugacity of the pure gas at the same temperature and at such a pressure as

* Laboratory contribution No. 220.

it must have to be in equilibrium with the mixture through a membrane permeable to it alone.

Given sufficient data on the pressure-volume-temperature properties of gaseous mixtures, the fugacity of each gas in a mixture can be calculated by means of rigorous thermodynamic relations from the assumption that the partition of any real gas through a semipermeable membrane is governed at sufficiently low pressure by the ideal gas relation. The product of the total pressure times the mole fraction has the same value for any constituent on both sides of the membrane when the system is in equilibrium. This was pointed out in a previous publication[1] and, by using a familiar differential equation due to Gibbs, $\partial\mu_1/\partial p=\bar{v}_1$, the following equation was derived:

$$RT\ln f_e=\int_0^p(\bar{v}_1-v_1)dp+RT\ln f_p+RT\ln x_1 \tag{2}$$

where f_e is the fugacity of gas 1 in the mixture, p is the total pressure and x_1 is the mole fraction of gas 1 in the mixture, f_p is the fugacity of gas 1 at the total pressure p, $\bar{v}_1$ and v_1 are the partial volume in the mixture of gas 1 and the molal volume of pure gas 1 at the pressure p, respectively.

Later, the thermodynamically equivalent Eq. (3)

$$\ln f_e=\frac{1}{RT}\int_0^p\left(\bar{v}_1-\frac{RT}{p}\right)dp+\ln px_1 \tag{3}$$

was derived by Van Lerberghe,[2] and Gillespie (from Eq. (2))[3] and by Gibson and Sosnick.[4]

Still another thermodynamically equivalent equation was given by Lurie and Gillespie,[5] a special convenience of which exists only when the equations of state used do not permit explicit integration of pdV or Vdp. An integrated equation in terms of V and T has been given by Beattie.[6]

Recently Van Lerberghe[7] has discussed Eq. (3) without limiting its application to the gaseous state. Note however that when x_1 denotes the mole fraction in the liquid phase, the integration from zero pressure must begin with a gas phase of the same composition and maintain this composition, as otherwise a relation other than (3) would be required. The integration implies therefore a continuous isothermal transformation of gaseous into liquid mixture such as that imagined by James Thomson for pure substances. Complete data for the integration can therefore never be obtained, and no equation of state exists at present even for pure gases which can be regarded as an accurate equation of continuity. Though the differential equation

[1] Gillespie, J. Am. Chem. Soc. **47**, 305 (Feb. 1925).

[2] Van Lerberghe, Comptes rendus Ac. Sci. Paris **181**, 851 (Nov. 1925).

[3] Gillespie, J. Am. Chem. Soc. **48**, 28 (Jan. 1926).

[4] Gibson and Sosnick, J. Am. Chem. Soc. **49**, 2172 (1927).

[5] Lurie and Gillespie, J. Am. Chem. Soc. **49**, 1146 (1927).

[6] Beattie, Phys. Rev. **32**, 691 (1928).

[7] G. Van Lerberghe "Le Calcul des Fugacités d'une Solution" Marcel Hayez, Brussels (1928).

leading to Eq. (3) is of course general, the integrated Eq. (3) appears limited in application to mixtures of gases, though it will be naturally of use in the discussion of liquid mixtures.

Application of Eq. (2) was made by Lurie and Gillespie[8] to certain mixtures of ammonia and nitrogen without the aid of any pressure-volume-temperature data for mixtures of these gases. This was done by assuming an equation of state for the mixtures. Comparison of the calculated and the experimentally determined results indicated a considerable degree of validity for the principle used for deducing the equation for the mixtures.

Equation (3) may be used in what may be called an empirical manner, the integral being determined not from an equation of state for mixtures, but from graphical analysis of pressure-volume-temperature data for the gaseous mixtures. This has been done by Gibson and Sosnick[4] for mixtures of ethylene and argon, using the pressure data for mixtures obtained by Masson and Dolley;[9] and by Merz and Whittaker[10] for nitrogen and hydrogen mixtures, using the pressure data of Bartlett[11] for a single mixture.

The principle used in deducing the equation of state of mixtures from the equations for the pure gases is as follows. The equation for mixtures has the same form as that for the pure gases, and the numerical coefficients are determined by combining the coefficients appearing in the equations for the pure gases. The principle has been found consistent with the pressure measurements of Keyes and Burks[12] on nitrogen and methane, both by them, using the Keyes equation of state, and by Beattie[13] using the Beattie-Bridgeman equation of state.[14] In combining the coefficients they as well as Lurie and Gillespie extracted the square roots of the cohesive pressure A constant and combined these roots as well as all the other constants according to the linear scheme

$$k_n = \Sigma(k_1 x_1 + k_2 x_2 + \cdots) \tag{4}$$

where the x's denote mole fractions. This procedure will be called hereinafter "linear combination of constants." It has been used frequently in the past as applied to equations of state of simpler type, the coefficients of which were generally inaccurately calculated from a theory of the critical state.[15] Eucken and Bresler[16] have recently published data on equilibria between liquids and gas mixtures and found scheme (4) for the square root of A

[8] Lurie and Gillespie, J. Am. Chem. Soc. **49**, 1146 (1927).
[9] Masson and Dolley, Proc. Roy. Soc. London **103A**, 524 (1923).
[10] Merz and Whittaker, J. Am. Chem. Soc. **50**, 1522 (1928).
[11] Bartlett, J. Am. Chem. Soc. **49**, 1955 (1927).
[12] Keyes and Burks, J. Am. Chem. Soc. **50**, 1100 (1928).
[13] Beattie, J. Am. Chem. Soc. **51**, 19 (1929).
[14] Beattie and Bridgeman, J. Am. Chem. Soc. **49**, 1665 (1927).
[15] See Beattie, reference 13, for summary of earlier references.
[16] Eucken and Bresler, Zeits. f. phys. Chem. **134**, 230 (1928). In their theoretical discussion they also calculated coefficients from critical state theory and did not observe that a rigorous thermodynamic theory for such equilibria had been published and that Lurie and Gillespie[8] had already applied it to some of the data of Pollitzer and Strebel.

consistent with certain vapor pressure measurements by the use of a certain expression for the partial pressure.

2. The Special Considerations Which Led to the Present Work

Upon the appearance of the article of Gibson and Sosnick it became of especial interest to test the principle upon mixtures of ethylene and argon. An equation of state for argon was available, derived by Beattie and Bridgeman[17] and one of the same form was then derived for ethylene.[18] It was found necessary in obtaining an equation for ethylene to rely exclusively upon the data of Amagat. Since, except at low pressures, these data do not agree well with those of Masson and Dolley, as they recognized,[9] the equation does not closely represent their data. Nevertheless it would be expected that fairly consistent results might be obtained, if instead of comparing the whole of the fugacity we should compare only the integral term of Eq. (2) calculated from the equation and determined empirically by Gibson and Sosnick from the data of Masson and Dolley. And this integral itself is of more interest than the whole fugacity since it is the only part of the fugacity which requires data on mixtures, the rest being rigorously determinable by well-known methods. The integral measures in fact[1] the error of the simple Lewis and Randall rule.

In an unfinished investigation of this matter these integrals were calculated at various pressures for the mixture of 20 mole percent ethylene and 80 mole percent argon, using an equation of state deduced by means of linear combination of constants. On comparing the values with those obtained by Gibson and Sosnick (in the form of the difference of two integrals) it was found that the agreement, while not without some significance, was not good. But the disagreement was practically constant (to 1 calorie in the "free energy") from 15 to 70 atmospheres, therefore the areas calculated from 15 to 70 atmospheres for intervals of 5 atmospheres did in fact agree. The disagreement above 70 atmospheres was not surprising in view of the inconsistency of the measurements upon ethylene of Amagat and of Masson and Dolley. It appeared improbable however that an equation holding between 15 and 70 atmospheres could give erroneous results between 0 and 15 atmospheres.

Turning to the data of Masson and Dolley it is remarked that they give no figures for mixtures below 30 atmospheres, so that the areas from 0 to 30 atmospheres were determined by Gibson and Sosnick entirely by extrapolation. Since the areas begin at zero pressure, errors in the fugacity due to extrapolation below 30 atmospheres affect all results. They did not discuss this extrapolation, but examination of their Figure 3 shows the principle used in the extrapolation. This may be stated as follows: $(RT/p-\bar{v}_1)$ approaches at zero pressure the same value for a given gas in all mixtures. This is equivalent to the following: $(\bar{v}_1-v_1)$ approaches zero for a given gas in any mixture as the pressure approaches zero.

[17] Beattie and Bridgeman, Proc. Am. Acad. Arts and Sci. **63**, 229 (1928) and J. Am. Chem. Soc. **50**, 3133 (1928).

[18] Gillespie, J. Phys. Chem. **33**, 354 (1929).

Now this principle, which has not previously been stated, is in conflict with the linear combination of constants, which gives the following result for a binary mixture:

$$\text{Limit}_{p=0}\ \bar{v}_1 - v_1 = \frac{1}{RT} x_2^2 \left[(A_1)^{1/2} - (A_2)^{1/2}\right]^2 \tag{5}$$

whether the Keyes or Beattie-Bridgeman equation is used or their prototypes the van der Waals and Lorentz equations. Note that the expression is invariably positive.[19]

We are led to conclude that if the extrapolation be repeated, bringing the curves to the intersections with the axis of zero pressure calculated from Eq. (5), the areas $\int_0^p (\bar{v}_1 - v_1)\, dp$ determined in this way for the 20 percent ethylene mixture from the mixture data of Masson and Dolley would agree with those calculated from the deduced equation of state of mixtures up to 70 atmospheres.

To see whether such choice of extrapolations is justified we may examine the curves plotted from the data; $(\bar{v}_1 - v_1)$ being plotted as a function of the pressure.

3. Empirical Extrapolation of the Expansion Curves

The quantity $(\bar{v}_1 - v_1)$ represents the expansion of a system consisting of a very great quantity of mixture together with a quantity of pure gas 1 at the same pressure and temperature when 1 mole of gas 1 is taken from the pure gas and added to the mixture at constant temperature and pressure. It may be termed the expansion of gas 1 in the mixture. Figures 1 to 4 show the type of curves for mixtures of argon and ethylene and of hydrogen and

[19] This expression has not been given before. A more general form for the limiting value of $v_1 - v_1$ is $(\bar{\beta}_1 + \beta_m - \beta_1)/RT$ (A) where β_1 is the coefficient of $1/v^2$ in the virial for gas 1 and β_m is the corresponding coefficient in the virial for the mixture when this is written in the form used by Beattie (Phys. Rev. **32**, 691, 699 (1928))

$$p = RT\Sigma n_1/v + \beta_m/v^2 + \gamma_m/v^3 + \delta_m/v^4$$

where v is the total volume containing Σn_1 moles, and $\bar{\beta}_1 = (\partial \beta_m/\partial n_1)_{T, n_1 n_2 \ldots}$, is evaluated from the virial in this form. The above expression (A) holds for any number of constituents and presuppóses only that the pressure of the mixture is expressible as a virial expansion, but it can be evaluated only after a special hypothesis is adopted for β_m. A very general hypothesis for the variation of β_m with composition is that it is a homogeneous quadratic in the mole numbers. Then $\beta_x \equiv \beta_m/(\Sigma n_1)^2$ is a homogeneous quadratic in the mole fraction, and may be written for binary mixtures without further hypothesis

$$\beta_x = x_1^2\beta_1 + 2x_1x_2\beta_{12} + x_2^2\beta_2 .$$

From this the curious relation can be deduced

$$\text{Limit}_{p=0}\ \bar{v}_1 - v_1 = \frac{-x_2^2}{2RT}\left(\frac{d^2\beta_x}{dx_1^2}\right)_T$$

where β_x is the coefficient in the virial when written in terms of the volume v of an average mole ($v = V/\Sigma n_1$), thus: $p = RT/v + \beta_x/v^2 \ldots$. The second derivative does not vary with the composition. The expression need not always be positive, but it appears unlikely, from the numerical applications so far carried out (with the aid of the Lorentz expression for β_{12}), that it will be negative except at temperatures high in comparison with the critical points of the gases.

nitrogen. These are the only mixtures for which partial volumes have been calculated from pressures of mixtures. Figures 5 to 9 show the volume increase when gases are mixed at constant pressure to form a total number of moles equal to 1. This increase equals

$$x_1\bar{v}_1+x_2\bar{v}_2-x_1v_1-x_2v_2=v_m-RT/p-x_1(v_1-RT/p)-x_2(v_2-RT/p)$$

This must approach zero as the pressure approaches zero if $(\bar{v}_1-v_1)$ and $(\bar{v}_2-v_2)$ approach zero. Substitution of values from Eq. (5) into this expression gives $x_1x_2[A_1^{1/2}-A_2^{1/2}]^2/RT$ as the limiting value at zero pressure when we apply the linear combination of constants.[20]

Thus all the figures may be examined in the same way to see whether the curves appear to approach zero or a positive intercept. The intercepts calculated from the linear combination of constants are in all cases shown by circles on the axis, $p=0$. In some cases a short line through the circle is drawn to show the tangent calculated for $p=0$.[21]

4. Detailed Discussion of the Plots

All volumes are in cubic centimeters per mole, whether they express, as in Figs, 1–4, the expansion of a single gas in a mixture $(\bar{v}_1-v_1)$, or, as in Figs. 5–9, the volume increase on mixing $(\Sigma x_1\bar{v}_1-\Sigma x_1v_1)$. All pressures are in atmospheres. Circles on the axis of ordinates indicate intersections calculated from linear combination of constants; points marked L are calculated differently (see footnote 23).

Figures 1, 2, argon (1) and ethylene (2). Values of $(\bar{v}_1-RT/p)$ and $(\bar{v}_2-RT/p)$ were taken from Table II of Gibson and Sosnick.[4] Values of (v_1-RT/p) and $v_2-RT/p)$ for the pure gases were taken from their Table I (for mole fractions 0 and 1 only). By subtraction the expansions, $(\bar{v}_1-v_1)$ and $(\bar{v}_2-v_2)$, were found for each value of the pressure given from 30 to 125 atmospheres. (The entries for mixtures at 1 atmosphere are calculated under the hypothesis of zero expansion and can in no way be used here). It is noteworthy that it is the expansion $(\bar{v}-v)$ which is directly found from the mixture data by their graphic procedure.[22] This graphic method

[20] J. P. Kuenen, "Verdampfung und Verflüssigung von Gemischen" in Bredig's Handbuch der angewandten physikalischen Chemie IV, Leipzig (1906) gives the expression (on page 105):

$$x_1x_2\left[\frac{A_1-2A_{12}+A_2}{RT}-(B_1-2B_{12}+B_2)\right]$$

for the volume expansion at low pressures (subject to the assumption of homogeneous quadratic functions mentioned above) and remarks that it is independent of the pressure at low pressures. This expression is however merely the limiting value at zero pressure and the tangent does not in general vanish at zero pressure, as may be seen by a glance at the plots here given.

[21] For the calculation of the tangents the γ term of the virials must be retained. The formula is, independently of the mode of combination of coefficients:

$$\text{Limit}_{p=0}\frac{\partial}{\partial p}(\bar{v}_1-v_1)=(\beta_1^2-2\beta_m\bar{\beta}_1+3\beta^2_m)/R^2T^2-(\gamma_1-\bar{\gamma}_1+2\gamma_m)/R^2T^2.$$

Formulas for the evaluation of the β's and γ's and derivatives in terms of the linear combination of constants are given by Beattie.[19]

[22] Sosnick, J. Am. Chem. Soc. **49**, 2255 (1927). Also described by Hildebrand, Solubility. New York, 1924, page 64.

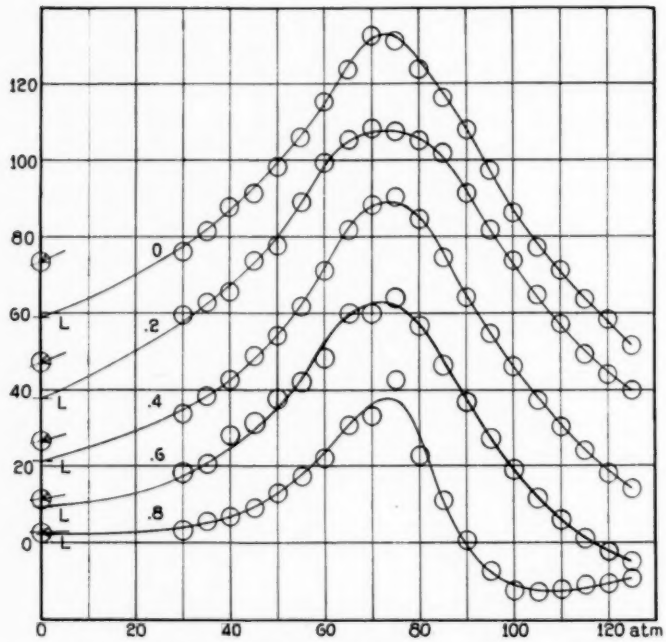

Fig. 1. Expansion of ethylene in argon-ethylene mixtures as a function of the pressure at various mole fractions of ethylene in cc per mole at 24.95°.

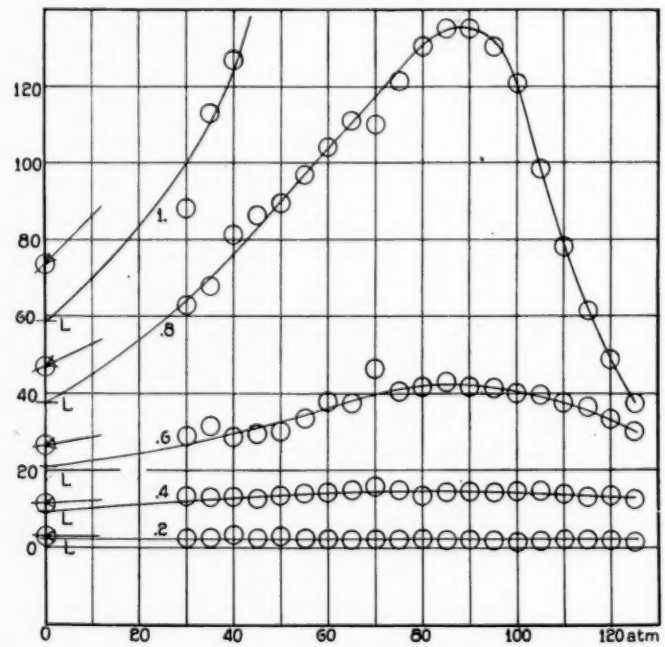

Fig. 2. Expansion of argon in argon-ethylene mixtures as a function of the pressure at various mole fractions of ethylene in cc per mole at 24.95°.

was used to check a few of their expansion values and it was concluded that, on account of the necessity of arriving at a smooth family of curves,

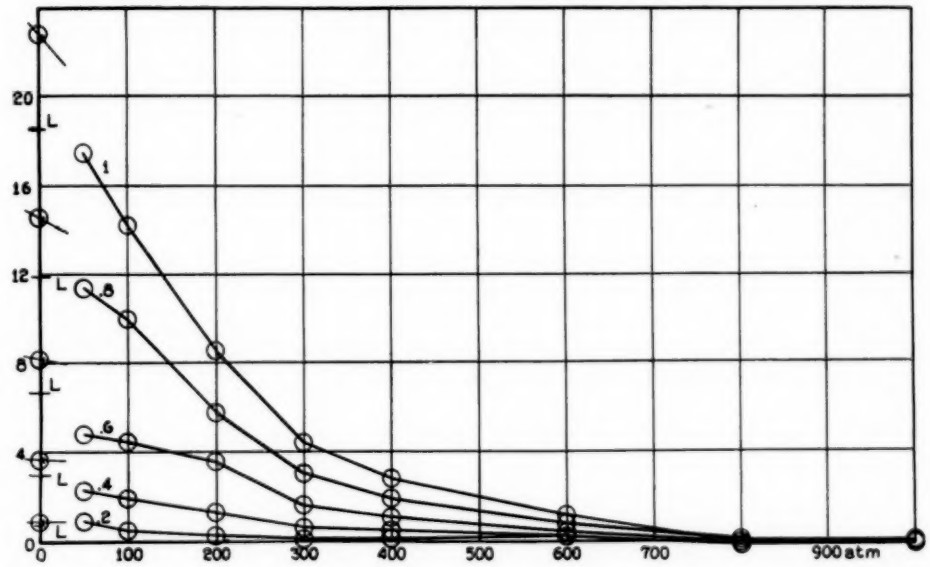

Fig. 3. Expansion of hydrogen in hydrogen-nitrogen mixtures as a function of the pressure at various mole fractions of nitrogen in cc per mole at 0°.

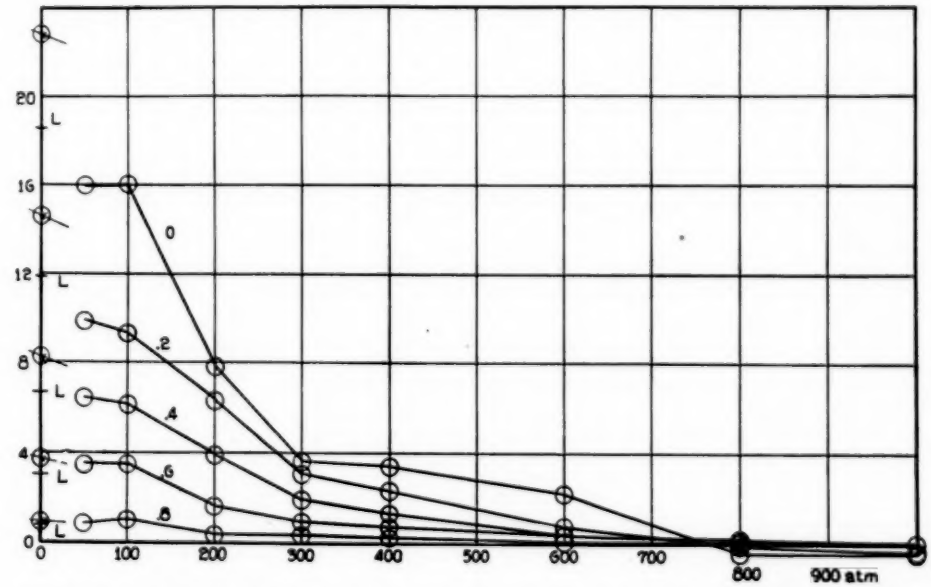

Fig. 4. Expansion of nitrogen in hydrogen-nitrogen mixtures as a function of the pressure at various mole fractions of nitrogen in cc per mole at 0°.

the results found in this present work would not be materially affected by a recomputation of the expansions.

In Fig. 2, in the interest of clearness no points are shown for argon in pure ethylene above 40 atmospheres. In both Figs. 1 and 2 the numbers within the diagram give the mole fraction of ethylene. The curves drawn pass through intersections on the axis, $p=0$, calculated by combining the $(A)^{1/2}$ constants linearly, but by combining the B's quadratically and putting $B_{12}=[B_1^{1/3}+B_2^{1/3}]^3/8$ according to Lorentz.[23] Smoothing to these intersections appears perfect, but this does not hold for other mixtures.

Figures 3, 4, hydrogen and nitrogen. The figures within the diagram show the mole fraction of nitrogen. The values plotted were determined from Tables I and II of Merz and Whittaker.[24]

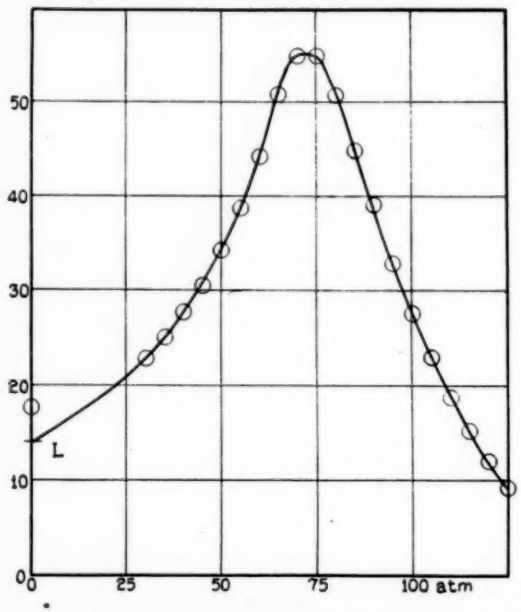

Fig. 5. Volume expansion in cc on mixing 0.4002 moles argon and 0.5998 moles ethylene as a function of the pressure at 24.95°.

For clearness it was thought better to connect the points for each mixture with straight lines than to show smoothed curves. It is evident that the points might have been smoothed either to the circles on the axis (linear combination) or to the Lorentz ("L" points)[23] and almost equally well.

The equation of state constants used for nitrogen were those given by Beattie and Bridgeman[17] for all observers exclusive of Smith and Taylor.

[23] Lorentz, Wied. Ann. d. Physik u. Chemie N. F. **12**, 127 (1881). Intercepts calculated in this way are indicated by an L on these and on other plots. The linear combination of $(A)^{1/2}$ constants is of course the same as quadratic combination of A's putting $A_{12}=(A_1A_2)^{1/2}$.

[24] Reference 10. Through the kindness of Dr. Merz I learned that the entry in Table II, 200 atm., $\bar{v}_1$ for 0.8, should be 133.6 instead of 113.6, and that in Table III, 1 atm., N_2 for 0.2, −874 should have been printed for −881.

Figure 5, argon-ethylene. Volume increase on mixing argon and ethylene at constant pressure to form one mole of the mixture of which the mole fraction x_2 of ethylene is 0.5998.[25]

This figure serves as a transition, and shows that plotting the volume increase leads to the same general results as plotting the expansion of one constituent. Extrapolation to the Lorentz intercept is obviously indicated just as in Figures 1 and 2.

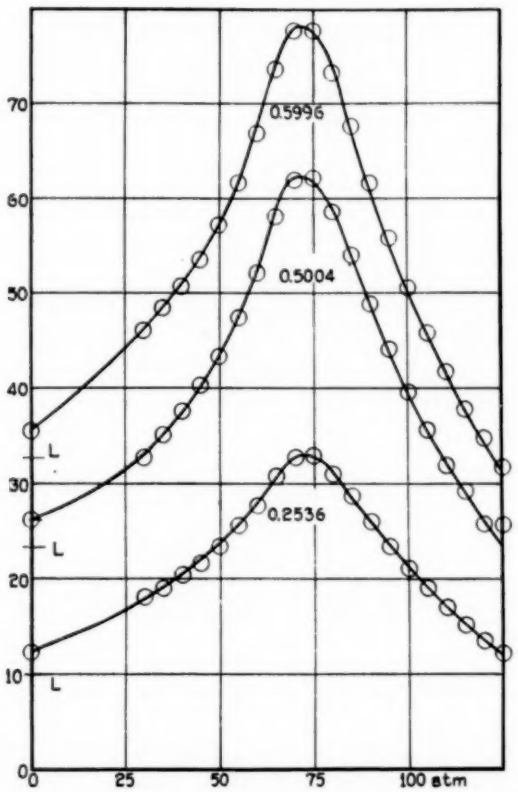

Fig. 6. Volume expansion in cc on mixing oxygen and ethylene to form a mole of mixture containing 0.2536, 0.5004, or 0.5996 moles ethylene, as a function of the pressure at 24.95°.

The volumes y_1 and y_2 of a mole of pure argon and pure ethylene at 1 atmosphere and 24.95° were computed from the equations of state. They are tabulated together with those for oxygen in Table I. By dividing the volume of a mole of pure argon by the density at the pressure p_1 given by Masson and Dolley, the volume v_1 of a mole of pure argon at the pressure was obtained.

[25] Gibson and Sosnick computed $x_2 = 0.6007$, assuming that the coefficient of expansion for 0°C to 24.95° is the same for both gases at 1 atmosphere. By using the equations of states available I compute the following mole fractions for the mixtures of Masson and Dolley: 0.2483, 0.5008, 0.5998, 0.7083, 0.9011. It is believed that the values of Gibson and Sosnick do not differ enough from these to produce any great effect on the comparisons under consideration. Figure 5, being based on recomputed values, confirms this opinion.

By dividing $(x_1y_1+x_2y_2)$ by the density given by Masson and Dolley for the mixture at the pressure p_1 the volume v_m of a mole of mixture for this pressure was obtained. Then the expansion $(v_m-\Sigma x_1v_1)$ was computed and plotted.

TABLE I. *Volumes in liters per mole of pure gases at 1 atmosphere and 24.95° computed from the equations of state.*

Gas	Argon	Ethylene	Oxygen
Volume	24.4448	24.3214	24.4440

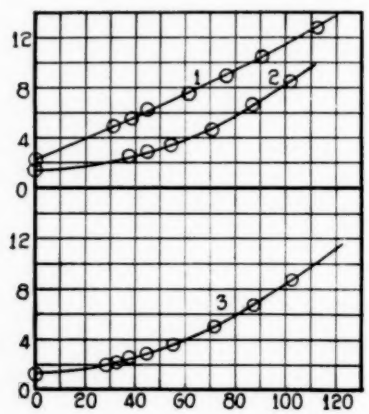

Fig. 7. A function of the pressure, in cc per mole, which is at zero pressure the volume increase on mixing nitrogen and methane at 0° to form 1 mole of mixture 1, 2, or 3.

Figure 6 shows the volume increase for oxygen-ethylene for all three mixtures of Masson and Dolley. Choice of limits for the extrapolation favor the linear combination of constants over the Lorentz[23] in two cases out of three.

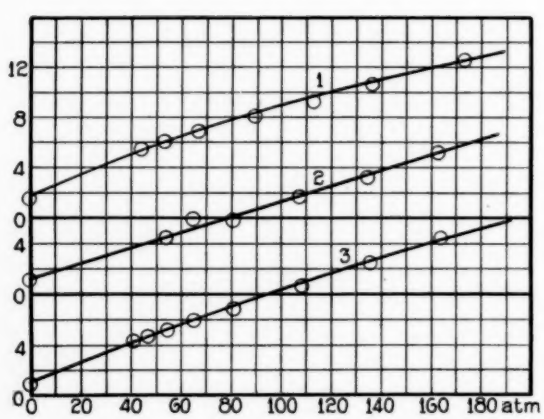

Fig. 8. A function of the pressure, in cc per mole, which is at zero pressure the volume increase on mixing nitrogen and methane at 100° to form a mole of mixture 1, 2, or 3.

Figures 7, 8, and 9 show similar plots for nitrogen and methane from the data of Keyes and Burks.[12] The variable plotted as a function of the pressure

is not exactly the same, except in the limit. Much computation was saved by using in the expression

$$v_m - RT/p - x_1(v_1 - RT/p) - x_2(v_2 - RT/p)$$

the limiting values at $p=0$ of the quantities in parentheses. These were calculated from the relation:

$$\text{Limit}_{p \doteq 0} \; v_1 - RT/p = B_{01} - A_{01}/RT - c_1/T^3$$

This expression will approach the same limit at zero pressure as if actual values at each pressure had been used as in the previous cases. Three temperatures are represented, the extreme and the middle of those given by Keyes and Burks, and all three mixtures. For the plots, the volumes were first recalculated from cc per gram to cc per mole. The mole fractions of methane in mixtures 1, 2 and 3 were 0.4334, 0.7954, and 0.8054, respectively.

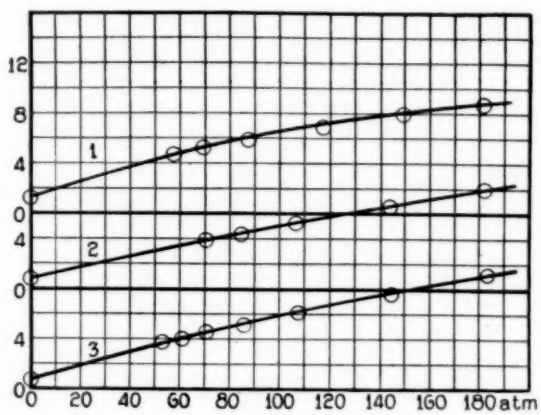

Fig. 9. A function of the pressure, in cc per mole, which is at zero pressure the volume increase on mixing nitrogen and methane at 200° to form a mole of mixture 1, 2, or 3.

For these two figures the equation of state constants used for nitrogen were those calculated by Beattie and Bridgeman[17] from the data of Smith and Taylor, which were determined in the same apparatus as the mixture data. The curves are drawn to the intercepts calculated by linear combination. The Lorentz intercepts are not shown as they are nearly equal to the linear ones.

5. General Discussion of the Plots

Remembering that the quantity plotted against the pressure is $(\bar{v}_1 - v_1)$ or a quantity which vanishes with it at zero pressure, one observes that the plots decide clearly against the hypothesis that $(\bar{v}_1 - v_1)$ vanishes at zero pressure. In no case is extrapolation to zero to be preferred to extrapolation to a positive finite value, and in a number of cases, including argon with ethylene and nitrogen with hydrogen, extrapolation of the families

of curves to zero would require the introduction of inflections in regions where no data exist.

The limiting value of $(\bar{v}_1 - v_1)$ at zero pressure can be reasonably well or even excellently calculated from the linear combination of constants. In the single case, argon with ethylene, in which the agreement is only fair, the Lorentz expression for B_{12} fits very well, but it is not so good for oxygen with ethylene as putting $B_{12} = (B_1 + B_2)/2$, which is equivalent to linear combination. This means that an adjustment of the ethylene A and a constants to make the equation of state of pure ethylene fit the Masson and Dolley isotherm somewhat better[26] would not suffice to make either expression for B_{12} fit both combinations of gases perfectly.

The question as to the proper expression for B_{12} is not exactly an open one, in view of the fact that high pressure data have been found consistent with linear combination, as cited above.[8,12,13]

In smoothing expansions for the calculation of fugacities it would appear well to supplement our empiricism with calculated intercepts, to be judged, like experimental points, by their consistency. The determination of fugacities with such "rational" aid would still be empirical as contrasted with those calculated from the equation of state of mixtures without the aid of mixture data.

6. Expansions at all Pressures

A relation accredited to Biron[27] by Hildebrand[28] gives the expansion of two liquids upon mixing to form a mole of mixture as

$$\Delta V = K x_1 x_2. \tag{6}$$

This is equivalent to

$$\bar{v}_1 - v_1 = K x_2^2. \tag{7}$$

It will be noted that our expressions for gases at zero pressure are of this form (whatever expressions for B_{12} or A_{12} are used). One must know whether this relationship holds for gases at high or even moderate pressures. Our equation of state for mixtures does not lead to simple relations of this type, *except at zero pressure.*

From the exact smooth curves of Figure 1, the quantity $K = (\bar{v}_1 - v_1)/x_2^2$ was calculated and examined. It varied with pressure and also with composition at constant pressure.

From the quantities plotted in Figure 5, the quantity $K = \Delta V/x_1 x_2$ was calculated and found likewise to vary with pressure and also with composition. Evidently these relations (6) and (7) are valid, in the case of gases, only at zero pressure.

[26] Making, for instance, $A = 5.95$ and $a = 0.0474$.

[27] Biron, J. Russ. Phys.-chem. Soc. **44,** 1264 (1912).

[28] Hildebrand, J. Amer. Chem. Soc. **51,** 66 (1929). Van Lerberghe[7] has also pointed out this relation.

7. A Curious Coincidence

It is a striking fact that, for mixtures of argon and ethylene and also of oxygen and ethylene, summits are seen in the curves at approximately the same pressure, which is about 70 to 75 atmospheres. It may therefore be of some significance that at 24.95°, the experimental temperature of Masson and Dolley, the pressure of pure ethylene is according to their measurements 73 atmospheres at the molal density 7.9, which is the critical density selected by Pickering[29] as the best value for ethylene.

8. Empirical Recalculation of Fugacities of Argon-Ethylene Mixtures at 24.95°

The whole series of plots give evidence which might justify extrapolation of the curves of Fig. 1 and 2 to the intercepts calculated linearly. However, if we wish not to miss points in a systematic manner, linear combination must be given up. Extrapolation to the Lorentz intercepts fits so well for both families of curves as to make the curves shown which were drawn to these intercepts, excellent empirical curves through the data. These curves are smooth at least at zero pressure, where we have no data, with respect to the variation of the ordinate with the parameter.

The areas under these curves were therefore determined from zero pressure to 50 atmospheres. Generally by 20 atmospheres the further increments of area for each increase of 5 atmospheres agreed with those obtained from the calculations of Gibson and Sosnick. The results are given in Tables II and III.

Table II. *Values of the areas* $\int_0^p(\bar{v}_1-v_1)dp$ *in calories for argon in argon-ethylene mixtures. The mole fraction* x_2 *given for the mixture refers to ethylene.*

p	$x_2=0.2$ area	diff.	$x_2=0.4$ area	diff.	$x_2=0.6$ area	diff.	$x_2=0.8$ area	diff.	$x_2=1.$ area
1	0.06	0	0.23	0	0.51	1	0.92	1	1.43
5	0.3	1	1.2	1	2.6	2	4.8	3	7.4
10	0.6	1	2.4	1	5.3	1	10.1	5	15.6
15	0.9	1	3.6	0	8.1	0	15.8	6	24.5
20	1.1	1	5.0	0	11.0	0	22.2	7	34.1
25	1.4	1	6.3	−1	14.1	0	29.0	7	44.7
30	1.7	1	7.8	−1	17.3	−1	36.6	8	56.2
35	2.0	1	9.2	−1	20.6	0	44.8	8	68.9
40	2.3	1	10.8	−1	24.1	−1	54.5	8	83.1
45	2.6	1	12.4	−1	27.8	−1	64.2	8	99.2
50	2.8	1	14.0	−1	31.6	−1	74.7	8	119.0

These areas are the values of $\int_0^p(\bar{v}-v)dp$ in calories. Division of the values by $2.3\ RT=1364.9$ would give log $(f_e/f_p x_1)$, from which the fugacity f_e could be determined by the aid of v_1dp integrations, which have been carried out by Gibson and Sosnick. Under the heading "diff" are given to 1 calorie the difference obtained by subtracting from the area given the value obtained from Gibson and Sosnick's calculations. Now an error of 1 calorie

[29] Pickering, U. S. Bureau of Standards, Sci. Papers 541 (1926).

corresponds to an error of $1/2.3RT$ in the logarithm of the fugacity; or to an error of 0.17 percent of the fugacity itself. This is not serious. It will be seen however that differences of 7 calories occur for several mixtures, at pressures as low as 30 atmospheres, and 7 calories corresponds to an error of 1.2 percent in the fugacity, which is not negligible in a thermodynamic recalculation.

The results of principal importance to chemical thermodynamics which can be found solely from the work of Masson and Dolley are believed to be given (up to 50 atmosphere) in Tables II and III. Further utilization to

TABLE III. *Values of the areas $\int_0^p(\bar{v}_2-v_2)dp$ in calories for ethylene in argon-ethylene mixtures. The mole fraction x_2 given for the mixture refers to ethylene.*

p	$x_2=0$ area	$x_2=0.2$ area	diff.	$x_2=0.4$ area	diff.	$x_2=0.6$ area	diff.	$x_2=0.8$ area	diff.
1	1.43	1.83	2	0.52	1	0.23	0	0.06	0
5	7.3	4.7	5	2.7	3	1.2	1	0.3	1
10	14.9	9.8	6	5.6	5	2.4	1	0.6	1
15	22.7	15.3	7	8.7	6	3.8	3	0.9	1
20	31.0	21.1	8	12.2	6	5.4	3	1.2	1
25	39.7	27.4	7	15.9	6	7.1	3	1.6	1
30	48.8	34.2	7	19.9	6	9.1	2	2.1	1
35	58.5	41.5	8	24.4	7	11.5	4	2.7	2
40	68.6	49.4	7	29.3	6	14.3	2	3.5	2
45	79.5	57.9	8	34.8	7	17.6	3	4.5	2
50	91.3	67.2	7	41.0	6	21.5	2	5.9	1

calculate fugacities would involve questions of judgment. The fugacity depends after all principally on the v_1dp integrations for the pure gases. Shall we utilize solely the data of Masson and Dolley, as did Gibson and Sosnick, or combine their single isotherms with the work of other investigators?

Another question also arises. In reporting such calculations, should fugacities themselves be reported or "free energies"? In the opinion of the writer confusion is to be feared in reporting free energies, for a convention has to be adopted quite other than the one adopted for free energy tables, whereas the convention in the case of the fugacity is a natural one and well established.

INCOHERENT SCATTERED RADIATION IN DIATOMIC MOLECULES

By F. Rasetti
California Institute of Technology, Pasadena

(Received June 15, 1929)

Abstract

Raman spectra excited in diatomic gases by the line λ2536 of mercury have been photographed with a quartz spectrograph. An apparatus for using gases at pressures from ten to fifteen atmospheres has been built, with great improvement as compared with the use of gases at atmospheric pressure. Results obtained with H_2, N_2, O_2, NO are reported. A particularly complete investigation has been made of the hydrogen spectrum, leading to an accurate determination of the constants of the molecule in the normal electronic state. The numerical values are (in cm^{-1}) $B_0 = h/8\pi^2 I_0 c = 59.40$; $\omega_{0/1} = 4162.1$. For N_2, the corresponding values resulted to be: $B_0 = 1.992$; $\omega_{0/1} = 2330.7$. For O_2: $B_0 = 1.436$; $\omega_{0/1} = 1554.7$. All these molecules are in Σ states, and the Raman spectra consist of Q-, double R-, and double P- form branches, as deduced from the Kramers-Heisenberg formula by the author and by Hill and Kemble. Nitric oxide is the only molecule so far investigated which is in a $^2\Pi$ state. The transition between the two terms of the doublet has been observed in the scattered radiation.

THE structure of the Raman spectrum for a diatomic molecule has been deduced from the quantum mechanical theory of dispersion by the author[1] and by Hill and Kemble.[2] It is easy to show, by means of the Kramers-Heisenberg formula, that rotational and vibrational transitions are to be expected in the scattering process for non-polar molecules also; and

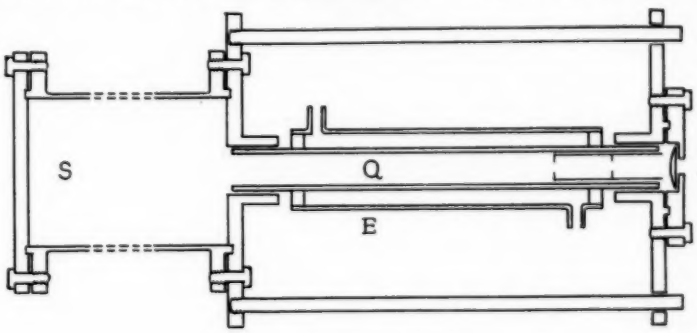

Fig. 1. High pressure tube.

that, if the molecule is in a Σ state, only transitions satisfying the selection rule $\Delta j = 0, \pm 2$ can take place, thus giving rise to Q-, double R-, and double P-branches. Hill and Kemble have worked out the theory more completely, to include a qualitative treatment of intensities and polarization.

[1] F. Rasetti, Proc. Nat. Acad. Sci., **15**, 234 and 515 (1929); Nature **123**, 757 (1929).
[2] E. L. Hill and E. C. Kemble, Proc. Nat. Acad. Sci., **15**, 387 (1929).

The author has already reported on the results of some experiments[1] in which the double R- and double P-form branches of the pure rotational bands, and unresolved Q-form branches of vibrational bands were recorded. Similar spectra have been obtained by Wood[3] in HCl.

The experimental arrangement has been considerably improved, bringing out new results. In order to avoid extremely long exposures, the intensity of the scattered radiation has been increased by the use of gases at pressures from ten to fifteen atmospheres. The apparatus was similar to the one which

Fig. 2. Raman spectrum of H_2, showing rotational and vibrational-rotational lines.

has been described,[1] except that it was built in such a way to stand the above-mentioned pressure. It will be sufficiently explained by Fig. 1. The illuminated part of the tube was made of thick-walled quartz Q, 2.2 cm internal diameter, and about 20 cm long. This quartz tube was fastened to a large steel tube S by means of sealing-wax. The external quartz tube E was filled with a solution of acetic acid in water, in order to absorb the $\lambda 1849$ radiation, which otherwise would have caused troublesome photochemical reactions in many gases (for example, the formation of ozone in oxygen).

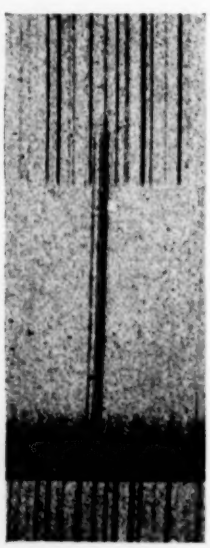

Fig. 3. Q-branch of the $0 \rightarrow 1$ band in H_2.

The primary source of light was a commercial mercury arc, 12 cm long. Water-cooling and deflecting the discharge by means of a strong magnet were employed as usual.

With the described apparatus, strong Raman spectra were recorded in exposures from 10 to 40 hours. The same Hilger quartz spectrograph as in the previous work was used.

Hydrogen

Spectrograms taken with H_2 at 12 atmospheres showed four positive and two negative rotational lines, and four lines in the Q branch, four in the positive branch, and two in the negative branch in the $0 \rightarrow 1$ vibrational band. Fig. 2 shows the appearance of the whole spectrum; Fig. 3 shows, much enlarged, the Q-form branch of the $0 \rightarrow 1$ band, resolved into four lines.

[3] R. W. Wood, Phil. Mag. **7**, 744 (1929).

Frequencies were measured by comparison with the iron spectrum. In measuring plates, I noticed that the position of the λ2536 line, as deduced from the symmetry of positive and negative rotational lines, was not exactly as given in the tables, that is 39412.6 cm^{-1}, but was shifted, and uniformly in all the plates, the observed value being 39411.1 cm^{-1}. I have considered it more correct to adopt this last value for the frequency of the exciting line in calculating Raman shifts.

The error in the measurement of the frequencies is believed to be always smaller than one frequency unit (except perhaps for a few weak lines). This follows both from the consistency of values from different plates, and from the agreement with the calculated values.

The energy E_{nj} of the nth vibrational and jth rotational state can be represented in first approximation by a formula of the following form:[4]

$$E_{nj}/hc+\text{const.}=\omega'_{0/n}+B_0'\left[1-\alpha(n+\tfrac{1}{2})\right](j+\tfrac{1}{2})^2-4(B_0'^3/\omega_0^2)(j+\tfrac{1}{2})^4$$

where B_0' is the value of $h/8\pi^2Ic$ for *zero* vibration, ω_0 the vibration frequency for zero amplitude, and α is a constant which measures the coupling between vibration and rotation. The frequency $\omega_{0/1}$ of the transition from the zero to the first vibrational state, and the moment of inertia, I_0, in the zero vibrational state and for zero rotation are evidently connected to the above used symbols by the relations:

$$\omega_{0/1}=\omega'_{0/1}-\alpha B_0'/4$$
$$B_0=h/8\pi^2I_0c=B_0'(1-\alpha/2)$$

Table I gives the calculated and observed values for 16 transitions (in cm^{-1}), using for the constants the values $\omega'_{0/1}=4162.8$, $B_0'=60.862$, $\alpha=0.0481$.

TABLE I. *Calculated and observed values for* 16 *transitions in the hydrogen molecule.*

n	j	ν calc.	ν obs.	difference
0→0	3→1	−587.3	−587.3	0
	2→0	−354.6	−354.5	−0.1
	0→2	354.6	354.1	−0.5
	1→3	587.3	587.5	+0.2
	2→4	814.4	814.4	0
	3→5	1033.9	1034.6	+0.7
0→1	0→0	4162.1	4162.1	0
	1→1	4156.2	4156.0	−0.2
	2→2	4144.5	4144.8	+0.3
	3→3	4126.9	4126.9	0
	0→2	4499.1	4498.4	−0.7
	1→3	4714.2	4713.3	−0.9
	2→4	4917.9	4917.8	−0.1
	3→5	5108.0	5109.8	+1.9
	2→0	3807.5	3807.4	−0.1
	3→1	3568.9	3568.9	0

From the difference between the observed and calculated values, I believe that we may assign the following limits of accuracy to the constants of the hydrogen molecule:

[4] A. Sommerfeld, Atombau, Wellenmechanischer Ergänzungsband, p. 29.

$$B_0 = 59.40 \pm 0.03$$
$$\omega_{0/1} = 4162.1 \pm 0.3$$

The intensities of the lines, so far as a qualitative inspection can tell, agree with those predicted by Hill and Kemble, including the fact that the Q-form branch of the vibrational band is more intense than the other branches, even when resolved into its components as is the case here. As to the ratios of the intensities of the lines in the same branch, we have to consider several factors, that is, the *a priori* statistical weights of the rotational states, the transition probabilities to rotational states of other electronic levels, and the Boltzmann distribution. The increasing statistical weight with increasing j partly compensates the Boltzmann factor and favors the higher rotational lines; then the fact that the odd rotational levels have three times the statistical weight of the even levels has to be taken into account. All this explains the observed distribution of the intensity. The $1 \rightarrow 1$ line is the most intense in the Q branch, the $1 \rightarrow 3$ line in the positive branches. These data on the normal state of the H_2 molecule are in very close agreement with those deduced by Hori[5] from the absorption bands in the far ultra-violet, $\omega_{0/1} = 4162.8$; $B_0 = 59.2$. Hori's value 4415 for ω_0 has been used in the correction term containing $(j+\frac{1}{2})^4$.

Nitrogen and Oxygen

No new features have been found in the Raman spectra of these molecules, but better plates (one of which is reproduced in Fig. 4) have been

Fig. 4. Raman spectrum of O_2

obtained. I give only the most probable values of the constants and of their uncertainty, as deduced from the consistency of the determinations from different plates:

$$N_2: \cdot \omega_{0/1} = 2330.7 \pm 2$$
$$B_0 = 1.992 \pm 0.005$$
$$O_2: \omega_{0/1} = 1554.7 \pm 1$$
$$B_0 = 1.436 \pm 0.005$$

Nitric Oxide

This molecule differs from all the others so far investigated in the Raman effect, being in a $^2\Pi$ state, with a separation of about 121 cm^{-1}. An inspection of the scheme of the $^2\Pi \rightarrow {}^2\Sigma$ absorption system[6] shows that here we have to

[5] T. Hori, Zeits. f. Physik **44**, 834 (1927).
[6] R. S. Mulliken, Phys. Rev. **32**, 388 (1928).

expect transitions with $\Delta j = 0, \pm 1, \pm 2$ which give a pattern of rotational lines too close to be resolved with the present apparatus. Therefore, we must expect continuous darkening of the plate near the exciting line. However, at a distance of 121 cm^{-1} from the exciting line, the intensity must increase suddenly, because we have, besides the transitions between rotational states of the lowest $^2\Pi_{\frac{1}{2}}$ level, also the transitions from those of the $^2\Pi_{\frac{1}{2}}$ to those of the $^2\Pi_{1\frac{1}{2}}$ level.

Nitric oxide was prepared by the action of acetic acid on a mixture of potassium nitrite and potassium ferrocyanide. It was used at atmospheric pressure and a very long exposure was necessary to obtain the spectrogram shown in Fig. 5. The darkening at the expected distance from the exciting line is clearly visible.

The measured shift is 119 ± 5, in agreement with the value deduced from the absorption bands.

In conclusion, I wish to express my thanks to Professor R. A. Millikan for the facilities of the Norman Bridge Laboratory placed at my disposal; and to the International Education Board, to whose grant of fellowship my vist to America was due.

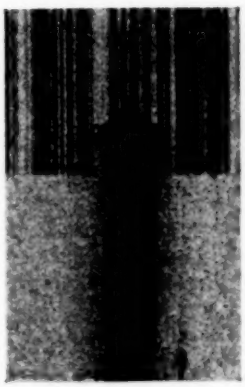

Fig. 5. Transition between the two terms of the $^2\Pi$ doublet in NO.

THE HEAT OF DISSOCIATION OF DIATOMIC HYDRIDE MOLECULES

WILLIAM W. WATSON*
LEIPZIG

(Received June 26, 1929)

ABSTRACT

The computation of the heats of dissociation for several diatomic hydride molecules from the vibrational data of their band spectra is given, as well as a brief discussion of an apparent discrepancy between these estimates and those deduced from the phenomenon of instability at high rotational speeds. This rotational distortion is attributed to an uncoupling action on the electronic angular momenta.

FOR many diatomic hydride molecular spectra it is difficult to apply the well-known method of Birge and Sponer for the determination of the heat of dissociation D because of the paucity of available data concerning the vibrational energy levels.[1] In some of these hydride spectra the anomalous behaviour of the rotational levels for the greatest speeds of nuclear rotation (examples; CaH, AlH bands) has been attributed to a high degree of molecular instability, and suggests the possibility of computing D from rotational data alone. Franck and Sponer,[2] in a recent discussion of several phenomena connected with the determination of heats of dissociation from band spectra, have considered this question, and have come to the conclusion that it is possible so to determine D from this maximum rotational energy in some cases where the excited electronic state is more unstable than the normal state.

There is evidence[3] that these diatomic hydrides are polar in character, thereby bringing somewhat into question the validity of the process of extrapolation of the known vibrational levels to zero separation in order to estimate D, a procedure which holds only for non-polar molecules. It is clear, however, that upon dissociation a neutral H atom results, since the excitation of the H atom involves much too large an energy. Therefore, even though the $\omega_n : n$ curve departs markedly from linearity, it should be possible to estimate the heat of dissociation, providing the data go to high enough n values to make evident the further course of the curve. It is of interest to note the accuracy of such calculations for some of the few hydride systems where the data are sufficient, and where a check on the findings exists. This check is to be found in the conservation of energy relation[4]

$$D''+E_a=E_m+D' \qquad (1)$$

* Fellow of the John Simon Guggenheim Memorial Foundation.

[1] For a detailed discussion of diatomic hydride spectra, reference should be made to recent articles by R. S. Mulliken in this journal, particularly Phys. Rev. **33**, 730 (1929).

[2] J. Franck and H. Sponer, Göttingen Nachrichten 1928, page 241.

[3] R. S. Mulliken, Phys. Rev. **33**, 737 (1929). R. Mecke, Zeits. f. Physik **42**, 393 (1927).

[4] H. Sponer, Ergebnisse der Exakten Naturwissenschaften, **6**, 84 (1927).

where D'' and D' are the dissociation heats in the lower and upper states respectively, E_a is the energy of the excited atom or atoms (only the M atom in our examples) resulting from the dissociation of the upper molecular state, and E_m is the molecular electronic energy for the band system. The quantities D'', D', and E_m are determined from the band spectrum analysis, and the resulting E_a should equal that of a (low-lying) excited level of the M atom.

Recently G. Nakamura[5] has reported a band system in absorption for LiH which, judging from its structure, is undoubtedly the predicted $^1\Sigma \rightarrow {}^1\Sigma$ principal combination for this molecule. Nakamura reports that the $\omega_n : n$ curve is linear for the vibrational levels in the normal state, yielding 2.56 volts for D'', but that for the excited state the spacing of the vibrational levels first increases to a maximum at $n' \leqq 7$, and then decreases in the usual fashion for higher values of n'. Such a spacing is unique among the recorded data for band systems but the necessary changes in the potential energy as a function of r, the internuclear distance, are comprehensible. The question of interest for us, however, is whether the area under this peculiar $\omega_n : n$ curve gives the correct value of D'. The extrapolation is not too long, for n'_{max} is but 30, whereas Nakamura has recorded the bands to $n' = 18$. The area under this curve is 1.1 volts, while the zero-point of the system (E_m) is given as 3.2 volts. Placing these values in (1), we obtain 1.74 volts for E_a. Now the predicted state for the Li atom in this dissociation process is the 2^2P resonance level at 1.84 volts. The discrepancy is only 0.1 volt.

The writer[6] and also E. Bengtsson[7] have studied an ultra-violet beryllium hydride band system, which, because of its singlet P, R branch structure and its definitely different lower state than that of the $^2\Pi \rightarrow {}^2\Sigma$ green BeH bands, has been thought to be due to the BeH^+ molecular ion. A computation of the heats of dissociation involved gives additional evidence in support of this conclusion. Bengtsson gives a more accurate vibrational energy level formula, including measurements of new bands. This formula contains a very appreciable term in n'^3, which is to be expected if the emitter is indeed BeH^+, while for the lower state the $\omega_n : n$ curve is quite linear. The resulting heats of dissociation are $D' = 2.52$ volts and $D'' = 3.66$ volts. Since the system origin, E_m, is at 4.87 volts, Eq. (1) gives $E_a = 3.73$ volts. Be II has its 2^2P levels at 3.93 volts, whereas the two lowest excited levels of Be I, 2^3P and 2^1P, lie at 2.84 and 4.84 volts respectively, thus making it rather certain, in view also of the other evidence just mentioned, that a Be^+ ion results from the dissociation of this molecule. The rough calculation as follows is also corroborative of the evidence for BeH^+. The analysis of the green BeH bands shows that there is scarcely any difference in the internuclear distance for the lower and upper electronic states ($r_0' = 1.34$, $r_0'' = 1.35$ A.U.), thereby indicating that ionized BeH is just about as stable as the neutral molecule.

[5] G. Nakamura, Zeits. f. Physikal. Chemie **B3,** 80 (1929), and Physikertag Jena, May, 1929. Article in press.

[6] W. W. Watson, Phys. Rev. **32,** 600 (1928).

[7] E. Bengtsson, Nature, **123,** 529 (1929).

Since only the $\Delta n = 0$ sequence is present in the green system, it is difficult to determine accurately D''. From the known [6,7] rotational constants of the $n'' = 0$ and 1 states, however, together with the formula $\omega_0^2 = -4B_0^3/D_0$ and the empirical relation $2 \cdot x \cdot B_0/\alpha = R \leqq 1.4$ given by Birge, it is possible to estimate the coefficients ω_0'' and $\omega_0'' \cdot x''$ of the n'' and n''^2 terms in the vibrational formula. One obtains in this way the values $\omega_0'' = 2025$ cm^{-1} and $\omega_0'' \cdot x'' = 38.47$ cm^{-1}, from which, assuming that the $\omega_n : n$ curve is linear for this lower state (probably the normal $^2\Sigma$ state of BeH), it follows that $D'' \leqq 25{,}650$ cm^{-1} or approximately 3.3 volts. This value is roughly about the same as the D'' computed above for the ultra-violet bands.

The vibrational constants of the analogous $^2\Pi \rightarrow {}^2\Sigma$ MgH band system are better known,[8] and give directly $D'' = 2.12$ volts as the heat of dissociation for the low $^2\Sigma$ state, and $D' = 2.18$ volts for the $^2\Pi$ state. These values placed in Eq. (1) give $E = 2.44$ volts as against 2.70 volts for the ^3P state of the Mg atom. The agreement here would probably be better if the course of the vibrational levels were known as well as for the LiH and BeH^+ systems cited above. Since in the corresponding CaH bands[9] only the 0, 0 and 1, 1 bands are known, the same difficulty in estimating D'' as in the case of the green BeH system presents itself. Employing the same rather crude methods again, however, with Hulthén's rotational data for the $n'' = 0$ and 1 vibrational states, one obtains $D'' = 1.9$ volts. There is apparently a decreasing stability of the $^2\Sigma$ normal state in passing down the series BeH, MgH, CaH, . . . HgH.

There is a rather large discrepancy for some molecules between values such as these for the heats of dissociation and those estimated from the phenomena of rotational distortion, the latter estimates being very much lower (0.6 volt for the low $^2\Sigma$ CaH level). It appears possible to explain some of these rotational distortions, such as the reverse bending of the branches of a band—examples; CaH, BeH, CH λ3143,[10]—as due to changes in the couplings of the electronic angular momentum vectors brought about by the nuclear rotation. Due to this uncoupling action, the molecule is perhaps in a state of "predissociation,"[11] quite a different situation from that of the non-rotating molecule dissociating because of its vibrational energy content. It is proposed to discuss later in some detail this rotational uncoupling phenomenon.

[8] W. W. Watson and P. Rudnick, Phys. Rev. **29,** 413 (1927). It is necessary to estimate the constants from the $n = 0$, 1, and 2 vibrational levels only.

[9] E. Hulthén, Phys. Rev. **29,** 97 (1927).

[10] R. Fortrat, C. R. **178,** 1247 (1925). This band has P, Q, and R branches which are very narrow doublets at the origin. Since the order of intensity is apparently $Q > P > R$, the R branch being so weak as to be undetectable at the origin, this may be the possible $^2\Sigma \rightarrow {}^2\Pi$ transition from a higher $^2\Sigma$ state than that of the λ3900 CH band to the same lower electronic level. Cf. F. Hund, Zeits. f. Physik **51,** 779 (1928), and R. S. Mulliken, Phys. Rev. **33,** 733 (1929).

[11] Cf. J. Franck and H. Sponer, ref. 2, especially their note 3, page 249, concerning the work of Bonhoeffer and Farkas.

LETTERS TO THE EDITOR

Prompt publication of brief reports of important discoveries in physics may be secured by addressing them to this department. Closing dates for this department are, for the first issue of the month, the twenty-eight of the preceding month; for the second issue, the thirteenth of the month. The Board of Editors does not hold itself responsible for the opinions expressed by the correspondents.

The Effect of Retardation on the Interaction of two Electrons

The problem of calculating positions of energy levels and probabilities of existing spectroscopic transitions is practically solved by the Dirac equation. As has been pointed out by Dirac even this simple case involves the fundamental difficulty of transitions to states with negative energy. It is hopeless at present therefore to have anything but an approximate treatment for two electrons since even one has not as yet been treated altogether satisfactorily. Nevertheless it seems reasonable to ask for a treatment correct to the order $(v/c)^2$. This is the approximation involved in the discussion of most problems of fine structure in spectroscopy.

In a paper which is to appear soon in this Review such an equation is set up. It is

$$\{p_0+\sum_{k=1}^{3}(\alpha_k^{\mathrm{I}}p_k^{\mathrm{I}}+\alpha_k^{\mathrm{II}}p_k^{\mathrm{II}})+(\alpha_4^{\mathrm{I}}+\alpha_4^{\mathrm{II}})mc+(e^2/2cr)(\sum_{k=1}^{3}\alpha_k^{\mathrm{I}}\alpha_k^{\mathrm{II}}+\sum_{k,i=1}^{3}\alpha_k^{\mathrm{I}}(x_k^{\mathrm{II}}-x_k^{\mathrm{I}})\alpha_i^{\mathrm{II}}(x_i^{\mathrm{II}}-x_i^{\mathrm{I}})/r^2)\}\psi=0$$

where $p_0=-(h/2\pi i)\partial/c\partial t+(e/c)(A_0^{\mathrm{I}}+A_0^{\mathrm{II}})-e^2/cr$; $p_k^{\mathrm{I}}=(h/2\pi i)\partial/\partial x_k^{\mathrm{I}}+(e/c)A_k^{\mathrm{I}}$; $p_k^{\mathrm{II}}=(h/2\pi i)\partial/\partial x_k^{\mathrm{II}}+(e/c)A_k^{\mathrm{II}}$, $r=[(x_1^{\mathrm{II}}-x_1^{\mathrm{I}})^2+(x_2^{\mathrm{II}}-x_2^{\mathrm{I}})^2+(x_3^{\mathrm{II}}-x_3^{\mathrm{I}})^2]^{1/2}$

and where A_0^{I} A_0^{II} are respectively the scalar potentials due to the external field for the coordinates $(x_1^{\mathrm{I}}\ x_2^{\mathrm{I}}\ x_3^{\mathrm{I}})$ and $(x_1^{\mathrm{II}}\ x_2^{\mathrm{II}}\ x_3^{\mathrm{II}})$ of the electrons I and II. The same convention is used for the vector potentials A_k^{I}, A_k^{II}. The above equation is derived in two ways. It is shown that in the configuration space of two electrons the relations between the momenta and the velocities $c\alpha_k^{\mathrm{I}}$, $c\alpha_k^{\mathrm{II}}$ are precisely those found by Darwin[1] for two electrons in the classical theory. It is also shown that the unified quantum theory of electrodynamics and matter recently developed by Heisenberg and Pauli leads to a first approximation in the Coulomb interaction to the same result as the equation just written. From the point of view of the later theory it becomes clear that another restriction should be made. The above equation applies only if the electrons in question are sufficiently close together to make $2\pi r/\lambda \ll 1$ where r is the distance between the electrons and λ is the shortest wave length of the term values of the electrons.

Presupposing the validity of the equation having 16 components it is reduced to a form involving only four. In this form the interactions of electronic spins with each other and with the orbits appear with the correct numerical factors used by Heisenberg in his discussion of the He fine structure. In addition another term of the same order of magnitude as the interaction of the electronics spins is found. It is hoped that its existence can be checked by an exact calculation of the proper functions of the ^2p state of He. For elements of high atomic number the effects of the interaction of electronic spins and of the new term are negligible and only the well known orbital spin interactions remain.

G. Breit

Department of Terrestrial Magnetism,
Carnegie Institute of Washington,
July 1, 1929.

[1] C. G. Darwin, Phil. Mag. **39**, 537 (1920).

An Isotope of Carbon, Mass 13.*

The bands belonging to the Swan spectrum of carbon appear in the vacuum electric furnace at about 2400°C. At temperatures above 2600° they are strong and clear-cut, even the the band at λ6191, difficult to obtain in the carbon arc, being well defined. It has been noted by one of us, during a variety of electric furnace investigations, that plates on which the band at λ4737 is very strong showed a faint band, not to be ascribed to a ghost, about 7.5A to the red of the strong band. The carbon arc shows a scattered structure in this region, which is suppressed in the furnace. It has however thus far failed to give the faint band, which in the furnace spectrum shows a distinct structure, essentially identical with the structure of the main band.

The recent discovery of isotopes of oxygen makes it very probable that other similar elements contain isotopes in small quantities. We have accordingly measured this faint band very carefully, using a first order exposure of a 15 ft. concave grating, the furnace being at about 2800°C. It is now generally agreed that the Swan bands are due to the neutral C_2 molecule, presumably $C^{12}-C^{12}$. We find that the new faint band corresponds quantitatively to that which should be given by an assumed $C^{13}-C^{12}$ molecule. The constants of the Swan band system are known with great precision (Int. Crit. Tables, V, 411, and J. D. Shea, Phys. Rev. 30, 825, 1927), and an accurate comparison with theory is therefore possible. With data of the precision now becoming available for oxygen, as well as in the present case, it is necessary to avoid various approximations which have commonly been used in previous work on isotopes. This will be fully discussed in later publications.

Because of the irradiation due to the strong band, it is to be expected that the measured distance between the two *heads* will be slightly *smaller* than the calculated isotope shift for the head. This is in fact the case, this distance being measured as 2.020 mm (=7.520A= 33.44 cm^{-1}) as compared to a calculated isotope shift of 2.028 mm (33.58 cm^{-1}). Fortunately, however, it is possible to distinguish six individual lines in the very faint isotope band. These have been identified as the unresolved triplets P_{26} to P_{31} (Shea's nomenclature). In the comparator P_{30} and P_{29} could be measured with reasonable accuracy, P_{28} and P_{27} less reliably, P_{26} very poorly, and P_{31} not at all. The corresponding triplets in the main band, also unresolved, could be measured with great precision. The observed isotope shifts in mm for P_{30} to P_{26}, with the calculated in parenthesis in each case are 2.059 (2.0515), 2.049 (2.0473), 2.037 (2.0429), 2.033 (2.0395), and 2.044 (2.0373) respectively. Multiplication by 16.58 gives the shift in cm^{-1}. The two good lines (P_{30} and P_{29}) give an average measured shift 0.082 cm^{-1} too large. Although with the present available data the fact may have no significance, it is interesting to note that this small discrepancy may be cancelled by assuming 12.0000 and 13.0026 for the two masses.

This 1–0 band (λ4737) is especially favorable for showing the faint isotope molecule, when one considers photographic intensity, position with respect to other bands (particularly CN) and size of the shift. We shall endeavor to get better plates, showing the isotope effect in other bands, and also showing more detailed structure. The present evidence seems however fully sufficient to establish the existence of an isotope of carbon, of mass 13. We cannot at this time make any statement as to its relative abundance, except to say that the isotope band is hundreds of times as faint as the strong band.

ARTHUR S. KING
RAYMOND T. BIRGE

Mount Wilson Observatory,
Carnegie Institute of Washington,
and
Phycial Laboratory,
University of California,
June 24, 1929.

*See later communication, page 379.

The Raman Effect of Ketones

A study of the Raman effect in three ketones, dimethyl (acetone), methylethyl, and diethyl, has been made in the manner described by Wood (Phil. Mag. October 1928). The spectrograph was a Hilger constant deviation instrument which gave a spectrum about 30 mm long from 3900A to 4900A. Eastman process plates were found to be the most satisfactory as they brought out the faintest lines in exposure-times of from twenty

to twenty-five hours. A copper arc comparison spectrum was used in making wave-length determinations. The lines were measured with a comparator to an accuracy of at least 0.005 mm, or about two wave-numbers at 4500A.

by Coblentz and LeComte. The number of the exciting line and the relative intensity of the Raman line due to each shift is also included. The intensity estimates do not take account of the variation of the sensitivity of the plate in different regions.

TABLE I. *Dimethyl ketone (acetone). S=sharp; D=diffuse; D+=very diffuse. Exciting lines: 1—3650; 2—3655; 3—4046; 4—4358.*

Exciting line	Shift in wave-number	Relative intensity	Infra-red wave-length (μ) Calculated	Observed Coblentz	Observed Le Comte
1	2928 cm^{-1}	4*S*			
2	2930	4*S*	3.42	3.40	3.41
3	2929	6*S*			
4	2921	4			
3	1717	2*S*	5.82	5.80	5.90
4	−1430	3*D*	6.97	7.00	7.07
4	1433	1*D*			
3	1222	2			
4	1222	2*D*+	8.18	8.18	
3	1064	1	9.40		
4	1077	1*D*	9.30	9.20	
4	795	6*S*	12.58		
4	−792	1	12.61		
3	787	5*S*	12.70	12.70	
4	534	1	18.75		
4	487	0	20.50		

TABLE II. *Methylethyl ketone.*

Exciting line	Shift in wave-number	Relative intensity	Infra-red wave-length (μ) Calculated	Observed Le Comte
1	2947 cm^{-1}	3*S*		
2	2948	3*S*	3.39	
1	2928	3*S*		
2	2930	3*S*		
3	2928	6*D*+	3.42	3.45
4	2928	3*D*		
4	1734	3	5.77	5.91
4	−1429	2*D*	7.00	
4	1444	2*D*	6.92	7.07
4	−1360	0*D*		
4	1351	1*D*		
3	1292	0	7.75	
4	1213	0*D*+	8.23	
3	1165	0	8.58	8.50
3	1085	4	9.22	9.70
3	955	0	10.47	10.90
4	768	3		
4	−763	0	13.10	13.60
3	760	6*S*		
4	*593	2	1351−760=591	
4	*406	0	1165−760=405	
4	*316	1	1087−760=327	

Tables I, II, and III give a comparison of the observed shifts in frequency with corresponding infra-red frequencies as observed

It is interesting to note several things in connection with the tables. For several lines (starred) whose shifts are small, it is assumed

TABLE III. *Diethyl ketone.*

Exciting line	Shift in wave-number	Relative intensity	Infra-red wave-length (μ) Calculated	Observed Le Comte
1	2947 cm^{-1}	4		
2	2948	4	3.39	
3	2910	3*D*		
4	2928	2*D*	3.42	3.45
4	1724	2*S*	5.80	5.92
4	1468	2	6.92	6.92
4	1428	2	7.00	7.10
4	−1360	1*D*	7.35	7.47
3	1232	0	8.10	
4	1224	1	8.16	
4	1180	3	8.48	
3	1095	3*S*	9.14	
3	1018	1*D*	9.83	
4	−801	1*D*	12.50	
4	794	0*D*	12.60	
3	786	2	12.70	
4	760	0*D*	13.60	
3	748	1	13.30	
4	*410	3	1180 − 786 = 394	

that absorption takes place while the molecule is in an excited state, so that the resulting Raman line differs in frequency from its exciting line by the difference of the infra-red frequencies of an initial excited state and a final state. The probability of such transitions has been suggested by Langer (Nature, March 9, 1929), although the Raman lines due to such transitions should be weak in intensity, since the absorption from a state is proportional to the number of molecules in that state, and ordinarily the number of molecules in an excited state is small.

The ketones as contrasted with the acids and aldehydes are characterized by an infra-red absorption band at 5.80–5.90μ which is attributed to the C=O band. Raman lines whose frequency shifts corresponded to an absorption band of this wave-length were found for the exciting line 4358A in the case of each of the three compounds. The Raman lines shifted from 4046 by this amount would have fallen on the region of 4358A which was greatly over-exposed.

Raman lines whose frequency shifts corresponded to the infra-red frequency of the fundamental C−H band at 3.42μ were the most intense. The ketones were C.P., obtained from the Eastman Laboratories.

In acetone, all four exciting lines, 3650A, 3655A, 4046A, and 4358A, gave rise to lines shifted by nearly 2928 wave-numbers, the Raman line being sharp in each case. In diethyl ketone, exciting lines 3650A and 3655A gave rise to Raman lines shifted by 2948 wave-numbers which were quite sharp. Exciting lines 4046A and 4358A gave rise to diffuse lines whose shift was about 2928 cm^{-1}. Methylethyl ketone had two lines scattered from 3650 A and two from 3655A. One line in each case was shifted by 2928 cm^{-1} and one by 2948 cm^{-1}. Exciting lines 4046A and 4358A gave rise as in diethyl to diffuse Raman lines of nearly 2928 cm^{-1} shift.

It seems then that the C−H binding in the methyl group rives rise to a rather sharp band at 3.42μ. The ethyl group, however, seems to have a complex band at this point. In addition to a maximum at 3.42μ, it has another at 3.39μ. The diffuseness of the Raman lines due to 4046A and 4358A scattered by absorption corresponding to these two maxima are then probably due to the fact that the Raman lines were not resolved by the spectrograph in the region of longer wave-lengths where they fell.

NEILL G. WHITELAW
Laboratory of Physics,
University of Wisconsin,
June 26, 1929.

Further Evidence of the Carbon Isotope, Mass 13

A few days ago Dr. King and I announced the discovery of an isotope of carbon, mass 13, appearing in the λ4737 Swan band of neutral C_2. Since then I have found this isotope in two additional sources, viz., in Hopfield's absorption spectrograms of CO, and in King's furnace (emission) spectrogram of the λ3883 CN band.

Two years ago J. J. Hopfield and the author presented to the American Physical Society (Phys. Rev. **29**, 922, 1927) an analysis of the emission and absorption spectra of carbon monoxide, based on extensive experimental material obtained by Professor Hopfield with his vacuum spectrograph. The most complete absorption system is the fourth positive group, in which we were able to measure the bands from 0–0 to 15–0 (λλ1544 to 1199). These bands degrade to the red, and it was noted at the time that a faint second head appeared to the red of each main head, at a systematically increasing distance. We were however not able to fit these heads into the band system. I have now carefully measured these second heads and find that they agree quantitatively with C^{13}–O^{16} as an assumed source. The heads can be measured with reasonable certainty in all the bands from 2–0 to 15–0, with the exception of two for which emission lines interfere. The calculated isotope shift, using reliable vibrational constants obtained by Professor Hopfield and myself, varies from 0.072 to 0.273 mm (55 to 316 cm^{-1}). The arithmetic average *obs*−*calc* value is 0.0035 mm and the algebraic average 0.0017 mm, in the sense that the observed shift is very slightly less than the calculated.

If the C^{12}–O^{18} molecule is also present, its absorption bands should lie to the *red* of the C^{13}–O^{16} band heads, by amounts varying from 0.006 to 0.024 mm. It is thus impossible, with the present spectrograms, to separate the two isotopes. In all cases the observed C^{13}–O^{16} head is wide enough to include a possible C^{12}–O^{18} head. Thus the evidence is conclusive that C^{13}–O^{16} is present, but is strictly neutral as to C^{12}–O^{18}.

The second source of information is King's furnace spectrogram of CN λ3883 (Astrophys. J. **53**, 161, 1921). Dr. King kindly loaned me all his CN furnace spectrograms, for my work on temperature and band spectra (Astrophys. J. **55**, 273, 1922), and I still have this material. He called attention (page 162, loc. cit.) to a very faint series of doublets lying between λ3872 and λ3876. I measured these roughly, in connection with my temperature work—but was unable to fit them into the band structure. I found, however, that two of the six doublets had been observed by Kayser and Runge, in the arc spectrum. I now find that these six doublets are the isotope lines P_{56} to P_{61}, due to C^{13}–N^{14}. They have the same doublet separation as the main doublets, and lie just to the red, in each case. In calculating the vibrational shift I have used the constants based on Heurlinger's original analysis, as calculated by Kratzer (Ann. d. Physik **71**, 72, 1923). For the rotational shift I have used new constants determined by R. T. Birge and W. O. Smith, in an unpublished quantum analysis of this band. The calculated shift varies from 0.228 to 0.451 mm (0.877 to 1.739 cm^{-1}).

Although the isotope lines are very faint, they can under favorable mechanical conditions be measured with reasonable acuracy. Excluding P_{56}, which lies too close to its parent line to measure properly, the observed isotope shift averages 0.014 mm greater than the calculated, with an average deviation from the mean of only 0.0033 mm. This indicates a small error in the vibrational constants, or an electronic shift of this magnitude (0.05 cm^{-1}). The latter explanation seems the more reasonable. The calculated isotope lines based on either C^{12}–N^{15} or C^{12}–N^{16} lie far outside the limits of error. There are definitely no other isotope lines observable in this region of the band, so that one may conclude that if isotopes of nitrogen exist, they are much less abundant, compared to N^{14}, than is C^{13} compared to C^{12}.

RAYMOND T. BIRGE
University of California,
June 29, 1929.

The Comet-tail Bands*

On plates obtained by passing a high frequency electrodeless discharge (10,000 kilocycles) through commercial nitrogen at about 10^{-4} mm pressure, it was found that nearly

* Released for publication by the Navy Department.

the entire spectrum from 2000A to 7000A was made up of the band spectrum of carbon monoxide. The tubes had been very carefully prepared, having been well cleaned and baked out. The CO was present therefore only as an impurity in the commercial nitrogen and at a total gas pressure of 10^{-4} mm, the partial pressure of the CO must have been less than 10^{-6} mm. Similar results were obtained when air or oxygen were used instead of nitrogen.

The spectrum of CO that was obtained in this manner has many striking characteristics. The only one, however, to which attention will be called here is the one pertaining to the comet-tail bands. These bands are now definitely attributed to CO^+ and they were first observed by A. Fowler in low pressure CO. Since their observation by Fowler these bands have been studied by Baldet, Merton and Johnson, and others.

Using a low dispersion instrument it was found that in the region from 4900 to 6300A the centers of the most intense bands agreed remarkably well with the measurements of Pluvinet and Baldet on the spectrum of Comet Morehouse. This agreement is interesting since the photographs of Pluvinet and Baldet were obtained with a prismatic camera and their measurements are thus to be compared only with spectra photographed with small dispersion.

On using larger dispersion an interesting fact was revealed. Fowler reported four bands having wave-lengths of 5510, 5473, 5078 and 5049A. These bands have since been identified with the bands of the comet-tail group lying at 5504.7, 5466.8, 5075.9 and 5043.8. These bands consist of narrow doublets that degrade to the red and only the long wave-length heads are given here. On our plates the doublet at 5504.7 is very intense, but in addition there is a band at 5510A which does not appear to be a comet-tail band. We do not observe the doublet 5466.8 with which Fowler's band at 5473 was identified, but there is a very intense band at 5473A which does not at all resemble the comet-tail bands. The doublets at 5075.9 and 5043.8 are very intense and beautifully developed on our plates. There is also an extremely intense band at 5052A which agrees with the 5049 band of Fowler to within the errors of Fowler's measurements in this region. This band also is not a member of the comet-tail group. There are several weak bands on our plates that agree very well with several of the bands in Comet Morehouse that have not been reported in terrestrial spectra. It has not been possible so far to determine the direction of degradation of the bands 5570, 5473 and 5052 and further study with larger dispersion is necessary.

It is interesting to compare these experiments with those of Merton and Johnson in which the comet-tail bands were excited in a small amount of CO mixed with helium at 20 or 30 mm.

L. H. Dawson
Joseph Kaplan
Naval Research Laboratory,
"Bellevue," Anacostia, D. C.
July 9, 1929.

The Molecular Scattering of Light from Solids. Plate Glass

The scattering of visible light with change of frequency was first observed in the case of pure liquids.[1] There was also discovered, independently and simultaneously, a similar scattering of light from solids.[2] This scattering has become known as the Raman effect. It is the purpose of this communication to report the results of a study of the Raman effect from ordinary plate glass, a substance which contains about 80% pure fused silicon dioxide, the remainder being made up of various other oxides. The results are as yet preliminary in character. There can, however, be no doubt concerning the presence of the Raman lines which are reported since they have been scattered from a number of samples of glass of various ages and have always made their appearance. They are of interest in connection with papers by Pringsheim and Rosen[3] and by Czerny[4] in which the Raman effect in pure crystalline quartz has been studied. Czerny has discussed frequency differences between the exciting and excited lines which correspond to infra-red absorption bands at 8.6, 12.5, 14.2, 21.5, 24.7, 38.2, 48.0,

[1] Raman and Krishnan, Nature **121**, 501, 619, 711; **122**, 12, 169, 278, (1928).

[2] Landsberg and Mandelstam, Naturwiss. **16**, 557, (1928).

[3] Pringsheim and Rosen, Zeits. f. Physik **50**, 741 (1928).

[4] Czerny, Naturwiss. **17**, 12 (1928).

80, 94, and 118μ. Pringsheim and Rosen state that while it was possible to observe the effect in crystalline quartz they could find no such effect in fused quartz.

There appears to be no reason, theoretical or otherwise, why fused quartz should not give a Raman effect. Indeed it will be evident from the data to be presented that the lines observed from plate glass must be identified with the infra-red spectrum of fused quartz which has been studied by Reinkober.[5] The transmission versus wave-length curve given by Reinkober shows absorbtion bands at 4.3, 5.4, 6.1μ, and a continuous region of absorption between 7.8 and 10μ.

It appears then that the lines observed have been caused by light quanta which have lost a part of their energy in encounters with silicon dioxide molecules, in other words the lines obtained are to be identified with fused quartz. The infra-red absorption bands of Reinkober at 4.3, 5.4, and 6.1μ all make their appearance. The plates also indicate the presence of the continuous region of absorption between 7.8 and 10μ, there being a very diffuse blackening of the plate between the Raman lines corresponding to 7.74 and 9.3μ which have been recorded in the table. These lines correspond to maxima in the intensity of the blackening in this region.

TABLE I. *Raman effect from plate glass: λ is the wave-length of Raman lines; ν the wave number of Raman lines; λ_{Hg} the wave-length of exciting lines; ν_{Hg} the wave number of exciting lines; $\Delta\nu$ the frequency difference between excited and exciting lines; λ_{RA} the wave-length in μ calculated from frequency differences; λ_{IR} the position of observed infra-red absorption bands in μ. Observer: R = Reinkober, fused quartz; C = Czerny, crystalline quartz (calculated from Raman lines).*

λ	ν	λ_{Hg}	ν_{Hg}	$\Delta\nu$	λ_{RA}	λ_{IR}	Observer
4748	21056	4359	22937	1881	5.33	5.4	R
4698	21280	4359	22937	1657	6.03	6.1	R
4619	21644	4359	22937	1293	7.73	7.8–10	R
4572	21866	4359	22937	1071	9.33	7.8–10	R
4513	22152	4359	22937	785	12.74	(12.5	C)
4513	22152	4078	24515	2363	4.23	4.3	R
4463	22400	4046	24709	2309	4.33	4.3	R
4410	22669	4359	22937	268	37.3	(38.2	C)
4410	22669	4078	24515	1846	5.42	5.4	R
4305	23222	4078	24515	1293	7.74	7.8–10	R
4229	23640	4046	24709	1069	9.35	7.8–10	R

The method used in photographing the spectra is exactly that which has been described in a previous article,[6] except that the tube containing the liquid has been replaced by a flat section of the plate glass. For this work a small Steinheil glass prism spectrograph was used. It was necessary to expose the plates about five times as long as is necessary to obtain a distinct Raman spectrum for a liquid, acetone or chloroform for example. The source of light was a 220-volt D. C mercury vapor arc. The lines, which were faint at best, were measured by means of a Gaertner comparator. The results of a number of observations on plate glasses of varying ages, but, as far as the authors are aware, of like composition are given in Table I.

The Raman lines scattered from plate glass which have been observed by us to date are eleven in number. Of these, nine correspond to infra-red absorption bands whch have been directly observed for fused quartz by Reinkober. The other two lines correspond approximately at least to Raman lines which were reported by Czerny to have been found to be scattered from crystalline quartz.

The data of this article are of interest in another connection. Experimental studies of the Raman effect are making their appearance so rapidly that certain of them appear to be improperly controlled. An obvious source of error, one which, however, seems to have been made in several cases, is the mistaking of the very weak lines of the mercury spectrum for Raman lines. It may also occur in the study of the effect in cases where longer exposures are necessary that lines caused by the containing vessels may be mistaken for lines caused by the substance under investigation. Thus, the complete Raman spectrum for a solution can probably be determined only after the lines caused by the glass or quartz containing vessel have been accounted for.

It is our purpose to continue this study, extending it to glasses of known and varying chemical content, and to compare the results with those for pure fused quartz and those which have already been obtained for crystalline quartz. These data will be communicated at a later date.

ALEXANDER HOLLAENDER
JOHN WARREN WILLIAMS

Department of Chemistry,
University of Wisconsin,
July 6, 1929.

[5] Reinkober, Ann. d. Physik **33**, 343 (1911).

[6] Williams and Hollaender, Proc. Nat. Acad. Sci. **15**, 421 (1929).

BOOK REVIEWS

Donneés Numériques d'Electricité Magnétisme et Electrochimie. By R. Audubert, Ch. de Massacre, A. Buffat, L. Durand, G. Foex. Extrait du Vol. VI des Tables Annuelles de Constantes (1923–1924)-I Vol. in-4° de 174 p. Prix: Relie, 90 Fr.; Broche, 70 Fr. Gauthier-Villars and Company, 55 Quai des Grands-Augustins, Paris VI°

This volume is a reprint of a certain number of the chapters contained in Volume VI of the Tables Annuelles de Constantes (1923-1924). It contains data on the following:

Electricity: Electrical conductivities, dielectric constants, thermoelectric effects; electrotechnics (insulation leakage, dielectric loss, breakdown voltage, current carrying capacities of bare and insulated wires, heating of electrical machines).

Magnetism: Influence of impurities and heat treatment upon magnetic properties of ferromagnetic metals, permanent magnets, magnetic viscosity, magnetostriction, para- and diamagnetism (gases, solutions, compounds). Atomic moments, magnetochemistry, magneto-optics, Hall effect.

Electrochemistry: Conductivity of electrolytes, electromotive forces, contact potentials, decomposition potentials, over-voltage, oxidation-reduction potentials, electrometric titrations.

John T. Tate

Handbuch der Experimentalphysik. Wien und Harms. Band 13, Teil I. Die Ionenleitung in Gasen, Shweidler. Teil II. Die Elektrischen Eigenschaften der Flamme, Becher. Pp. 314, figs. 55. Akademische Verlags gesellschaft. Leipzig, 1929. Price 29.60 RM.

The first part of this book contains about 100 pages on the electrical conductivity of gases and the second part 200 pages on the electrical conductivity of flames. Both parts are well written and give a very useful summary of available information with full references to original sources. The descriptions given are brief and in many cases could have been improved by being made longer. A reader who wishes thoroughly to understand the subject will probably find it necessary to refer to the orginal papers in many cases.

Experimental methods are described without much discrimination between good and bad methods. For example the method of measuring the current through an ionized gas, by allowing it to charge a condenser and then discharging the condenser through a ballistic galvanometer, is described fully with a diagram as though it was an important method.

The history given of the earlier determinations of the ionic charge e is inadequate. The method of measuring e by means of charged droplets in a vertical electric field is wrongly attributed to Millikan and Ehrenhaft.

On page 117 some very good photographs of the deflection of metal vapors in a flame by an electric field are reproduced. These seem to show that the vapor is attracted by the negative electrode.

The measurements of the conductivity of alkali metal vapors in flames using cold electrodes, by Zachmann are very fully described. With cold electrodes nearly all the potential drop occurs in the layers of cold gas at the electrodes so that the potential gradient in the flame is very small. Zachmann's results are very different from those obtained by other observers who used hot platinum electrodes and no adequate explanation of the difference has been suggested. Zachmann's claim that his method is superior seems doubtful.

The account of the Hall Effect in flames is not very good. Marx' early experiments are described in detail but the later work using greatly improved methods is only briefly mentioned.

The defects of the book are mainly such as can be put down to lack of space and are not serious. The full references to original sources and the valuable critical discussions of many important parts of the subjects treated make the book a very useful one.

H. A. Wilson

Acoustic Experiments with the Pin-Hole Probe and the Interferometer U-Gauge. CARL BARUS. Pp. 158+x, 288 figures. Published by the Carnegie Institution of Washington, November 1927.

This monograph by the Emeritus Professor of Physics at Brown University presents in detail a vast number of interesting experiments forming an extension of his first work with the pin-hole probe described in Carnegie Institution of Washington Publication No. 310. Some ten years ago Barus discovered that if a narrow tube with a pin-hole orifice (generally of a conical shape) is inserted in a vibrating a column while its other end is connected to one arm of an interferometer U-gauge, measurable static pressure differences (e.g. as much as 300 dynes/cm²) can be observed when the pin-hole is at a displacement node. This affords a direct experimental method of exploring the pressure distribution in a sound field. The present work is not theoretical but describes in straightforward inductive fashion with the liberal use of graphs the behavior and use of the probe under widely varying experimental conditions.

The probe is first applied to study the standing wave patterns in short narrow tubes excited by telephone diaphragms at the two ends. The attempt is made to use the results in the acoustical measurement of inductance but without great quantitative success. Evidence is shown, however, of resonance between electrical oscillations in the telephone circuit and the acoustical oscillations in the tube. The use of probes in pairs is next studied in detail and much information is obtained as to the effect of the type of opening. The theory of the probe's action still remains rather obscure, though there seems to be no doubt that it is due to complicated vortex motions in the vicinity of the opening.

The remainder of the monograph treats of experiments with larger air blown pipes in which the observed acoustic pressures attain values well over 500 dynes/cm². Conical horns are also investigated with the probe, and there is a short final chapter on miscellaneous experiments mainly concerning the pressure associated with the electric wind.

The reviewer considers it unfortunate that frequencies are everywhere referred to the musical scale instead of being given in cycles per second. And in general a slight change to more modern notation would render the results more easy to follow. Nevertheless there seems to be no question but that this text contains a vast amount of interesting and useful acoustical data which should prove a challenge to the theoretical worker in acoustics.

R. B. LINDSAY

Vom Erz zum Metallischen Werkstoff. DR. W. GUERTLER AND W. LEITGEBEL. Pp. xxiii+426, 176 diagrams and 30 tables. Akademische Verlagsgesellschaft m. b. H. Leipzig, 1929. Price, bound RM 32.

This is the first volume of a projected series entitled Der Metallische Werkstoff, Gewinnung, Behandlung, Veredlung, to be edited by W. Guertler. The text of the present volume was written by W. Guertler, and the numerous figures and tables were supplied by W. Leitgebel.

The book was evidently largely inspired by the difficulties in which the German metallurgist has found himself because of the readjustments of the war, and the necessity for conducting his craft with the absolute maximum of intelligence if he is to maintain his economic position. It aims to give a survey of all the factors involved in any of the operations after the removal of the ore from the ground up to the production of the pure metal or alloy ready to be turned into the finished product, in such completeness that the student will be able to understand the various steps and to adapt himself to changing conditions in practice. For example, an extensive discussion is given of the physical chemistry involved in ore reduction, and in particular of the way in which equilibrium shifts when the nature and physical conditions of the gaseous atmosphere are altered. Naturally in a book of this character all the details of the theoretical discussion cannot be given, and emphasis is laid on the approximate behavior under practical conditions. The physicist will find much of interest mentioned incidentally, and in particular will find convenient the extensive tables of various properties of pure metals and alloys.

P. W. BRIDGMAN

An Introduction to Crystal Analysis. SIR WILLIAM [H.] BRAGG. Pp. viii+168, figs. 105, plates 8. D. Van Nostrand, New York, 1929. Price $4.25.

This little book records a series of lectures delivered at Aberystwyth in the autumn of 1926. It is frankly selective, but most of the phases of crystal analysis by the use of x-rays are sufficiently explained for clear understanding and some methods are worked out in detail. Perhaps the most valuable feature to the specialist in the subject is the novelty of some of the ways in which new concepts are developed. The treatment of two-dimensional space-groups is particularly striking. The author expresses every idea in English which it is a pleasure to read. The only really difficult bits occur when the inadequacy of some of the diagrams makes it necessary to present a tricky geometrical argument in words. It looks as though the author had in such places cut his text to fit ready-made pictures (lantern-slides?). This suspicion grows when it is noticed how widely the figures vary in style and excellence. The technically trained reader whose main interests lie else-where will find the book of value in pointing out how the study of crystal structures is progressing into related domains and in giving a very fair account of the state of the subject a short time ago. The paper is good, the typography and binding only passable, considering the price.

L. W. MCKEEHAN

Handbuch der Experimentalphysik. WIEN AND HARMS. Bd. XXIII. **Phosphoreszenz und Fluoreszenz.** P. LENARD, F. SCHMIDT AND R. TOMASCHEK. Pp. 741+xxiii, 162 figs. Akademische Verlagsgesellschaft, m.b.H., Leipzig, 1928. Price bound RM 71.

This volume of Wien and Harms' Handbuch really forms two volumes, each of which contains more than 700 pages. The whole of the first volume and half of the second are devoted to phosphorescence and fluorescence. The work thus forms the most extensive treatise on luminescence that has yet appeared. While there are relatively short chapters on the fluorescence of gases and of solutions, on triboluminescence, and on chemiluminescence (including the luminescence of living organisms) the work deals chiefly with the luminescence of solid solutions and more particularly with phosphors of the Lenard and Klatt type. The treatise cannot therefore be regarded as a balanced treatment of the whole field. But the loss in breadth and perspective is offset by the fact that the book gives an authoritative and unified presentation of the almost unbelievably extensive investigations of Lenard and his associates, which have contributed so much to development of our present day views regarding radiation. It should not be forgotten that the first suggestion that absorption and radiation are accompanied by electron transitions occurs in one of Lenard's papers on luminescence and came as a natural result of his attempts to find an explanation of the behavior of the Lenard and Klatt phosphors.

The book is not easy reading; nor is the arrangement such as to make it easy to find the experimental material bearing upon any particular class of luminescence phenomena. In the opinion of the reviewer the book would be more useful if the material were presented in more compact form and if greater stress were laid on the experimental facts rather than on their interpretation. Before going far, however, in adverse criticism one should remember the extremely difficult position in which the subject of luminescence now finds itself. An enormous amount of experimental material has been accumulated, much of it obviously of great significance. Especially in the European laboratories there is evidence of greatly increased interest in this field. But a really satisfactory theory of luminescence, which may serve as an aid in correlating the observed phenomena and as a guide in planning new investigation, is still lacking. Workers in the field of luminescence will appreciate the difficulties that the authors have had to contend with in presenting the complex experimental material in systemmatic form and will find this book extremely useful.

ERNEST MERRIT

Zur Nomenklatur der 32 Kristallklassen. FRIEDRICH RINNE. **Über eine neue Herleitung und Nomenklatur der 230 Kristallographischen Raumgruppen.** ERNST SCHIEBOLD. Abhandlungen der mathematisch-physikalischen Klasse der sächsischen Akademie der Wissenschaften **40.5.** Text 204 pp. Atlas 22 pp. 349 figs. (36 in colors) on 46 plates. S. Hirzel, Leipzig 1929. Price unbd. Text 13 RM. Atlas 13 RM.

The new system for describing crystal classes given by the senior author in the first eight pages of the text appeared in abstract two years ago and has certain striking simplicities to recommend it. The symbols are especially compact and significant. A further slight saving might have been made by dropping the parentheses in 6 cases, e.g. $4sd$ for $4(sd)$. The names as distinct from the symbols, are rather awkward,but this is forgotten as soon as the long monograph concerning the 230 space-groups is fairly under way. The junior author here offers a symbol (with from 1 to 9 significant parts) for each space-group. This symbol tells the initiate how the space-group can be built up by the combination of symmetry elements. More astonishing still are names which tell all that the symbols do and alternative names for the most general complex of planes (or points) in the group. Examples will indicate the sort of thing that happens in simple and complicated cases. Space-group C_2^3 (Schoenfliess' notation) becomes s'; the name suggesting its derivation is Γ_m'−sphenoidisch; the name describing its four-fold complex of planes is Γ_m'−sphenoid. Space-group O_h^{10} becomes $\tilde{t}''(s\delta_k)[1/4\ 0\ 3/8]$; the two names are Γ_c''-tetraedroidisch-gyroklinodomatoidisch, and Γ_c''-Dyshexaoktaedroid. Graeco-German masterpieces like these are offered after the promise (p. 32) "that no outlandish word too long and difficult in pronunciation will arise, which would make an application [of the new system] impossible, especially in teaching." The explanation of the system suffers from poor proof reading of symbols and coordinates on pp. 23–24 (9 omissions or mistakes), otherwise it is clear enough. The 141-page list of space-groups (still fortunately accessible by simple numerical reference) gives, in more compact form than in Niggli's compendium of 1919, all the symmetry elements with their relative positions in the elementary parallelopiped. The division into generating and resulting symmetry elements is not wholly logical. For example, the symmetry centers included in the first category arise, with one exception, fro n the combination of elements already listed. The separation of symmetry centers into sets, apparently non-equivalent, is often not justified. There are very few mistakes in this part of the work to judge by a partial check. (Mistakes appear in V_h^7 and V_h^{14}.) The diagrams are apparently even more free from mistakes, but the scale is too small for the more complicated space groups (except in the really beautiful three-color plates for the cubic space-groups) and the care taken in the drawing varies greatly (cf. Figs. 44b and 52). The symbols used in the diagrams are more perspicuous than those chosen by Astbury and Yardley in a similar presentation.

The work as a whole is recommended for purchase by reference libraries rather than by individuals.

L. W. McKeehan

Handbuch der Astrophysik. Bd. IV. G. Eberhard, A. Kohlschutter, H. Ludendorff. Pp. 501, 221 figs. Julius Springer, Berlin, 1929. Price, bound, RM 78.80.

This volume—the second part of the *Handbuch* to appear—maintains the high standard set by volume VI, which was published last year. It is of thoroughly international character—the separate chapters which comprise it coming from Austrian, German, Italian and American authors. Seventy percent of the text deals with the Sun—which owes this prominence not so much to its dominant position in the solar system as to its high temperature, which adapts it to astrophysical investigation.

In chapter 1 Dr. Bernheimer, of Vienna, discusses the temperature and radiation of the Sun, and gives a very complete survey of past investigations in this field, without obtruding his own opinions. Chapter 2—the longest in the book—by Professor Abetti of Florence, deals (in excellent English) with solar physics. After a rather full description of the instruments employed in solar research, the immense mass of detailed knowledge which has been accumulated by the observations of the last thirty years is reviewed with admirable clearness.

Many topics are treated historically—the earlier observations or theories being discussed first—and the novice should realize that the various sections should be *read through* in order to arrive at the latest data.

The final section on solar theories deals almost entirely with the various dynamical theories which have been advanced to explain the circulation in the solar atmosphere and the body of the Sun. More than a brief mention might have been given to Eddington's fundamental investigations upon the internal constitution of the Sun and the stars.

Chapter 3, by Professor S. A. Mitchell of Virginia, deals with eclipses of the sun. The style is here considerably more popular, and one-third of the 120 pages are devoted to historical accounts of observation of total eclipses since 1836. The present state of knowledge of the chromosphere, the flash spectrum and the corona are well summarized, and the equipment and condition required to secure the best results at future eclipses are clearly discussed—though all observers would not agree with the author's judgment on some technical points.

Chapter 4, on the planets, by Professor Graff of Vienna, is again successful in summarizing a mass of detail with relatively small compass. The latest observations, such as those of Moore and Menzel in 1928 on the rotation of Neptune, are included. Some of the opinions expressed would, in the reviewer's judgment, be shared by few astronomers—for example, the disbelief in the 88-day period of rotation for Mercury, and the acceptance of Seeliger's view that the attraction of the matter which produces the zodiacal light is responsible for the advance of the perihelion of Mercury. A very interesting discussion of the surface features of the Moon deserves specific notice.

The last chapter, on comets and meteors, comes from Dr. Kopff of Berlin. It is well brought out how many unsolved problems are still presented by the forms and changes of the envelopes and tails of comets, and by the sudden lighting up of meteors when they enter the Earth's atmosphere.

Two features of the book in general deserve especial praise, the number and excellence of the illustrations, and the abundance of references to original papers on all the subjects which are discussed, which is likely to be of great and permanent aid to the student who desires to go further.

The price, as in the case of many recent German works, appears to be very high.

HENRY NORRIS RUSSELL